NOTICE

The quality of this microform is heavily dependent upon the quality of the original thesis submitted for microfilming. Every effort has been made to ensure the highest quality of reproduction possible.

If pages are missing, contact the university which granted the degree.

Some pages may have indistinct print especially if the original pages were typed with a poor typewriter ribbon or if the university sent us an inferior photocopy.

Previously copyrighted materials (journal articles, published tests, etc.) are not filmed.

Reproduction in full or in part of this microform is governed by the Canadian Copyright Act, R.S.C. 1970, c. C-30.

AVIS

La qualité de cette microforme dépend grandement de la qualité de la thèse soumise au microfilmage. Nous avons tout fait pour assurer une qualité supérieure de reproduction.

S'il manque des pages, veuillez communiquer avec l'université qui a conféré le grade.

La qualité d'impression de certaines pages peut laisser à désirer, surtout si les pages originales ont été dactylographiées à l'aide d'un ruban usé ou si l'université nous a fait parvenir une photocopie de qualité inférieure.

Les documents qui font déjà l'objet d'un droit d'auteur (articles de revue, tests publiés, etc.) ne sont pas microfilmés.

La reproduction, même partielle, de cette microforme est soumise à la Loi canadienne sur le droit d'auteur, SRC 1970, c. C-30.

Canada

ISBN 0-315-46866-1

UNIVERSITÉ D'OTTAWA
UNIVERSITY OF OTTAWA

ACKNOWLEDGMENTS

First, I would like to thank Dr. B.E. Conway, my thesis advisor, for advice and discussions throughout this work, especially during the writing of this thesis. His immense knowledge of electrochemistry and chemistry in general was greatly appreciated.

I also would like to acknowledge Dr. H. Angerstein-Kozlowska for many useful discussions during the analysis of the results obained in this work. Her profound understanding of metal oxidation processes was invaluable.

I especially thank Mr. Egon Kristov for constructing my glass electrochemical cell and Theresa W. for the SEM pictures. I also thank the other members of the support staff, Werner, Joe, Eva, Cass, Fern, Mike, Dan and others, for all the help they have given me during the course of this work.

I would also like to thank my colleagues in the electrochemistry laboratory, especially David T. and David H., for their help with the computer; Simon, for many useful discussions; and Viola, for being a bit of a mentor.

Thanks are also due to my parents and my sister for all their encouragement; they had more confidence in me than I had in myself.

Most of all, I thank my husband, Frank Houlihan, to whom I dedicate this thesis. Without his patience, help, encouragement and love, this work would not have been possible.

TABLE OF CONTENTS

LIST OF FIGURES

LIST OF TABLES

ABSTRACT

The surface oxidation of Au electrodes has previously been shown to be a complex process, consisting of several distinguishable stages, observed as peaks in cyclic voltamograms. This process was also found to be very sensitive to the type of anions in the solution, temperature and the structure of the electrode surface on an atomic scale. Commencement of surface oxide formation arises at less positive potentials in the presence of weakly adsorbed anions, such as ClO_4^-, than with more strongly adsorbed anions, such as SO_4^{2-} (HSO_4^-).

In the present work, findings of those previous investigations were expanded upon by studying Au electrodes in solutions containing $HClO_4$, H_2SO_4, HF and mixed $HClO_4/H_2SO_4$. Existing techniques, developed to prevent contamination, were improved by employing new potential-time programs and better data collection and processing with a digital oscilloscope and a mini-computer. These new techniques allowed precise measurements of very small charges, corresponding to less than 1 % of a monolayer of OH species, whereas previously, sensitivity was limited to about 5% .

It was found that adsorbed F^- anions blocked the initial stages of surface oxide formation to a greater extent than $HClO_4^-$, but less than sulfate ions. This indicates that the relative strength of adsorption at Au electrodes of these ions is SO_4^{2-} (HSO_4^-) > F^- > ClO_4^-.

In mixed $HClO_4/H_2SO_4$ electrolytes ($[H_2SO_4] = 4X10^{-4}$ M, $4X10^{-5}$ M), SO_4^{2-} adsorption at 1.2 V, which was studied by its displacement effect upon surface oxide formation, was found to follow adsorption kinetics which are first order in anion concentration and sites. In these mixed electrolytes, anions may be prevented from adsorbing at the surface ("anions off" situation) or be allowed to attain almost equilibrium coverage ("anions on" situation) by using different potential-time programs. "Anions off" I vs E profiles resemble those found for 1 M $HClO_4$, and those for "anions on" resemble those found for 0.5 M

H_2SO_4.

Surface oxide growth in 1 M $HClO_4$ is characterized by observing the reduction of OH/O species in three cathodic peaks, OC1, OC2 and OC3; in 0.5 M H_2SO_4, four peaks, OC1, OC1', OC2 and OC3, are observed. The OC1 peak arises from the reduction of reversibly deposited OH species, and its potential is less positive in $HClO_4$ than in H_2SO_4 solution. The OC1' peak is the reduction of OH electrosorbed in the presence of a lower coverage of sulfate than the initial OC1 state. This is a result of the time-dependent desorption of anions. There is an important relationship between the co-adsorbed anions and OH's, and their associated isotherms, causing time-dependent desorption and relaxation of the adsorbed anion layer, especially for sulfate. The OC3 peak is due to reduction of species which have been turned-over and is in the beginning of phase-oxide formation. The coverage by the species reduced in the OC2 peak reaches a saturation limit, indicating that this is the reduction of surface OH species remaining at the surface.

Surface oxide growth in both electrolytes is characterized by a non-logarithmic region in time followed by logarithmic regions. In $HClO_4$, a plateau is temporarily reached in growth after the OC1 peak has attained its maximum charge at relatively negative potentials; this behavior is not found in H_2SO_4. At these plateaus, the oxide charge formed in $HClO_4$ increases very little in time, and an isotherm for the OA1/OC1 OH species is given for these conditions.

The change of state of the intially electrosorbed OH species, reduced in the OC1 peak, to states characterized by reduction in the OC2 and especially the OC3 peak, was examined in $HClO_4$. The charge associated with the conversion of state of the OH species, is also found to follow a logarithmic relation with time.

A $t^{1/2}$ relation for surface oxide growth at Au has been found for a relatively short time after growth was controlled by solution resistance (iR

drop) and before the well established log t relation sets in. These $t^{1/2}$ relations were found under several conditions, i.e. different concentrations of H_2SO_4 and temperatures. The slopes for these lines, $dQ/d(t^{1/2})$, depend linearly on potential, and not exponentially as is usually the case. Possible mechanisms for this behavior are discussed.

Surface oxide growth was also examined in mixed $HClO_4/H_2SO_4$ solutions. Under "anions off" conditions, this process initially resembles that found in $HClO_4$, but in this case OH species at the surface are displaced by readsorbing SO_4^{2-} anions, characterized by a decrease in total surface oxide charge with time. "Anions on" growth resembles that observed in H_2SO_4. Although the "anions off" and "anions on" growth behavior are quite different at short holding times, understandably they become more similar at longer holding times and more positive potentials.

Temperature effects on Au surface oxidation were studied by cyclic voltammetry and growth experiments.

The double-layer charging I vs E profiles for polycrystalline Au electrodes in 0.5 M H_2SO_4 and 1 M $HClO_4$ are nearly the same for $E \leq 0.1$ V (i.e. well negative to the potential of zero charge) where no anions are adsorbed at the surface, but are quite different for more positive potentials where anion adsorption and some charge transfer occurs. For the double-layer capacitance of Au in mixed $HClO_4/H_2SO_4$ electrolytes, the currents in the cathodic I vs E profile increase with holding time at 1.2 V, as SO_4^- (HSO_4^-) anions adsorb with time.

Roughening of Au electrodes by means of rapid potential cycling begins when the potential is sufficient in the anodic sweep for the appearance of the OC3 and OC2 peaks during the reduction cycle, i.e. when the turn-over process commences. Gold electrodes roughen more rapidly in 0.5 M H_2SO_4 than in 1 M $HClO_4$.

CHAPTER I

INTRODUCTION

1.1. General Area of Interest

In many ancient and primitive mythologies, the boundary between two different things, for example the threshold between a house and outdoors, was considered to be partially under the influence of supernatural forces and, for this reason, it was thought things might happen there that were quite out of the ordinary[1]. In physical science, boundaries are also found to be of special significance. It is known that an "interphase", i.e. that matter of finite dimensions that resides just at the interface between phases, may exhibit properties which are different from those of either of the adjacent bulk phases[2]. The special properties of these interphases are of practical importance in such areas as heterogeneous catalysis, adhesion and the corrosion and passivation of metals. Of all the many types of interphases, the work described in this thesis is concerned with those between polycrystalline gold and electrolyte solutions, particularly for the case of the gold surface being partially covered with electrosorbed oxygen species.

In most electrochemical studies of metal oxidation, fairly thick oxide films, involving several, or many, atomic layers, are examined[3]. However, as shown in a smaller number of investigations, generally concerned with noble metals[4], the very first layer, or monolayer, of oxygen species at the metal surface can be distinguishably examined. Such studies are important for a fundamental understanding of the elementary processes of metal oxidation, in general, and for the elucidation of its initial stages, in particular. Although several studies have been made in the past of this behavior down to coverages less than about ten percent of a monolayer[255-260], the present work represents an improvement, mostly because of better instrumentation, but to some extent also on account of a lack of appreciation of the major importance of

characterizing and understanding the elementary processes that occur at such coverages. With recent advances in scientific equipment, particularly for digital collection and manipulation of data, it is now possible to study very low coverages, down to < 1% of a monolayer, as has been done in the present work, and to follow the kinetics of conversion of sub-monolayer levels of adsorbed oxygen species from one state to another at such coverages.

Gold is particularly well suited to studies of surface oxide formation and reduction down to monolayer and sub-monolayer levels because the various stages of these processes can be precisely and uniquely resolved by potentiodynamic techniques[5-9], including the initial, reversible electrosorption and desorption of OH at very low coverages. In addition, the anions that are present in the electrolyte, and hence usually adsorbed at the electrode surface, are found to have very strong and chemically specific effects upon the initial and subsequent surface oxidation processes at gold. Also, gold surface oxidation had been examined previously in this laboratory[5-7] and the required special, high-purity techniques had already been developed for some of these experiments, since gold electrodes are particularly sensitive to the presence of organic and certain ionic impurities[6] so that extreme care is needed in cleaning the experimental cell, electrodes and other equipment, and in solution preparation.

Previous research in this laboratory on noble metal oxidation processes has been recorded in two earlier theses by Barnett[6] and Sharp[7], and papers that have resulted from that work. Because their respective theses, particularly that of Sharp, contain extensive reviews of pertinent literature, the present introduction will be only brief.

1.2. Metal Oxidation Mechanisms

1.2.1. Direct Dissolution as Metal Cations

This is the simplest of metal oxidation mechanisms and is of particular

importance in corrosion and battery reactions, especially those involving base metals. No oxide film is formed. This type of mechanism occurs in the corrosion of any relatively active metal, such as zinc, in an acidic electrolyte[10,11] or, in some cases, also in strong alkali where soluble metallate species can be formed. In the simplest case, metal atoms at the electrode surface react to give metal cations in solution and electrons remaining in the metal:

$$M \rightarrow M^{Z+}_{soln.} + Ze \qquad (1.1.)$$

1.2.2. Dissolution-precipitation

In this mechanism, the previously described dissolution is followed by the formation of an insoluble metal oxide or hydroxide in solution. This material precipitates at the electrode surface, since this insoluble product forms faster than the metal cations can diffuse away:

$$M \rightarrow M^{Z+}_{soln.} + Ze$$

$$M^{Z+}_{soln.} + Z\,H_2O \rightarrow M(OH)_Z + Z\,H^+ \qquad (1.2.)$$

A porous, thick oxide film results, and its growth is usually controlled by diffusion of M^{Z+} cations through the film[3,12]. This type of oxide film formation often occurs in alkaline solutions on such metals as silver[13] or zinc[14,15], and is often pH dependent when the anodically formed oxide has amphoteric properties.

1.2.3. Direct Oxide Film Formation

Unlike the two previously mentioned mechanisms, which are bulk processes, a surface process may also be involved in the very initial stages of oxidation of some metals, as is the case with noble metals[3,4] and nickel under certain conditions[16]. No dissolution step is involved. Oxygen-containing species (O or OH) are reversibly electrosorbed at the metal surface:

$$M + H_2O \rightleftharpoons M\text{-}OH_{surface} + H^+ + e \qquad (1.3.)$$

Although formation of a complete monolayer of oxygen species and subsequent

formation of thicker oxide films usually involves a more complex mechanism, as will be explained later, the process starts with this sort of electrosorption step, which is therefore fundamental for oxidation of this type.

1.2.4. Film Growth Mechanisms

Several different kinetic laws have been proposed to describe oxide growth on a variety of metals under various conditions. Since many reviews[3,11,17-21] have already covered this subject extensively, it is only necessary here to describe breifly some of the general laws that are found to describe the rates of thin film oxide formation at metals. These are the so-called direct logarithmic law, the inverse logarithmic law and the parabolic law. Most work indicates that the direct logarithmic rate law seems to be followed for oxide film formation at noble metals[21-31], but the results of some experimental work are not always consistent with this[32-38]. For some cases, the type of law that applies depends upon the stage or extent of oxide film growth at a given metal.

The logarithmic oxide growth laws are found for conductive oxide films, such as those found with noble metals and some transition metals[21]. Growth often proceeds through a place-exchange mechanism[3,39], where adsorbed oxygen species (O or OH) are exchanged with surface metal atoms, as will be described in greater detail later. The free energy of activation, $\Delta G^{\ddagger}$, for oxide growth is often assumed to increase linearly with film thickness[3,40], x.

$$\Delta G^{\ddagger} = \Delta G_o^{\ddagger} + bx \qquad (1.4.)$$

where b is constant. The resulting integrated rate law is:

$$x = k \ln t + k' \qquad (1.5.)$$

where k and k' are constants and t is time.

The inverse logarithmic law[3] is usually found for growth of films of insulating oxides, as is the case, for example, with the valve metals[3,18,21]. In the treatment of Mott and Cabrera[41], the growth is considered in terms of ions (generated at the metal/oxide interface) passing over a series of energy

barriers associated with a jumping mechanism of ionic transport through the film.

The integrated form of this law is:

$$\frac{1}{x} = k' - k \ln t \qquad (1.6.)$$

Parabolic growth of oxides is found where field-assisted diffusion of ions though the film determines the rate of growth[3,11], yielding for this case an integrated growth law of the form:

$$x = k\, t^{1/2} + k' \qquad (1.7.)$$

for the case of diminishing field, at constant potential, due to the growth of the film.

1.3. Experimental Methods for the Study of Electrochemical Surface Processes

1.3.1. The Need for Transient Methods

Electrochemical methods detect changes in the state of the electrode surface or of species reacting at this surface by the the passage of charge. Unlike bulk Faradaic processes, where the reaction of essentially unlimited amounts of material give rise to steady-state currents, surface processes, by their nature, are always limited by the coverage of products at the surface, a monolayer or less for any given state. For this reason, transient methods are essential for the effective examination of electrochemical surface processes. Several excellent reviews dicuss these techniques in detail[42-45].

Two kinds of transient methods are generally used in these experiments:

1. Galvanostatic, where a constant current (I) or current pulse is passed, and the resulting change in potential (E) is examined as a function of time and hence charge.
2. Potentiostatic, where a known potential or time-dependent function of potential (a triangular wave in cyclic-voltammetry[46,47] or sinusoidal in a.c. impedance), is applied, and the resulting current response is

examined as a function of time and/or potential, or frequency and phase.

Both methods depend on the two characteristics of electrochemical reactions, viz. current magnitudes are some function of electrode potential and integration of current in time corresponds to the passage of a well-defined charge that can be related to chemical material changes through Faraday's laws applied on a microscopic scale.

1.3.2. Galvanostatic Method

This method was developed by Bowden and Rideal[48] for double-layer capacitance studies, and subsequently used by Frumkin et al.[49] and Butler et al.[50,51] to examine adsorption and desorption of hydrogen and oxygen species at Pt electrodes. Since each reaction has a particular energy change and corresponding potential associated with it, the shapes of the charging curves give information about successive processes occuring at the electrode surface. Partial arrests in the curve may be due to the predominance of a single reaction[42] or to distinguishable stages of a process.

1.3.3. Cyclic-Voltammetry

The first potentiostat was developed by Hickling in 1939[52] for steady state measurements at solid metals, but was not extensively used in electrochemical surface studies until reliable and more sensitive instrumentation was available in the late 1950's. Cyclic sweep polaragraphy was introduced by Sevcik[46] and Will and Knorr[47], in one of the most widely quoted papers in modern electrochemistry, used a repetitive linear potential-time program employing an electronic potentiostat, to examine the electrosorption and desorption of hydrogen and oxygen species at Pt and other noble metals.

A cyclic-voltammogram is illustrated in Figure 1.1. for a Pt electrode in 0.5 M H_2SO_4[53], which shows features typical for I vs E profiles at noble metals in general. Between the potentials for molecular hydrogen and oxygen evolution

from water, three major potential regions corresponding to three processes are found:

1. electrosorption (cathodic sweep) and desorption (anodic sweep) of atomic hydrogen between 0.0 V and ca. 0.35 V.
2. double-layer charging between ca. 0.35 V and ca. 0.78 V.
3. electrosorption of oxygen species and subsequent oxide film formation and growth (anodic sweep) at potentials above ca. 0.78 V.

In the cathodic sweep, a large peak due to the reduction of the surface oxide is found over a less positive potential range than that for its formation, indicating hysteresis or irreversiblity in this process. This hysteresis will be discussed in greater detail later in this introduction, and in relation to new results to be described later in this thesis.

Cyclic-voltammetry is a very sensitive technique for the study of surface properties, since the number, size and shape of the peaks in the I vs E profiles give relative energy information about the different states as well as the kinetics of the adsorption/desorption processes[43-45]. An important feature of the technique is that it gives differential information (dQ/dE) since the potential, E, of a process is related to current (dQ/dt) rather than just charge, Q, so that a sort of "spectrum" of states of electrosorbed species is resolved in terms of potential or Gibbs energy for their adsorption or desorption. Coverages and adsorption isotherms may be obtained from the areas under these adsorption peaks. The shape and symmetry of the peaks are related to the kinetics and reversibility of the processes involved[54-56], and the width of the peak becomes greater with repulsive interactions and narrower with attractive interaction between adsorbate species in the monolayer[57,58]. By varying the sweep-rate, diffusion-controlled and reversible or irreversible faradaic surface processes may be differentiated by examining the dependence of peak currents on sweep-rate; they increase with sweep-rate as the square-root

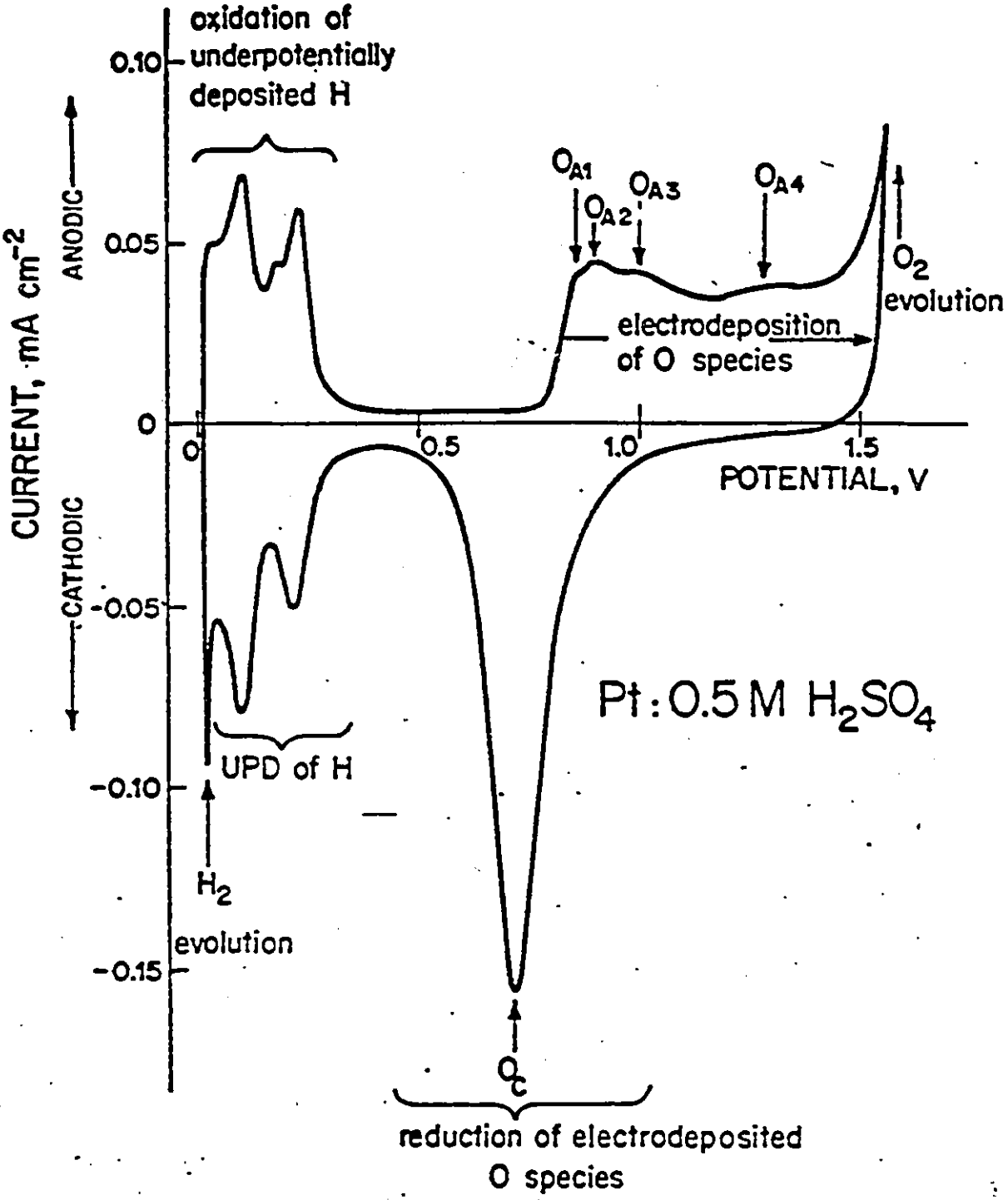

Figure 1.1. Typical potentiodynamic I-E profile for Pt at 0.050 V s^{-1} in 0.5 M H_2SO_4.

or linearly, respectively. Also, electrochemical rate constants for adsorption may be obtained from the variation of peak potential with sweep-rate[59].

One of the advantages of linear sweep voltammetry is the flexibility in the types of potential-time programs that may be used. Programs with assorted potential sweeps and arrests may be used to obtain a variety of information, as has been done in this laboratory[5,6] and others[60-65].

Single or repetitive linear potential sweeps give general information about adsorption processes occurring at the electrode surface. This approach is especially useful when the potential limit is taken to a series of successively increasing or decreasing anodic values within the range of the particular process being examined, so that the desorption or reduction may be examined after different stages or extents of adsorption or oxidation, or growth of an oxide film. By varing the sweep-rate, kinetic information may also be obtained as was previously mentioned[59].

Surface oxide may be aged by using a potential cycle in which the surface oxide formed is only partially reduced before reoxidation. The surface oxide formed in this way is found to be in a different state from that developed in a single potential sweep[6,61-69].

Application of a controlled constant potential arrest in potential "holding" experiments may be used to examine the growth or time-dependent reduction of surface oxide at a single potential or to allow time for anion adsorption to reach equilibrium. In oxide growth experiments, surface oxide which is formed at a set potential during several different holding times is analyzed by a cathodic sweep in which oxygen species in various states at the surface are reduced in characteristic peaks[5,6] at different potentials, i.e. for different Gibbs energies. In these experiments, it is important to minimize surface oxide formation before the growth potential is reached, so a very fast anodic potential sweep (approaching a step), taken from a potential

below that for the onset of surface oxide formation, is used. In studies of surface oxide reduction, surface oxide formed under the same conditions (sweep-rate and potential limit) is reduced at a particular potential for several holding times, and then the oxide remaining is measured in a cathodic sweep[6]. The adsorption of anions and their subsequent effect on surface oxide formation may be studied by holding the potential at a value slightly negative to that for the onset of surface oxide formation[6,65].

1.3.4. Complementary Non-Electrochemical Methods

Since electrochemical methods give only indirect information about chemical changes in state, complementary, non-electrochemical methods are sometimes used to obtain more direct information about the nature of oxygen species or other adsorbates at the electrode surface. A useful review of some these techniques has been given by Yeager[70]. Several in-situ methods have been used to measure various properties of the surface in conjunction with electrochemical experiments. Ex-situ methods may also be used, but usually the electrochemical experiment must be interrupted and the surface may change during the time between emersion from solution and the measurement.

In some of the earlier in-situ work, the metal solution interface was examined by means of reflectivity and ellipsometry, yielding information about the refractive index, optical adsorption coefficient and thickness of adsorbate films at the surface. These measurements may be used for examining surface charge, adsorption isotherms, the state of water in the compact double-layer, surface roughness and the electronic properties of films at the electrode surface[70-73]. It is also possible to make this type of measurement as a function of wavelength[74,75] of the incident radiation used. This method has been used extensively to examine surface processes at Pt[76-79] and Au[80-85]. Surface plasmon polaron spectroscopy, which is a special type of visible-UV reflectance measurement involving excitons on intrinsically highly reflective

metals[86], has been used to examine Au electrodes at potentials for both the double-layer charging[87,88] and surface oxide formation[89-91] processes.

Surface enhanced Raman spectroscopy (SERS) has also been used to look at adsorption at Au in solution[92-94], but this method may only be used to obtain qualitative information, since it is still uncertain why the signal is enhanced despite many theories on the origin of this effect.

Very recent advances in infrared spectroscopy, in particular Fourier transform infrared spectroscopy[95,96], in which very small signals may be measured with respect to a much larger background signal, has facilitated the use of IR spectroscopy in surface studies. In electrochemical work, the best results have been obtained using a specular reflectance method in which IR light, polarized parallel to the surface, is used as a reference, since adsorbates only absorb light polarized perpendicular to the surface[97,98]. Photoacoustic spectroscopy, in which absorption of modulated IR radiation results in a detectable sound wave, and photothermal spectroscopy have also been used to examine the surface oxide on Au[99-101].

Photoelectrochemistry has also been used to examine surface oxides at gold electrodes[105], especially somewhat thicker oxides which are known to have photosensitive semiconductor properties.

Radiotracer studies[103] using radioactive anions have given information on anion adsorption and its competition with subsequent surface oxide formation at Pt[104] and Au[105]. An indirect examination of surface oxide formation at gold has been made using labelled Ca^{2+} [106].

Information about the state of the electrode, such as adsorption, simple charging and the potential of zero charge, may be obtained by measuring the resistance of a microscopically thin electrode during electrochemical experiments[107-111].

Recently, an investigation of Au dissolution and surface oxide formation

and dissolution used a piezoelectric microbalance to measure very small weight changes[112], and found corroborative evidence for a place exchange mechanism.

Some recent work showed, surprisingly, that electrodes may be emersed from solution under certain conditions with the double-layer unchanged[111,113-115], i.e. the charge at the metal surface is unchanged and the distribution of adsorbed water and anions remains intact after emersion. However, it is doubtful if submonolayer oxide films at noble metals would remain the same after emersion, at the very least they would age[6,61,63]. After an electrode is emersed, various techniques not available in-situ, including ultra high vacuum measurements such as LEED[116-118] or XPS[113,119-130], may be used. Work functions have been measured at an emersed gold electrode[115,131,132] with and without surface oxide, and reflectivity measurements on the emersed gold have been found to be similar to those made in solution[114].

1.4. Electrochemical Direct Oxide Film Growth at Noble Metals

1.4.1. Indications of Direct Surface Processes and their Resolution at Sub-monolayer Levels of Coverage

Two electrochemical surface processes are generally found at noble metal electrodes between the potentials for hydrogen and oxygen evolution, the underpotential deposition and desorption of hydrogen (except at gold) and electrosorption of oxygen species (OH or O). As with some other surface processes, electrosorbed oxygen species in different states existing at submonolayer coverages can be distinguished through their resolution as current peaks in cyclic-voltammetry experiments, as was described in the previous section. These processes may depend upon the orientation and microscopic structure of the surface, pH, anions in solution, temperature and potential.

It was shown in this laboratory that there are three peaks, designated OA1, OA2 and OA3, that can be distinguished in the electrosorption of OH up to monolayer coverage (220 $\mu C\ cm^{-2}$) in the I vs E profile for polycrystalline

Pt[7,53,133] (Figure 1.1.). Since the charges associated with these peaks are about 55, 55, and 110 $\mu C\ cm^{-2}$ for OA1, OA2 and OA3, respectively, it was suggested that these peaks correspond to the formation of successive ordered overlattices of OH with coverages $\theta \approx 0.25$, 0.5, and 1.0, respectively. These states were denoted "Pt_4OH", "Pt_2OH" and "PtOH" and theoretically correspond to (2 X 2), $(\sqrt{2} \times \sqrt{2})R45^{\circ}$ and (1 X 1) superlattices of OH on Pt(100), giving maximized spacing between mutually repelling Pt-OH dipoles. Oxidation of the surface beyond monolayer coverage of OH, seen as a broad plateau anodic to these three peaks in the I vs E profile, is due to further oxidation of the electrosorbed OH to O:

$$Pt\text{-}OH \rightarrow Pt\text{-}O + H^{+} + e \qquad (1.8.)$$

and to the simultanious formation of a rearranged layer of oxide by a place-exchange process (reconstruction mechanism) between metal atoms and surface oxygen species. At higher potentials and/or for extended times, more than one monolayer of oxide species can be formed.

A reversible electrochemical surface process is one in which adsorption and desorption occur, for a given fractional coverage, θ, at the same potential over an appreciable range of rates. In a cyclic-voltammogram, the I vs E profile for desorption should then be the mirror image of that for the adsorption process; experimentally, such reversible behavior is, to a substantial degree, realized in the deposition and desorption of H at Pt (Figure 1.1), especially in dilute electrolyte solutions where anion adsorption is minimized. The electrosorption of OH at Pt electrodes up to a coverage of about 0.15 and a potential of 0.9 V[53] is also an almost reversible process but the reduction of surface oxide becomes irreversible as greater extents of OH deposition are generated either in time or at higher positive potentials. Similar behavior can be demonstrated in optical reflectivity measurements[78]. The initial stages of electrosorption of OH at gold electrodes are also found

to be reversible, but irreversible processes arise already after a fractional coverage by OH $\geq$ 0.02 is deposited[5,6], as will be reported and discussed further in later sections of this thesis.

A cyclic-voltammogram for surface oxide formation and reduction at polycrystalline gold in 0.001 M $HClO_4$ at 0.02 V s^{-2} and in 1 M $HClO_4$ at 20 V s^{-1} is shown in Figure 1.2.[5,6]. Four peaks, identified as OA1, OA2, OA3 and OA4, are resolved in the anodic I vs E profile and three, identified as OC1, OC2 and OC3, in the cathodic profile, and are designated according to the following convention: the peaks are numbered in the order in which they appear on the anodic (A) and cathodic (C) sweeps with increasing end potential of the anodic sweep in cyclic-voltammetry experiments. This leads to a situation in which peak OC3 lies on the cathodic sweep potential scale between the peaks designated OC1 and OC2, as seen e.g. in Figure 1.2. The three reduction peaks have previously been observed by Gol'dshtein et al.[8,9] and Sotto[60], and previously in this laboratory by Barnett[5,6]. However, only those oxygen species resulting in the peak designated as OA1/OC1 (Figure 1.2.) are deposited reversibly, further oxidation being irreversible with resulting species being reduced in the peaks designated as OC2 and OC3. It is important to note that these designations for the anodic and cathodic peaks observed at Au are used thoughout the remainder of this thesis without further explanation.

The state in which the OH species are initially reversibly deposited at gold in H_2SO_4 solutions is very short lived, and can only be observed using relatively rapid sweep-rates. The onset of surface oxide formation is also more positive in the presence of the strongly adsorbed anions from H_2SO_4 (HSO_4^- and SO_4^{2-}). The large OC3 peak corresponds to the the main reduction process, thought to be the reduction of oxygen species which have undergone place-exchange with Au metal atoms into a quasi-3-dimensional surface oxide phase, but only a nominal monolayer in thickness.

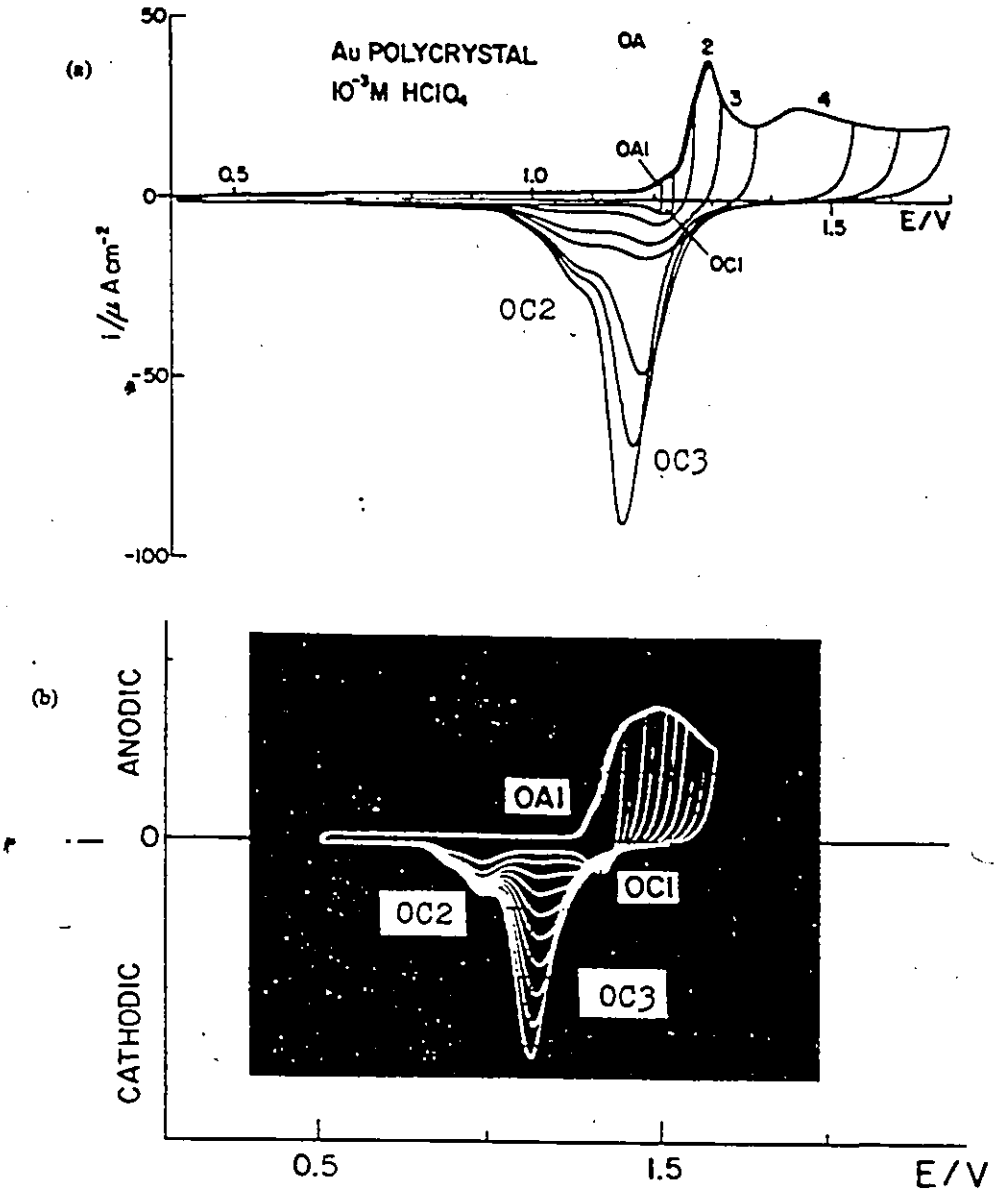

Figure 1.2. Potentiodynamic I-E profiles for Au taken to a series of anodic end potentials:

(a) in 0.001 M $HClO_4$ at 0.02 V s^{-1}

(b) in 1 M $HClO_4$ at 20 V s^{-1}

The species reduced in the OC2 peak reaches a limiting coverage (see e.g. Figure 4.4.7.) which depends characteristically on the anions of the electrolyte and their concentration, as well as temperature. It is thought, however, that this peak corresponds to the reduction of electrosorbed oxygen species that are arranged in two-dimensional overlattices in the relative absence of strongly adsorbed ions such as HSO_4^- (SO_4^{2-}). Such a situation arises especially (but not only) when an appreciable coverage by oxygen species in the reconstructed OC3 state has been generated and is reduced in the cathodic sweep. After the completion of the OC3 reduction process, some sub-monolayer quantity of electrosorbed OH species appears to remain on the surface at relatively low coverages in the absence of strongly adsorbed anions (this is because the ions were desorbed in the preceeding anodic sweep during the oxidation process). Such ions may, however, become readsorbed if the transit time of the sweep is lengthy over the OC2 peak region. The OC2 peak corresponds to the reduction of these residual electrosorbed OH species. This behavior is evidently general, since it is also observed for the three principal index planes of Au[194]. Note that the potential range for the "OC2" reduction process (see Figure 1.2.) is always much less positive than that for the "OA1" or other "OA" process. This is because, due to the chemisorption of anions in the anodic sweep, OH species are always initially competively deposited ammongst these adsorbed anions, therefore at a more positive potential. The evidence for this mechanism has been given in earlier papers[5,6,194,195].

The I vs E profiles for gold in alkaline solutions are characterized by a wider double-layer charging region (larger double-layer capacitance)[5,6], which seems in fact to be due to a sort of reversibly electrosorbed (upd-like) OH species, possibly with a fractional electrosorption valency[134].

Results similar to the above have been found by Nguyen et al.[83] in

double-capacitance and electroreflectance spectra of Au electrodes in neutral and alkaline NaF solutions. A relatively slow adsorption of 10 to 20 % of a monolayer of OH at potentials substantially less positive than that for the onset of surface oxidation was characterized and referred to as the "incipient oxidation". The electroreflectance spectrum for this "incipient oxide" was also found to be different than that for double-layer charging alone.

1.4.2. Irreversible Processes and Hysterisis in Metal Surface Oxidation

As discussed previously, although initially the adsorption of OH is reversible, subsequent surface oxide formation processes are irreversible. Electrochemical surface processes may become irreversible because of either kinetic irreversibility[54,56] or hysteresis. In kinetic irreversibility, the electrochemical rate constant for the desorption process is small (relative to the sweep-rate), and a relatively large overpotential is needed for an appreciable rate of desorption to be achieved; however, the desorption is microscopically simply the opposite of the chemical process involved in the adsorption. In hysteresis, however, the adsorbate undergoes an irreversible change in state after the initial adsorption process, so that the desorption process proceeds through a different kinetic pathway as was found e.g. in the adsorption and desorption of benzene on active charcoal as a function of pressure by Everett and Whitton[135]. The irreversiblity of the surface oxide formation at noble metals is due to hysteresis, because the I vs E profile does not become more reversible with decreasing sweep-rate, as would be expected for kinetic reversiblity as it does for H adsorption and desorption at Pt. As well, the reduction process seems to occur principally in one peak while the oxidation process is resolved into several stages (Figure 1.1.). The irreversible, post-electrosorption change in the state of the oxygen species at the surface is thought to occur through a reconstructive place-exchange

process, resulting in a new state having lower energy[53].

1.4.3. Reconstructive Place-Exchange Process

In place-exchange, adsorbed oxygen species interchange with underlying metal atoms and are incorporated into the substrate. A schematic illustration of this is given as follows[58] in terms of OH species, but may equivalently arise with O species:

OH OH OH OH OH OH ⟶

M M M M M M M M

OH M OH M OH M

M OH M OH M M M OH

This type of mechanism was first suggested for oxide film formation at metals exposed to oxygen in the gas phase[39]. Changes in work function during the initial stages of oxide film formation[136] under such conditions indicated a reversal in metal/oxygen dipoles, which reduces the total energy of the film and increases its thermodynamic stability.

There is the evidence, listed below, that a post-electrochemical place-exchange process occurs also in electrochemical surface oxide formation:

1. The observed hysteresis of surface oxide formation and reduction at noble and other metals;
2. The logarithmic decline of current in time due oxide film formation at constant potential[7,81,136].
3. The cathodic potential shift of the main cathodic growth peak (OC3 in Au I vs E profile, Figure 1.2.) with increasing coverage[5,6].
4. The "aging effects" found with respect to the thermodynamic states of oxide films[6,61,63].
5. Weight gain at gold electrodes (measured by a piezoelectric microbalance) only after considerable OH or O is adsorbed. This is

thought to occur because of adsorption of additional water molecules at the newly exposed metal atoms after place-exchange[112].

6. Certain small organic molecules are only oxidized at potentials at which reversibly electrosorbed oxygen species are present[137].

Place-exchange in oxide film formation is assisted by the repulsive interaction between metal/oxygen dipoles and adsorbed anions, and by increasing electrode field[5,6,53,138]. By place-exchange, these repulsive forces arising from chemisorbed oxygen species (M-OH or M-O surface dipoles) are relieved, and a more stable state of the surface oxide is then formed. Place-exchange is an activated process, which is generally slower than the initial adsorption step, and so its rate increases with temperature.

This type of mechanism was first treated in Sato and Cohen's interpretation of anodic oxide film growth at Fe[139], and later applied to Pt surface oxidation by Reddy et al.[23]. Before this, Schuldiner et al.[140] qualitatively suggested that oxygen species may be "dermasorbed" after electrosorption.

The rate-determining step in the reduction of place-exchanged surface oxide at gold electrodes was found by Barnett[6] in previous work from this laboratory to be a simple irreversible electrochemical process with the transfer of two electrons. It was also found by Cadle and Bruckenstein[141], using a ring-disk electrode, that the reduction of this type of surface oxide was associated with some dissolution of gold.

1.4.4. Specific Adsorption of Anions and Surface Oxide Formation

In many cases, the surface concentration of ions found at the electrode surface is greater than that which would be due just to electrostatic physisorption. These ions, especially anions such as the halides and SO_4^{2-} (HSO_4^-), are chemisorbed at the electrode. This phenomenon is known as "specific adsorption" and was first observed as an increase in double-layer capacitance in electrocapillarity measurements at Hg[142]. More recently, specific adsorption of anions has been studied by a variety of techniques at polycrystalline and single-crystal surfaces of several metals[143,144]. Anion adsorption may depend upon anion concentration, potential, surface orientation and structure on a microscopic level, and temperature.

The d-orbital bonds between the chemisorbed anions and the metal are similar to ligand bonds found in metal complexes[145,146]. The increase in double-layer capacitance found with specifically adsorbed anions may be because either the larger concentration of anions at the surface causes a greater positive charge at the metal surface by inducing image charges[147] or because partial charge transfer occurs, determined by the electrosorption valency[134], between the anion and the metal. In the latter case, the extra capacitance is not strictly an electrostatic capacitance.

In general, the halides (excepting F^-), followed by SO_4^{2-}, are the most strongly adsorbed anions at noble metal electrodes, a trend that is also found for the formation of complexes of these metals with anions in solution. Previously the order of strength of anion adsorption at gold was given as $Cl^- > Br^- > OH^- > Cl^- > SO_4^{2-} > ClO_4^- > F^-$ [148], but the double-layer capacitance measurements made at that time were not sensitive enough to determine the small difference in specific adsorption between ClO_4^- and F^-. In more recent work, in which adsorption of weakly adsorbed anions at Ag single-crystal planes was examined, it was found that the relative strength of adsorption is $SO_4^{2-} >> F^-$

> ClO_4^- ≥ BF_4^- = PF_6^- [149]. F^- has also been found to be more strongly adsorbed at Au than ClO_4^- by both double-layer capacitance measurements[150] and electrode resistance measurements[110]. The double-layer capcitance behavior of Au in perchlorate solutions is quite complex[151] and BF_4^- seems to be the only anion which does not specifically adsorb at all gold surfaces[152]. Anion adsorption is also dependent upon the sub-microscopic structure of the electrode surface, and the relative strength of adsorption of anions for different Au single-crystal planes has been found to be (111) > (100) > (110) > (210) [153,154], which is also the relative order of hydrophobicity of these surfaces[156].

The nature of anions in solution and hence their adsorption behavior at electrode surfaces has an important effect on surface oxide formation at noble metals[5,6,157,158], especially gold. Some of ways in which this is manifested are:

1. The adsorption of anions is competitive with the electrosorption of OH and causes either "blocking" of the initial states of surface oxide formation, resulting in a diminution of charge in the corresponding peaks[5,6,159], or "displacement", in which the initial OH is electrosorbed in a different energy state (corresponding to a different current peak) at a more positive potential. "Blocking" is found with Cl^- adsorption at Pt[159] and "displacement" is found for SO_4^{2-} adsorption at Au[5,6].
2. The inner-layer potential profile is changed by adsorbed anions, affecting charge transfer kinetics[160,164].
3. The charged adsorbed anions influence the place-exchange between the metal and oxygen species[5,6,23,133,138].
4. Co-adsorbed anions may stabilize or destabilize certain states of adsorbed oxygen species[5,6].
5. Adsorbed anions affect oriented water at the surface[165,166], possibly

though Gurney co-sphere/electrode co-plane water interactions[167].

6. Anion adsorption may cause surface reconstruction (e.g. of the (100) plane) under certain conditions[154,168], when water does not already cause such reconstruction to occur[169-171].

Gold electrodes are particularly sensitive to the nature of the anions adsorbed; the onset of surface oxidation is 100 mV more positive in solutions containing H_2SO_4 than in those containing $HClO_4$[5,6]. As little as 10^{-8} M H_2SO_4 in a $HClO_4$ solution can cause displacement of the potential for the initial stage of deposition of OH species. The competition between strong adsorption of this anion and surface oxide formation was shown in a radiotracer study in which the surface concentration of SO_4^- was found to increase with potential until surface oxide formation commences, after which which almost no adsorbed SO_4^{2-} was found[105].

Arvia et al.[65] have recently examined the inhibiting effect of holding long periods of time (20 - 1800 s) at potentials just cathodic of those for surface oxide formation upon the I vs E profiles for subsequent surface oxide formation. This was interpreted as being due to the slow adsorption of anions; however, it was determined by the results presented in this thesis that the adsorption of anions at $[H_2SO_4] > 10^{-4}$ M is nearly complete after 1 s. The effect observed by Arvia et al. may actually be due to the slow restructuring of the water/anion film or more likely to the slow adsorption of trace organic impurities from solution.

One of the reasons why surface oxide formation at Au electrodes is so strongly influenced by adsorbed anions is that this process occurs at a potential that is considerably positive to the potential of zero charge (p.z.c.). The p.z.c. depends upon surface orientation[172], temperature[173-176], and the nature of anions adsorbed at the electrode[177]. The values reported are usually between 0.1 and 0.54 V s.h.e. for different faces of gold and about 0.2

V for polycrystalline surfaces[178,179].

1.4.5. Behavior at Single-Crystal Surfaces

Studies of surface oxide formation at Pt[180-189], Ir[199] and Au[27,60,83,150-152,168,175,176,190-195] single-crystal planes have shown that the submicroscopic structure (lattice geometry) of the metal surface has an important effect upon this process as might be expected. This is particularly true for gold single-crystal surfaces, where the cyclic-voltammograms for the different principal index planes are quite different from each other and display several different peaks in the anodic and cathodic I vs E profiles (Figure 1.3.[168]), and far more detailed information may be obtained than is possible with polycrystalline gold. Different potentials for the onset of surface oxide formation are found for the different planes[60,191-194]. The OC3 reduction peak is, however, nearly the same for all the single-crystal planes, but the OC1 and OC2 type reduction peaks vary considerably. Surface oxide formation at single-crystal gold surfaces is also quite sensitive to the nature of the anions in solution[194], and the adsorption behavior of a particular anion is different on different planes[144], a phenomenon probably determined by the the electronic work function, ϕ, of that plane.

Dickertmann et al.[27] found that the orientation of the surface of single-crystal gold electrodes had a role in the growth of thin oxide films. Their cyclic-voltamograms for (100), (111) and polycrystalline gold in 1 M $HClO_4$ differed considerably in the anodic profiles, but the cathodic profiles coincided. Contrary results were found by Kozowska and Hamelin[194], whose cyclic-voltammograms were characteristically different for the three principal index planes, both in the cathodic as well as the anodic sweeps. The relatively anodic potential for the onset of surface oxide formation and the lack of structure in the I vs E profiles, when compared with the results of more recent single-crystal work in $HClO_4$[194,195], indicate that organic or some

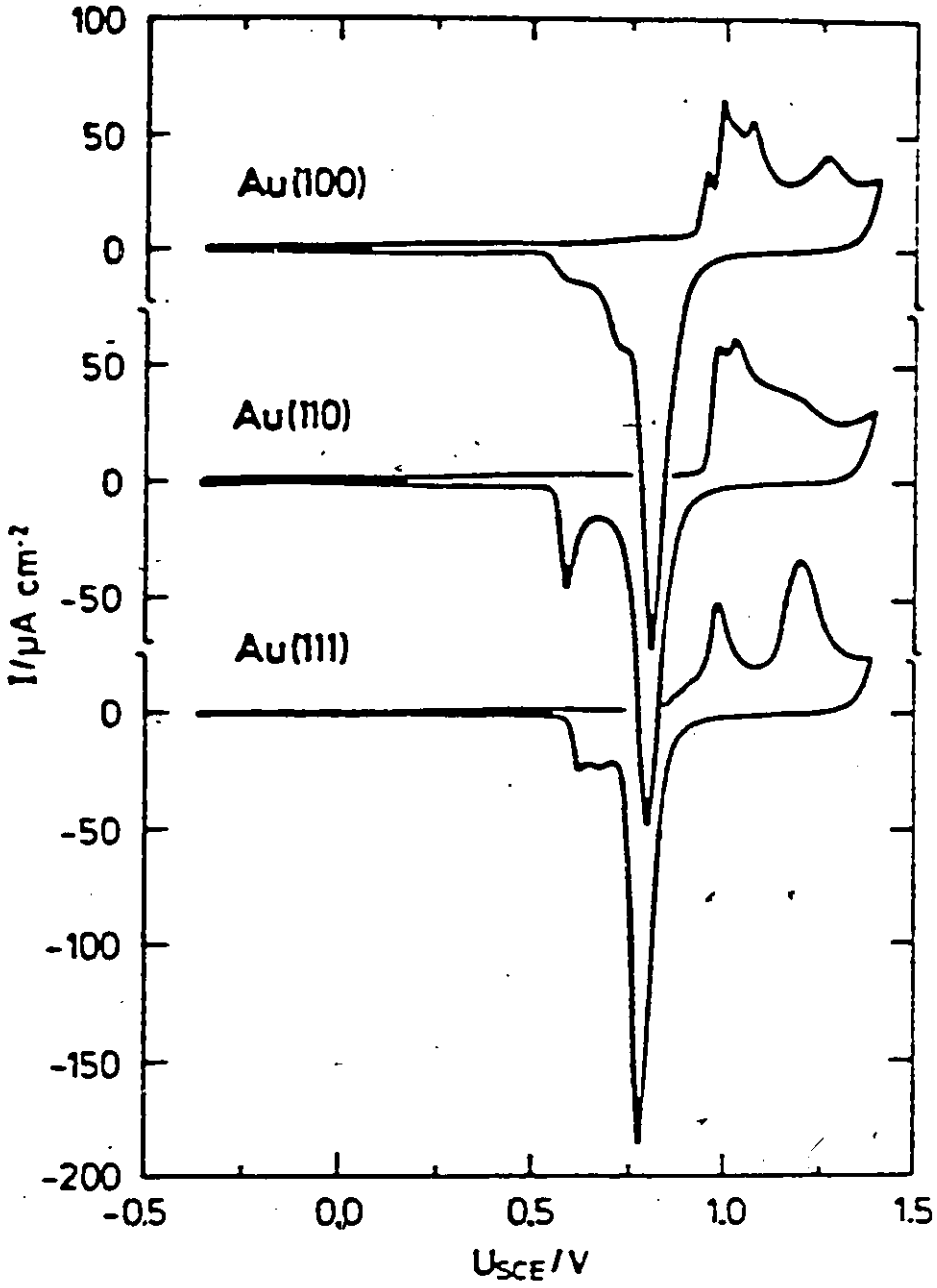

Figure 1.3. Potentiodynamic I-E profiles for the principal index planes of Au at 0.050 V s^{-1} in 0.01 M $HClO_4$ (from Reference 168).

other impurities probably had contaminated the electrodes, even though the preparation of the crystallographic planes seems to have been satisfactorily done.

Sotto et al.[60,191-193] studied how surface oxide formation and reduction at single-crystal surfaces changes as a function of pH, temperature and sweep-rate in cyclic-voltammetry studies at gold. The reduction of the surface oxide formed was examined by a cathodic sweep taken to a particular potential, which was then held for a variable amount of time, after which the remaining surface oxide was reduced by resuming the cathodic sweep. An electrochemical pretreatment of extensive potential cycling to an anodic end potential of 1.9 V was used to obtain reproducible I vs E profiles; this must have caused some restructuring and roughening of the electrode surface by dissolution[141] and redeposition of the gold. However, some recent LEED studies have shown that more gentle cycling of gold[190] and Pt[188] single-crystal electrodes may not cause much damage to the single-crystal surface.

Sotto found from one to three peaks for the reduction of the surface oxide; this result was thought to indicate the reduction of three oxidation states of gold, all existing at the electrode surface at the same time: Au III as $Au_2O_3 \cdot H_2O$ phase oxide, and Au II and Au I as oxides or hydroxides only existing at the surface. These different states were simultaniously present because of a supposed "energetic heterogeneity" even existing at single-crystal surfaces.

Hamelin et al. have recently made I vs E profiles for Au(210)[175] and (111)[178] in $HClO_4$ electrolyte for a series of temperatures between 274 and 334 K. The results show the same general trends for surface oxide formation and reduction with temperature found at polycrystalline Au electrodes, e.g. the initial formation peak becomes less positive with increasing temperature[7].

In recent examinations of surface oxide formation at gold single-crystals,

it became recognized that effects associated with co-adsorption of anions are of great importance. For example, the distinguishable adsorption behavior of anions[144] at different single-crystal planes is considered to be responsible for the differences observed in the potential for the onset of surface oxidation and other aspects of surface oxide formation, as was recently found by Angerstein-Kozlowska et al.[194] in a careful and detailed examination of the Au(100), (111), and (110) planes in $HClO_4$ and H_2SO_4 solutions of varying concentration. Adsorbed anions are thought to form an ordered hydrated layer, which depends strongly on the orientation of the electrode surface[195](tetrahedral anions will adsorb most strongly on the (111) surface which has similar 3-fold symmetry to that of the anions). Gas-phase studies of the co-adsorption of halides and water vapor at Pt[165] and Ag[166] single-crystal surfaces showed that hydrated-anion complex films are formed, with certain hydration states being more stable than others. Anion adsorption may even cause surface reconstruction in some cases[154,168], as is found in the gas phase with adsorption on a very clean (100) surface[196-198]. In addition, considerable extents of charge transfer can arise when anions are strongly chemisorbed[195].

It is thought that the initial reversible stages of surface oxide formation originate from discharge of water molecules within this hydrated-anion complex layer and may involve only partial charge transfer[195]. Completion of the surface oxidation processes requires desorption of the anions, which, it is believed, begins to take place when place-exchange sets in, and the very sharp peaks found in the I vs E profiles may be due to desorption of the anions, followed by the process of further oxidation of the surface.

1.4.6. Transition to Thick Film Growth and Aging of the Oxide

Logically, the formation of the initial monolayer of oxygen species should be considered differently from the process of growth of thicker oxide films.

However, experimentally there is usually no distinct transition between monolayer formation and multilayer growth, since no inflection is found experimentally in oxide growth curves as the monolayer level OH or O coverage[5,6,24,200] is attained and exceeded. Examinations of the formation of thicker oxide films at noble metal surfaces have usually found direct logarithmic[21-31] or inverse logarithmic[32-38] growth laws, which have been described earlier. The disagreement over the the kinetics for the growth of noble metal surface oxides is partially due to the fact that oxide growth must be examined over 4 to 5 decades in time in order to distinguish between logarithmic and inverse logarithmic kinetics. In addition, it does not seem reasonable that thin noble metal oxide films, especially those less than a monolayer in extent, are insulating as is the basis of the model for high-field, inverse logarithmic film growth. Work of this kind has been extensively reviewed elsewhere[3,11,17-21].

Damjanović[35-38,201] found "inverse" logararithmic kinetics for oxide growth at Pt electrodes over a wide range of pH, using galvanostatic and other techniques. At low pH, growth was not found to depend on pH, but for pH > 12, growth increased linearly with pH[201]. This indicates that the mechanism of growth of surface oxide at Pt in alkaline solutions is different for that in acid. Ord and Ho[34] also found inverse logarithmic kinetics. Experimentally, Vetter and Schultze found "direct" logarithmic kinetics for up to 5 decades of time and three layers of O species for potentiostatic growth of surface oxide at Pt[25] and Au[32]. They also used a high-field model in an attempt to interpret the kinetics of these processes even though their data could not be fitted to the predictions of that model.

The growth of the initial monolayer (2e / surface Au atom) had been extensively investigated by Barnett in this laboratory[5,6] by using potentiostatic holding experiments at several growth potentials and in several

electrolyte solutions. Generally, an initial non-logarithmic growth region, followed by two direct logarithmic growth regions in time, were found. The initial non-logarithmic growth was thought to follow a log(1-θ) vs t relation, which could be explained by the electrochemically controlled adsorption of O with a two electron transfer:

$$Au + H_2O \rightarrow AuO_{ads.} + 2\,H^+ + 2e \qquad (1.9.)$$

The logarithmic growth behavior is thought to correspond to growth of the monolayer by the place-exchange mechanism, since those oxygen species reduced in the OC3 peak seem to be associated with this type of growth. Direct logarithmic growth of surface oxide at sub-monolayer levels of coverage was also found at Pt electrodes[25,26].

Barnett also examined the formation of oxide films on gold, greater than a monolayer in thickness, by cycling to very anodic potential limits, and he also performed "aging" experiments of the type described in Section 1.3.3.[6]. It was found that the potential of the OC3 peak shifts to less positive values and becomes narrower as the coverage by oxygen species (thickness of the film) at the surface increases, indicating that the surface oxide becomes more stable with respect to reduction though a time and potential-dependent restructuring process. This process continues as multilayer oxide formation is developed to $Q > 400\ \mu C\ cm^{-2}$. For high extents of oxidation, where this process approaches bulk oxide formation, the surface oxide is reduced in a single peak, OC4. In alkaline solution, an additional peak negative to OC2 is found during aging experiments at high coverages. Under some aging conditions, where the actual charge due to surface oxide is increased very little, it is possible to increase the charge of the OC2 peak at the expense of that for the OC3 peak. These changes were considered to be the result of time-dependent changes in the structure of the surface oxide, such as place-exchange. Similar results for aging experiments were found by Arvia et al.[61,63] and Burke et al.[66-69];

however, Arvia attributed these changes to stepwise oxidation processes and Burke to the formation a porous "hydrous" oxide, similar to those observed at Ir and Ru.

Thicker anodic films on Au are found by XPS to be in oxidation state III[123,202]; however, there is some controversy as to the actual composition of such oxide films. Different researchers have suggested that they may be anhydrous Au_2O_3[28,32,91,203], hydrated Au_2O_3[57,66], AuOOH[204-206], and $Au(OH)_3$[66,202,207]. In some of these studies, the electrode surface was examined in high vacuum, and, in such experiments, the oxide may have changed after emersion from the electrolyte.

1.4.7. Monolayer Oxide Formation in the Gas Phase

The interaction of gaseous oxygen with some metals parallels the electrochemical surface oxide formation in that both reversibly chemisorbed oxygen at the surface and place-exchanged surface oxide are found. This is especially true of the Group VIII transition metals: Ni, Pt, Pd, Rh, Ir and Ru[208]. At low temperatures, oxygen merely chemisorbs reversibly but, at higher temperatures, the oxygen binds very strongly and irreversibly at the metal surface in a state more like that of a bulk oxide than chemisorbed oxygen[209,210]. In some cases, the oxygen may be under metal atoms at the surface and form more than one monolayer of surface oxide or even an epitaxial metal oxide film. The temperature at which the surface oxide forms depends upon the paticular metal, for example Ni forms a surface oxide at much lower temperature than Pt[210].

Experimental evidence from the literature, clearly contrasting the two very different states of oxygen found at Pt surfaces, has been summarized by Niehus and Comsa[211], and an abbreviated version of their classification is given in Table 1.1.

Table 1.1.

A Comparison of Chemisorbed Oxygen and Surface Oxide at Pt

	Chemisorbed Oxygen	Surface Oxide
Formed by exposure to O_2 at	< 800 K	> 800 K
Desorption	begins at 550 K; complete at 1000 K	decomposes at 1200 K
Reaction with CO and H_2	at room temperature	none
Binding energy of CO and H_2 w.r.t. clean Pt	same	greater
Catalytic activity w.r.t. clean Pt	same	generally greater
Auger oxygen signals	496 & 517 eV	491 & 511 eV
Work function change w.r.t. clean Pt	+ 0.5 eV	- 1.0 eV

The change of reactivity of H_2 and CO with respect to the two types of oxygen species at the Pt surface[212,215] indicates a difference in their chemical nature. Similarly, reversibly electrosorbed oxygen species at Pt electrodes are also found to be more reactive towards the electro-oxidation of small molecules than oxygen species which have been place-exchanged[137]. The Auger shift of 5 to 6 eV indicates that there is a difference in the valence (oxidation state) of oxygen between the two states[212]. The difference in work function change with respect to clean Pt [213,216,217] indicates a difference in the orientation of the metal-oxygen dipole at the surface and that place-exchange has occurred in surface oxide formation.

At single-crystal surfaces, the chemisorbed oxygen has been shown by LEED to form ordered superlattices[218], just as has been proposed for electrosorbed oxygen species at electrode surfaces[53]. The surface oxide also forms superlattices, and epitaxial film growth is found as well[208,214]. Oxygen has been shown to be chemisorbed more readily at kink and step sites on Pt surfaces than

at the principal index planes, where adsorption is very slow[215,219-221].

Unlike Pt, oxygen forms only chemisorbed monolayers at single-crystal Au surfaces in the gas phase[222]. Although older work reported thicker Au_2O_3 films[223,224], more recent work using much improved experimental techniques indicates that only monolayer-type surface oxide is formed via dissociative adsorption of oxygen at gold surfaces[225-227] and, in some work, no dissociative adsorption of oxygen was found on clean Au surfaces at all[228]. These results are quite different from those found for the electrochemical oxidation of gold, where large hysteresis arises between surface oxide formation and reduction, indicating place-exchange. Of course, in the electrochemical case, a variable driving force for the oxidation of Au is provided, different from the affinity change available in the spontaneous oxidation from molecular oxygen. It has also been found that the dissociative adsorption of oxygen at Au is highly activated, occuring only at temperatures above 373 K[208], but may be catalyzed by kinks or steps[229], or Ca[230,231] and Si[232,233] impurities at the surface. Water vapor may also react dissociatively with the gold surface to give chemisorbed oxygen and hydrogen[227].

1.5. New Areas of Work Required

The brief review given above indicates that there have been a number of experimental studies of surface oxide formation at gold in the past. However, there are still important areas where new work, or extensions of previous work in this laboratory, needs to be carried out. For example, the kinetics of anion adsorption in the absence of mass transport effects has not been properly examined. The effect of temperature on the kinetics of anion adsorption, surface oxide formation and place-exchange has not been thoroughly studied. It has been shown recently that electrochemical measurements can be made in frozen $HClO_4 \cdot 5.5\ H_2O$[234], in which the proton has been found to be surprisingly mobile. This means noble metal surface oxide formation processes may be examined in a

range of temperatures between 150 and 360 K.

Recent work suggests that more detailed and revealing information concerning the initial stages of surface oxide may be obtained using single-crystal surfaces rather than polycrystalline ones, as has generally been done in the past. Much of the previous work done using single-crystals has been marred by insufficient care in surface preparation and/or solution and cell cleanliness; however, better experiments have been made in the past few years. A careful examination of gold single-crystal surfaces in alkaline solutions has yet to be made.

The introduction of new scientific instrumentation and improved techniques always suggests new areas for research which were not previously possible. The recent introduction of digital data acquisition and manipulation, especially using digital oscilloscopes, allows the precise measurement of very small coverages of electrosorbed species during rapid potential sweeps which were not possible previously using analog equipment. Since some of the species formed in the earliest stages of surface oxide formation are very short lived (< 10 ms), new information about these processes should be obtained, as has been done in the present work. Very recently, advances in spectroscopy, particularly Fourier-transform infrared spectroscopy, have been made, which will facilitate in-situ measurements during electrochemical experiments. It may be anticipated that this will allow more direct characterization of the bonding of oxygen species, anions and adsorbed water molecules found before and during the initial stages of surface oxide formation, giving useful information complementary to data derived from purely electrochemical measurements.

CHAPTER II

AIMS OF THE EXPERIMENTS

Before describing the experimental procedures used and the results of the experiments, it is desirable to give a summary of the aims of the work. This is because the choice of experimental techniques and the conditions used, as well as the chemical choice of systems to be studied, depend very much on what type of information is required in the program of work. Accordingly, the principal aims of the work are summarized below.

1. To characterize the relation between distinguishable processes in the anodic oxidation of Au (over an appropriate potential range) and corresponding processes of oxide redution in the cathodic sweep.

2. To establish the conjugate effects of potential and time in the successive processes.

3. To evaluate the role of anions in the surface oxidation processes, as observed by the manifestation of their effects through the I vs E profiles. Two oxyanions, ClO_4^- and SO_4^{2-} (HSO_4^-), and a monatomic anion, F^-, were investigated.

4. To evaluate, on a new scale of much improved sensitivity, the very initial stages of suface oxidation of Au.

5. From the results of (4), to evaluate the conversion in time of the distinguishable states of the oxidation of the surface below 20 % θ_O (two electrons per metal atom site), with the possiblity of evaluating the kinetics of this process.

6. To examine the role of anions in the formation of those interconvertible species and evaluate the kinetics involved.

7. In relation to (6), to establish how the distinguishable states are influenced by temperature and to include the effect of temperature on the interconversion rates.

8. To establish the "growth laws" in time for the development of oxide films at low coverage and higher coverage (log t):

   a) for the two types of anions;

   and

   b) as a function of temperature;

   in terms of possible mechanisms.

9. To compare, by means of an appropriate potential program, the behavior of the distinguishable stages of surface oxidation, as manifested in the reduction I vs E profiles, with and without strongly adsorbed anions ($SO_4^=$) present on the surface.

10. To relate the oxidationbehavior to the two type of anions to the double-layer charging profile as a function of potential, prior to Au surface oxidation.

11. To compare Au surface roughening during rapid potential cycling in 0.5 M H_2SO_4 and 1 M $HClO_4$, and thus to determine at what potential and corresponding stage in surface oxide formation this roughening process begins.

CHAPTER III

EXPERIMENTAL PROCEDURES

3.1. Choice of Methods

Because the initial stage of electrochemical oxidation of gold and some other noble metals is a 2-dimensional surface process, it can only be effectively examined using non-steady state electrochemical techniques, analogous to thermal desorption spectroscopy and similar procedures in gas phase surface studies[235]. In the present work, the potentiodynamic sweep method[47] was used for almost all the electrochemical studies. This technique is exceptionally well suited to surface studies, in that it provides a powerful method for distinguishing different states of adsorption at an electrode surface and allows the examination of the energetics and kinetics of these processes with high sensitivity and/or reduction of the processes involved. Complex potential-time programs, with one or more single potential arrests, were often used to facilitate the study of the kinetics of submonolayer surface oxide formation and the effect of anions upon this process at the gold electrode.

As in ultra-high-vacuum gas phase studies, cleanliness is critical to electrochemical surface studies, especially those involving gold or platinum. Therefore, it is necessary that special care be taken in preparing cells, electrodes and solutions for this type of experiment[6], because organic impurities or undesired traces of strongly adsorbed anions can easily block sensitive surface processes. These aspects were therefore emphasized in the present work and involved demanding requirements in the careful execution of most of the experiments.

3.2. Electrodes

Working, counter and internal reference electrodes were prepared from 99.999% pure, Johnson Matthey "Spectapure" gold wire having a diameter of

0.5 mm. Initially, the wire was degreased in refluxing acetone in a Soxhlet extractor. A 50 to 70 mm piece of the clean wire was welded to a longer piece of silver wire and sealed in a 6 mm O.D., lead free, soft-glass tube, approximately 280 mm long. The cleaned wire was handled only by means of cleaned Pt tipped forceps. 10 to 30 mm of the gold wire was left exposed, and the gold-silver contact was well above the glass seal. The soft-glass tube was cleaned in concentrated CrO_3-H_2SO_4 solution, rinsed with doubly-distilled water, then completely dried before the electrode was sealed. The finished electrode was stored in concentrated H_2SO_4.

Soft-glass/gold seals are fragile because of the difference in the thermal expansion behaviour of the two materials. For this reason, a drop of "Araldite" epoxy was placed just behind the glass seal to reinforce it. Well cured "Araldite" epoxy, when directly exposed to 1 M $HClO_4$, did not significantly contaminate the solution with respect to the electrochemical behaviour of gold. The electrodes with an additional "Araldite" seal introduced no more impurities into the solution and were much less likely to leak than electrodes without this extra reinforcement. A leaky seal at a gold electrode leads to serious time dependent distortion of voltammograms.

To provide a relatively large surface area of the counter electrode, a 1 cm^2 piece of 99.999% pure gold sheet was spot welded to a gold wire electrode. This electrode was then etched briefly in aqua regia.

For all experiments, the reference electrodes were platinized platinum hydrogen electrodes in the same solution as the working electrode, but maintained in a separate compartment of the cell. All potentials reported in this thesis are given with respect to this electrode in the same solution. For convenience, this potential scale is called "E_H".

Although monolayer surface processes are associated with very small charges (less than 400 $\mu C\ cm^{-2}$), quite high currents are generated during

rapid potentiodynamic sweep experiments when sweep rates are greater than 1 V s^{-1}. This can give rise to significant ohmic drop errors between the working electrode and the Luggin capillary of the H_2 reference electrode[6], despite the relatively low solution resistance between them (ca. 1 ohm in 0.5 M H_2SO_4). Also, the much higher impedance of the stopcock between this reference electrode and the Luggin capillary can cause feed-back problems at higher sweep rates in the potentiostatic circuit, producing significant potential oscillations (electronic ringing). These problems were alleviated by using an internal reference electrode during experiments involving fast sweep rates. A gold wire electrode in the cell's working compartment was used for this purpose. It was possible to place this internal reference electrode very close to the working electrode. Even though this type of electrode does not have a reversible potential associated with it, it maintained a constant potential to within ± 1 mV over periods of several minutes during the experiments. The potential of this internal reference was constantly monitored against the external H_2 electrode during experimentation, so that the potential of the working electrode was always indirectly and accurately measured against the E_H scale. This is important as quite fine differences of potentials of current-potential peaks for various processes of Au oxide film formation and reduction are significant and measurable.

Electrodes used in HF and KHF_2 electrolyte could not be sealed in soft-glass, since these solutions readily attack glass. For experiments involving HF or KHF_2, a special triple electrode assembly was made from Teflon (Figure 3.1.) which included the working, counter and internal reference electrodes all together. A TFE Teflon sleeve was made with three 0.45 mm holes drilled in it. Degreased pieces of 0.5 mm diameter, Johnson Matthey "Spectrapure" gold wire, welded to silver leads, were force-fitted into the three holes, with the wires extending a few mm beyond the Teflon-gold seals. 1/16" O.D. FEP Teflon tubes

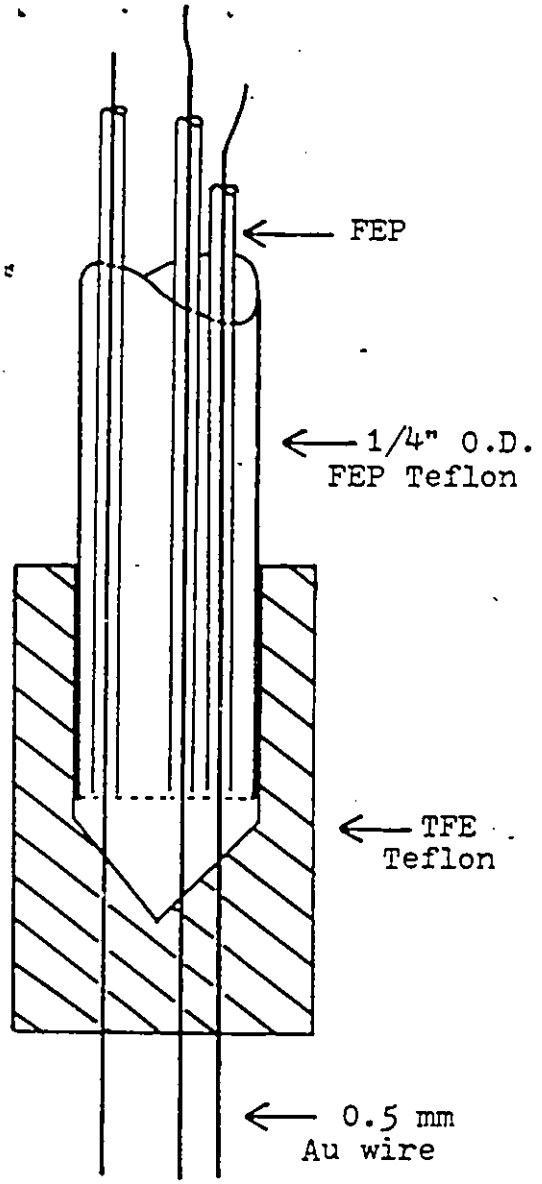

Figure 3.1. Teflon triple electrode assembly employed in studies in aq. HF and KHF_2.

were fitted over the leads behind the seals to insulate them electrically. The sleeve was fitted over a short 1/4" O.D. FEP Teflon tube.

The platinum electrode used for the H_2 reference in HF and KHF_2 solutions consisted simply of a piece of platinized platinum gauze attached to a platinum wire lead (Figure 3.3.).

3.3. Cells for the Electrochemical Experiments

It has been found that simplifying the cell design can significantly reduce the amount of impurities in solution, which could poison the gold electrode surface[6]. This is mainly because such a cell can be more conveniently and effectively cleaned than a complicated one with several stopcocks and joints. It is important that the ratio of glass surface area to solution volume is minimized and solution contact with ground glass joints is avoided in experimental cells. Also, small simple cells require smaller quantities of purified water for cleaning and rinsing, and less volume of the required electrolyte solutions. This is important because of the complicated cell cleaning procedures necessary in these experiments, requiring several rinses with pyrocatalytically distilled[236] water. The cell and attached reference electrode system, shown in Figure 3.2., represents an attempt to optimize these design criteria. This glass cell was used for all work carried out in H_2SO_4 and $HClO_4$ electrolytes.

For experiments done in HF and KHF_2, it was necessary to design a small, easily cleaned cell not made of glass. It was found that TFE Teflon was not a good material to use for this purpose, even though, chemically, it is very inert and itself will not contaminate the test solution. However, it is a very porous material, and therefore difficult to clean, as illustrated in the following section. Leaching of H_2SO_4, used in cleaning, from the cell walls was a major problem because fluoride does not adsorb as strongly as sulfate ion. High density polypropylene was found to be easier to clean and introduced

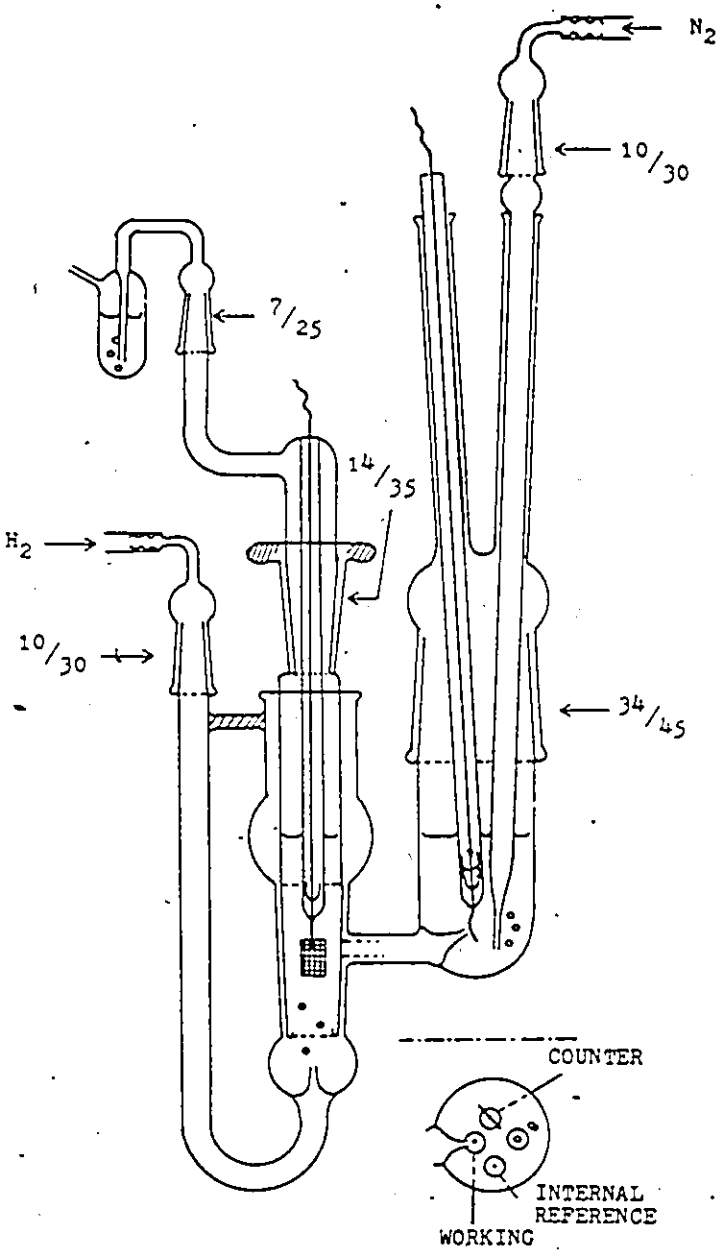

Figure 3.2. Glass experimental cell.

less impurities into the electrolyte than TFE Teflon. Polypropylene is less chemically inert, than Teflon; however, it is stable towards H_2SO_4 and HF. Polypropylene is also relatively inexpensive and available in many forms.

A small cell and reference electrode assembly for work in HF and KHF_2 was fabricated from two 30 cm^3 "Nalgene" polypropylene bottles (Figure 3.3.). The gas inlets and outlets, and the electrolyte connection between the main cell and reference electrode bottles, was made of 1/16" O.D. FEP Teflon tubing.

3.4. Difficulties in Cleaning Teflon Experimental Cells

Originally a large, conventional, TFE Teflon cell was used for measurements in HF and KHF_2 solutions, and was similar to those generally used for electrochemical experiments in solutions containing F^- or alkaline solutions. However, when tested with 1 M $HClO_4$ as the electrolyte, in which the behavior of gold electrodes is well established[6], this cell was found to be unsatisfactory for measurements of surface oxide formation on Au, which are highly sensitive to the presence of SO_4^- and organic impurities. This problem arises because the a Teflon cell is difficult to clean properly. Teflon is a very porous material, analogous to a sponge, and will adsorb or even absorb H_2SO_4 (used during the cleaning of the cell), and particularly organic impurities. Even after repeated rinsing, SO_4^- continued to be leached from the cell walls, evidence for which will be shown later. It is impossible to boil or steam such a cell in order to remove SO_4^-, because Teflon becomes deformed at this temperature, and the cell would become leaky when reassembled.

Cyclic-voltammetry measurements at gold electrodes in 1 M $HClO_4$, which had already previously been studied[6,7], gave consistently unsatisfactory results in the Teflon cell despite the rigorous cleaning procedures employed (Figure 3.4.). Figure 3.4.a. shows the cyclic-voltammogram obtained for this system at a sweep rate of 0.05 V s^{-1} and at room temperature. The Teflon cell had been soaked in concentrated H_2SO_4 for several hours, rinsed ten times with

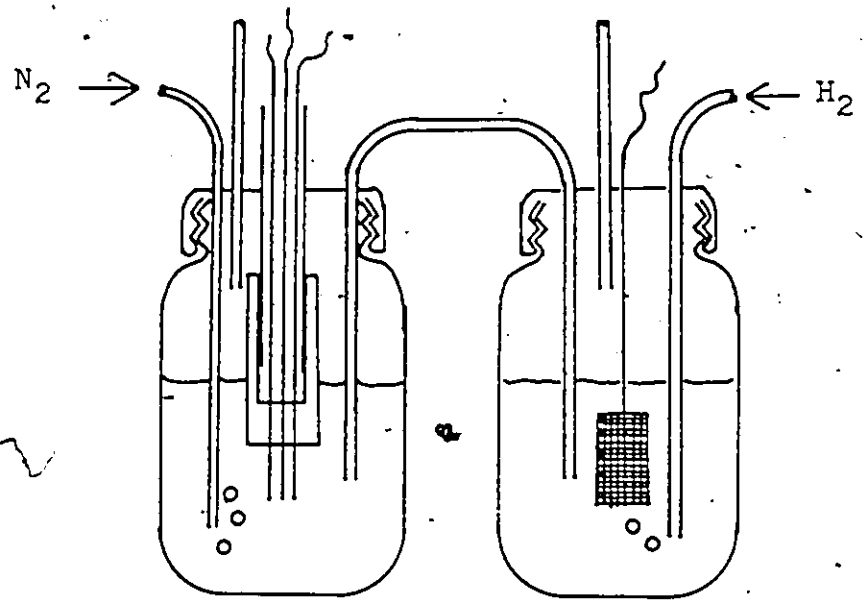

Figure 3.3. Experimental cell for studies in aq. HF and KHF_2, made of two "Nalgene" high density polypropylene 30 ml bottles.

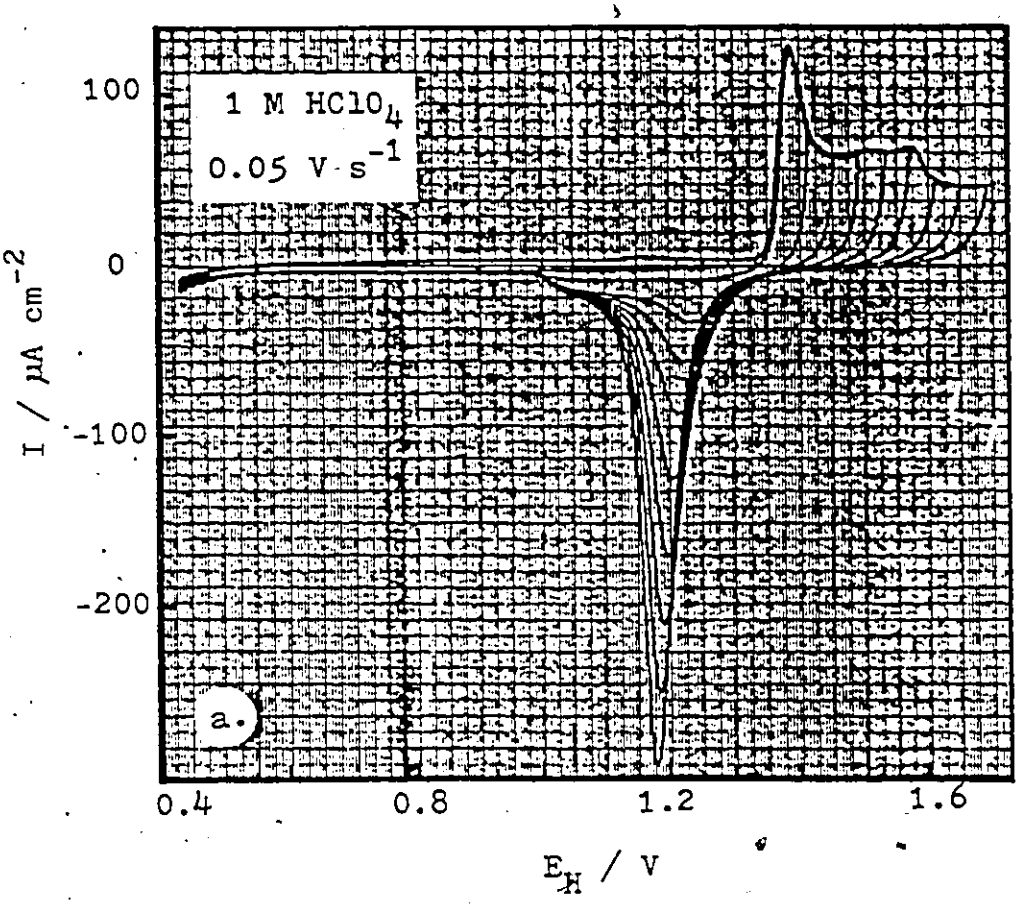

Figure 3.4. Potentiodynamic I vs E profiles for Au at 0.050 V s^{-1} in 1 M $HClO_4$ in a large Teflon cell showing H_2SO_4 contamination even after extensive cleaning procedures.

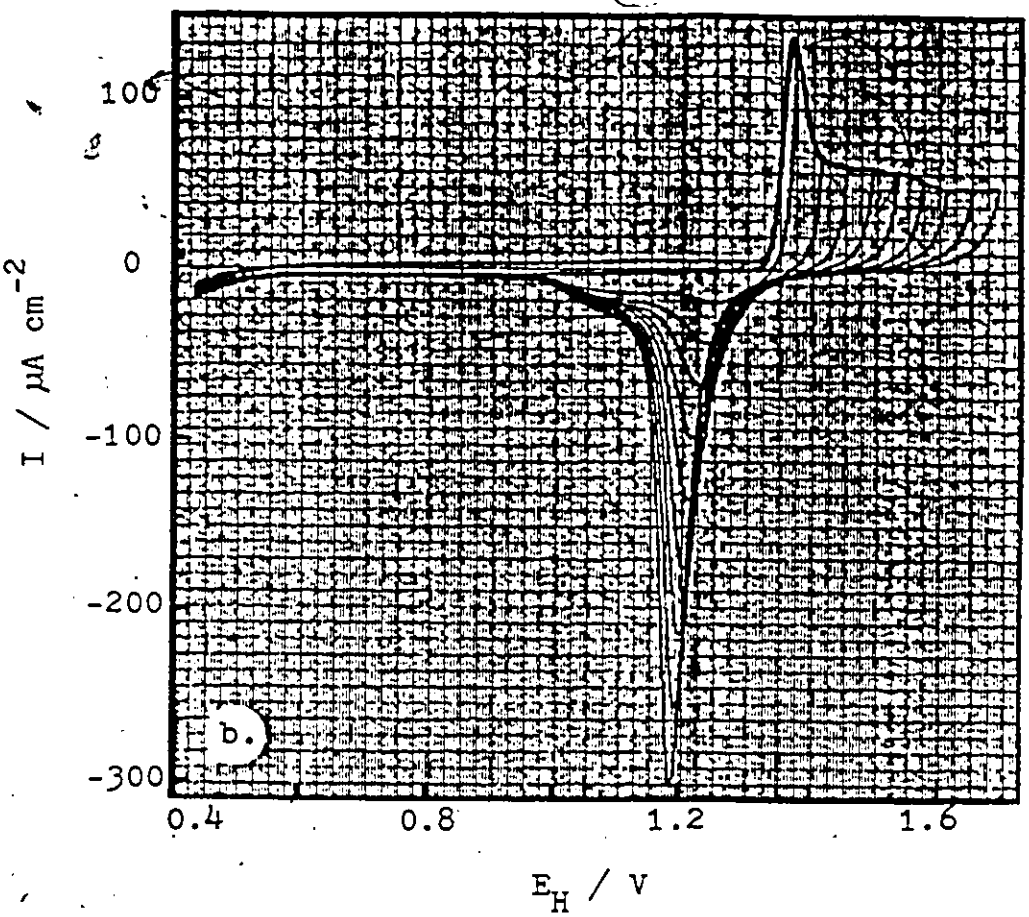
100
0
-100
-200
-300
I / μA cm^{-2}
b.
0.4
0.8
1.2
1.6
E_H / V

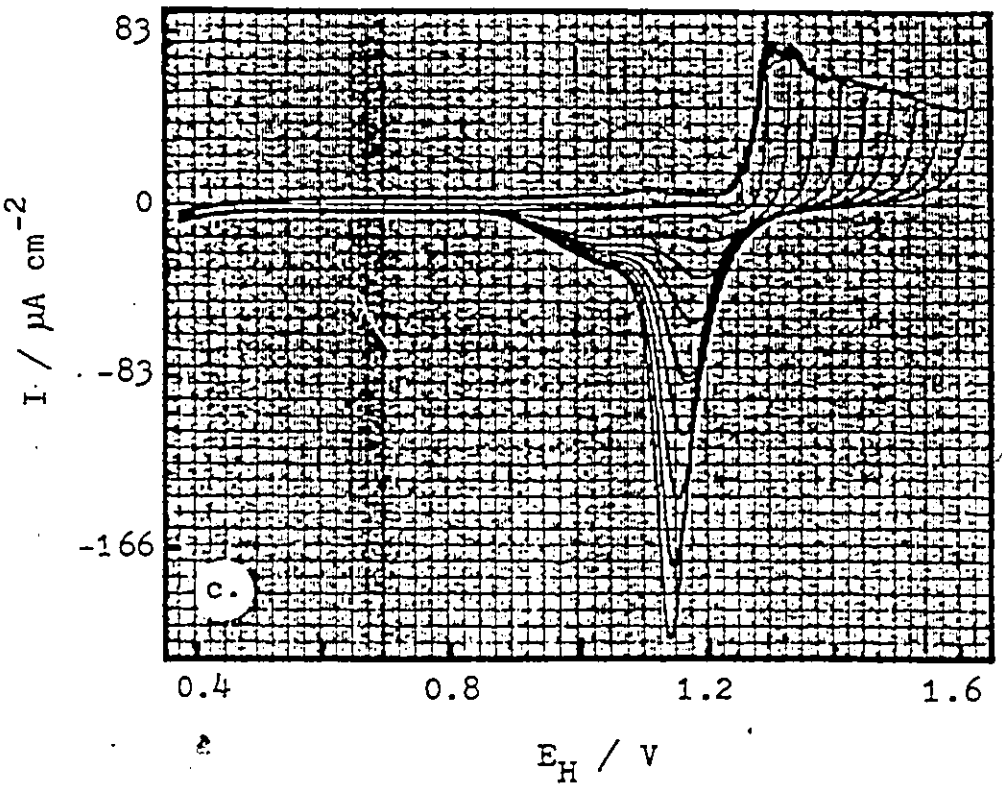
83
0
-83
-166
I / μA cm^{-2}
c.
0.4
0.8
1.2
1.6
E_H / V

doubly distilled water and twice with hot pyrocatalytically distilled water[236] before it was filled with the electrolyte used in the measurements. The initial surface oxide formation peak for 1 M $HClO_4$ (with H_2SO_4 contamination) then arose at 1.388 V, which is far more anodic than the first peak found in a properly prepared and cleaned Au / 1 M $HClO_4$ system, with a potential of 1.332 V (Figure 4.1.1.). The small hump in the anodic sweep at 1.17 V also indicates the presence of traces of oxidizable organic impurities. The electrolyte in the cell was then discarded and, using doubly distilled water, the cell was again rinsed ten times, soaked for twelve hours, rinsed ten times more, soaked for three hours, and finally rinsed twice with hot and ten times with room-temperature double distilled water. After this elaborate cleaning procedure, the traces of organic impurities were eliminated but the traces of SO_4^- were not (Figure 3.4.b.). The cell was then soaked for an additional twelve hours in doubly distilled water and rinsed again ten times afterwards. After this treatment, the cell was initially free of organic impurities and SO_4^-, but after less than an hour, results showed that both impurities had reappeared in the electrolyte solution (Figure 3.4.c.). The cyclic voltammogram shows two initial peaks at 1.348 V and 1.382 V, indicating a very small concentration (10^{-7} - 10^{-8} M) of SO_4^- in the electrolyte, since the less anodic peak is only partly displaced by the anion[6]. Since satisfactory results could not be obtained, despite extremely careful cleaning of the cell, it was concluded that Teflon is a poor material for fabrication of cells for use in electrochemical investigations of sensitive surface processes, e.g. as at gold.

3.5. Water Purification

In order to prevent blocking of the surface processes on gold and other noble metal electrodes by organic impurities, it is necessary to use extremely pure water for solution preparation and cleaning purposes. It was found in this laboratory that some organic impurities are not completely removed from

water twice distilled, the second time from alkaline $KMnO_4$. However, pyrocatalytic distillation does produce sufficiently pure water for electrochemical surface studies.

In pyrocatalytic distillation, water vapour and oxygen are passed over a Pt/Rh catalyst at 1050 K, which oxidizes any organic impurities. This process has been described in detail elsewhere [7,236,237] in earlier papers from this laboratory.

All water used for solution preparation and rinsing cells and electrodes during this work was first distilled from city water, then from alkaline $KMnO_4$, pyrodistilled and given a final simple distillation from a glass still attached to the pyrostill apparatus. This latter procedure is desirable for work with gold electrodes in order to ensure that no hydrothermally distilled Pt species are present in the final water for solution preparation.

3.6. Solution Preparation

BDH "Aristar" grade $HClO_4$, H_2SO_4 and HF were employed, without further purification, to make experimental solutions. The limits of impurities in these acids are specified by the manufacturer to be less than 1 ppm. In previous work, the purity levels of this grade of acids was found to be satisfactory. Pyrodistilled water was always used as the solvent. All experimental solutions were deoxygenated by slow bubbling of purified N_2 through them for 30 minutes in the cell before experimental measurements were commenced.

3.7. Gas Puification

The N_2 used to deoxygenate solutions was purified in a conventional gas train[238]. It consisted of BDH type 4A molecular sieves, $Mg(ClO_4)$ drying agent, Cu turnings at ca. 723 K to remove oxygen and three traps cooled in liquid N_2, two of these containing activated charcoal. The Cu turnings were regenerated, when needed, by heating them in purified H_2. H_2 gas for the reference

electrode was purified in a gas train similar to the N_2 one, except that it had a palladized on asbestos section at 623 K in addition to copper turnings[138,238]. For experimental temperatures above 300 K, the gases were also passed through presaturators containing the same solution at the same temperature as that in the cell, so that the solution examined would not change concentration due to evaporation during the program of experiments.

3.8. Cleaning Procedures

The all-glass cells were initially soaked in concentrated CrO_3-H_2SO_4 solution for at least 12 hours. They were then rinsed several times with doubly-distilled water and refilled with fresh concentrated H_2SO_4. Before starting experiments, the acid was poured out and the cell was rinsed 10 - 12 times with pyrodistilled water. Before experiments where traces of H_2SO_4 were undesired, the cell was also rinsed twice with hot pyrodistilled water. The cell was then rinsed with the experimental solution and set up in a glove bag. This time consuming but unavoidable procedure was repeated before all sets of experiments.

Electrodes, presaturators and all glassware used for solution preparation were cleaned in a similar way to that for the cells.

Teflon and polypropylene cells, and other apparatus for use with HF and KHF_2 solutions, was cleaned by soaking for a few hours in concentrated H_2SO_4 only, followed by extensive rinsing several times with pyrodistilled water followed by soaking for one day in pyrodistilled water.

3.9. Temperature Control

Experiments at ca. 273 K were performed by immersing the cell and the reference electrode in a crushed ice bath in a Dewar flask. Experiments at temperatures between 274 and 364 K were obtained by immersing the cell and reference electrode in a Colora NB-32781 thermostated water bath.

3.10. Electrical Circuitry

The basic electrical circuit for potentiodynamic measurements used during this work is shown in Figure 3.5. A high output voltage Wenking electronic potentiostat was used to control the potential of the working electrode according to a program set by a Tacussel GSATP function generator.

The Tacussel function generator is quite versatile and can be programmed to supply complex potential-time functions with up to eight different potentiodynamic sweeps and single stage holdings of potential for times from 0.0001 to 10 s. These complex potential-time programs greatly facilitate electrochemical surface studies, especially those sensitive to anion adsorption, as in the case of experiments at gold. Because several different complex potential functions were used during this work, their forms will be included with the respective results for continuity in the presentation.

The potential of the working electrode was measured with respect to the H_2 reference electrode by means of a Cimron DMM 15 multimeter, with the signal sometimes passed first through a Tektronix Type O operational amplifier acting as a cathode follower. Currents passed between the working electrode and the counter electrode were measured, as a potential, across a Leeds and Northrup 4755 precision decade resistance box. Current vs potential data were recorded on a Hewlett-Packard Moseley model 7001 AM X-Y recorder, on a Hewlett-Packard 181 A storage oscilloscope or on a Nicolet model 2090 III digital oscilloscope, with a built-in flexible disk drive.

Digital oscilloscopes have many advantages over conventional analog oscilloscopes. The data collected are more precise than those obtained on analog instruments. This allows accurate measurements to be made of the very small charges associated with submonolayer coverages of less than 1% which are not possible otherwise. Digital data are in many ways easier to handle than analog data. For example, it is easier to obtain accurate peak potentials from

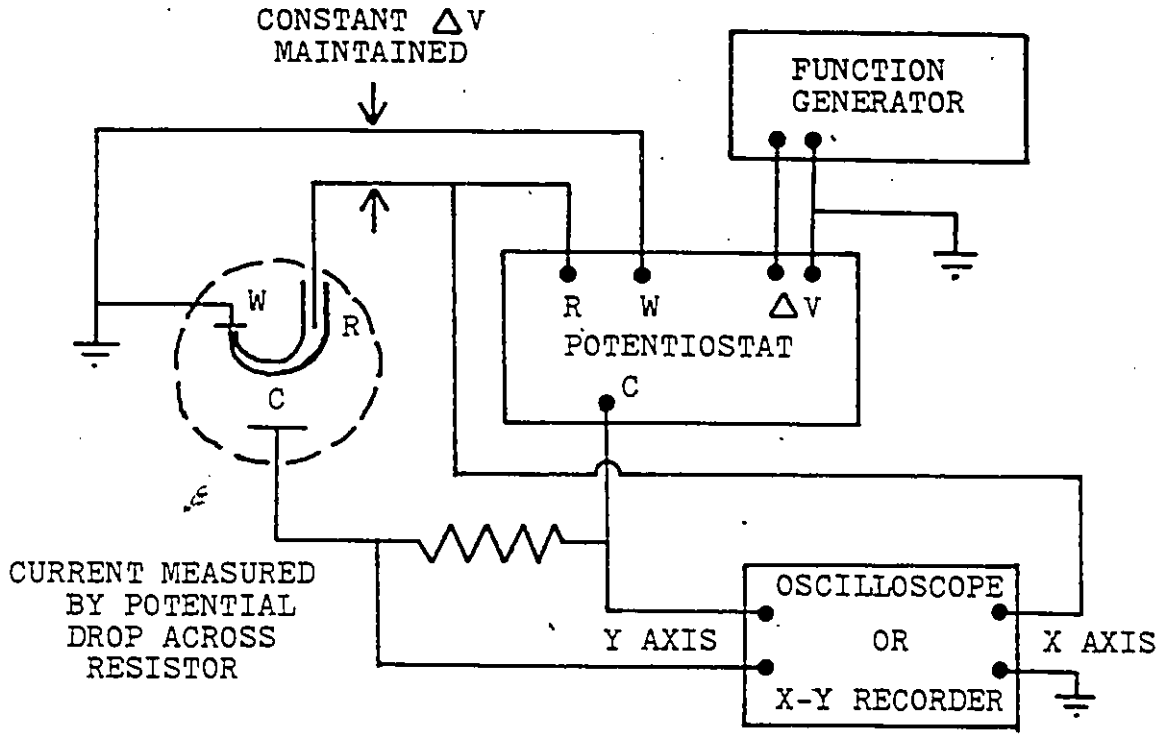

Figure 3.5. Electrical circuitry employed in potentiodynamic sweep studies.

digital data than from a Polaroid oscilloscope photograph. The data may also be easily transferred into a computer for further analysis and processing. Finally, these oscilloscopes have "pretriggering" facilities, which allow data collection **before** or after the instrument is triggered.

3.11. Computer Aspects

Extensive work pertaining to the use of computers for various electrochemical applications has been done in this laboratory[239-241]. Although nothing especially original concerning the use of computers was developed during this work, a Digital PDP 11/34 mainframe computer was used extensively to analyze data obtained via the Nicolet oscilloscope. Various FORTRAN and MACRO programs used for these operations are included in Appendix I. Many of these programs are modifications of programs previously written by D.F. Tessier and D.A. Harrington in this laboratory, or utilize subroutine packages written by them.

Data were transferred from the oscilloscope to the computer by means of a Nicolet 2082 RS-232C interface connected between the computer and the VT-55 terminal. The current vs potential data were then stored on 8 inch flexible diskettes. Coverage information was obtained by using the computer to integrate the current data in the files with respect to time, subtracting appropriate double-layer charging data. Hard copies of I-V profiles were produced by outputting the data via an RS-232 interface to a Hewlett-Packard 7470 A digital plotter.

3.12. Electrode Area Determination

It is not possible to determine accurately the **real** surface area of an electrode from its geometric area because of its surface roughness. On Pt and some other noble metals, a monolayer of H atoms is electrodeposited[242,243] already before the H_2 reversible potential, allowing an easy determination of real area. However, electrodeposition of H does not occur on Au[6,244], so this

method is not applicable.

However, an effective method of determining the areas of gold using the discharge of O species was developed by Michri, Pshchenichnikov and Burshtein[245]. They found that the charge due to surface oxidation of gold below the potential of the current minimum in the cyclic-voltammagram just before significant O_2 evolution currents arise in 0.5 M H_2SO_4 corresponded to discharge of 2 electrons per surface Au atom, corresponding to a monolayer coverage of O species or 400 $\mu C\ cm^{-2}$. These authors calibrated the areas of their electrodes using B.E.T. measurements and showed that their electrochemical method was valid over a range of temperatures and sweep rates, as later verified in this laboratory[7]. The method is also valid for oxidation of gold in media other than H_2SO_4, where a current minimum can also be observed in the cyclic-voltammogram before O_2 evolution.

In this way, the real areas of the gold electrodes were calculated by integrating (weighing paper or using the computer method) the cyclic-voltammogram up to the "Burshtein minimum" and then obtaining the "Burshtein charge", Q_B, less an estimated amount due to double-layer charging. Dividing this charge by 400 $\mu C\ cm^{-2}$ then gave the required real area.

CHAPTER IV

RESULTS AND DISCUSSION

4.1. General Aspects of Surface Oxide Formation at Gold and the Role of Anion Adsorption

As was mentioned in the introduction, formation of the first monolayer of surface oxide at Au electrodes is a complex process, involving three to four distinguishable states of electrosorbed OH and O-species[5,6]. This process is also very sensitive to the nature of the anions adsorbed at the electrode surface[5-7,60,191-195].

In order to facilitate the description and understanding of the results to be given in the material which follows, a general outline of the current ideas on the sequential steps in the surface oxidation of Au is necessary here. Some of these ideas were developed in earlier work in this laboratory, as will be exemplified by reference to several typical potentiodynamic I vs E profiles, also recorded in the present work. Particular attention will be given to the influence of anions upon surface oxide formation in its very early stages at low coverage by OH or O species. It should be mentioned that cyclic-voltammetry measurements have previously been made in aq. H_2SO_4 and $HClO_4$ solutions[5-7], and some of those results have been included here only for the purpose of illustration of the behavior of Au in these solutions. Some of the results obtained in this earlier work are, however, not as accurate or as well resolved as those obtained in the present work using more modern equipment, in particular a Nicolet Explorer III digital oscilloscope.

The study of very low oxide coverages, down to 0.5 %, or less, of a monolayer, has been made possible by recent improvements in data acquisition and processing, using digital oscilloscopes and computers, through techniques developed in this laboratory, mainly in the course of the present work. The use of the digital oscilloscope was essential in order to obtain

the · the very precise data needed to study the earliest stages of surface oxide formation, especially those corresponding to coverages of less than 1 % of a monolayer. The digital oscilloscope also greatly facilitated data collection during the variety of complex potential-time programs used during the course of the present work. The acquired data could also be processed better using a mini-computer.

4.1.1. Reversible Processes and Hysterisis in Formation and Reduction of Surface Oxide Formation at Gold

The main feature of an I vs E profile for formation and reduction of surface oxide species at Au, as seen in Figure 4.1.1.a. for $HClO_4$ and in Figure 4.1.1.b. for H_2SO_4, made in each case to various end potentials, is the well known hysteresis between the oxidation peaks (denoted by OA) and reduction peaks (denoted by OC). Similar behavior is observed at most other noble metals. The OH species deposited on the surface of Au at certain potentials in the OA2-4 peaks (Figure 4.1.1.a.) undergo transformation in a surface reconstruction (turn-over) process into a pseudo-3-dimensional phase, the precursor to the 3-dimensional bulk phase. This form of surface oxide is reduced in the OC3 peak at much more negative potentials than those at which it was formed, indicating conversion to a more stable species. Because of the turn-over reconstruction process, which is relatively slow, the relative charges and peak currents associated with the anodic peaks are sensitive to changes in sweep-rate, temperature and the crystallograghic surface of the electrode. Two more broad and overlapping oxidation peaks (OA3 and OA4) arise at more positive potentials and are believed to be associated with oxidation of OH to O species in the film[5,6].

In the anodic direction of sweep, several stages of the surface oxidation process are resolved (this resolution is better at single-crystal surfaces of Au[194,195]), including firstly a reversible region observed at low coverages in

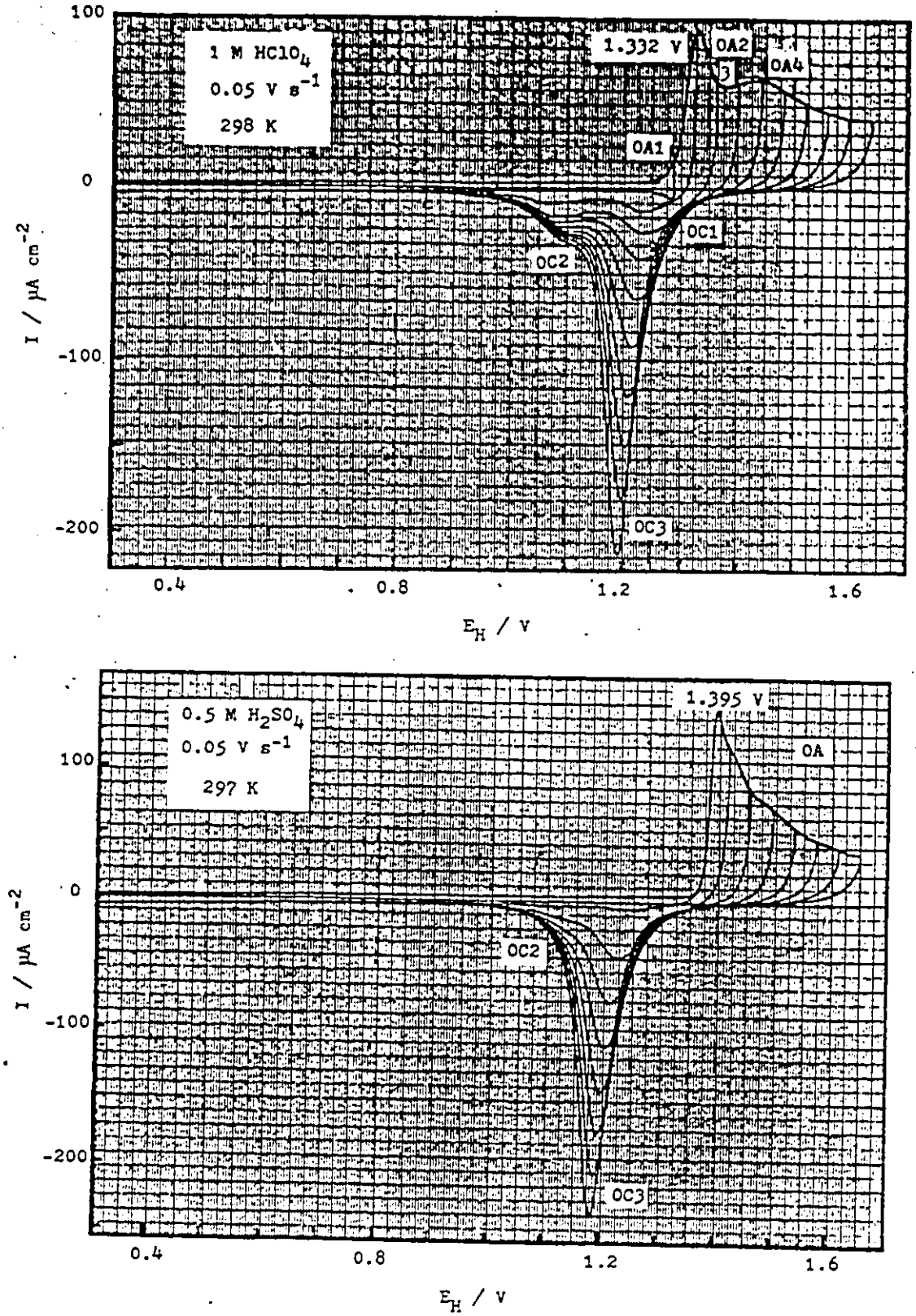

Figure 4.1.1. Potentiodynamic I vs E profiles for Au at 0.050 V s^{-1} taken to a series of anodic end potentials in

a. 1 M $HCLO_4$ at 298 K,

b. 0.5 M H_2SO_4 at 297 K.

$HClO_4$, as was also seen at Pt electrodes[53]. The stages of progressive surface oxidation, revealed in the anodic sweep, can be characterized by the behavior exhibited in corresponding peaks or shoulders in the cathodic sweeps, depending on the potential limit that is taken in the previous anodic sweep. The commencement of the anodic I vs E profile and the reversibility of the initial stage of oxidation depends very much on the chemical nature of anions in solution and their concentration[5,6,60,191-195], as will be emphasized below.

Three peaks are observed in the reduction profile under the conditions of Figure 4.1.1.a.: first the peak due to reduction of reversibly electrosorbed OH, designated OC1; the main reduction peak, CC3; and the most cathodic peak, OC2. For the first end potential of the anodic sweep, the reduction profile is almost the mirror image of the oxidation profile, which clearly indicates a reversible electrosorption of some O-species, most likely OH, at the Au electrode surface. In this respect, it bears a qualitative resemblance to an underpotential deposition (u.p.d.) process, such as H adsorption at Pt[242,243]. However, it is not possible, strictly speaking, to call this a u.p.d. process, without knowing the reversible potential "under" which the electrosorption occurs, as in H adsorption with respect to H_2 evolution at platinum. This potential for the initial stage of surface oxide formation is substantially less positive (by about 50 mV) than any that could be examined in 0.5 M H_2SO_4 to achieve a similar result (see Sections 4.3. and 4.4.). Although surface oxide will grow slowly in 0.5 M H_2SO_4 at potentials as low as 1.300 V, the OC1 reduction peak does not appear for oxidation potentials less than 1.380 V at room temperature. The OC1 peak in 1 M $HClO_4$, however, appears at oxide formation potentials as low as 1.280 V. This peak for reversible reduction has a potential of 1.285 V, which is about 90 mV less positive than the OC1 peak in H_2SO_4 under similar conditions (see Sections 4.3. and 4.4.).

For the second anodic end potential shown in Figure 4.1.1.a., a small

shoulder due to the OC1 reduction peak is seen, but most of the surface oxide formed is reduced at more negative potentials in other peaks. Following the sweep to the third end potential (1.365 V), no OC1 peak is distinguished and the surface oxide is reduced entirely in the OC3 and OC2 peaks. Finally, with further increase in the potentials of anodic sweeps, the OC3 peak continues to become larger. The same type of behavior is observed when the oxide film is grown at fixed potential for longer times[5,6] (potential "holding" experiments), as will be shown in Section 4.3.

The OC3 peak shifts cathodically and becomes narrower with increasing surface oxide formation charge, i.e. with the increase of end potential of the anodic sweep. This behavior is typical of that for a phase-type material.

The OC2 is smaller than the OC3 peak, and it can be seen that its potential does not shift with coverage and that it saturates in charge, i.e. it does not continue to grow as the OC3 peak does. This behavior is characteristic of a 2-dimensional surface species. The potentials of the OC3 and OC2 reduction peaks are much less positive than those of any of the oxidation peaks, corresponding to the well known hysteresis effect[5-7] exhibited in surface oxide formation and reduction at noble metals, including Au.

The effect of the strongly adsorbed anions in H_2SO_4 electrolyte[5,6], as opposed to weakly adsorbed ClO_4^- in $HClO_4$, can be clearly seen from a comparison of the series of sweeps in Figure 4.1.1.b. with that in Figure 4.1.1.a. The apparent onset of surface oxidation and the first large current maximum (the OA2 peak) arise at more positive potentials in the presence of strongly adsorbed anions. The position of the OA2 peak can be used, in fact, as an indication of the strength of adsorption of anions when other parameters (sweep-rate, concentration and temperature) are kept constant.

The main reduction peak, OC3, of the turned-over material differs little in the two solutions; this peak is smaller in $HClO_4$ solution because a compara-

tively larger portion is passed in the OC2 peak, i.e. the peak ascribed[5,6,194] to the reduction of domains of sublattices of surface OH on a Au surface more or less free of adsorbed anions. In H_2SO_4 solution, for the relatively slow sweep-rate used in obtaining the curves of Figure 4.1.1.b., the fast adsorption of anions does not leave much free space on the surface on which OH sublattices could be formed; therefore, as seen in Figure 4.1.1.b., the OC2 peak is somewhat obscured by the OC3 peak. It is much smaller and arises at more positive potentials than in $HClO_4$ solution.

The numerical values of the potentials of the various anodic and cathodic peaks are given in Table 4.1.1.

Table 4.1.1.

E_p / V r.h.e.

(s = 50 mV s^{-1}, room temperature)

	1 M $HClO_4$	0.5 M H_2SO_4
Onset of oxidation	1.25	1.35
OA1/OC1 (reversible)	1.285	----
OA2	1.332	1.397
OA4	1.440	1.490
OC3 (as $\theta \rightarrow 0$)	1.235	1.248
OC2	1.080	1.130

The species involved in the initial reversible surface oxidation step (OA1/OC1) are relatively very short-lived in the respective energy states at which they were initially electrosorbed, especially in the presence of strongly adsorbed anions such as SO_4^{2-} (HSO_4^-). They become transformed in a relatively slow process to states from which they are reduced at less positive potentials, indicating an increase of stability. The rate of this "post-electrochemical"

transformation process determines the effective lifetime of the initially deposited OH species (OA1 process).

Even at the least positive end potential of the anodic sweeps in aq. H_2SO_4 (Figure 4.1.1.b.), where only a few percent of a monolayer of OH-species are formed, no reversible reduction peak due to a 2-dimensionally electrosorbed species is observed. This state of surface oxide at small coverages has already changed and the resulting species in the changed state are reduced in the OC3 and OC2 peaks. However, by using an electrolyte with a weakly adsorbed anion, such as $HClO_4$, or employing a very rapid potentiodynamic sweep or operating at low temperature[5,6], it is possible to observe reversibility in the deposition and reduction of this species since, under such conditions, the turnover process has had little oportunity to take place.

Fast anodic potentiodynamic sweeps 50 V s^{-1} taken to a series of successively increasing end potentials in 1 M $HClO_4$ and 0.5 M H_2SO_4 at Au enable the formation and reduction of the initial, reversibly generated oxide species (OA1/OC1) to be clearly distinguished (see Figures 4.1.2.a. and 4.1.2.b.) in both electrolytes before such species have had time to change their state at the surface as would be the case at smaller sweep-rates. Note that in Figure 4.1.2.a. in comparison with Figure 4.1.2.b., the OA1/OC1 region is much better resolved with a charge in OA1 of 90 $\mu C\ cm^{-2}$. At the high sweep-rate in $HClO_4$, the initial stage of oxide formation (OA1) is much better separated from the subsequent stages. This is evidently due to the greater shift in potential of the OA2-OA4 peaks with sweep-rate than that of the OA1 peak. A feature of the OC1 region of Figure 4.1.1.a. is that the currents in this peak at first increase, then decrease, as the end potential of the anodic sweep is extended into the OA2 region; correspondingly, OC2 and OC3 species are generated in small quantities, as seen in Figure 4.1.2.a. Further details of the experimental behavior of this important process are given in

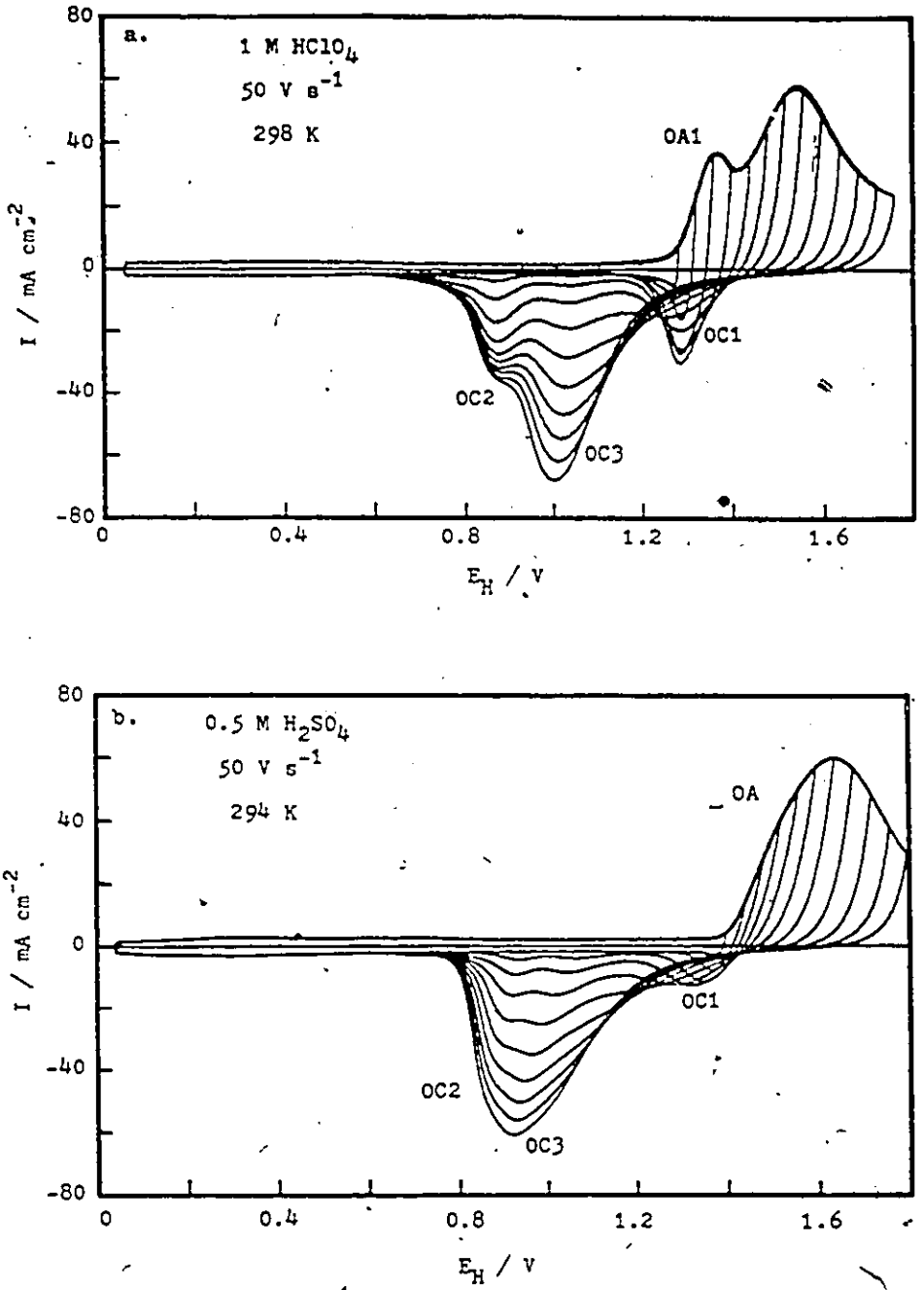

Figure 4.1.2. Potentiodynamic I vs E profiles for Au at 50 V s^{-1} taken to a series of anodic end potentials in

a. 1 M $HClO_4$ at 298 K,

b. 0.5 M H_2SO_4 at 294 K.

Section 4.3., together with an evaluation of the kinetics of the transformation process.

By contrast, in H_2SO_4 (Figure 4.1.2.b.), only a small region of reversible anodic/cathodic currents pass in the OA1/OC1 region and no OA1 peak of the kind resolved in Figure 4.1.2.a. is observed. In fact, the magnitude of such charge corresponding to these reversible currents in 0.5 M H_2SO_4 is less than that in 1 M $HClO_4$ at 100-times smaller sweep-rate.

4.1.2. The Relative Strength of Fluoride Adsorption at Gold

Recognizing that the initial stages of surface oxide formation at Au are so strongly affected by anion adsorption[5-7,194,195], an attempt was made to find an anion which is less strongly adsorbed than ClO_4^- in order to examine the oxidation processes with very little or no influence of anions adsorbed at the surface. Older studies of specific adsorption of anions at Au[148] suggested that fluoride (F^-) is less adsorbed than ClO_4^-, or not at all. However, from results to be reported below, it is evident that F^- is actually more strongly adsorbed than ClO_4^- at polycrystalline Au surfaces, but less so than sulfate. The principal, but indirect, indication of the strength of adsorption of a particular anion is the extent to which the initial stage of surface oxide formation is blocked in solutions containing that anion compared with other anions[5,6,159].

If the I vs E profile for surface oxide formation at Au in 1 M aq. HF (Figure 4.1.3.) is compared with that for 1 M $HClO_4$ (Figure 4.1.1.a.), it is seen that the potential for the onset of surface oxide formation (OA1 region) is shifted positively by ca. 30 mV relative to that in $HClO_4$, clearly indicating a greater blocking effect on the initial stages of surface oxide formation by F^- over ClO_4^-, hence stronger adsorption of F^- is indicated. Also the potential of peak OA2 is shifted to a value of 1.359 V. Comparison with the behavior in both $HClO_4$ and H_2SO_4 (Figures 4.1.1.a. and b.) shows that F^-

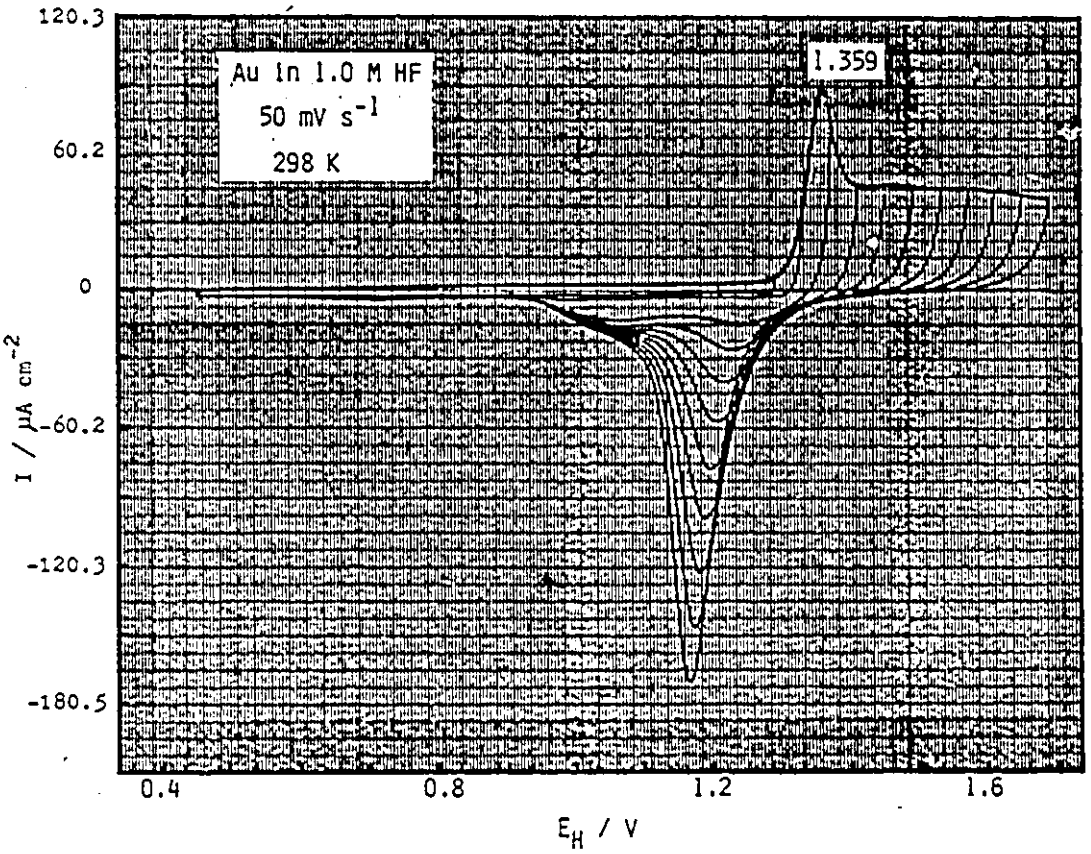

Figure 4.1.3. Potentiodynamic I vs E profiles for Au at 0.050 V s^{-1} taken to a series of anodic end potentials in 1 M HF at 298 K.

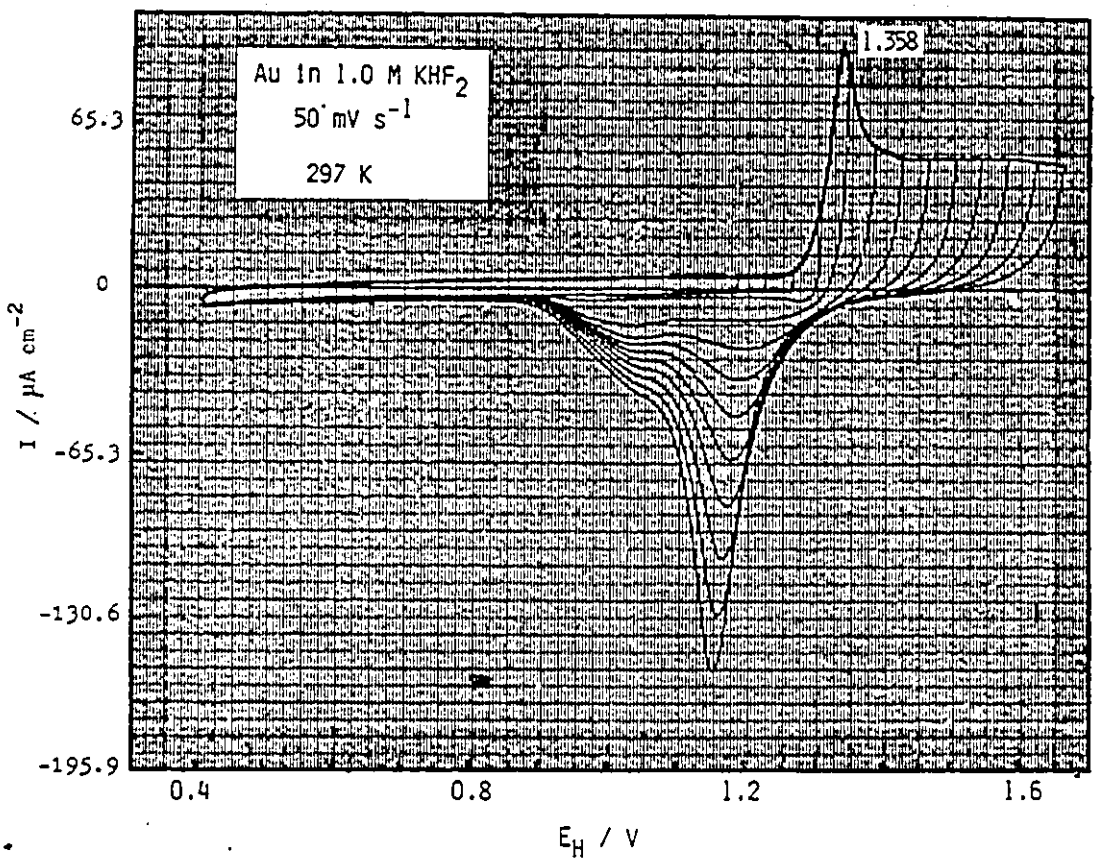

Figure 4.1.4. Potentiodynamic I vs E profiles for Au at 0.050 V s^{-1} taken to a series of anodic end potentials in 1 M KHF_2 at 297 K.

is, in fact, adsorbed at Au to an extent intermediate between that of ClO_4^- and SO_4^{2-} (HSO_4^-), as indicated by a) the potential for the onset of surface oxidation and b) the small but significant change in the extents of reversibility in the OA1/OC1 region.

In 1 M aq. KHF_2 (Figure 4.1.4.), the reversibility in the OA1/OC1 region and the OA2 peak potential, are the same as in 1 M HF*, but the OC2 region is more developed, probably due to higher pH.

Recent double-layer capacitance measurements on silver[149] and Au[150] single-crystals, and electrode resistance measurements on vapor-deposited thin films of Au[110] in solutions containing F^- are consistent with a small but significant adsorption of this anion at gold surfaces. A recent cyclic-voltammetry study of Au(111) in 0.4 M HF and in 0.09 M $NaClO_4$ with 0.01 M $HClO_4$ gave voltammograms that differed considerably, presumably because of the different adsorption behavior of the two anions [246].

4.1.3. Initial Peak Potential vs Sweep-Rate and the Relative Strengths of Anion Adsorption

In section 4.1.1., it was suggested that the peak potential of the first distinctive peak of Au oxidation can be considered as a measure of the strength of adsorption of anions on the Au surface. This current peak is due to OH deposition on a surface partially or fully covered by adsorbed anions, which block the surface. The anions are desorbed in the process of OH deposition, and the surface OH's formed undergo a transformation in a turn-over process (replacement turn-over process, RTO). In order to evaluate the effects of anions only, the step of electrodeposition of OH in the overall surface oxidation process should be reversible and the pH effect is avoided by using a hydrogen reference electrode in the same solution as that for the working

---

*Note that from the commonly accepted pK_a of HF in aqueous solution, 1 M HF will actually be ca. 10^{-1} M in free F^- ions. There will also be a small concentration of HF_2^- ions.

electrode. The comparison of peak potentials is meaningful only if there is no kinetic irreversibility in the electrodeposition of OH. In the replacement/turn-over process, turn-over becomes possible[194,195] when the stabilizing effect of adsorbed anions on OH's on the surface is removed by anion desorption; therefore the extent of turn-over is also influenced by the strength of anion adsorption. Both processes, since they are connected with anion desorption, are much slower than the OH deposition and are not reversible under the conditions of the experiments. As earlier work on Pt[53] and Au[5,6] indicates, the OH deposition is fast, therefore any shift of peak potential with sweep-rate, s, and with the kind or concentration of anions must be due to processes connected with or influenced by the adsorbed anions. In this respect, the differences in the peak potentials observed can be taken as a measure of the strength of anion adsorption.

The effects associated with F^- adsorption at Au, as indicated from Figures 4.1.3. and 4.1.4., are more clearly and quantitatively represented in Figure 4.1.5., where the potentials for the first main anodic peak (OA2) associated with oxide formation coupled with anion desorption[5,6,194,195], are plotted as a function of log(s) for several electrolyte solutions containing the anions F^-, ClO_4^- and SO_4^{2-} (HSO_4^-) at 298 K.

The results in 1 M $HClO_4$. 0.5 M H_2SO_4, 1 M HF, 1 M KHF_2 and 0.1 M HF, obtained during the course of the present work, were supplemented by some data from Barnett[6,247], previously obtained in this laboratory, to illustrate better the behavior of Au in solutions containing various anions.

Evidence of kinetic irreversibility is seen (Figure 4.1.5.) in the case of 0.1 M KHF_2, when, from s = 0.05 V s^{-1}, the slope of the line changes to 41mV dec^{-1}. In the case of 0.05 M H_2SO_4 and especially 0.001 M $HClO_4$, the observed increase of slope at higher sweep-rates may be due to kinetic irreversibility as well as some iR effects in dilute solution. However, at 0.02 V s^{-1}, the

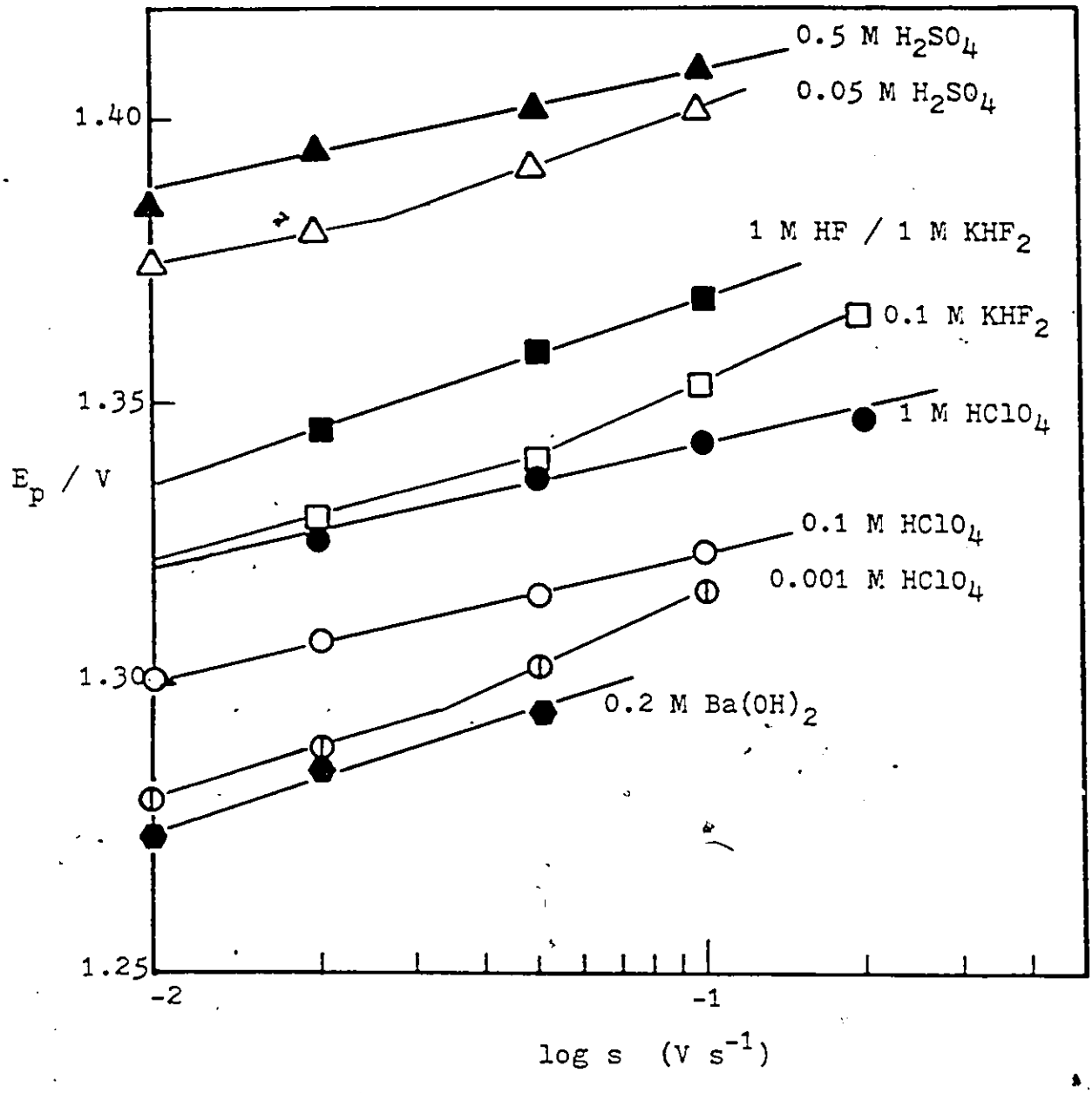

Figure 4.1.5. First anodic peak (OA2) potential, E_p vs log(s) for several different electrolyte solutions at about room temperature.

values of peak potential for all the solutions in Figure 4.1.5. seem to fulfill the criteria mentioned above.

The potential of the initial anodic peak is more positive in potential for 1 M HF and KHF_2 than for 1 M $HClO_4$ by about 19 mV, but not as much as for 0.5 M H_2SO_4, for which the initial anodic peak is shifted positively, relative to that for $HClO_4$ by about 70 mV. This same trend is also seen at lower concentrations of these anions. This result corresponds to the same relative strengths of adsorption found before: ClO_4^- < F^- < SO_4^{2-} (HSO_4^-).

The first surface oxide formation peaks in 0.2 M $Ba(OH)_2$ are the least positive, which is logical because the OH^- anion is the actual reactant for surface oxide formation and cannot compete by its own adsorption. 0.001 M was the lowest concentration of the most weakly adsorbed anion, ClO_4^-, considered here, and the initial peak potentials for Au in this solution are the closest to those in $Ba(OH)_2$, where there is no foreign anion interference in the surface oxide formation. However, the peak potentials are slightly more positive than those in $Ba(OH)_2$, indicating some specific adsorption of the anion.

The value of E_p at s = 0.02 V s^{-1}, the differences, ΔE_p relative to the first peak in $Ba(OH)_2$ and the slopes of the lines of E_p vs log(s) for the various electrolyte solutions illlustrated in Figure 4.1.5. are summarized in Table 4.1.2.

Table 4.1.2

Electrolyte	E_p/V at s = 0.02 V s^{-1}	ΔE_p/mV relative to E_p, $Ba(OH)_2$	$dE_p/d(\log(s))$ mV per decade
0.5 M H_2SO_4	1.395	110	22
0.05 M H_2SO_4 *	1.371	96	23/35
1 M HF, 1 M KHF_2	1.345	60	33
0.1 M KHF_2	1.330	45	23/41
1 M $HClO_4$	1.326	41	22
0.1 M $HClO_4$ *	1.307	22	21
0.001 M $HClO_4$ *	1.289	4	29/45
0.2 M $Ba(OH)_2$ *	1.285	(0)	32

* From B. Barnett, Ph.D. Thesis, U. of Ottawa, 1979, and unpublished results.

The values of the slope, $d E_p/d \log(s)$ observed are ca. 23 mV $dec.^{-1}$ for most of the solutions and ca. 33 mV $dec.^{-1}$ for 1 M HF or KHF_2 and $Ba(OH)_2$ solutions. This seems to suggest different mechanisms for the ion effects on the initial stage of surface oxidation at the electrode surface in the above two types of solutions. Certainly these two anions have different molecular geometries and chemical constitutions, as well as hydration structures, which could lead them to interact differently with the electrode surface.

From the cyclic-voltammograms of Au in HF, $HClO_4$ and H_2SO_4 (Figures 4.1.3., 4.1.1.a. and 4.1.1.b., respectively) and E_p vs log(s) results (Figure 4.1.5.) for the first clear peak, it can be concluded that the strength of specific adsorption of F^- and its effect on the initial stages of surface oxide formation of gold lies between those of HSO_4^- and ClO_4^-.

The results discussed above show that, among the simple anions examined in

this work, the anion least chemisorbed on Au in acid solution is actually ClO_4^-. Therefore, this anion was used in the course of this work in supporting electrolytes and to study the oxidation of gold under the conditions of weak chemisorption of anions.

4.2 The Effects of Sulfate Anion Adsorption at Gold in Mixed $HClO_4/H_2SO_4$ Electrolyte

It is possible to examine the kinetics of anion adsorption at gold electrode surfaces by observing, in time, the blocking effect the adsorbing anions have upon the initial stage of surface oxide formation.

In Section 4.1., clear indications were shown that the initial stages of surface oxidation of Au are very sensitive to the influence and chemical type of anions of the electrolyte that are adsorbed at the metal interface. Here, further experiments are described that enable the anion adsorption effects to be identified and quantified, in particular by means of an electrochemical technique that enables the onset of surface oxidation of Au to be observed in the effective absence and in the presence of strongly adsorbed ions such as SO_4^{2-} (HSO_4^-) in a given mixed electrolyte (H_2SO_4 + $HClO_4$) solution. Although experiments which changed the coverage of SO_4^{2-} (HSO_4^{2-}) at a gold electrode have been done before[5,6], the coverage of anions was less controlled than in the present work, since it was varied by solution stirring.

The special potential-time programs, which were developed to study SO_4^{2-} (HSO_4^-) anion adsorption kinetics and their effects on the Au oxidation processes are described below.

As very high rates of potential sweep (50 and 500 v s^{-1}) were used in parts of the program, a very conductive electrolyte was needed; for that reason 1 M $HClO_4$ was used as a supporting electrolyte.

The complicated nature of the potential-time programs, with two or more potential holding times, and the very small changes in surface oxide coverages that were to be observed, required the use of a digital oscilloscope to collect the data generated by these experiments.

The inset diagram in Figure 4.2.1.a. shows potential-time program required for this type of experiment. Initially, the electrode potential was held at a

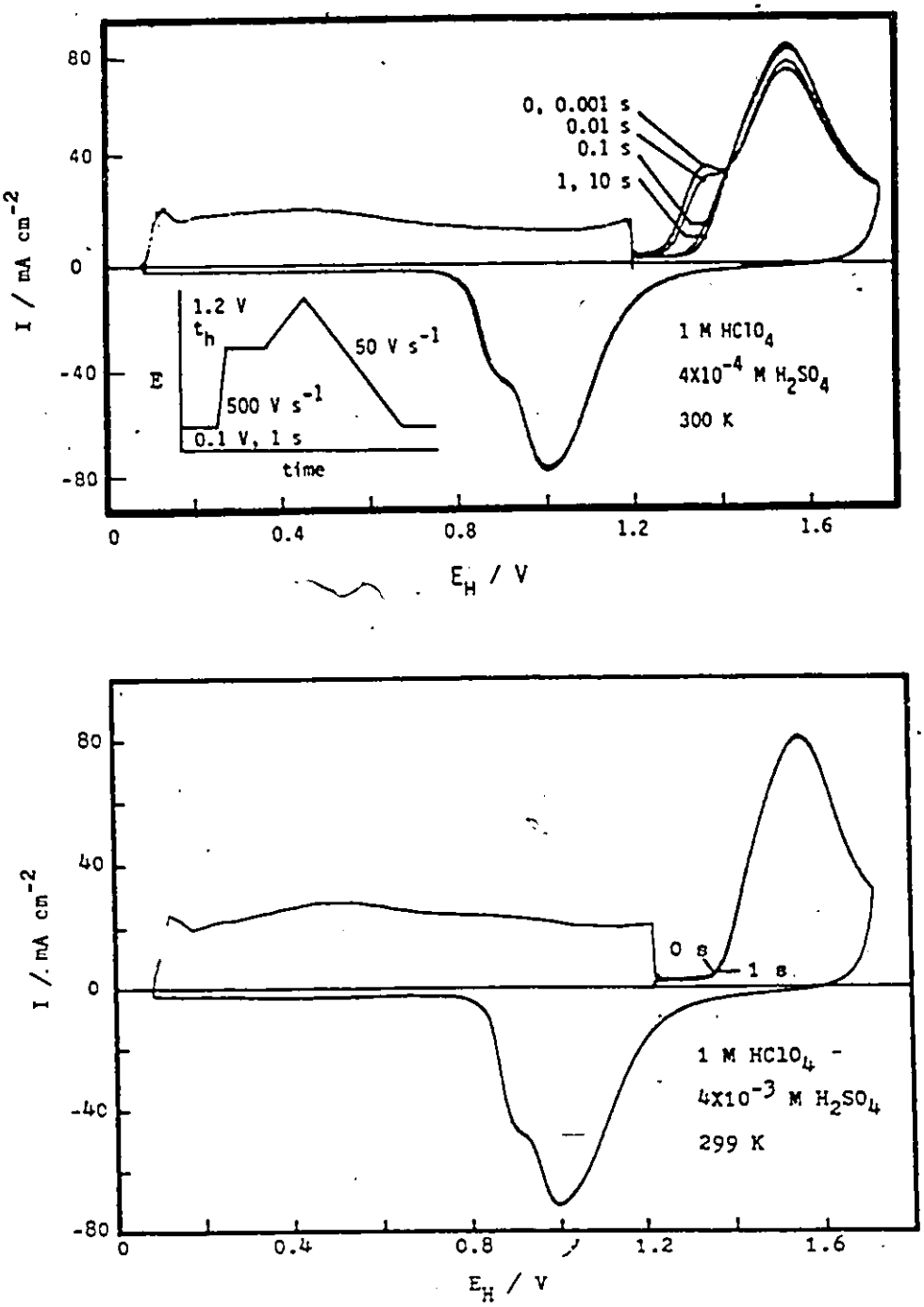

Figure 4.2.1. Potentiodynamic I vs E profiles for Au using the special potential-time program shown (inset) for several holding times at 1.2 V to examine the kinetics of anion adsorption in 1 M $HClO_4$ with (a.) 4X10^{-4} M H_2SO_4; (b.) 4X10^{-3} M H_2SO_4.

cathodic potential limit, E_c = 0.1 V to allow any chemisorbed anions present on the surface to become desorbed. This potential is well below the potential of zero charge of gold[144,173] and is negative to 0.4 V, the potential at which no measurable coverage of HSO_4^- was found by a radiotracer study in a solution of the same concentration of $HClO_4$ and H_2SO_4[105]. The ion desorption step was followed by a potential sweep at 500 V s^{-1} to E_h = 1.2 V, a potential just before surface oxide formation commences and at which maximum HSO_4^- adsorption was found by the radiotracer study. A very high sweep-rate was needed to minimize the time during which anion readsorption could take place during this step. The comparatively large current transients produced during this portion of the program were due only to double-layer charging at the high sweep-rate and have no special significance. The potential was then held at E_h = 1.2 V for a variable time, t_h, to allow various extents of anion adsorption to take place. An anodic potential sweep at 50 V s^{-1} was used to examine surface oxide formation from this potential and finally a cathodic sweep at 50 V s^{-1} was applied to reduce and characterize the surface oxide, and return the electrode to the initial potential (E_c) of 0.1 V.

Figure 4.2.1.a. shows the effect that holding at 1.2 V from 0.001 to 10 s has upon surface oxide formation in 1 M $HClO_4$ with 4 X 10^{-4} M H_2SO_4. For t_h < 0.001 s at 1.2 V, there is a minimal coverage of SO_4^{2-} (HSO_4^-) and the resulting I vs E profile resembles behavior observed in H_2SO_4-free 1 M $HClO_4$ under similar conditions (Figure 4.1.2.a.). As the electrode is held for increasingly longer times at 1.2 V, the initial peak for reversible surface oxide formation and reduction is decreased in charge. This is due to increased coverage of the anions which block the surface oxide formation in this peak. There is no significant difference between the the I vs E profiles for 1 and 10 s; therefore, after 1 s, a maximum coverage of anions, near equilibrium, has been attained, and the processes corresponding to the initial peak have been

completely blocked. The resulting I vs E profiles then resemble those obtained in 0.5 M H_2SO_4 (Figure 4.1.2.b.).

There is a distinct isopotential point at 1.42 V, and the electrosorption charge corresponding to OH blocked by the adsorbed anions is approximately equal to the extra charge recovered positive to that potential. At the anodic end potential, the I vs E profiles have all converged, indicating that the state of oxidation of the gold electrode has become similar for all the holding times studied. This is supported by the fact that there are then no significant differences between the various reduction profiles. Similar behavior was observed in 1 M $HClO_4$ with 4 X 10^{-5} M H_2SO_4, except that the SO_4^{2-} (HSO_4^-) anions became adsorbed about 10 times more slowly at this lower concentration of anions in solution; then a very small shoulder due to the initial reversible peak is observed, even after holding 100 s at 1.2 V.

This time-dependent blocking of the surface oxide formation by holding at 1.2 V is due to anion readsorption. The kinetics of this process are not determined by mass transport or diffusion of the anions, contrary to what was previously observed using a much lower concentration of H_2SO_4 and a lower sweep rate[6]. Measurable differences were not observed between results of experiments conducted in stirred and quiescent solutions, except in 4 X 10^{-5} M H_2SO_4 at 273 K, where a small but hardly significant difference was found. It should also be noted that much faster adsorption kinetics for SO_4^{2-} were found here than those reported by Arvia et al.[65].

Figure 4.2.1.b. shows results of a similar experiment conducted in 1 M $HClO_4$ with a higher concentration of H_2SO_4, 4 X 10^{-3} M. There is no significant difference between the behavior after holding for 0 or 1 s at 1.2 V, and the I vs E profile is similar to that in 0.5 M H_2SO_4 (Figure 4.1.2.b.). Near equilibrium coverage by the anions is attained too rapidly at this concentration of HSO_4^- for the ion adsorption kinetics to be followed using

this technique. Holding at 1.2 V also had no significant effect on gold surface oxide formation in 0.5 M H_2SO_4 or in 1 M $HClO_4$ (i.e. for ClO_4^- adsorption) with no H_2SO_4, as would be expected.

4.2.1. The Kinetics of SO_4^{2-} Adsorption

Figure 4.2.2. shows the extent of blocking of the initial reversibly formed, oxide (measured as a charge, Q_b) as a function of holding time (logarithmic scale) at 1.2 V with H_2SO_4 added at a concentration 4 X 10^{-4} M in 1 M $HClO_4$ at 318, 300, and 273 K and with 4 X 10^{-5} M H_2SO_4 at 273 K. The inset diagram shows how Q_b was determined from the appropriate I vs E profiles. Although the coverage by adsorbed anions is not equal to the coverage of O or OH species blocked, owing to geometrical factors, it is reasonable to assume that these two coverages are directly proportional to each other. Therefore, it is possible to obtain information about the kinetics of SO_4^{2-} (HSO_4^-) adsorption indirectly from Q_b.

The rate of SO_4^{2-} (HSO_4^-) adsorption, as expected, increases with temperature; it also increases linearly as a function of H_2SO_4 concentration, since the curves for Q_b as a function of time for 4 X 10^{-4} and 4 X 10^{-5} M H_2SO_4 at 273 K are separated by a factor of 10 on the time scale.

Before any meaningful calculations can be made, the limitations of the method and the program used must be considered. The process of adsorption of HSO_4^- consists of chemisorption on free surface sites, where, in 1 M $HClO_4$, OH species would already have been deposited, i.e. blocking of the surface for OH deposition takes place. Some replacement of ClO_4^- anions on the surface by HSO_4^- (ion exchange) also takes place. This process does not produce any measurable signal on the I vs E profile recorded after potential holding. It is evident from Figure 4.1.5. that ClO_4^- ions are themselves appreciably adsorbed in 1 M solution, where the OA2 peak for this solution is 37 mV more positive than that for a more dilute solution (10^{-3} M). This is also supported

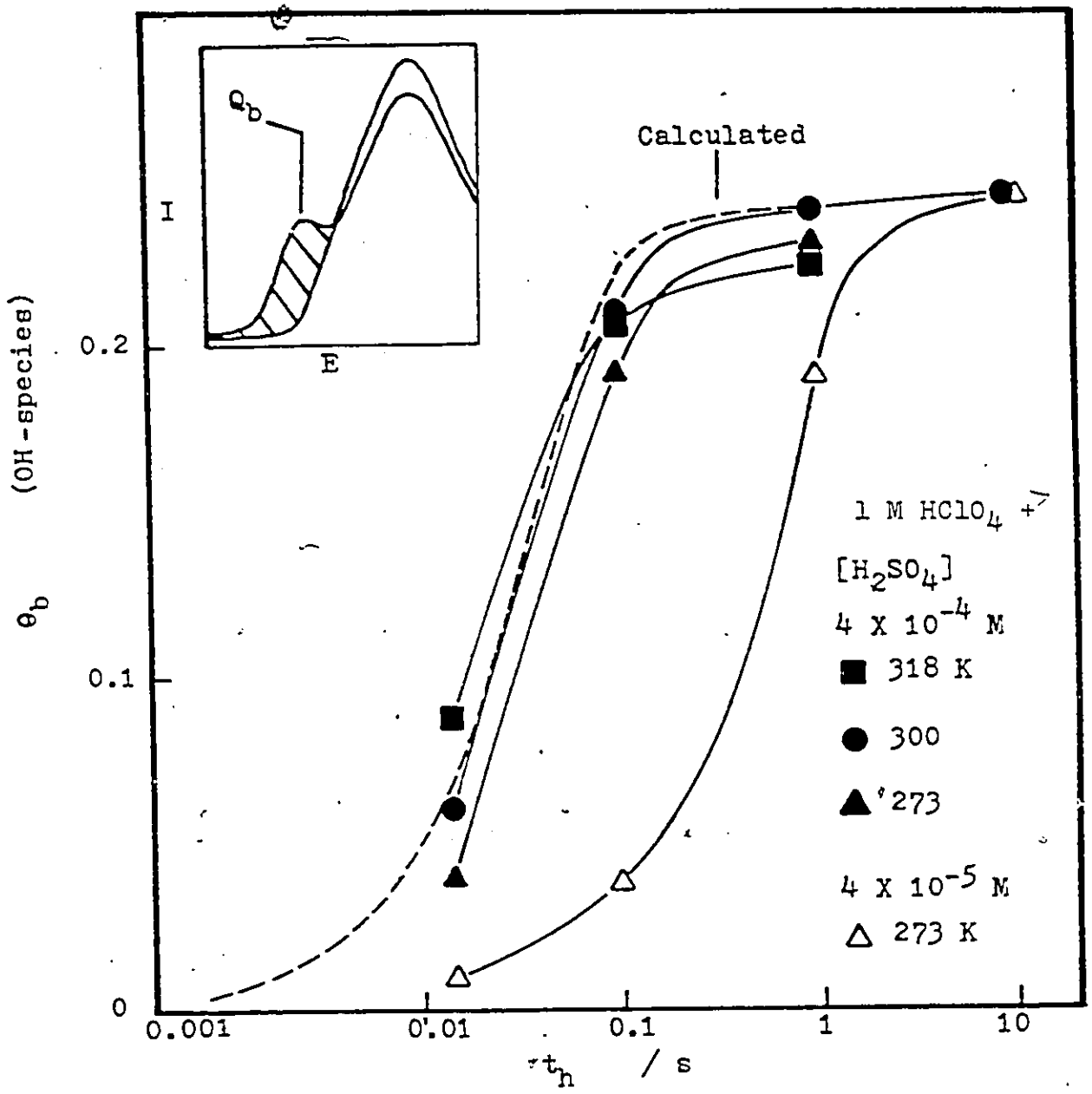

Figure 4.2.2. Coverage of surface oxide blocked (as OH-species) plotted against holding time at 1.2 V. The dotted line was calculated using:

$$\theta = \theta_{eq.} (1 - e^{-bt})$$

where $\theta_{eq.} = 0.23$ and $b = 23\ s^{-1}$.

by the fact that holding the potential at 1.2 V in 1 M $HClO_4$ does not change the subsequent I vs E profile.

The blocking of the initial stage of oxide deposition can therefore provide a quantitative measure of the chemisorption of HSO_4^- only if the above anion replacement reaction has a rate similar to that for chemisorption on free surface sites. Considering the large difference in the strength of adsorption of the two anions, this may actually be the case, but the blocking effect may certainly be semi-quantitatively evaluated.

The second factor which complicates the quantitative interpretation of these results is the finite excursion time of the sweeps, even at 50 V s^{-1}. Thus, to traverse the potential though the range of the reversible process peak, i.e. between 1.2 and 1.45 V, takes $\frac{0.25\ V}{50\ V/s}$ = 0.005 s, i.e. 5 times longer than the shortest holding time, 0.001 s, and 1.5 times longer than the second holding time, 0.01 s. Therefore, the values at the lowest t_h in Figure 4.2.2. must be rejected and the second t_h must be corrected from 0.01 to 0.015 s. Also, the values for 4 X 10^{-5} M H_2SO_4 would be better if there were no diffusion limitation.

A simple calculation which simulates how surface oxide formation might be blocked by anion adsorption is shown by the dotted line in Figure 4.4.2. The anion adsorption process is assumed to have kinetics which are first order in anion concentration and available sites, and desorption kinetics which are first order in coverage, θ_A, by adsorbed anions; one can then write

$$\frac{d\theta_A}{dt} = k_1\ c_A\ (1 - \theta_A) - k_{-1}\theta_A \qquad (4.2.1)$$

Integrating equation (4.2.1) yields

$$\theta_A = \frac{a}{b}(1 - e^{-bt}) \qquad (4.2.2)$$

where

$$a = k_1\ c_A \quad \text{and} \quad b = k_{-1} + k_1\ c_A.$$

As t becomes large, θ_A will tend to approach its equilibrium value, $\theta_{eq.}$, so that

$$\theta_{eq.} = \frac{a}{b}$$

and

$$\theta_A = \theta_{eq.} \ (1 - e^{-bt}) \qquad (4.2.3)$$

When the coverage by ions is directly reflected in the diminution of surface oxide coverage due to the ion adsorption, then obviously

$$\theta_b = \theta_{b,eq.} \ (1 - e^{-bt}) \qquad (4.2.4)$$

In practice, the HSO_4^- adsorption is kinetically irreversible, so that $k_{-1}\ \theta_A$ in equation (4.2.1.) is near zero. Under these conditions, this equation will integrate to

$$\ln (1 - \theta_A) = k_1\ c_A\ t = at \qquad (4.2.5)$$

with a defined as $k_1\ c_A$. Then

$$\theta_A = 1 - e^{-at} \qquad (4.2.6)$$

is a particular case of equation (4.2.3), and, for these conditions, $b = k_1\ c_A$. The result will obviously be more complex when some adsorbed ion interchange e.g. between HSO_4^- in solution and ClO_4^- already adsorbed is significant, which represents a parallel process for HSO_4^- adsorption.

For surface oxide blocked under conditions of holding at 1.2 V in 4×10^{-4} M H_2SO_4 at 300 K, it was determined from the data that $\theta_{b,eq.} = 0.23$ (calculated as OH species, i.e. 1 e per site) and $b = 23\ s^{-1}$. Although the species at the surface under these conditions are probably OH, the stoichiometry of the adsorption reaction and consequently the kinetic equation will formally remain unchanged if θ is defined as coverage by either O or OH species. Furthermore, as was previously stated, the extent to which surface oxide formation is blocked is probably not equal, but proportional, to the surface concentration of adsorbed anions.

The fit between the actual data and the calculated curve is surprisingly

good, especially considering that this simple model of anion adsorption does not take into account repulsive interactions between the anions. Values of b for the three temperatures studied in 4 X 10^{-4} M H_2SO_4 are given in the following table:

Table 4.2.1.

Data for the Kinetics of Blocking of OH Deposition by Adsorption of Anions

T / K	b / s^{-1}
273	18 ± 2
300	23 ± 2
318	30 ± 3

Because the supposed equilibrium coverages of anions and the extent of blocking of surface oxide are nearly equal for the three temperatures examined, it follows that the rate of anion adsorption is equal to the b value, as concluded above.

4.2.2. "Anions Off" and "Anions On" Situations with Sulfate on Gold

As previously shown, the Figures 4.2.1.a. and 4.2.2. illustrate the effects of readsorption of HSO_4^- ions following their desortion at 0.1 V, i.e. negative to the potential of zero charge of Au. It is useful to identify two limiting conditions associated with these profiles: a) an "anions off" situation corresponding to the t_h = 0.0 s in Figure 4.2.1.a., for which sulfate ions have been desorbed but have not had time to become appreciably readsorbed; and b) an "anions on" situation in which the surface oxidation process commences with sulfate initially adsorbed on the surface.

In the light of these two conditions, it was of interest to examine the reversibility of the initial surface oxidation region (OA1/OC1) for the "anions off" and "anions on" situations by means of a series of potential sweeps taken to successively increasing positive potentials, as shown in Figures 4.2.3.a.

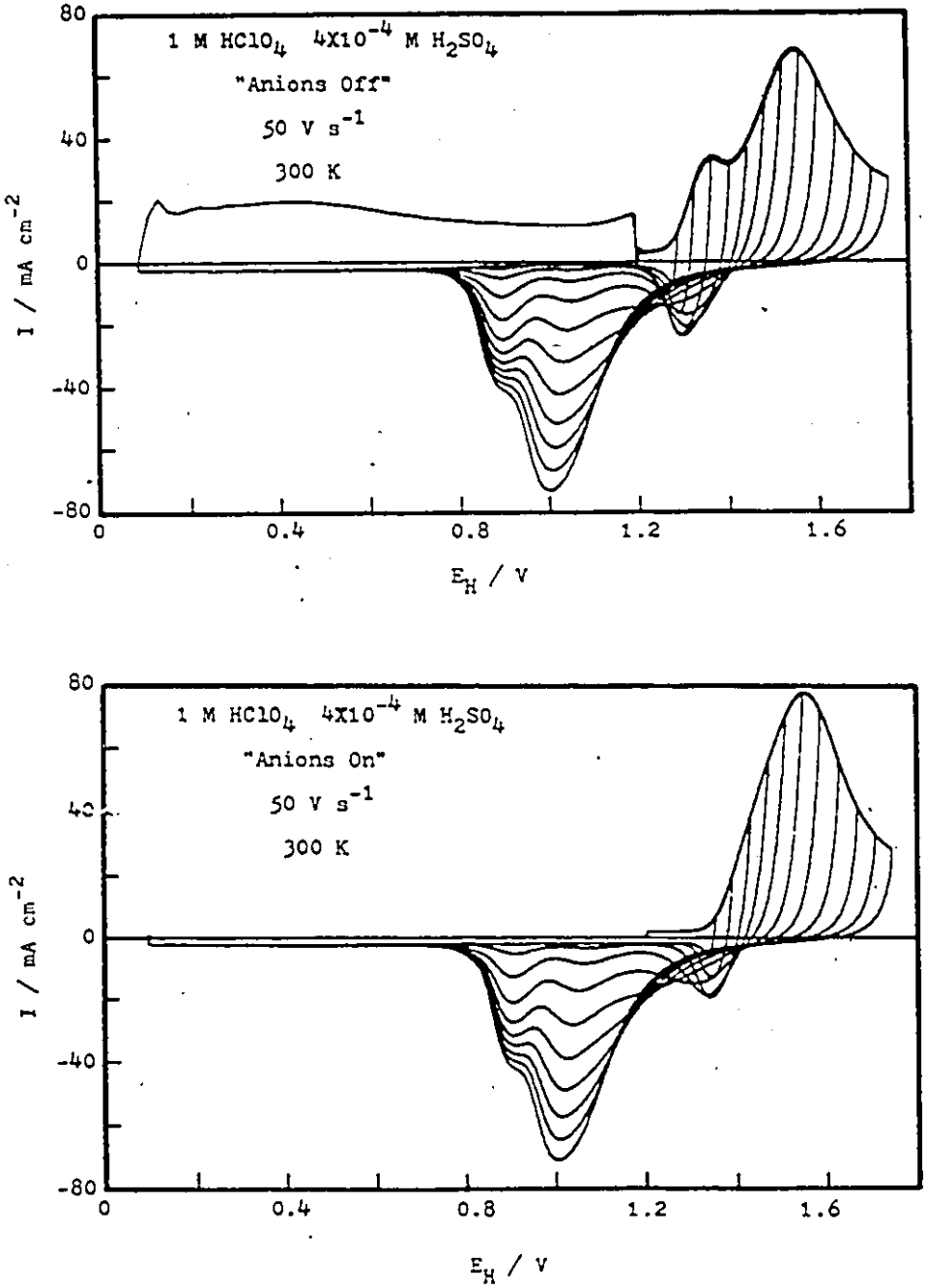

Figure 4.2.3. Potentiodynamic I vs E profiles for Au at 50 V s^{-1} taken to a series of anodic end potentials in 1 M $HClO_4$ with $4X10^{-4}$ M H_2SO_4 at 300 K. The potential program used was the same given in Figure 3.2.1., where t_h at 1.2 V was (a.) 0 s ("anions off") and (b.) 1 s ("anions on")

("anions off") and 4.2.3.b. ("anions on"). For these conditions, respectively, the potential was not held at 1.2 V (0 s) to minimize sulfate adsorption and held for 1 s at this potential to allow nearly complete readsorption of the ions.

In the "anions off" case, the I vs E profile is very similar to that obtained at 50 V s^{-1} in 1 M $HClO_4$ with no added H_2SO_4. It is seen that well developed reversible OA1 and OC1 peaks of the kind found with $HClO_4$ are observed. In the "anions on" profile, however, the OC1 peak is much smaller and has a more positive peak potential. For both cases, the more cathodic OC2 and OC3 reduction peaks are similar, but the species to which they correspond are initially formed at a somewhat less positive potential for the "anions off" case. This indicates that the initial reversible processes associated with the OA1 and OC1 surface oxide formation/reduction peaks are more sensitive to the presence of strongly adsorbed anions at the surface than are the oxide formation processes that arise at more positive potentials or longer times.

Figure 4.2.4. shows a series of I vs E profiles for gold in 1 M $HClO_4$ with 4 X 10^{-3} M H_2SO_4 at 50 V s^{-1} and 299 K. The results for this electrolyte clearly resemble the behavior of the "anions on" case in 1 M $HClO_4$ with 4 X 10^{-4} H_2SO_4, except that the the onset of surface oxide formation is somewhat more positive in 4 X 10^{-3} M H_2SO_4, which may be explained by a rather higher equilibrium coverage of SO_4^{2-} (HSO_4^-) at gold at the higher SO_4^{2-} concentration than that for 4 X 10^{-4} M H_2SO_4. Also, the OC2 reduction peak has a more positive potential in the 4 X 10^{-3} M H_2SO_4 electrolyte than in the 4 X 10^{-4} M solution.

4.2.3. Time Effects in the "Anions Off" and "Anions On" Experiments in the Initial Stages of Surface Oxide Formation at Gold

It is usually more informative to examine the I vs E profile for reduction of surface oxide when studying very low OH/O coverages (here down to θ =

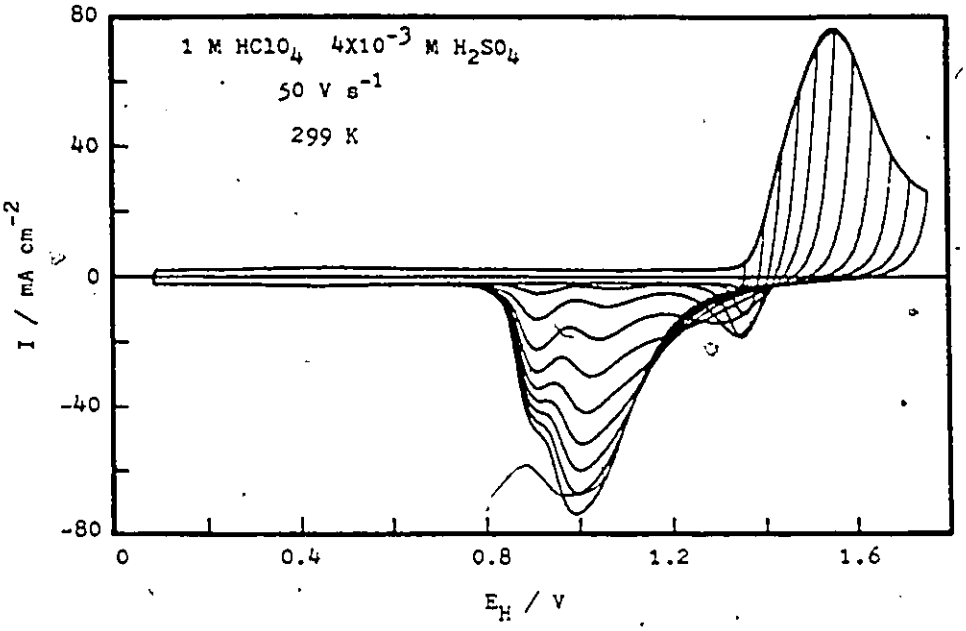

Figure 4.2.4. Potentiodynamic I vs E profiles for Au at 50 V s^{-1} taken to a series of anodic end potentials in 1 M $HClO_4$ with $4X10^{-3}$ M H_2SO_2 at 299 K.

0.5%) because the peaks corresponding to the different stages of OH/O formation are usually better defined and resolved than in the corresponding anodic direction and, in the cathodic direction, the results of effects of holding times and anion adsorption or desorption can be accurately followed. For this reason, special potential-time programs were devised (see Figure 4.2.5.) in order to controllably investigate time effects in sulfate ion adsorption and desorption at gold in relation to the growth and reconstruction of the surface oxide in the very initial stages (up to 5% coverage by OH) of its formation.

In Figure 4.2.5., t_C is a time of holding the potential at an initial potential E_C = 0.1 V (i.e. negative to the potential of zero charge) in order to desorb anions; followed by a 50 V s^{-1} linear sweep to a potential, E_B = 1.2 V, where a time of holding, t_B, allows controlled readsorption of anions; following this, an anodic sweep of 500 V s^{-1} (which is just enough to minimize oxide growth during this sweep) to a particualr anodic potential. E_A, where holding allows growth for various times, t_A, under conditions where the sulfate ion coverage is determined by the holding times at potentials E_B and E_C. Finally, the electrochemical behavior of the oxide film grown in this way is determined in a cathodic sweep of 50 V s^{-1} taken back to E_C = 0.1 V.

The results of various combinations of "hold, sweep and hold" in these programs are presented in Figures 4.2.6.a., b. and c. for examining the initial stages of surface oxidation of gold in 1 M $HClO_4$ with 4 X 10^{-4} M H_2SO_4 at 300 K and E_A = 1.328 V according to the conditions given in the following table:

Figure #	t_C/s	t_B/s	t_A/s
4.2.6.a.	1	0	0, 0.001, 0.01, 0.1, 1
4.2.6.b.	1	0, 0.001, 0.01, 0.1, 1	0
4.2.6.c.	0, 0.001, 0.01, 0.1, 1	0	0

These figures illustrate* the various effects of the presence or the absence of sulfate ions at the gold surface and time-dependent effects associated with their desorption or adsorption.

In Figure 4.2.7. are shown the various charges calculated from the results of Figures 4.2.6.a., b. and c. as a function of potential holding time for total surface oxide formation and for the initial reversible region (peak OC1), obtained by integrating the currents generated in these experiments with respect to time. The I vs E reduction profile for t_A = 0 s, t_B = 0 s and t_C = 1 s was used to calculate the double-layer charges that are subtracted in the integration of surface oxide charges from the overall I vs E profiles to obtain surface oxide charges.

Figure 4.2.6.b. and the curves labelled "B" in Figure 4.2.7. show how the increasing extent of adsorption of anions with time (0 to 1.0 s) at 1.2 V affects the OC1 peak, eventually eliminating it (see below). In this experiment, t_C = 1 s to allow the anions at the surface to become desorbed and t_A = 0 s so that only the reversible and anion-sensitive OC1 type surface oxide was formed, but t_B was varied between 0 and 1 s to allow various coverages of adsorbed SO_4^{2-} (HSO_4^-) to be attained at the surface. There is no significant difference in the OC1 reduction peak between 0 and 0.001 s holding at 1.2 V. After 0.01 s at 1.2 V, the peak is somewhat decreased and there is also a slight increase in the double-layer charging current cathodic to the peak.

The change of double-layer charging with holding at 1.2 V and increased anion coverage is examined in greater detail elsewhere in this thesis (see Section 4.7.). After holding for 0.1 s at 1.2 V, the OC1 peak is no longer observed, because the free space on which OH could be deposited is now completely blocked by the anions that have become adsorbed at the surface.

---

*This term is purposely used here, recognizing that effects observed with t_A = 0 or 0.001 s are complicated by the comparible but unavoidable time of traverse of the sweep at 50 V s^{-1} from E_C to E_A (Figure 4.2.5.).

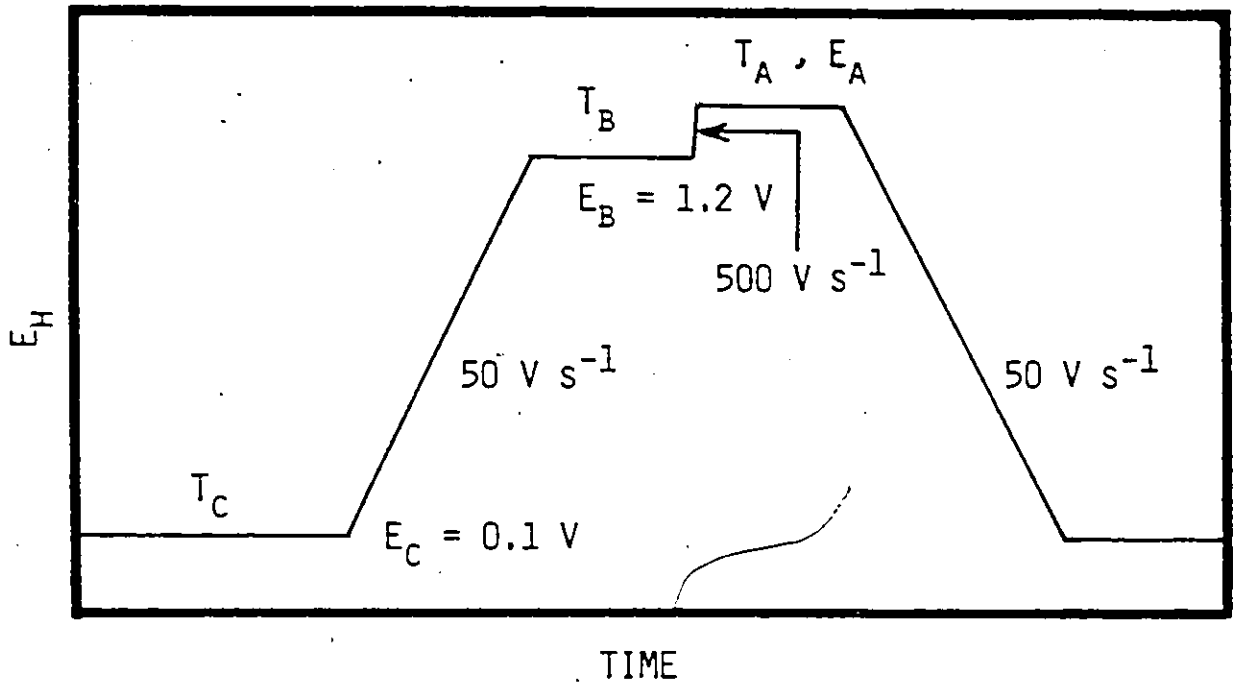

Figure 4.2.5. The potential-time program employed to obtain the results in Figure 4.2.6.

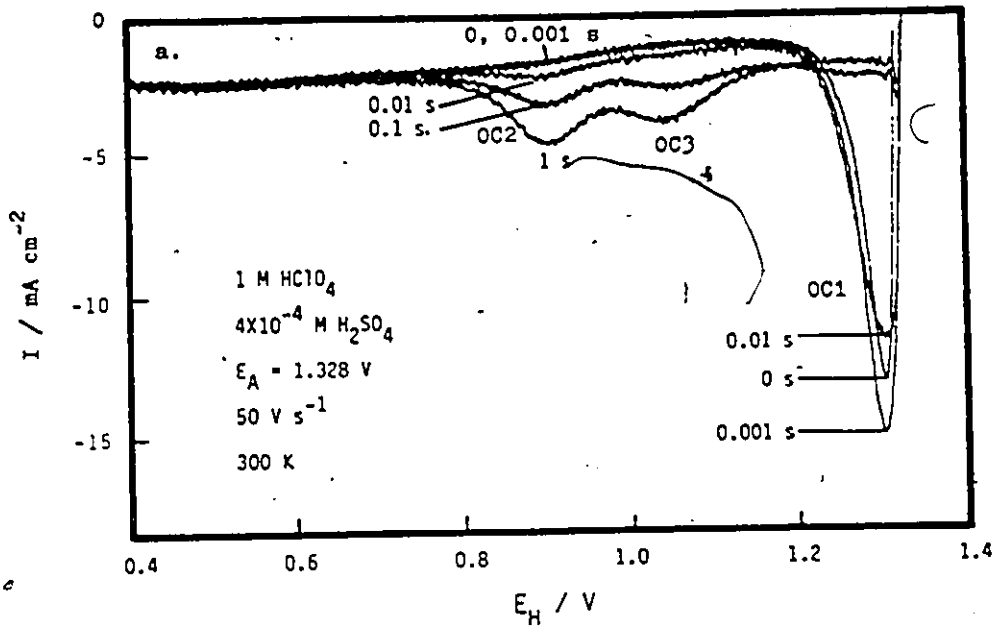

Figure 4.2.6. Series of potentiodynamic profiles showing the effect of holding at 0.1, 1.2 or 1.328 V (E_C, E_B and E_A respectively)for time between 0.001 s and 1 s upon Au in 1 M $HClO_4$ with $4X10^{-4}$ M H_2SO_4 at 300 K. (a.) varied t_A where t_C = 1 s and t_B = 0 s; (b.) varied t_B where t_C = 1 s and t_A = 0 s; (c.) varied t_C where t_B and t_A = 0 s

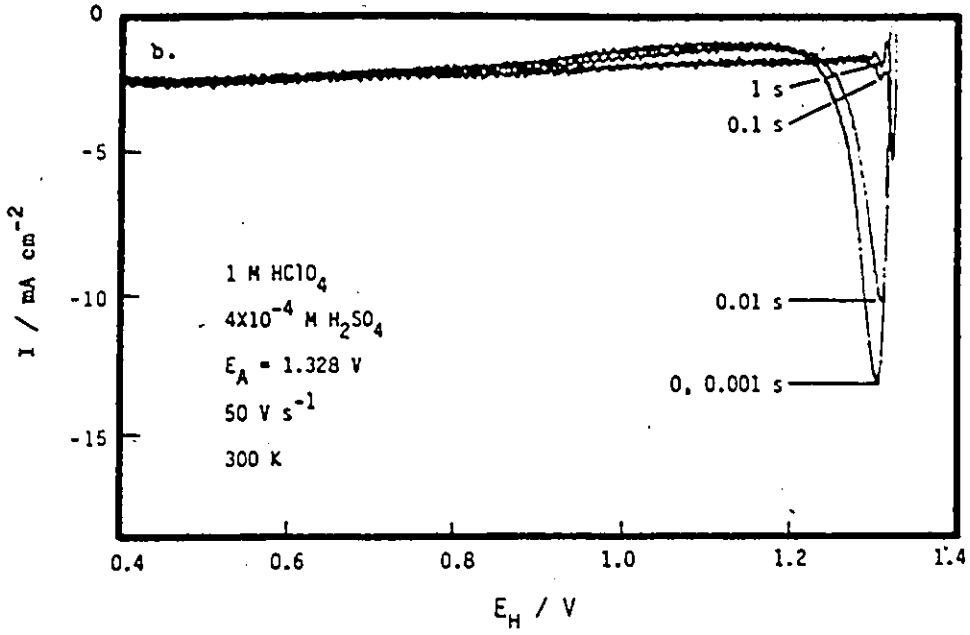
b.
1 s
0.1 s
0.01 s
0, 0.001 s
1 M HClO4
4X10-4 M H2SO4
EA = 1.328 V
50 V s-1
300 K
I / mA cm-2
EH / V
0
-5
-10
-15
0.4
0.6
0.8
1.0
1.2
1.4

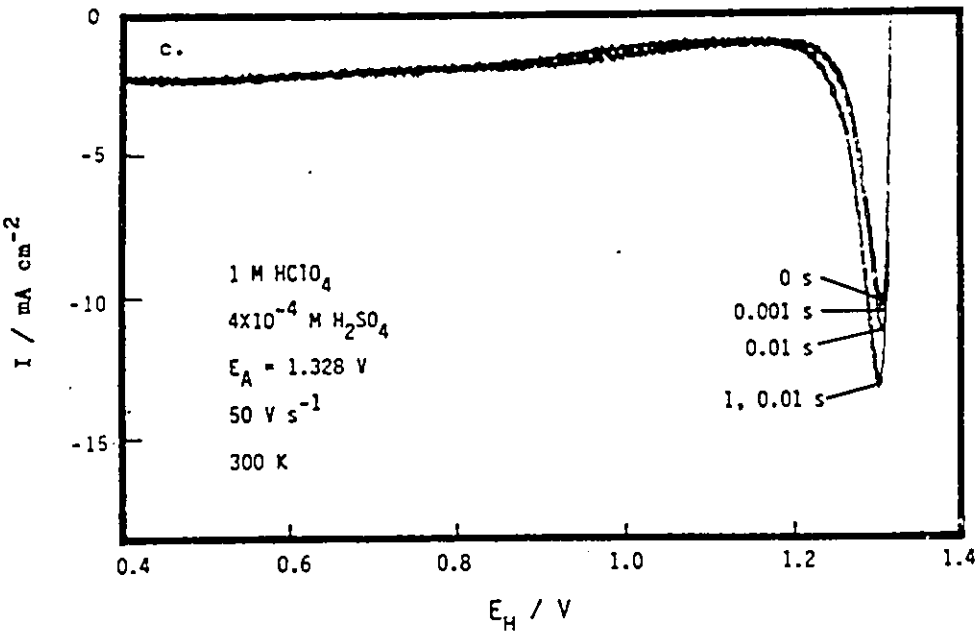
c.
0 s
0.001 s
0.01 s
1, 0.01 s
1 M HClO4
4X10-4 M H2SO4
EA = 1.328 V
50 V s-1
300 K
I / mA cm-2
EH / V
0
-5
-10
-15
0.4
0.6
0.8
1.0
1.2
1.4

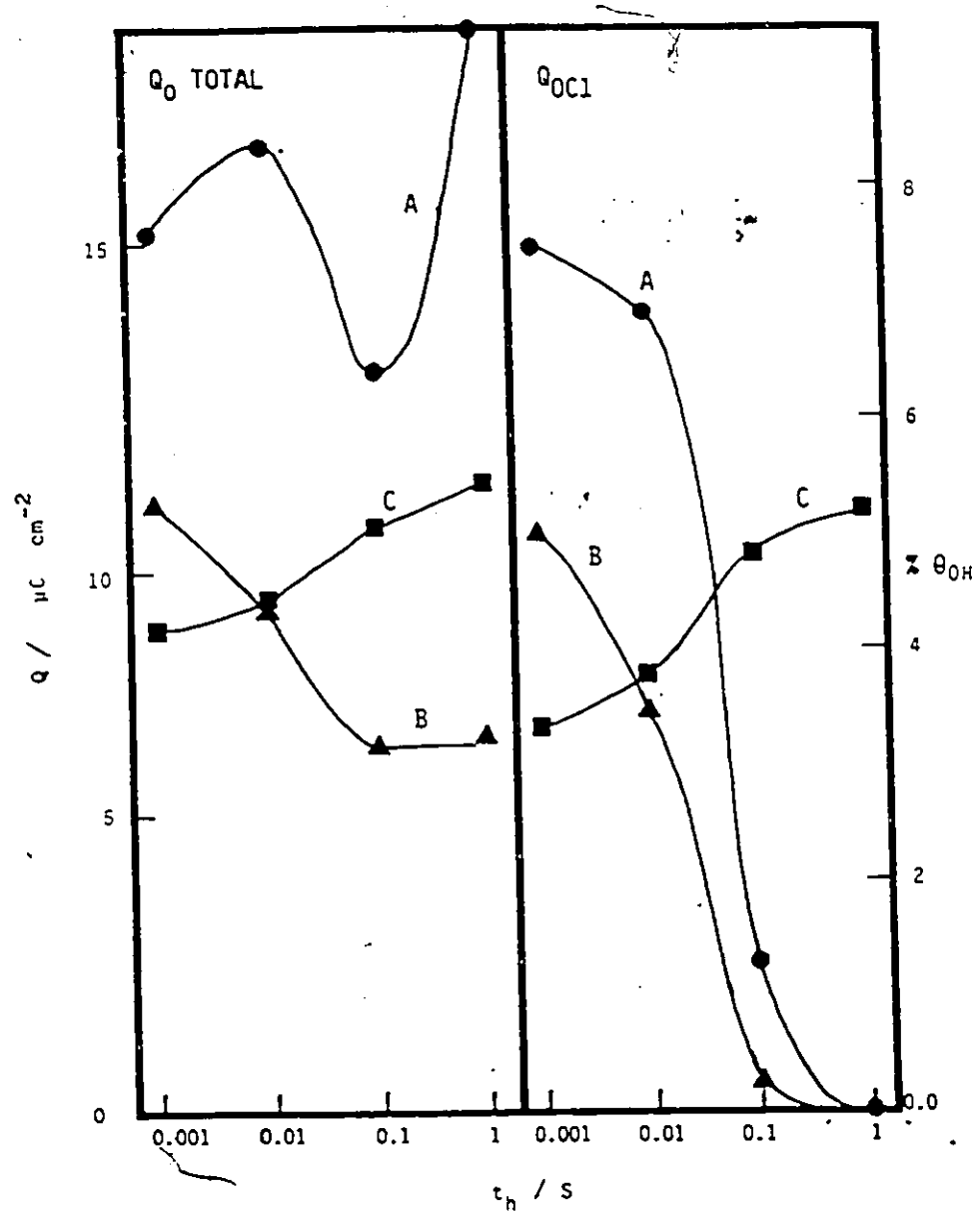

Figure 4.2.7. Variation of surface oxide charge and coverage (as O-species) formed at Au in 1 M $HClO_4$ with $4X10^{-4}$ M H_2SO_4 at 300 K with holding times between 0.001 and 1 s at 1.328 V (A), 1.2 V (B) and 0.1 V (C) for both total surface oxide and OCl.

There is very little difference between the I vs E reduction profiles after 0.1 and 1 s holding. Since the double-layer charge for t_B = 0 s was subtracted from computer-integrated charges to obtain the total Q_O, the charges measured at holding times of 0.1 and 1 s, shown in Figure 4.2.7., are only those due to the changed double-layer charging and not to surface oxide formation.

Figure 4.2.6.c. and the curves marked "C" in Figure 4.2.7. show how the OC1 peak is affected by anion desorption. In this case t_B = 0 s to allow only minimal anion adsorption and t_A = 0 s to produce only the OC1 surface oxide species; t_C was varied between 0 and 1 s to examine the effects of desorption of anions. There is little difference between the surface oxide reduction peaks for t_C = 0 or 0.001 s, but the OC1 peak increases with holding time at 0.1 V. This is because the anions at the surface are becoming desorbed during the period of holding at this potential and the decreased coverage of anions in turn involves less blocking of formation of surface oxide. After 0.1 s, in fact, most of the sulfate anions at the surface have become desorbed as is indicated by the only small difference between the results for 0.1 and 1 s holding at the desorption potential, E_C = 0.1 V.

Figure 4.2.6.a. and the curves marked "A" in Figure 4.2.7. show how the very earliest stages of surface oxide grow in this electrolyte when t_C = 1 s and t_B = 0 s. Under these conditions, there is a minimal amount of SO_4^{2-} (HSO_4^-) adsorbed at the gold surface just before oxide formation commences. Initially, the OC1 peak increases with holding time at 1.328 V but between 0.001 and 0.01 s, this peak decreases with time and this decrease continues at longer times. The total surface oxide charge also <u>decreases</u> with time between 0.01 s and 0.1 s, but <u>increases</u> between 0.1 and 1 s. The OC2 and OC3 peaks appear after holding for 0.01 s and continue to increase as a with time.

It is interesting to mention that on any oscilloscope, using a continuously repeated potential sweep but with successively more positive

values of E_C, this effect of decrease and increase of the oxide charge can be visibly seen in a novel way[6].

If the initial decrease of the OC1 peak were due only to this species becoming interconverted to the more stable OC2 and OC3 states, as in the case of more extensive surface oxide formation at higher E_A values, the total quantity of surface oxide formed would not decrease with holding time. These results clearly indicate that anions are competing with the reversibly and relatively weakly electrosorbed OH species for surface sites at the electrode. Although the initial, reversibly formed, surface oxide is generated quickly when compared to the rate of SO_4^{2-} (HSO_4^-) adsorption in 4 X 10^{-4} M H_2SO_4, the anions eventually displace the electrosorbed OH species and actually cause the total surface oxide charge to decrease as a function of time. When t_A becomes longer than 0.1 s, the surface oxide mostly exists in states that are characterized by reduction in the OC2 and OC3 peaks. These states are much less sensitive to the influence or displacement by anions, and the total quantity of surface oxide then increases as a function of time in the usual way (see Section 4.3. of this thesis, which follows).

4.3. Surface Oxide Growth in 1 M $HClO_4$

As was previously shown in Section 4.1., ClO_4^- anions are more weakly adsorbed at Au surfaces than are most simple anions; therefore surface oxide growth will tend to be faster at lower growth potentials in 1 M $HClO_4$ than with comparable concentrations of other anions. The behavior of the initial, reversibly electrosorbed species also depends upon the type of anions adsorbed at the electrode surface. Because the peak for this initial surface oxide is well resolved from the main reduction peak in this electrolyte[5-9], it possible to examine the interconversion of this species to more stable states of surface oxide upon ageing at constant potential.

4.3.1. General Aspects of Surface Oxide Growth in 1 M $HClO_4$

Figure 4.3.1. shows a series of potentiodynamic I vs E profiles resulting from a surface oxide growth experiment at Au in 1 M $HClO_4$. In this particular experiment, the growth potential was 1.340 V and the temperature 298 K. The potential-time program used (Figure 4.3.2.) consisted of an anodic sweep at 500 V s^{-1} from the cathodic end potential (E_C) of the sweep to the growth potential, $E_A = E_h$ (holding). The growth potential was then held for a variable but contolled time, t_h, between 0.0002 and 5 s. The surface oxide formed was reduced at 50 V s^{-1} and the resultant I vs E profiles were recorded and analyzed. This relatively high sweep-rate was needed to minimize any further time-related changes in the surface oxide during reduction.

As was noted before, three reduction peaks are seen in $HClO_4$: OC1, OC2 and OC3, as was noted in previous work[5-9]. At a growth potential of 1.340 V, the initial peak for the OC1 state is well developed; its growth and its interconversion to other states of surface oxide, which are reduced in the OC3 and OC2 peaks, are easily followed. These two peaks begin to grow as the OC1 peak begins to decrease, but the gain in charge for the OC2 and OC3 peaks is greater than the loss in charge in OC1. There is a clear isopotential point

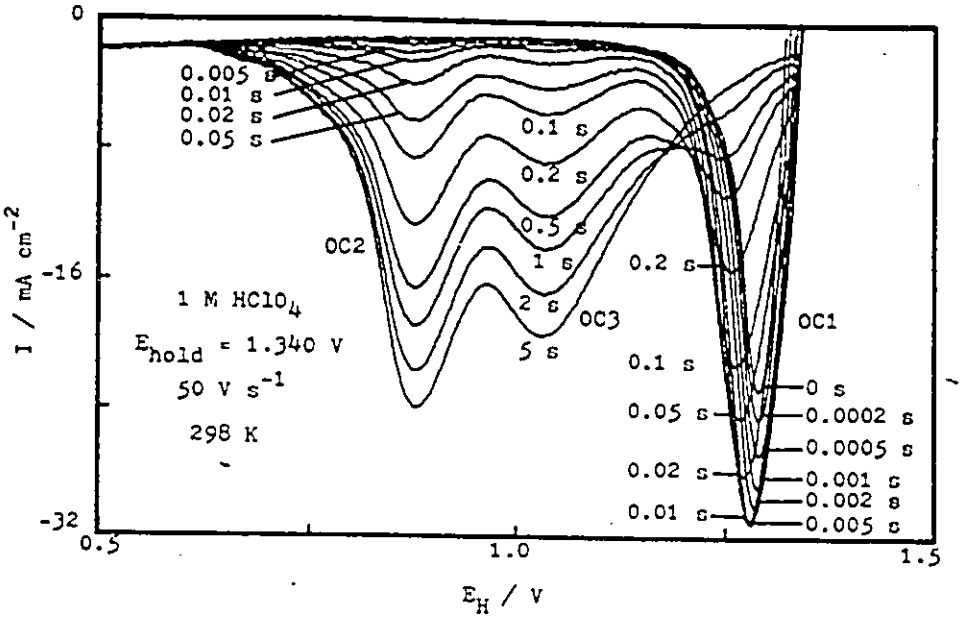

Figure 4.3.1. Series of potentiodynamic I vs E profiles for surface oxide growth at Au at E_h = 1.340 V and several t_h between 0.0002 and 5 s in 1 M $HClO_4$ at 298 K.

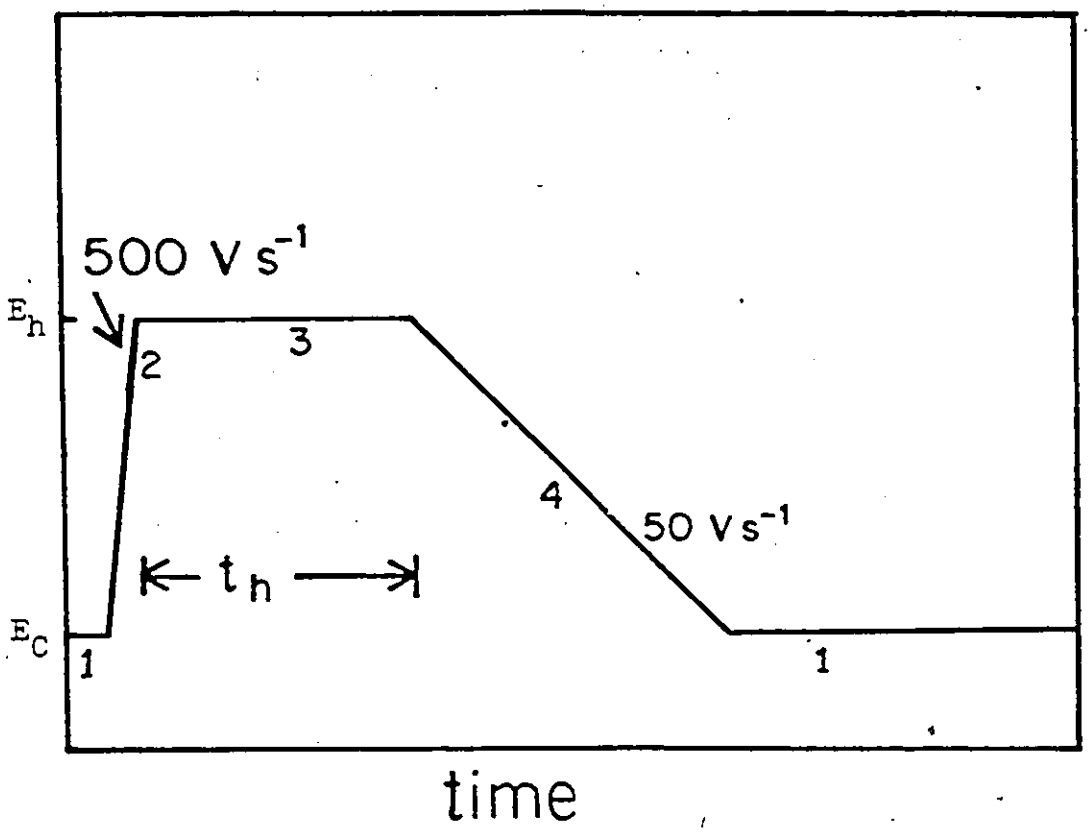

Figure 4.3.2 Potential-time program for studying surface oxide growth in 1 M $HClO_4$.

between the OC1 and OC3 peak, which suggests a conjugate relation between the states of the species involved. The OC2 peak is always larger than the OC3 peak for small coverages of surface oxide formed, but the OC3 species is the one that is eventually associated with the main growth process in time (see below).

The initial 500 V s^{-1} potential sweep (almost a potential step) in the program of Figure 4.3.2. provides for very little surface oxide being formed before the growth potential, E_h, is attained. This high rate of anodic sweep introduces, however, irreversibility in that electrosorption of OH which does take place as as E -> E_h and some also unavoidable iR drop, owing to the finite resistance of the electrolyte and the relatively high currents that arise when the sweep-rate is large. The effects of irreversibility and iR drop are seen if the beginning (right-hand side) of the cathodic sweeps in the OC1 region of Figure 4.2.1. are carefully examined.

With potential holding, the current decreases and distortion of the electrode potential by iR drop eventually disappears and the real holding potential will be attained. This iR effect is what influences the data points for holding times $\geq$ 2 ms (Figures 4.3.3.a) and leads to the small "knee" observed in the curves of Figure 4.3.4. at short holding times. Effects associated with this iR drop require special consideration in relation to oxide growth during the earliest periods of holding and will be further discussed in Section 4.4.5. and Chapter V. Thus the peak potential and charge for OC1 should not change with time if the process behaves reversibly and there are no other changes at the surface. However, the OC1 charge may change, for example, if anion desorption or adsorption is taking place.

As with other experiments at very short holding times, the actual holding times are increased by a small fraction of the time of traverse of the 500 V s^{-1}, i.e. in some range of potential in that sweep that are near E_h.

Figure 4.3.3.a. and b. show integrated charges for the OC1, OC2, OC3 species and total surface oxide plotted against holding time, t_h, on a logarithmic scale for surface oxide growth at 1.290 V and 1.340 V (see Figure 4.3.1.), respectively. First, for growth at 1.340 V, the charge in the OC1 peak increases during the time interval 0 to 2 ms, because of the reasons previously given and reaches a quasi-plateau at about 50 $\mu C\ cm^{-2}$, but after longer holding times, as the OC3 and OC2 charges grow, the OC1 charge decreases. In $HClO_4$, the OC2 peak appears before the OC3 peak, and its charge reaches a saturation value at about 60 $\mu C\ cm^{-2}$. The species associated with the OC3 peak shows logarithmic growth, as expected. The total surface oxide charge shows a slight inflection at the quasi-plateau for OC1 charge just before it begins to follow logarithmic growth. A flattened section of the curve for surface oxide formation is also seen for other growth potentials, especially those between 1.280 and 1.320 V (Figure 4.3.4.a.), for which values the OC1 remains almost constant over several holding times. This behavior of the growth of surface oxide in its various states is more clearly seen in Figure 4.3.3.a., for which the potential is lower (1.290 V) than that for the data of 4.3.3.b., so that the growth processes are slower. Apart from the points for which $t_h \geq 1$ ms, which are influence by iR drop, the OC1 charge clearly has a constant value over 2.5 decades of t_h, indicating that an equilibrium coverage of OC1 species has been attained. When the OC1 charge eventually decreases, it is seen to be accompanied by the onset of growth of the OC2 and OC3 species ($t_h > 0.2$ s). The effects are the same as in Figure 4.3.3.b. (1.340 V), but the plateau region is much shorter in that case.

Figures 4.3.4.a. and b. show the total charge for surface oxide reduction plotted against holding time on a logarithmic scale for growth in 1 M $HClO_4$ at several potentials. Growth in this electrolyte is initially non-logarithmic (for the reasons indicated above), followed by a flattening in the curve for

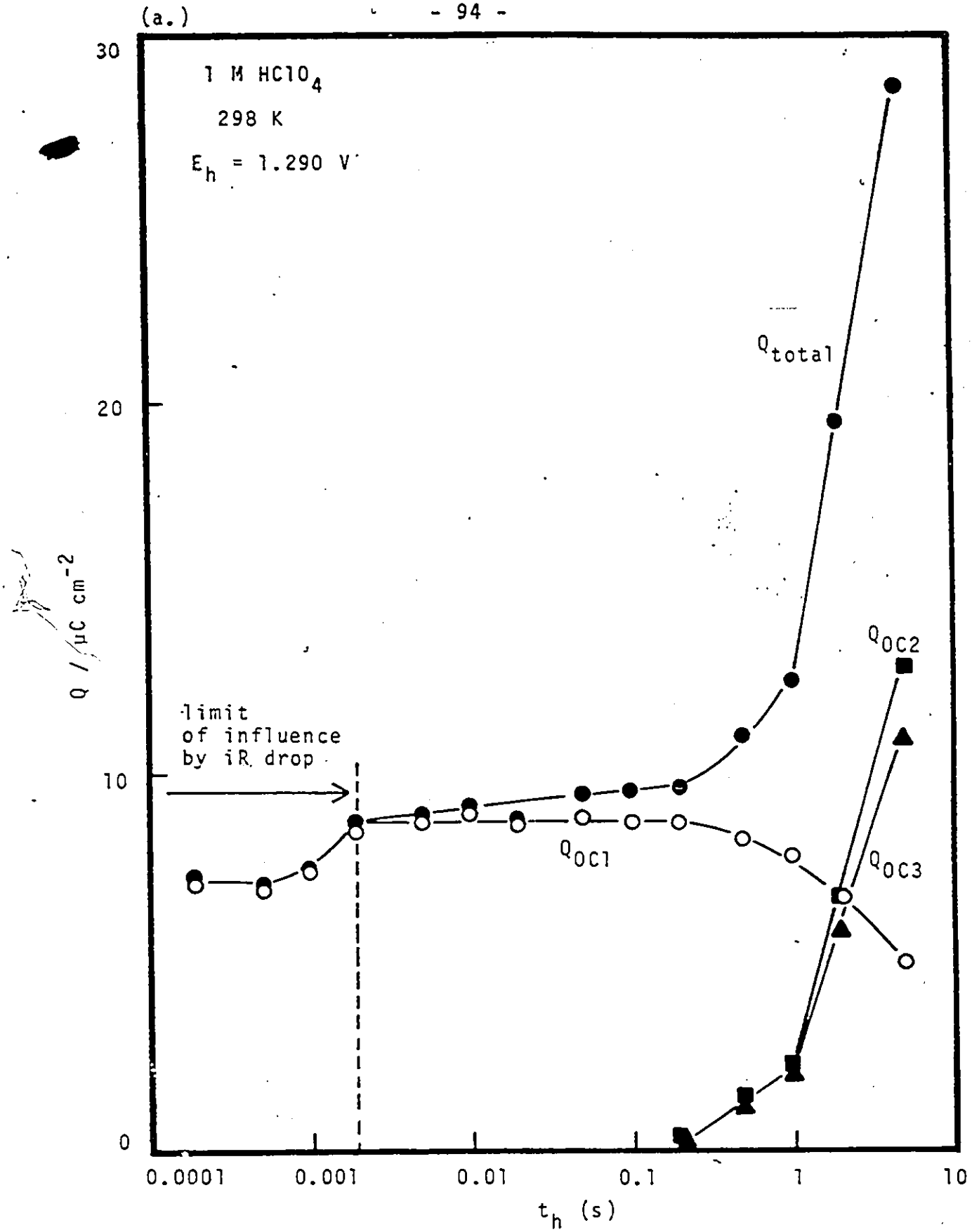

Figure 4.3.3. Variation of surface oxide charge formed for the OC1, OC2 and OC3 peaks and total O-species at Au in 1 M $HClO_4$, 298 K for t_h from 0.0002 to 5 s; (a.) at 1.290 V and (b.) at 1.340 V.

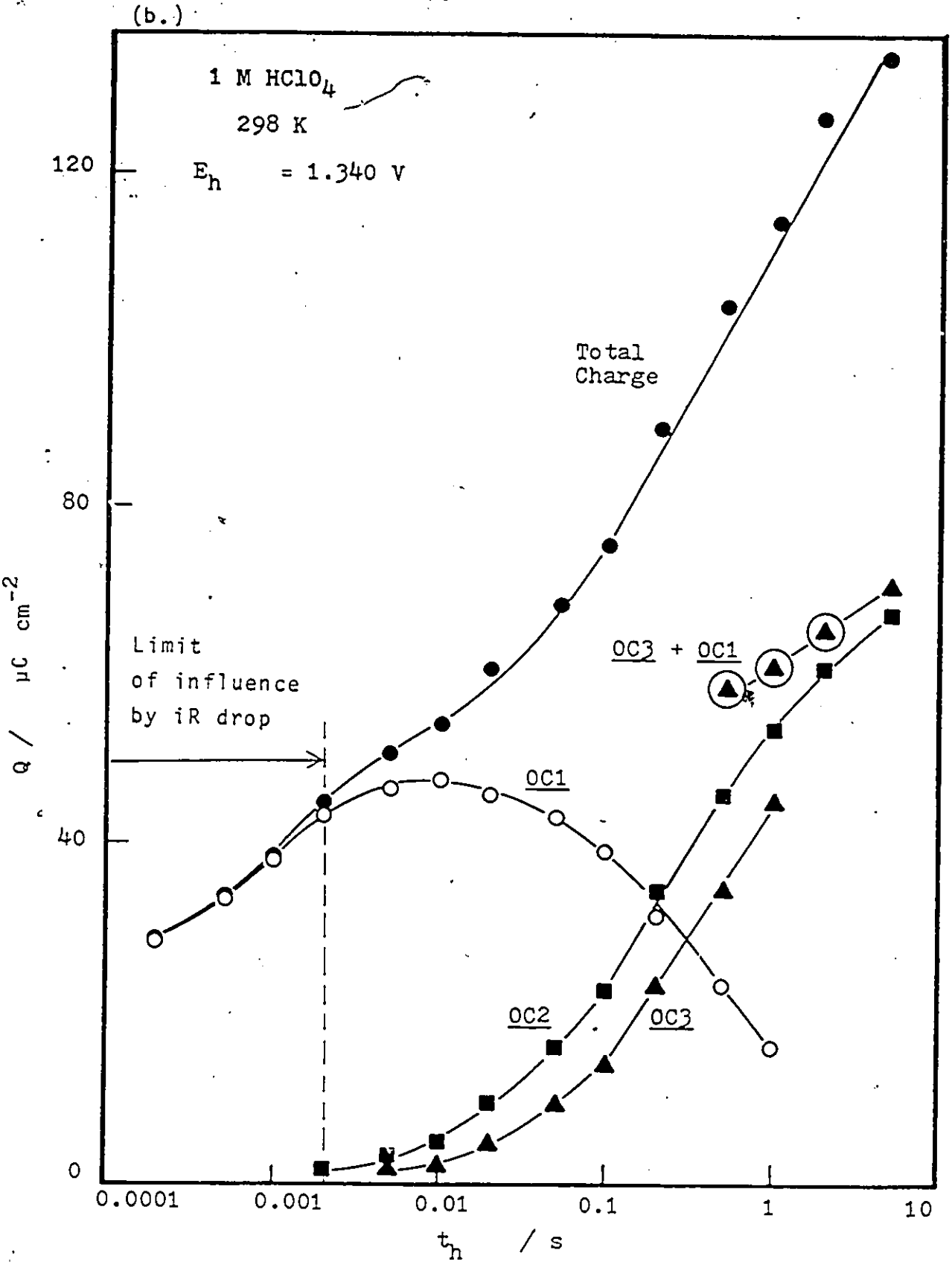
(b.)
1 M HClO4
298 K
Eh = 1.340 V
120
80
40
0
Q / µC cm-2
Total Charge
Limit of influence by iR drop
OC3 + OC1
OC1
OC2
OC3
0.0001
0.001
0.01
0.1
1
10
th / s

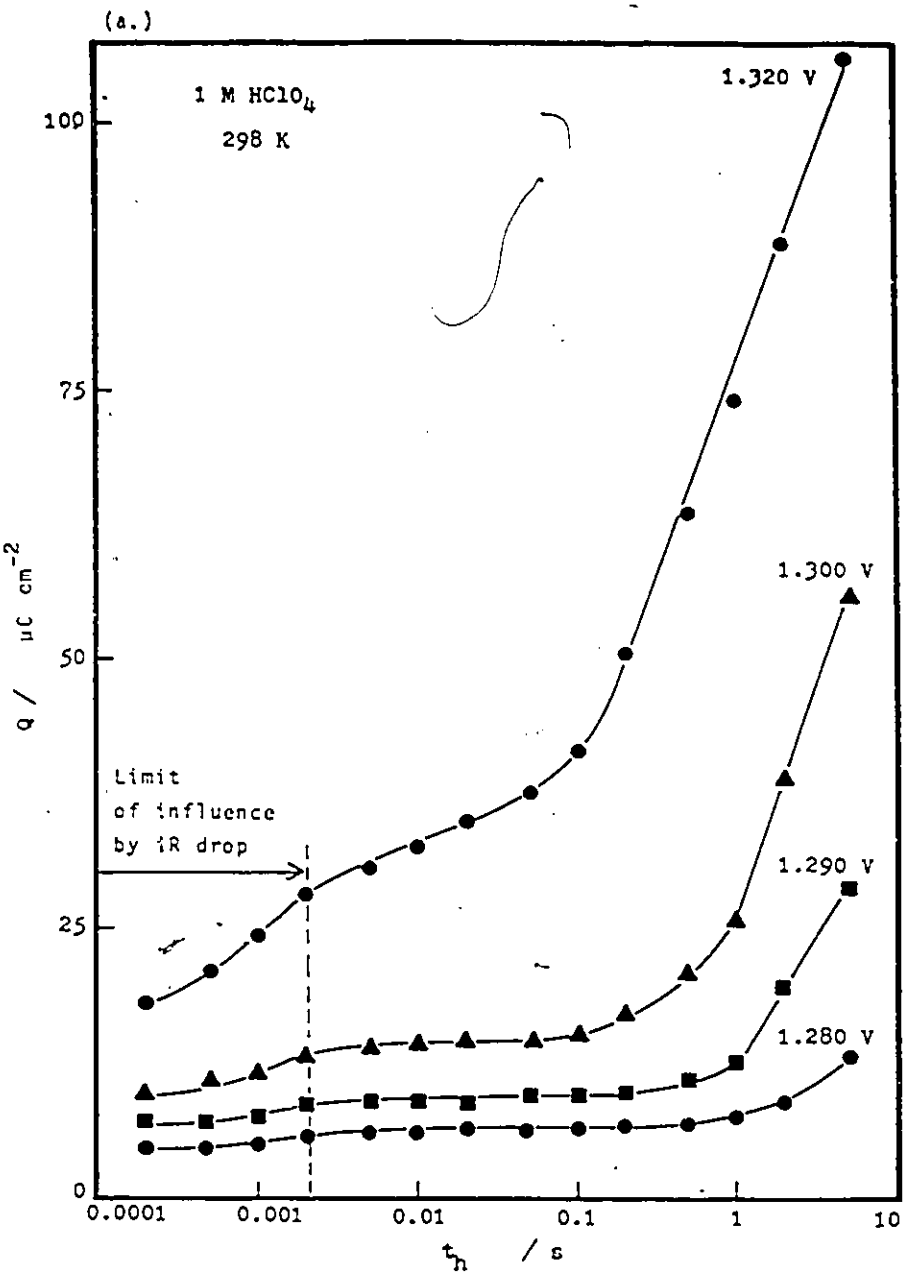

Figure 4.3.4. Variation of surface oxide charge formed at Au in 1 M $HClO_4$ at several E_h at 298 K for t_h from 0.0002 to 5 s.

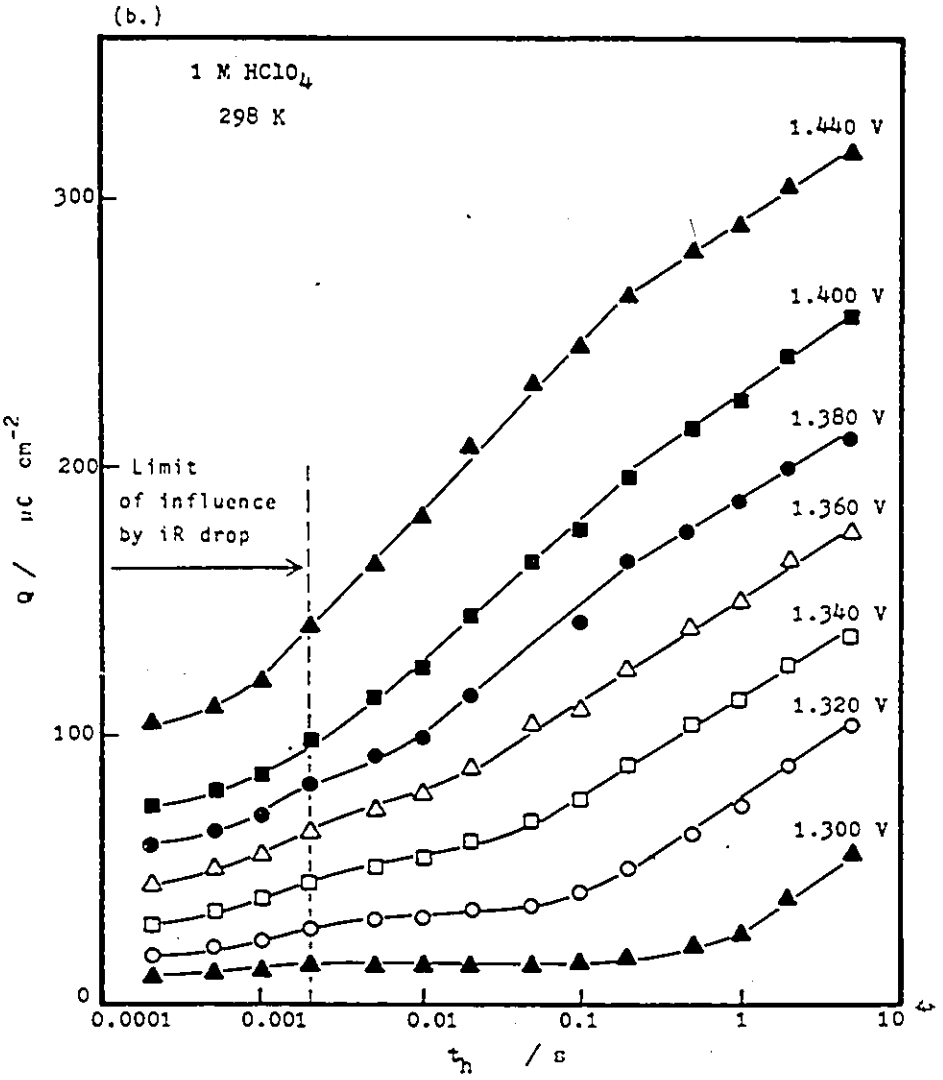
(b.)
1 M $HClO_4$
298 K
1.440 V
1.400 V
1.380 V
1.360 V
1.340 V
1.320 V
1.300 V
Limit
of influence
by iR drop
q / μC cm^{-2}
300
200
100
0
0.0001
0.001
0.01
0.1
1
10
t_h / s

growth at potentials less than 1.400 V. For growth potentials above 1.400 V, a plateau in growth is not found, while for longer holding times, growth is logarithmic. For growth at 1.440 V, two distinct logarithmic regions are seen, as was found in earlier work in this laboratory[5,6].

At this stage, it is useful to outline the phenomenology of the early stages of growth of surface oxide at Au in 1 M $HClO_4$ which can be summarized as follows; further details will be discussed later (Chapter V).

1. Reversible electrosorption of OH species arises first in between the weakly adsorbed ClO_4^- anions (OA1/OC1 peaks).
2. Conversion of the OC1 species occurs, giving rise to states of surface oxide that are reduced in the OC2 and OC3 peaks.
3. The species identified with the OC2 peak reaches a saturation coverage, while a direct logarithmic growth law applies to the species of the OC3 peak.

Values of peak potentials and maximum coverages (as O-species, 2 e/site) for the different stages of growth in this electrolyte are given in Table 4.3.1. The coverages for both the OC1 and OC2 peaks are larger than coverages of corresponding states in 0.5 M H_2SO_4 (see Table 4.4.1. in Section 4.4). The OC1 peak potential is less positive with respect to both the OC1 and the OC1' peaks in 0.5 M H_2SO_4. The OC3 and OC2 peak potentials are about 25 mV and 62 mV less positive, respectively, than those developed in 0.5 M H_2SO_4. This shows that the species associated with the OC2 peak are more sensitive to the nature of anions in the electrolyte than those of the OC3 peak, as was shown before.

Table 4.3.1.

Values of Peak potentials and Maximum or Saturation Coverages for Surface Oxide Formation in 1 M $HClO_4$ at 298 K

	θ_{max}*	E_p / V
OC1	0.34	1.285
OC2	0.40	0.875
OC3 (as θ_{OC3} -> 0)	no max.	1.040

* θ_{max} data are calculated here as coverages for OH-species (1 e/site).

4.3.2. Conversion of the Initial Reversibly Generated Surface Oxide to Other States

In 1 M $HClO_4$, the charge associated with the OC1 peak is easily separated from that for the main reduction peak, OC3, as species associated with the OC1 peak are converted to those the OC3 peak. This allows examination of this process in detail in this electrolyte; in particular, the kinetics of conversion process can be followed.

In order to quantify the conversion process, it is necessary to define the charge involved. This conversion charge, $Q_{con.}$, is defined as the maximum charge for the OC1 peak for the particular growth potential minus the OC1 charge at a particular time after the conversion process begins:

$$Q_{con.} = Q_{OC1,\ max.}(E) - Q_{OC1}(E,t)$$

This gives the charge for the OC1 species that has become converted (to OC3) after a particular time.

Figure 4.3.5. shows the charge associated with this conversion process plotted against holding time, t_h, for growth potentials of 1.320, 1.340 and

1.360 V. For holding times longer than 0.1 s, $Q_{con.}$ evidently follows a logarithmic relation with time, the slope of which increases with growth potential, an effect which can be due to either or both anion desorption and the oxygen/metal turn-over process, which is field dependent.

Growth of the surface oxide charge continues, however, as interconversion takes place. It is found that the OC1 charge when added to the OC3 charge is logarithmic in time (Figure 4.3.3.b., encircled triangles); therefore it is reasonable to assume that the disappearance of OC1 species is more closely related to the development of the species reduced in the OC3 peak than in the OC2 peak.

Figure 4.3.6. shows $Q_{OC3} - Q_{con.}$ (i.e. the increase in the charge for the OC3 peak that is not due to conversion) plotted against time on a logarithmic scale for growth at 1.320, 1.340, and 1.360 V. These plots show two distinct logarithmic regions, the slopes of which do not change with growth potential.

The slopes of $Q_{con.}$ and $(Q_{OC3} - Q_{con.})$ vs log(t) plots for the three growth potentials examined are given in Table 4.3.2.

Table 4.3.2.

Conversion of OC1 Species to OC3

E / V	$\frac{dQ_{con.}}{dt}$	$\frac{d(Q_{OC3} - Q_{con.})}{dt}$	
	$\mu C\ cm^{-2}$ / decade		
		region	
		1st	2nd
1.320	4.5	1.2	3.7
1.340	7.0	1.2	3.2
1.360	8.7	1.3	3.7

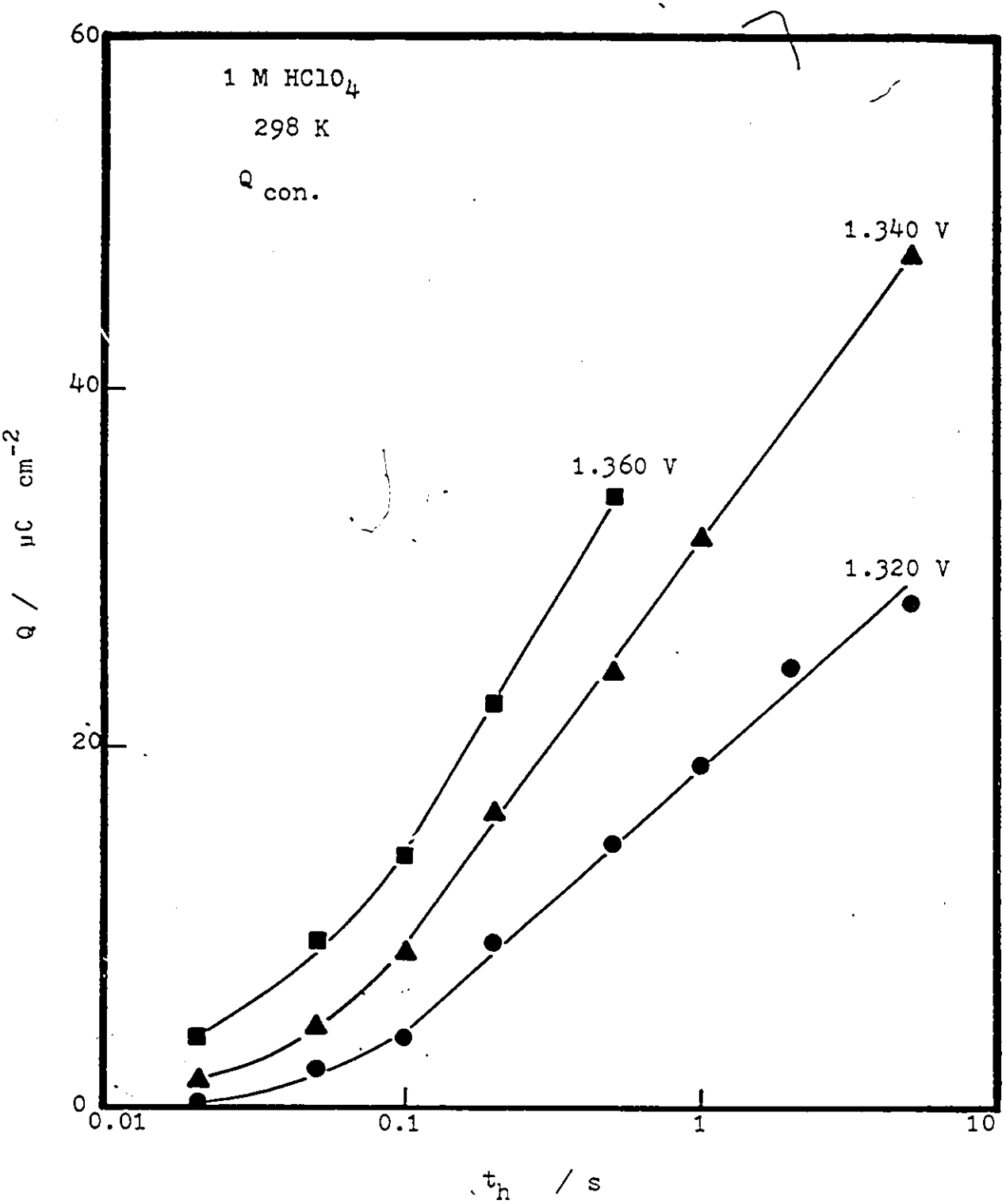

Figure 4.3.5. Q_{OC1} converted, $Q_{con.}$, to OC2 and OC3 as a function of t_h at 1.320 V, 1.340 V, and 1.360 V for oxide growth at Au in 1 M $HClO_4$ at 298 K.

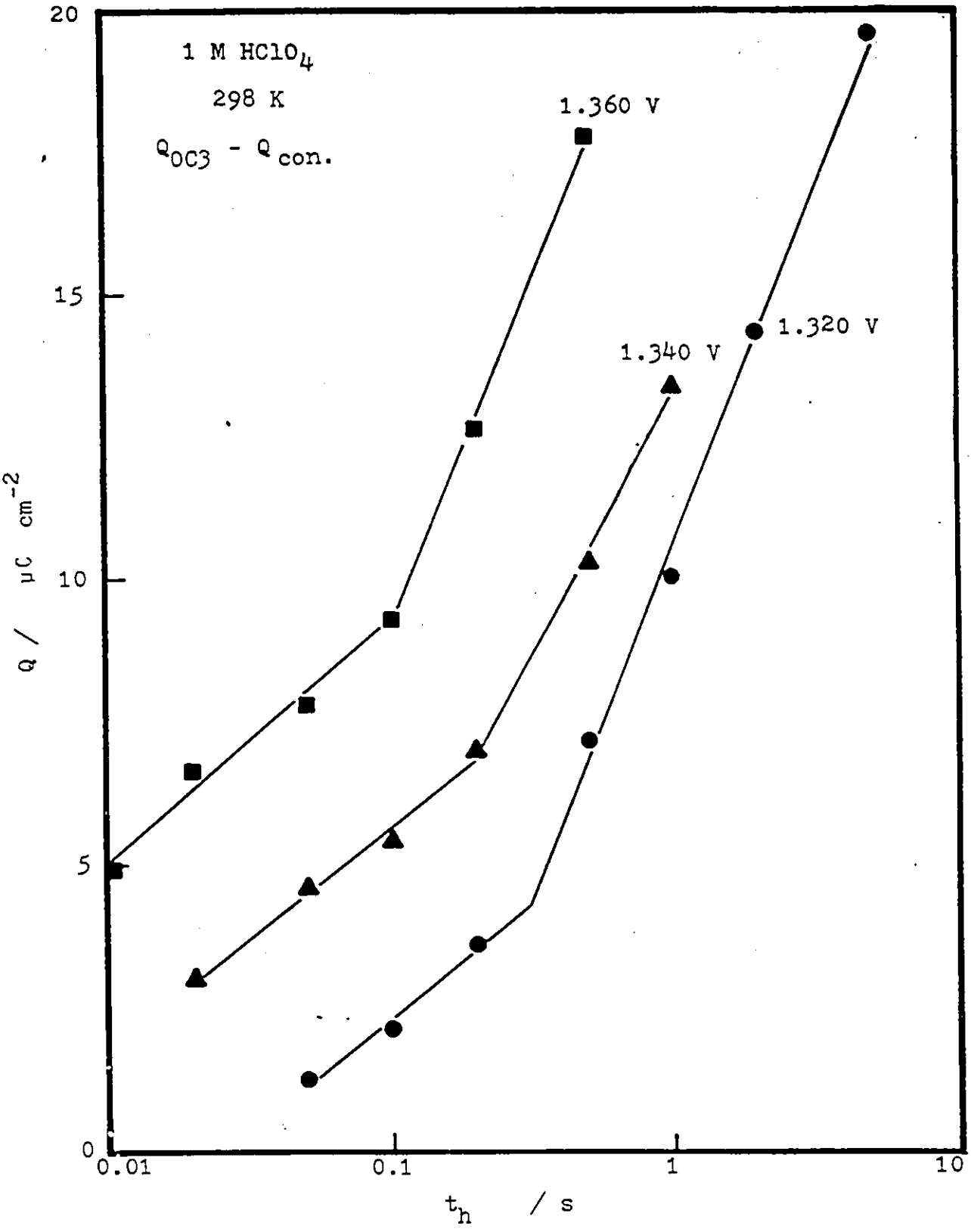

Figure 4.3.6. $Q_{OC3} - Q_{con.}$ vs t_h for oxide growth at Au in 1 M $HClO_4$ at 1.320 V, 1.340 V and 1.360 V, and 300 K.

4.4. Surface Oxide Growth in 0.5 M H_2SO_4

Although some previous work has been done on the various stages of surface oxide formation at gold electrodes in several different electrolytes[5-9], little work of this type has been conducted on the effects of changing temperature effects in the same electrolyte. A detailed examination was therefore undertaken of surface oxide growth at Au in 0.5 M H_2SO_4 at four temperatures, paying particular attention to the very early stages of monolayer formation (down to 0.2 $\mu C\ cm^{-2}$ in charge or $\theta_{OH} = 0.001$).

4.4.1. The Initial Stages of Surface Oxide Growth in H_2SO_4

The potential-time program used for surface oxide growth experiments in 0.5 M H_2SO_4 is shown in Figure 4.4.1.; it is similar, but not identical with that employed in the experiments in 1 M $HClO_4$. Initially, the potential was swept at 50 V s^{-1} to some potential, $E_B = 1.330$, just before the onset of surface oxide formation. This was followed by a very rapid sweep at 500 V s^{-1} to the growth potential, E_h; surface oxide formation *during* this sweep over the time period $(E_h-E_B)/s$ is minimized by use of such a high sweep rate, as was the case in the experiments in $HClO_4$. The growth potential was then held for a variable growth time, t_h, between 0.0002 and 5 s. Finally, the resultant surface oxide formed was reduced at 50 V s^{-1}. The portion of this potential-time program during which actual I *vs* E data were collected by the digital oscilloscope is shown by the part marked "b" in Figure 4.4.1.

A series of I *vs* E potentiodynamic profiles resulting from one of these surface oxide growth experiments is shown in Figure 4.4.2. In this particular case, the growth potential was 1.400 V and the temperature was 296 K. As previous studies of surface oxide growth in H_2SO_4 have shown[6], under certain conditions the reduction profiles are resolved into four peaks corresponding to distinguishable stages in surface oxide reduction, rather tnan the the three peaks observed in 1 M $HClO_4$ (Section 4.3.). This behavior arises because, with

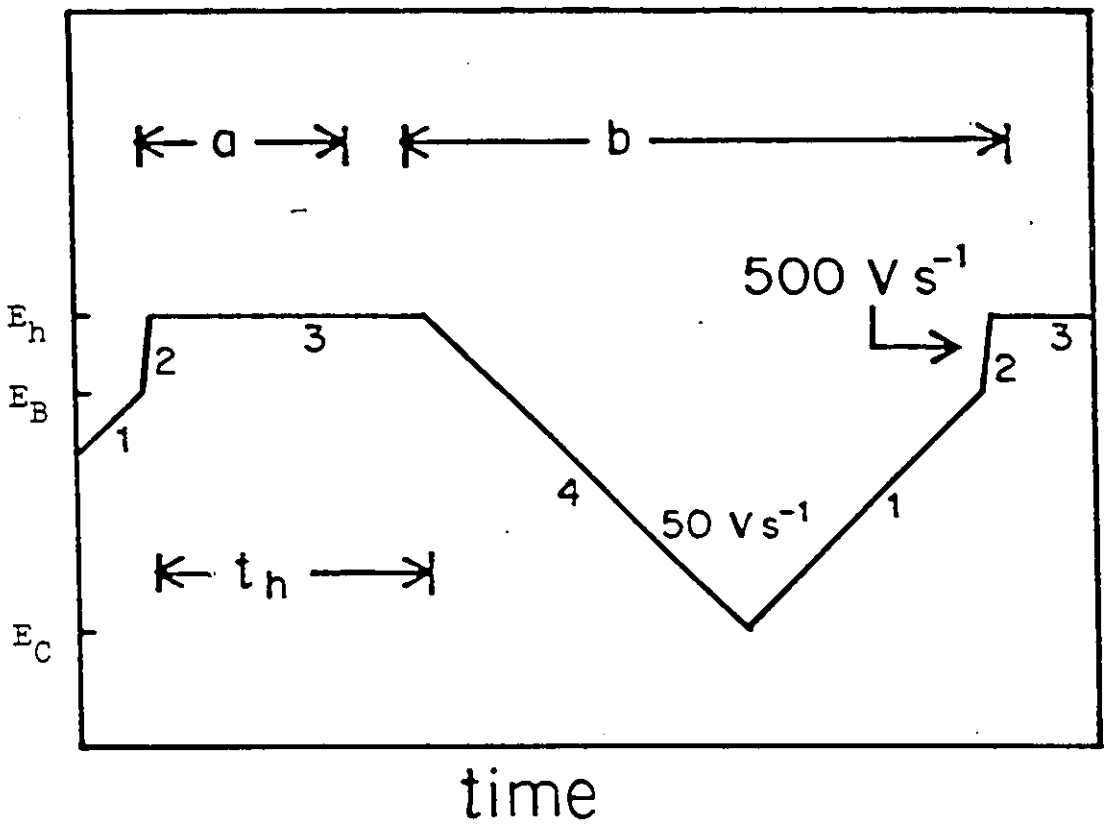

Figure 4.4.1 Potential-time program for studying surface oxide growth in 0.5 M H_2SO_4.

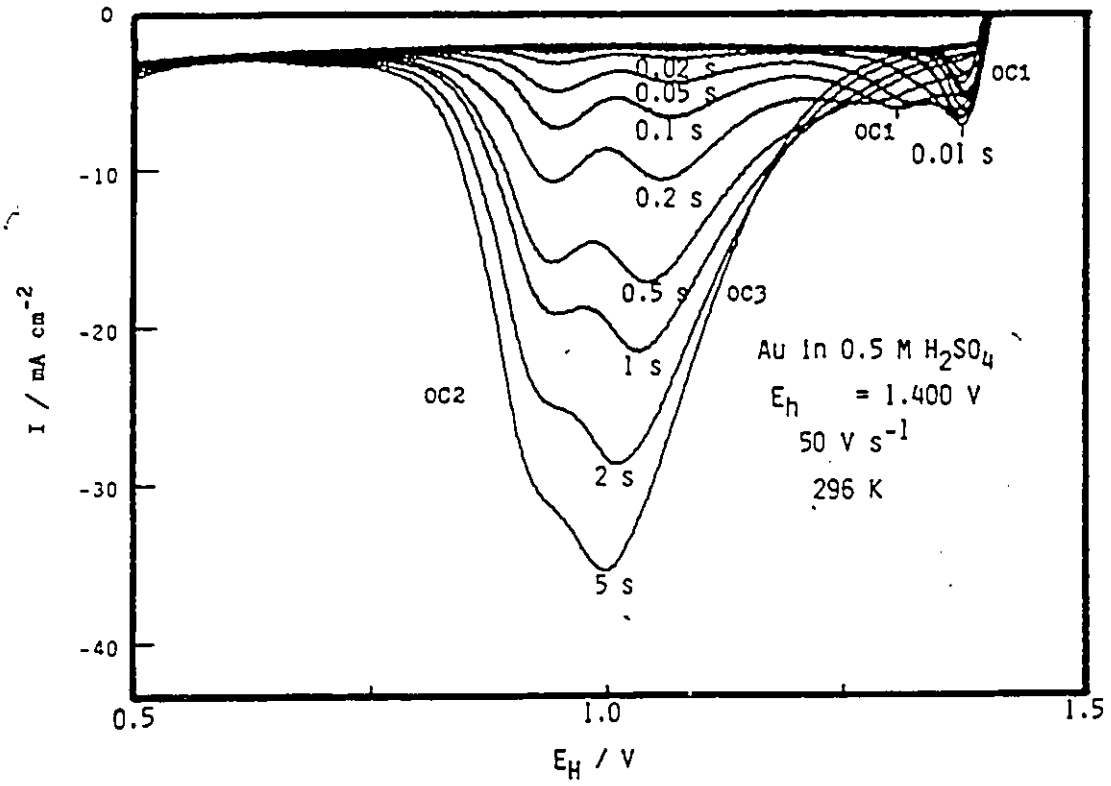

Figure 4.4.2. Series of potentiodynamic I vs E profiles for surface oxide growth at Au at E_h = 1.400 V and several t_h between 0.0002 and 5 s in 0.5 M H_2SO_4 at 296 K.

the more strongly adsorbed sulfate ions that are nearer full coverage than are ClO_4^- ions in 1 M $HClO_4$, the OC1 region is split into two components that overlap and depend on the environment of the adsorbed OH's, perhaps in patches with different coordination of the ions by OH's. The two components are designated here as OC1 and OC1'. In $HClO_4$, the same effect arises, but in a much less significant way. Also, owing to the stronger adsorption of sulfate than ClO_4^-, the OC2 peak grows comparably with OC3 at low coverages by OH (Figure 4.4.2.). Note also that in H_2SO_4, the surface oxidation process commences at more positive potentials than in $HClO_4$, so that the turn-over process (Section 4.1.) leading to the OC3 state occurs more rapidly than in ClO_4^- solutions.

Because of the overlap of many lines in Figure 4.4.2. in the OC1 region, the I vs E profiles in the initial reduction region are plotted on expanded potential and time scales, and split into three separate holding time ranges in Figures 4.4.3.a. through c. In these diagrams, it is easier to represent the growth and visualize the eventual conversion of the electrosorbed species associated with these two peaks to more stable states. It should be noted that these I vs E profiles correspond to very small coverages (5% or less of a monolayer of OH of surface oxide). During relatively short holding times, t_h = 0 to 0.005 s (Figure 4.4.3.a.), the reversible OC1 peak grows for reasons explained in Section 4.3.1. connected with iR effects. After 0.01 s (Figure 4.4.3.b.), the OC1 peak decreases and the OC1' peak starts to become larger. The OC1' peak shifts to less positive potentials with time and eventually (Figure 4.4.3.c.) it also decreases in charge as more stable states, characterized by reduction in the peaks, OC2 and OC3, grow.

Figure 4.4.4. shows integrated charges for the I vs E profiles shown in Figure 4.4.2 plotted against t_h on a logarithmic scale. The charges due to the OC1 and OC1' peaks are plotted in Figure 4.4.4.a. and those for OC2, OC3 and

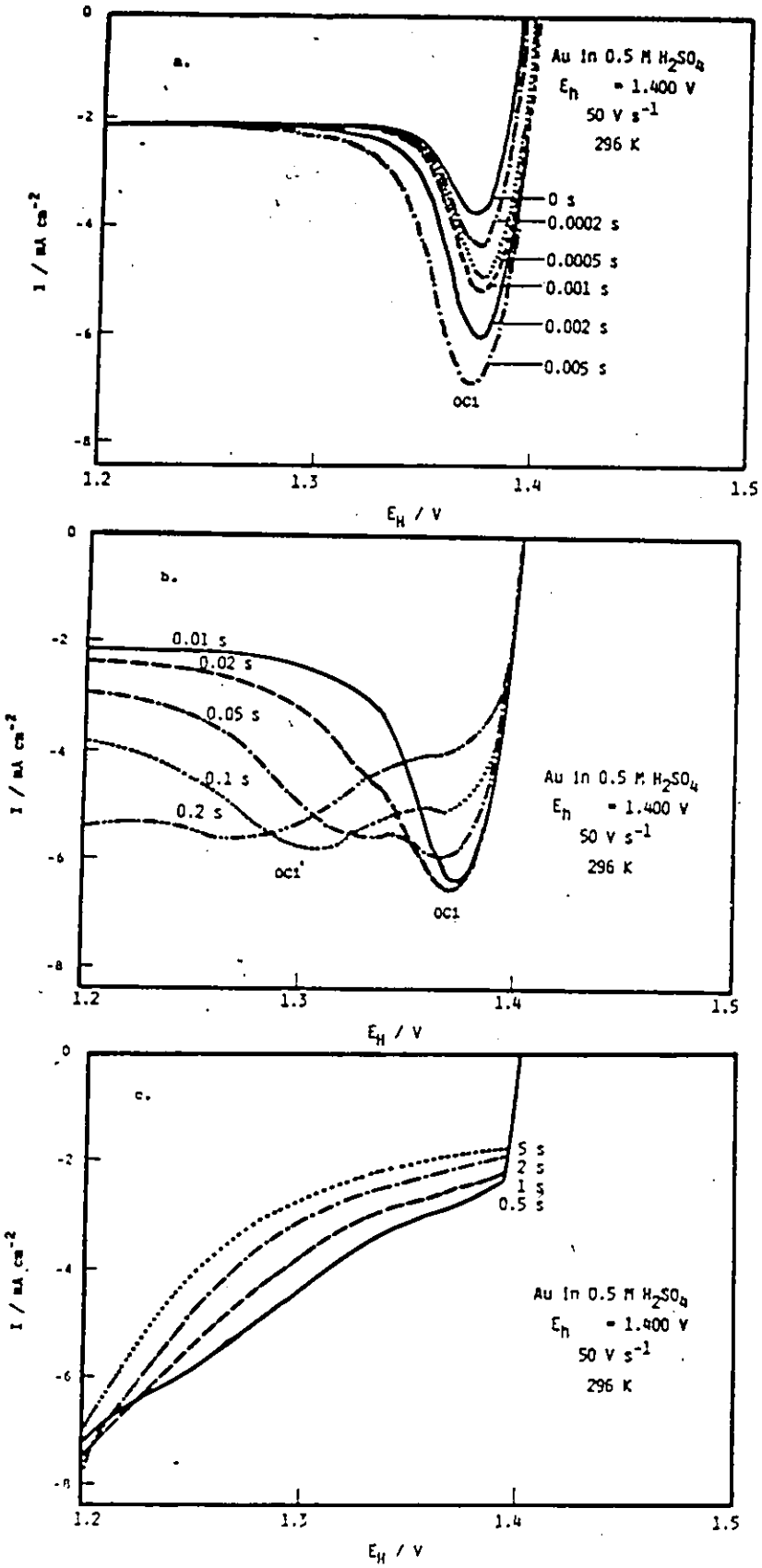

Figure 4.4.3. Potentiodynamic I vs E profiles showing the growth and disappearance of OC1 and OC1' at Au at E_h = 1.400 V in 0.5 M H_2SO_4 at 296 K with ranges of t_h of (a.) 0.0002 to 0.005 s; (b.) 0.01 to 0.2 s; (c.) 0.1 to 5 s

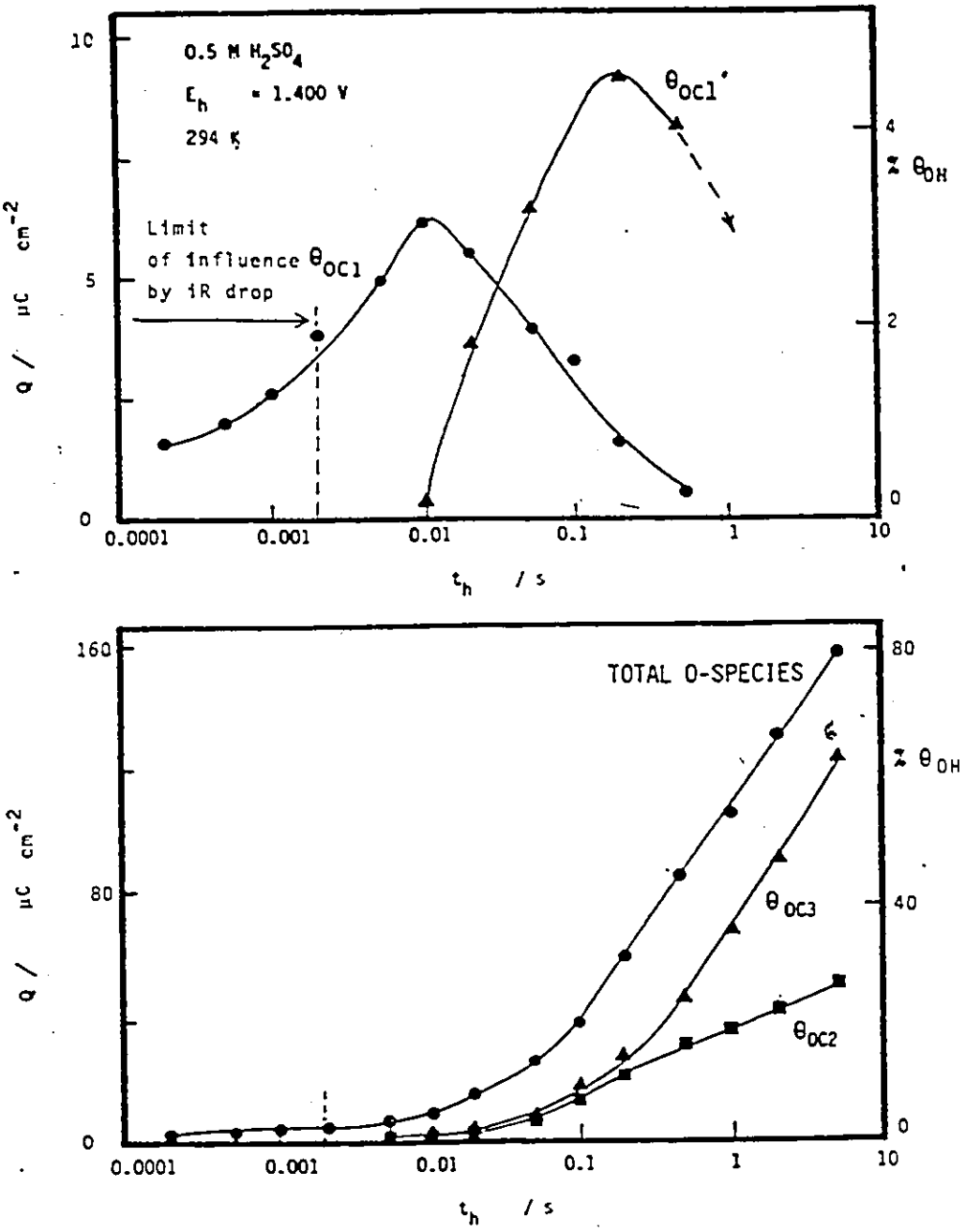

Figure 4.4.4. Variation of surface oxide charge formed at Au in 0.5 M H_2SO_4 at 1.400 V and 296 K for t_h from 0.0002 to 5 s. (a.) OC1 and OC1'; (b.) OC2, OC3 and total surface oxide charge.

total O-species in Figure 4.4.4.b.

As was also found with 1 M $HClO_4$ (Section 4.3.), the charge associated with the OC1 peak increases with t_h due initially to the iR drop effect, then at t_h = 0.01 s (Figure 4.4.4.a.) it reaches a maximum of ca. 6 μC cm^{-2} . No plateau is found in the plot of OC1 charge vs t_h is seen at this potential as is observed with 1 M $HClO_4$ (Figure 4.3.3.a. and b.). For t_h values greater than 0.01 s, the OC1' charge first increases but, after 0.2 s, the OC1' charge also decreases. As the surface oxide is converted to the OC2 and OC3 states for times longer than 0.5 s, the OC1' peak is not separated from the OC3 peak.

The total surface oxide charge and that component due to the OC3 state grow initially in a non-logarithmic manner, followed by logarithmic growth typical of development of surface oxide on Au in general[5,6]. Initially, the OC3 and OC2 peaks grow at the same rate, but, at longer t_h, the OC2 peak grows more slowly and eventually reaches a saturation charge of about 60 μ C cm^{-2}.

In terms of the above results, the processes involved in the early stages of surface oxide growth in 0.5 M H_2SO_4 (compare Section 4.3.1. for $HClO_4$) can be summarized as follows:

1. Reversible electrosorption of OH species between adsorbed anions (OA1/OC1 peaks).
2. Conversion of the OC1 species to states of surface oxide that are reduced in the OC3 peak, causing some desorption of the anions, in turn allowing relaxation to a new co-adsorbed anion/OH layer, with diminished coverage of anions, reduced in the OC1' peak (to be further discussed in Chapter V), and also the electrosorption of OH at vacancies left by the anions, such states of OH being reduced in the OC2 peak.
3. Completion of the conversion of the OC1 type surface oxide states (with continuing desorption of the anions) to states that are reduced

in the OC2 and OC3 peaks.

4. Saturation of the state corresponding to the OC2 peak and growth of the OC3 species in a logarithmic way with time.

4.4.2. Comparison of Methods for Measuring the Total Surface Oxide Charge

Figure 4.4.5. shows total surface oxide charge measured by two different methods for Au electrodes in 0.5 M H_2SO_4 at 296 K at a growth potential of 1.400 V. The circular points represent surface oxide charges that were measured in the usual way, that is by integrating the I vs E reduction profiles (with subtraction of appropriate double-layer charges) after holding at the growth potential for a particular time. The solid line represents data obtained by continuous integration of I vs time data obtained while the potential is held constant for the growth condition being studied. In order to do this, data had to be collected with the digital oscilloscope during potential holding (portion "a" of the potential-time profile shown Figure 4.4.1.).

Total surface oxide charge values determined by the two methods of measurement agree very well. This indicates that the two procedures are consistent and that the experimental cell and the solution were free of any impurities which could interfere with surface oxide formation. For example, if appreciable concentrations of electrochemically active impurities had been present, extra some charge due to their oxidation would have been observed during potential holding.

4.4.3. The Initial Stages of Surface Oxide Formation at 1.430 V and 294 K

It is of interest to examine the dependence of the OC1 and OC1' charges and peak potentials as a function of time for changes of OH charge at Au in 0.5 M H_2SO_4 at 294 K and a growth potential of 1.430 V; this is done in Figure

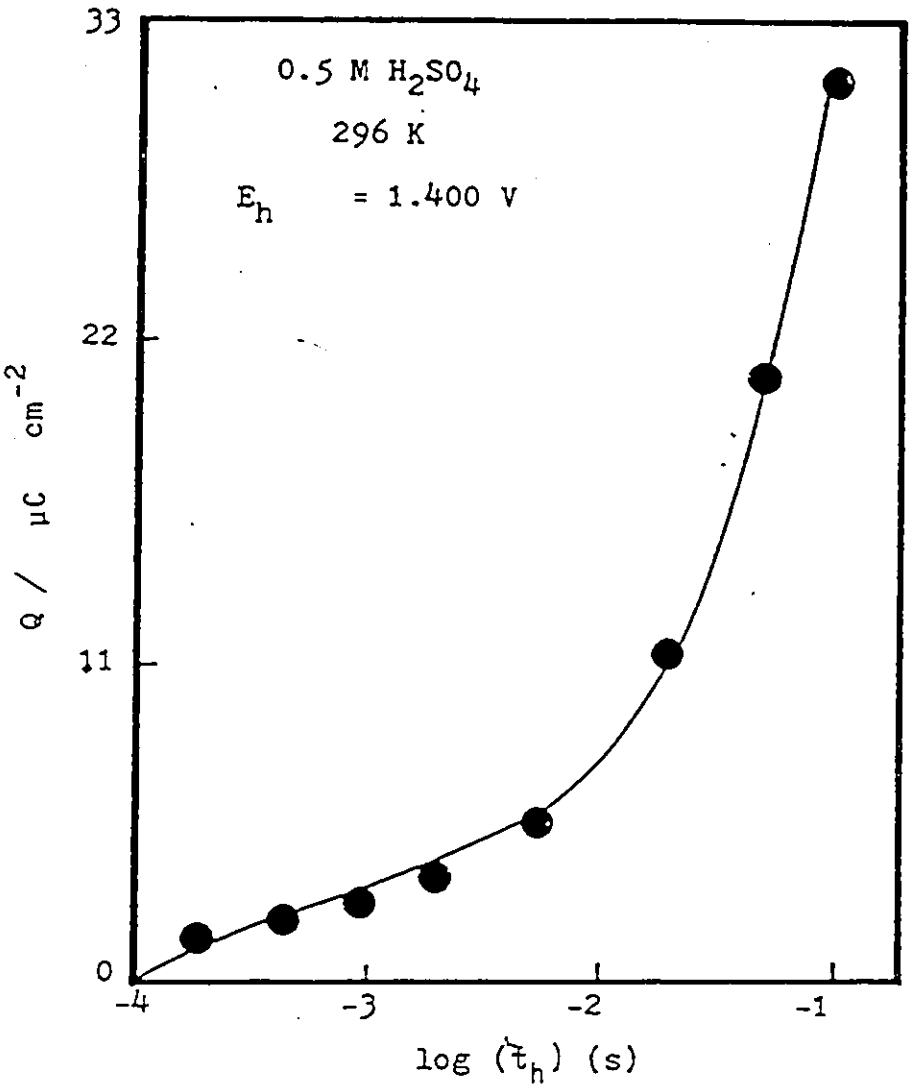

Figure 4.4.5. Total surface oxide charge at Au at E_h = 1.400 V in 0.5 M H_2SO_4 at 296 K calculated by integrating reduction I vs E profiles after potential holding (circular points) and current decay vs time during potential holding (solid line).

4.4.6. on a logarithmic scale for t_n as also in Figure 4.4.7., which shows similar information for the OC2 and OC3 peaks. These particular growth conditions were chosen because the OC1 and OC1' peaks are still clearly distinguished and the OC2 charge reaches saturation before 2 s. The corresponding potentiodynamic I vs E profiles are shown in Figure 4.4.8.c.

At this growth potential, 1.430 V, the OC1 peak attains a maximum charge of 15 $\mu C\ cm^{-2}$, after a growth period of 0.005 s, and then begins to decrease in the usual way (compare Figure 4.3.3. for Au in 1 M $HClO_4$). This maximum charge is greater than it is at 1.400 V, and the decrease in the charge under this peak occurs after a shorter time than it does at the lower growth potential. The maximum charge associated with the OC1 peak for a particular potential increases with potential until this peak charge reaches an ultimate maximum (about 21 $\mu C\ cm^{-2}$ at 294 K) for the electrolyte solution and temperature being studied. Also, the OC1 species begin to become converted to other surface oxide species after a shorter growth time with higher potential, as is also seen in $HClO_4$. It should be noted that the encircled OC1 and OC1' charge points in Figure 4.4.6. represent estimated values, a situation which arises because the OC1 and OC1' peaks could not be properly separated; however, the total OC1 charge (i.e. for OC1 + OC1') could be measured reliably. Again, the OC1' peak appears as the OC1 peak stops growing and begins to decrease. Unfortunately, the final decrease of the OC1' peak after $t_n > 0.1$ s cannot be shown because the OC1' peak could not then be resolved from the OC3 peak.

The OC1 peak potential shifts to less positive potentials with time and increasing total surface oxide charge, an effect that probably arises because the influence of the adsorbed anions upon the potential of this peak decreases as the coverag of surface oxide increases, leading to smaller co-adsorption of the anions. When the OC1' peak appears beyond 0.002 s, the interpretation is that the anions are being desorbed and new states of coordination between OH,

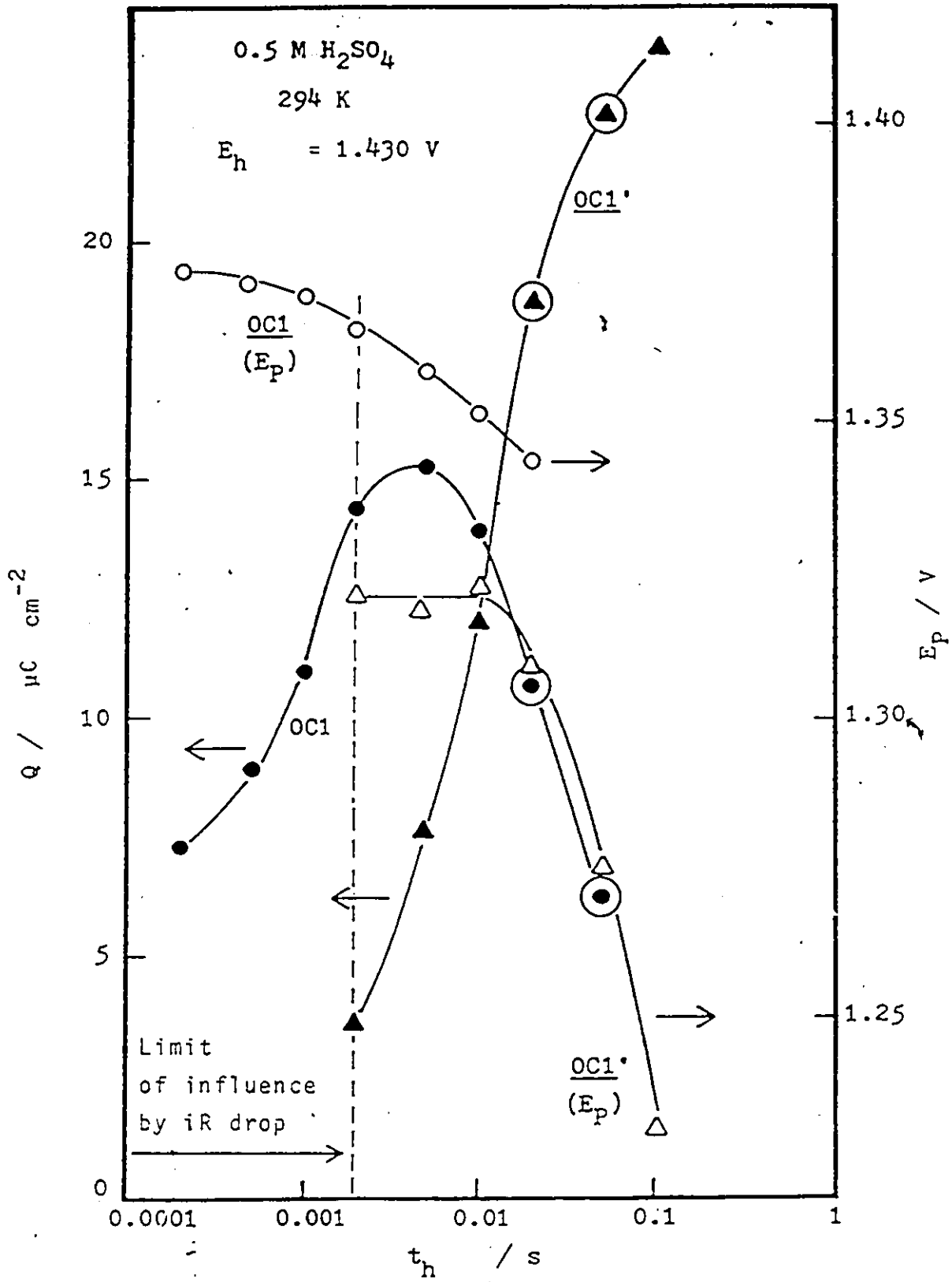

Figure 4.4.6. Surface oxide charge and peak potentials for OC1 and OC1' at Au at E_h = 1.430 V in 0.5 M H_2SO_4 at 296 K.

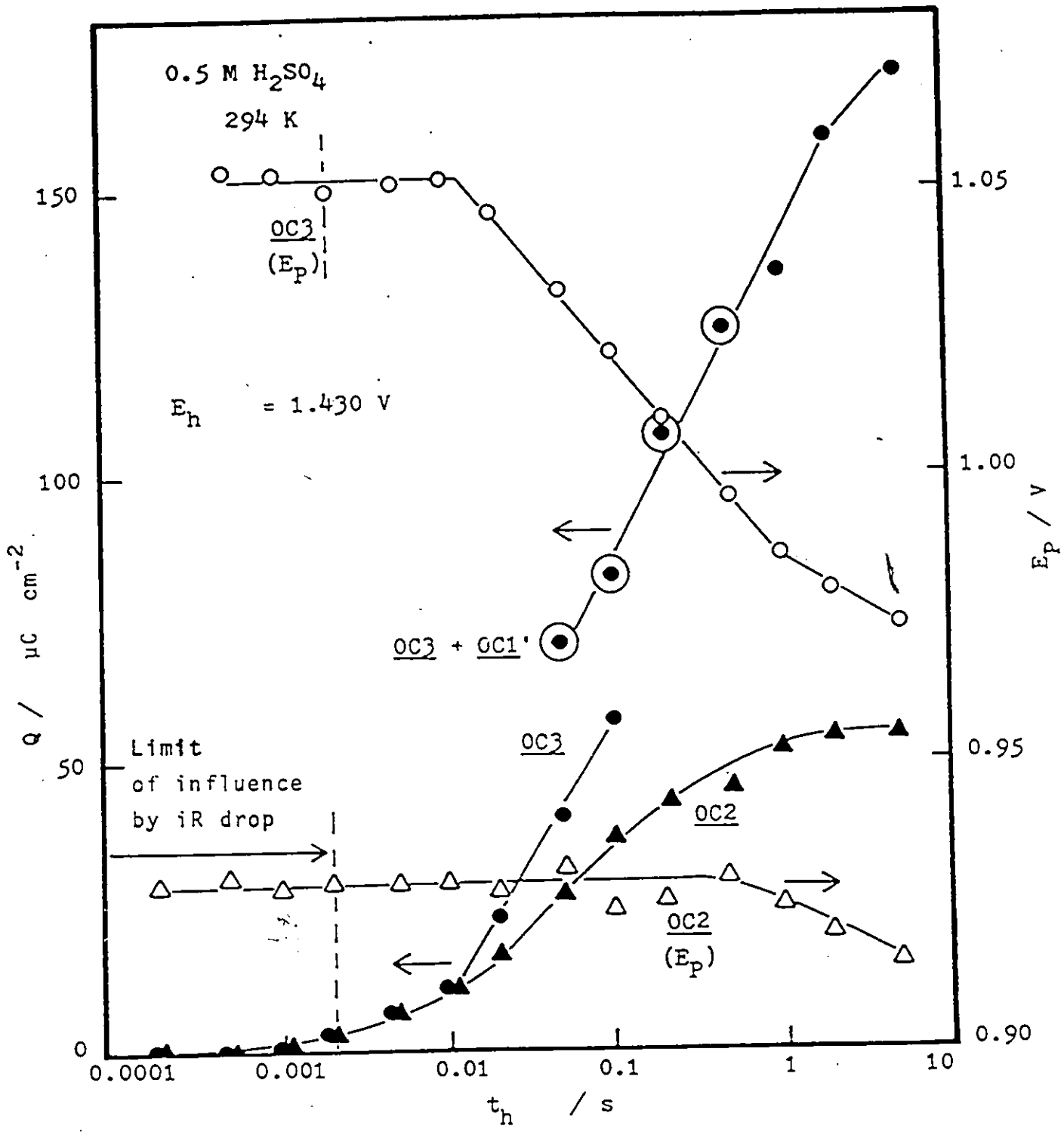

Figure 4.4.7. Surface oxide charge and peak potentials for OC2 and OC3 at Au at E_h = 1.430 V in 0.5 M H_2SO_4 at 296 K.

remaining anions and water molecules arise. The OC1' peak potential also shifts to less positive potentials with time and surface oxide coverage, but to a greater extent than does OC1. This is possibly due to the decreasing influence of anions.

As mentioned previously, the OC2 and OC3 peaks initially increase at similar rates. For times greater than 0.01 s at this particular growth potential, the OC3 peak starts to grow logarithmically in time. The OC2 peak, however, increases only until it reaches its saturation charge, here about 60 $\mu C\ cm^{-2}$. The encircled OC3 charge values represent the sum of the OC1' and the OC3 charges. For t_h = 0.2 and 0.5 s, the OC1' and OC3 charges could not be resolved from each other; however for t_h = 0.05 and 0.1 s, the OC1' and OC3 charges were deliberately added together. It is significant that these composite OC1' + OC3 charges then fit a logarithmic growth relation quite well (Figure 4.4.7.). This indicates that the logarithmic growth of the OC3 peak and the decline of the OC1' peak are closely related, as was also concluded for oxide growth in 1 M $HClO_4$ (see Section 4.3.).

In contrast, the OC2 peak potential does not shift with either coverage or time (Figure 4.4.7.), as is also seen for the OC1 peak in dillute acid solution[6]. This indicates, from general principles, that the OC2 state is generated in a simple surface reaction that is at equilibrium, since the coverage by this species remains independent of t_h over 3 decades of time. The apparent shift in peak potential at longer holding times is due to the fact that the OC2 peak becomes obscured by the growing OC3 peak, making the peak potentials difficult to determine. The OC3 peak potential does not change significantly with time while the OC3 peak remains still relatively small, but it does shift to less positive potentials and logarithmically with growth time, as well as linearly with peak charge, when the OC3 species are growing logarithmically in time at the Au surface.

4.4.4. Surface Oxide Growth at Various Temperatures

Potentiodynamic I vs E profiles for surface oxide growth in 0.5 M H_2SO_4 at 274, 283, 294 and 319 K and at growth potentials between 1.430 and 1.435 V are shown in Figures 4.4.8.a. through d. A summary of the results in terms of the peak potentials and maximum charges, as coverages, θ_{OH}, for the different stages of growth at the four temperatures is given in Table 4.4.1.

Several characteristics of the growth and reduction profiles change with temperature. Surface oxide grows more quickly at higher temperatures, as is to be expected. The states characterized by the OC1 and OC1' peaks also become converted to those that are reduced in the OC2 and OC3 peaks more rapidly with increasing temperature, and this is probably the reason for the decrease of the maximum observed OC1 charge (OC1 + OC1') with increasing temperature. Generally, of course, all the related surface processes involved here will tend to increase in rate with the increase of temperature, but not necessarily to the same extents.

In general, as temperature is increased, the anodic oxidation process takes place at less positive potentials than at lower temperature and, correspondingly, the cathodic processes are observed at more positive potentials, i.e. there is less apparent hysteresis between the processes for oxide formation and reduction. Such behavior is found at other noble metals also.

At Au, in particular, this effect is exemplified by a slight shift of the OC1 peak potential to less positive values with increasing temperature, and this corresponds to a similar shift of the reversible OA1 peak with temperature (not shown), since the processes corresponding to the OA1/OC1 peaks is reversible. It is to be expected that the SO_4^{2-} (HSO_4^-) anions would adsorb less strongly with increasing T, allowing the OA1/OC1 species to be formed at lower energy.

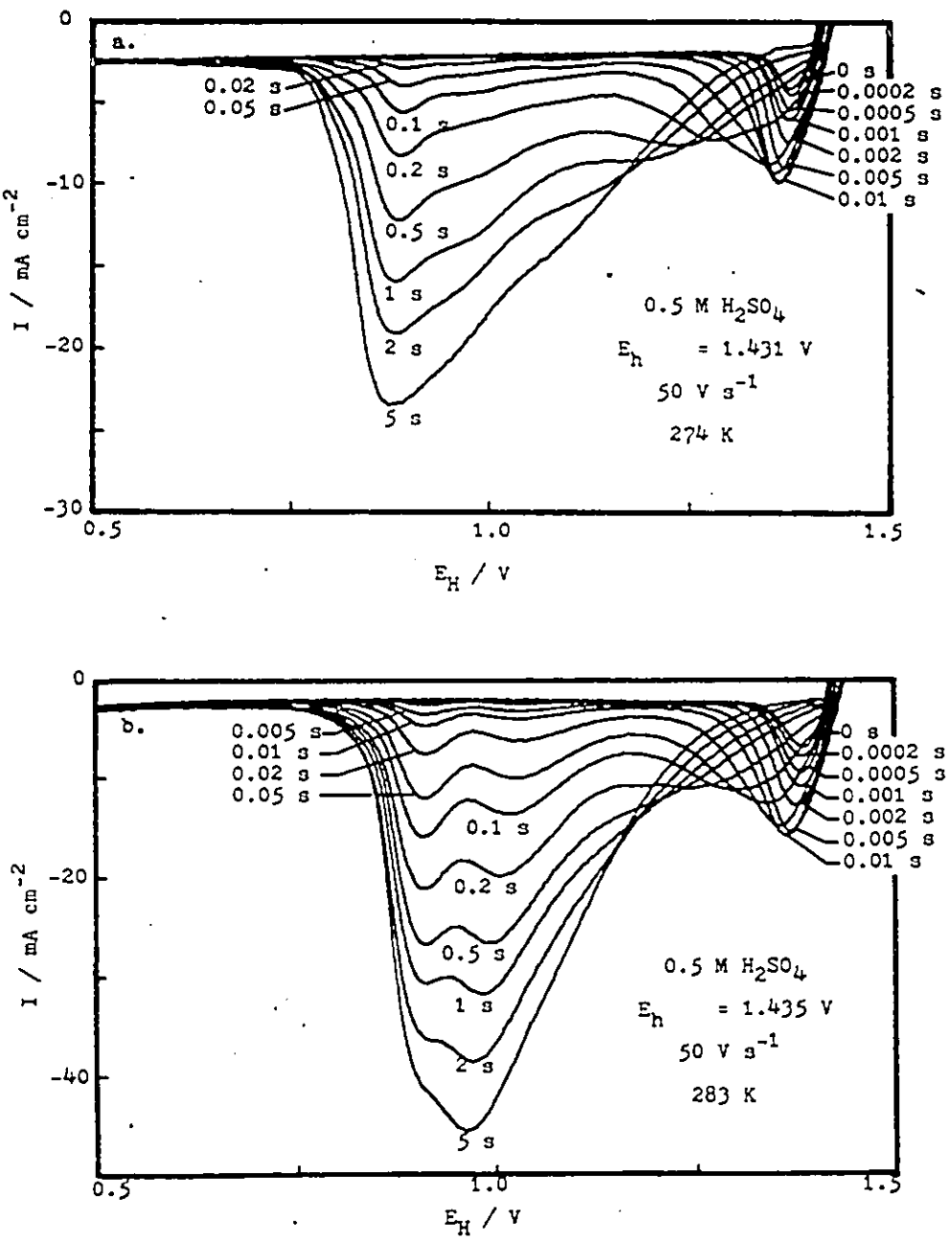

Figure 4.4.8. Series of potentiodynamic I vs E profiles for surface oxide growth at Au at several t_h between 0.0002 and 5 s in 0.5 M H_2SO_4. (a.) 1.431 V and 274 K; (b.) 1.435 V and 283 K; (c.) 1.430 V and 294 K; (d.) 1.435 V and 319 K.

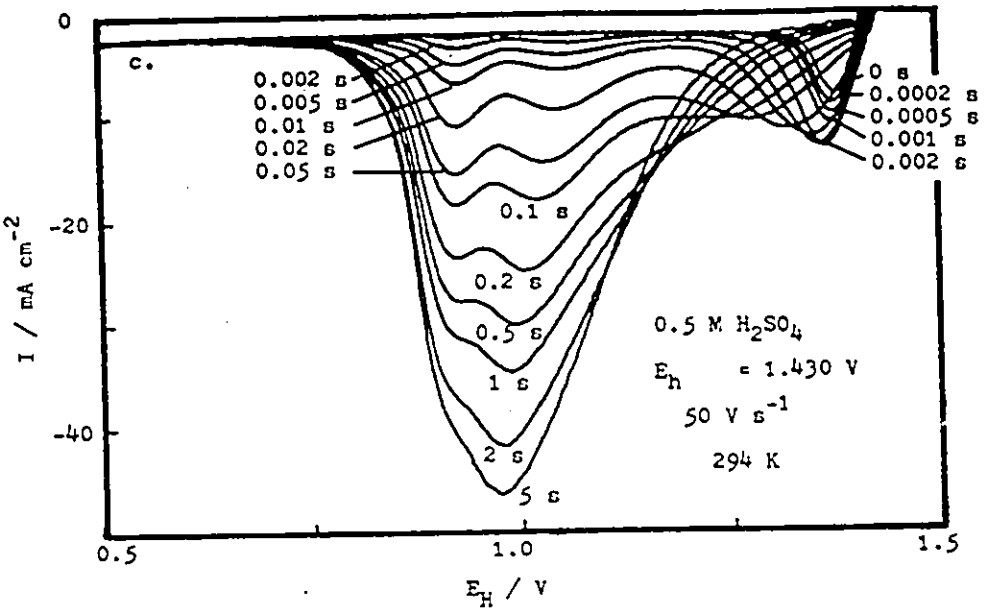
c.
0
-20
-40
I / mA cm^{-2}
0.002 s
0.005 s
0.01 s
0.02 s
0.05 s
0.1 s
0.2 s
0.5 s
1 s
2 s
5 s
0 s
0.0002 s
0.0005 s
0.001 s
0.002 s
0.5 M H_2SO_4
E_h = 1.430 V
50 V s^{-1}
294 K
0.5
1.0
1.5
E_H / V

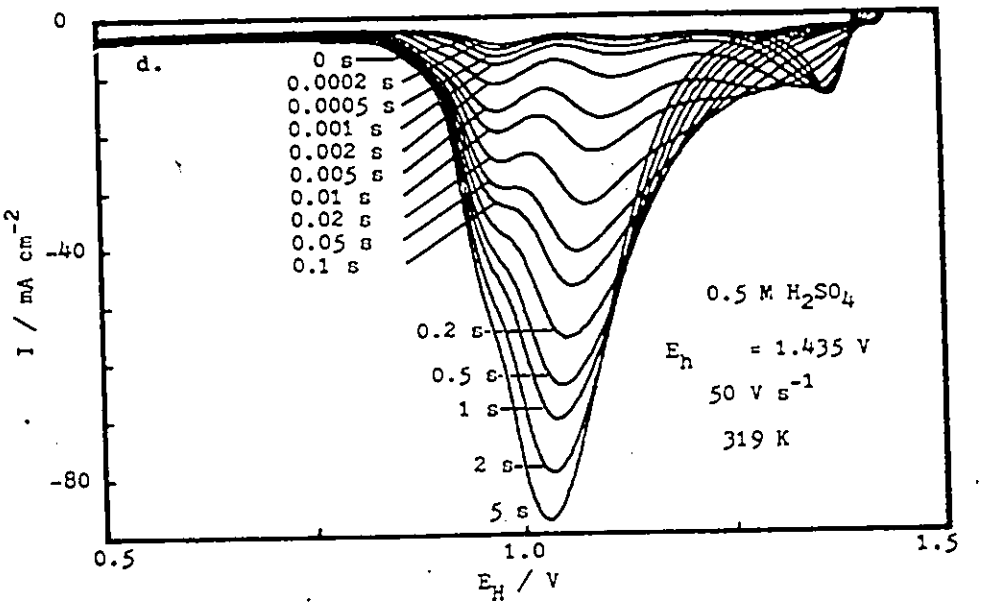
d.
0
-40
-80
I / mA cm^{-2}
0 s
0.0002 s
0.0005 s
0.001 s
0.002 s
0.005 s
0.01 s
0.02 s
0.05 s
0.1 s
0.2 s
0.5 s
1 s
2 s
5 s
0.5 M H_2SO_4
E_h = 1.435 V
50 V s^{-1}
319 K
0.5
1.0
1.5
E_H / V

Table 4.4.1.

Summary of Oxide Growth Behavior in 0.5 M H_2SO_4 at Four Temperatures

T / K	274	283	294	319
OC1				
θ_{max}*	0.26	0.30	0.26	0.18
OC1 + OC1'				
E_p / V				
OC1	1.378	1.380	1.375	1.372
OC1'	1.300	1.305	1.320	1.330
OC2				
θ_{max}*	--	0.28	0.30	0.26
E_p / V	0.890	0.913	0.930	0.975
OC3				
E_p / V (as $\theta_{OC3} \rightarrow 0$)	0.975	1.035	1.055	1.120

* θ_{max} data are calculated here as coverages for OH-species (1 e/site)

The OC1' peak shifts to more positive potentials with increasing temperature. The OC2 and OC3 peaks (as Q_{OC3} -> 0) also shift in the same direction with temperature; this effect is, of course, probably due to increases in reduction rates with temperature for these species. The OC2 peak potential changes linearly with temperature (about 1.84 mV K^{-1}), while the OC3 potential changes in a more complex way with temperature. than linearly.

The saturation coverage of the OC2 species does not seem to change significantly with temperature. At 274 K, the saturation coverage of the OC2 species could not, however, be measured because the peak is not sufficiently separated from that for the OC3 species. Also, the OC2 peak current and width do not seem to change appreciably with temperature. However, the OC3 peak becomes higher and narrower with increasing temperature. At the lower temperatures, the OC2 and OC3 peaks are relatively close together, while at higher temperatures, the converse occurs.

Figures 4.4.9.a through d. show total surface oxide charge plotted against time on a logarithmic scale for growth at several potentials for the four temperatures examined. In general, these growth curves show three distinct growth regions, as was found in earlier work[6]. Surface oxide growth at Au in 0.5 M H_2SO_4 occurs initially in a non-logarithmic way in time, which will be discussed in more detail later. This is followed by two logarithmic regions, as observed for each of the temperatures of the experiments. As stated earlier, surface oxide grows faster with increasing temperature; moreover, the non-logarithmic and the first logarithmic growth regions also last for shorter durations on the growth time scales at higher temperatures.

It should be noted that the surface oxide charges determined in this work are somewhat higher than those in the earlier work[6]. This is probably because the Au electrodes used in this work have a significantly different surface structure on a atomic level from those used before. Thus, surface crystallinity

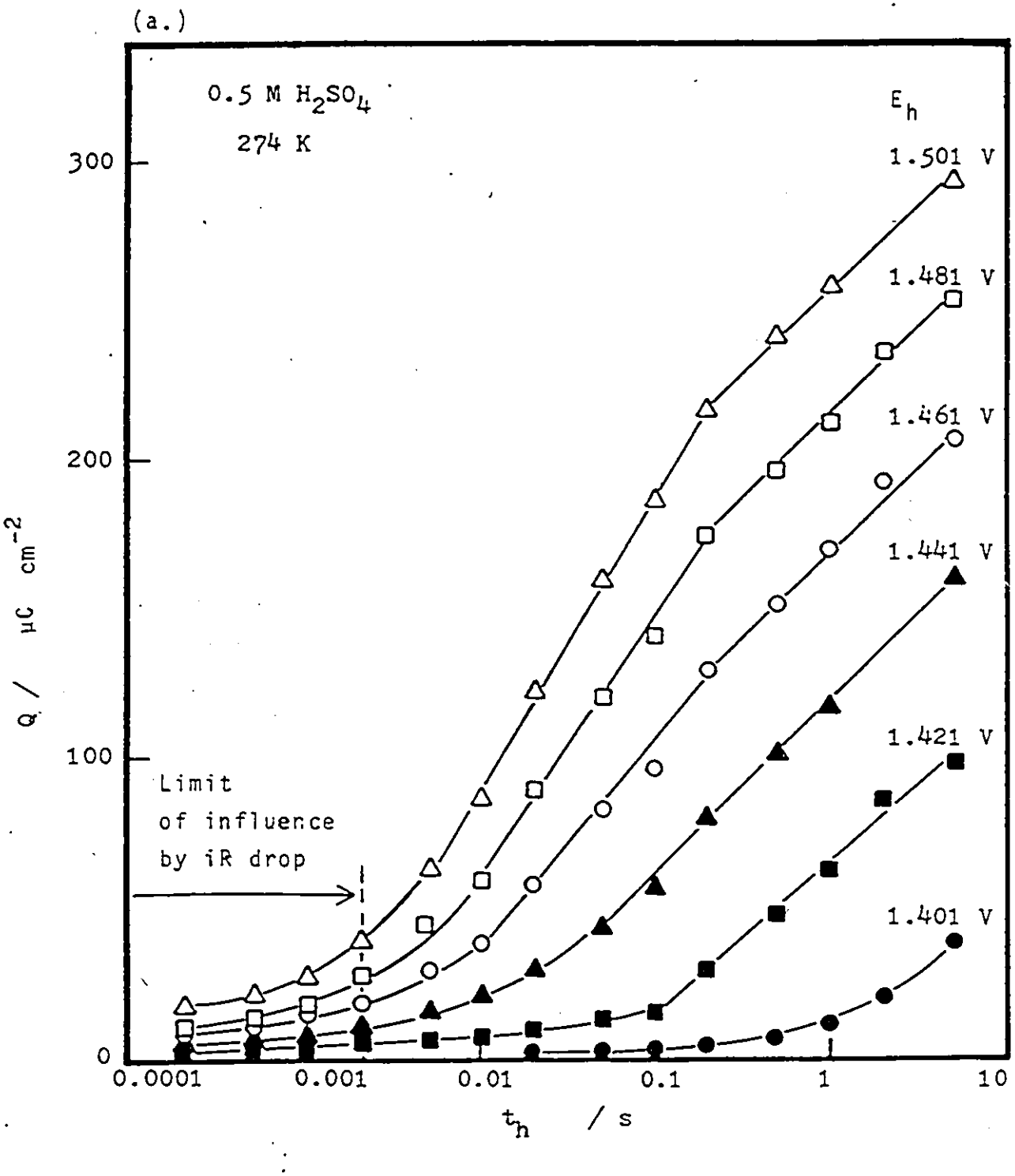

Figure 4.4.9. Variation of surface oxide charge formed at Au in 0.5 M H_2SO_4 at several E_h for t_h from 0.0002 to 5 s. (a.) 274 K; (b.) 283 K; (c.) 294 K; (d.) 319 K.

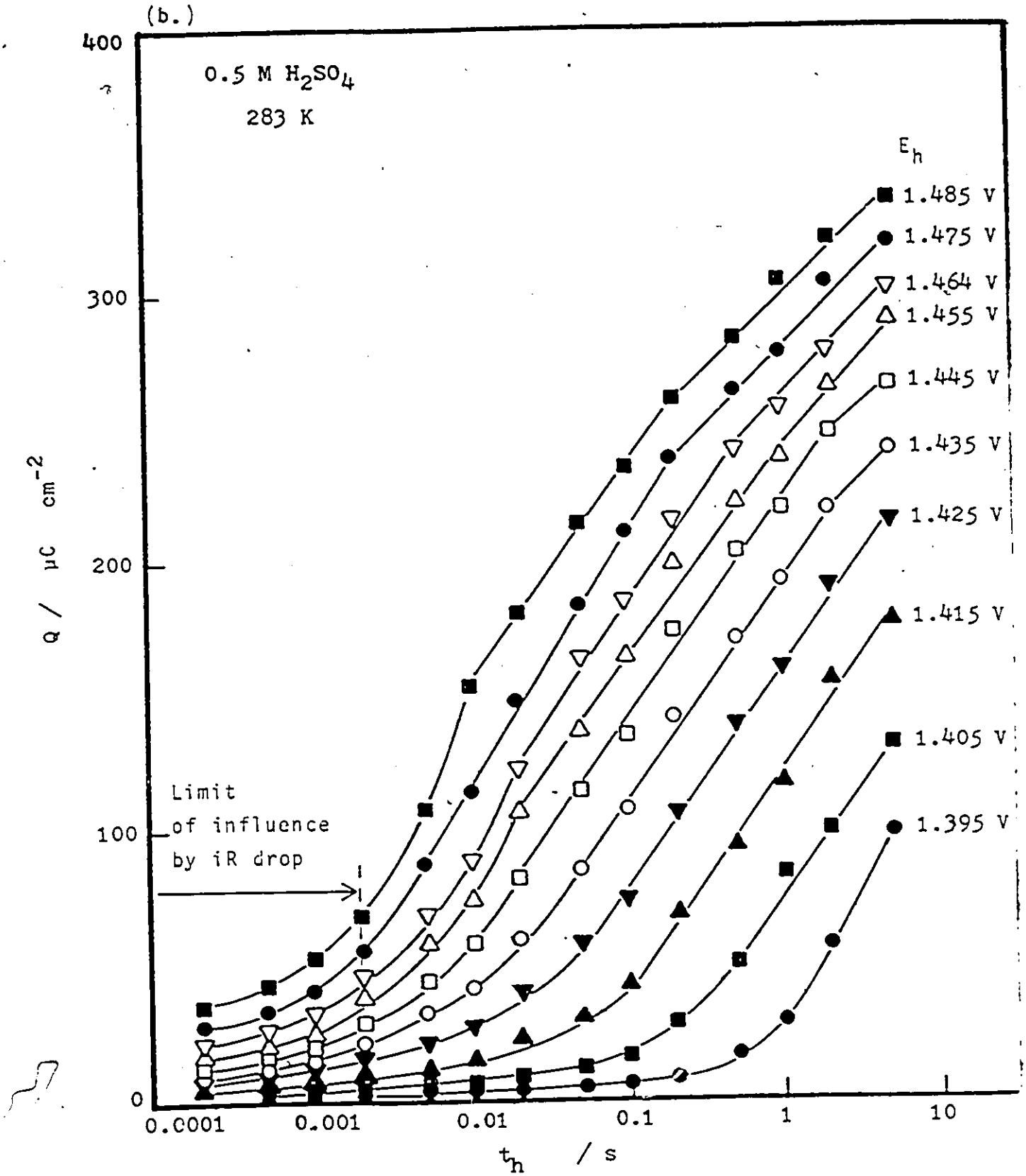
(b.)
0.5 M H_2SO_4
283 K
E_h
1.485 V
1.475 V
1.464 V
1.455 V
1.445 V
1.435 V
1.425 V
1.415 V
1.405 V
1.395 V
Limit
of influence
by iR drop
Q / µC cm^{-2}
400
300
200
100
0
0.0001
0.001
0.01
0.1
1
10
t_h / s

(c.)

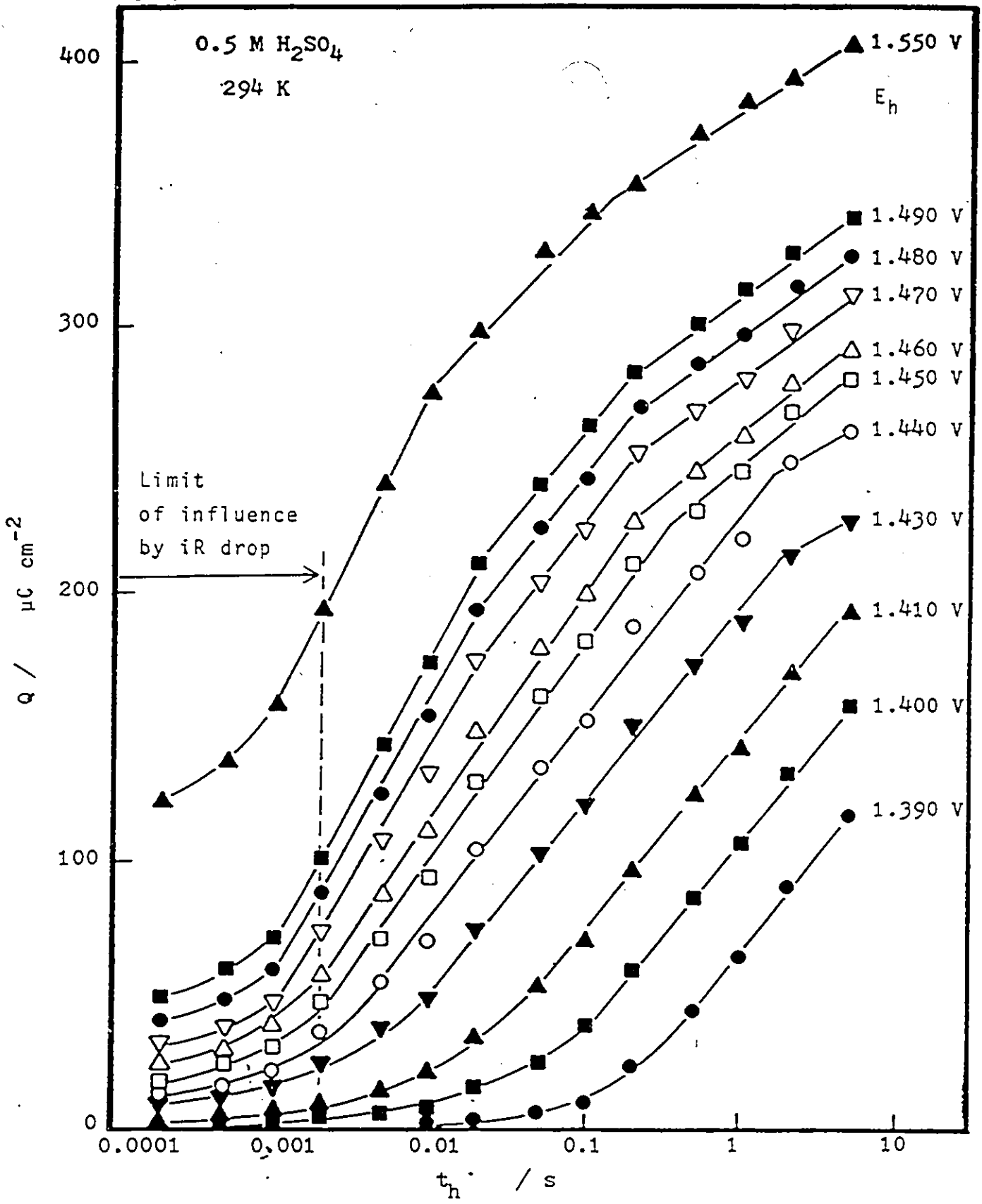
0.5 M H_2SO_4
294 K
1.550 V
E_h
1.490 V
1.480 V
1.470 V
1.460 V
1.450 V
1.440 V
1.430 V
1.410 V
1.400 V
1.390 V
Limit
of influence
by iR drop
Q / µC cm^{-2}
400
300
200
100
0
0.0001
0.001
0.01
0.1
1
10
t_h / s

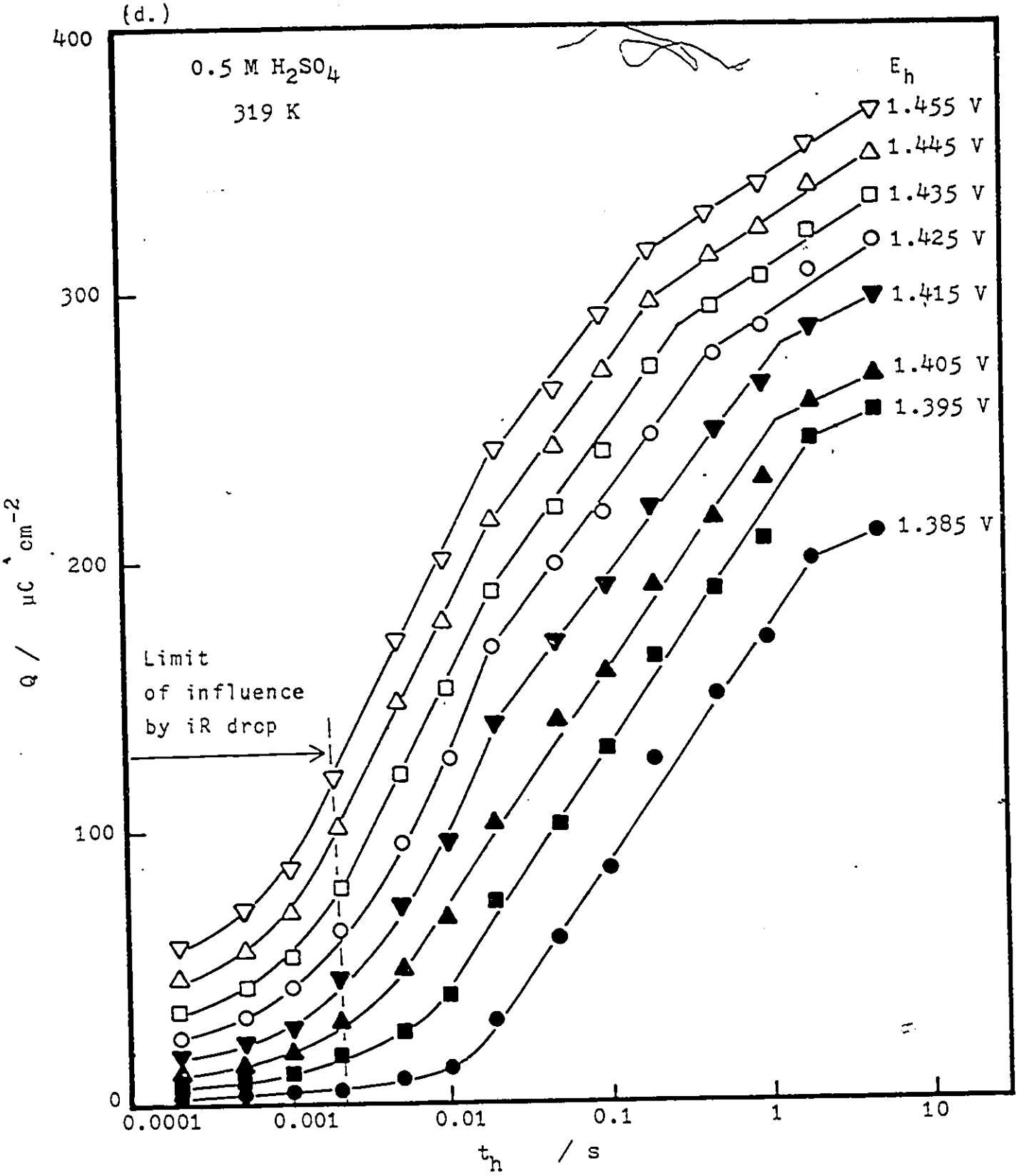
(d.)
0.5 M H_2SO_4
319 K
E_h
1.455 V
1.445 V
1.435 V
1.425 V
1.415 V
1.405 V
1.395 V
1.385 V
Limit
of influence
by iR drop
Q / μC cm^{-2}
t_h / s
400
300
200
100
0
0.0001
0.001
0.01
0.1
1
10

is found to have a profound effect on surface oxide formation at Au[194,195].

4.4.5. Oxide Growth Kinetics at Low Coverage in the First Few Milliseconds

Inspection of the initial region of the logarithmic plots for surface oxide formation at Au in Figures 4.4.9.a.,b.,c. and d. shows that the earliest stages of growth are not logarithmic in t_h, even though for longer t_h and higher coverages, they are, as was also found in other work at Pt. For this reason, exploratory plots were made for Q_{total} values in the low t_h region in terms of a) linear and b) square-root relations in t_h. At first, as will be discussed in Section 4.5.6. and Chapter V, it appeared that the growth behavior for short times could, to some approximation, be represented by plots in the square-root in t_h, as shown in Figure 4.4.10. However, Q_{total} values for $t_h < 2$ ms did not fit this relation very well. These plots also exhibit slopes that increase aproximately linearly with potential, E_h, while any electrochemically-controlled growth rate might be expected to be expotentially related to potential. Such a linear relation with E is suggestive of an effect connected with resistance through Ohm's law.

The initial oxide growth data for various conditions were therefore plotted linearly against t_h. Examples of the resulting plots for t_h values from 0.2 to 2 or 5 ms in experiments at T = 294 K are shown in Figures 4.4.11.a. and b. for 13 E_h values. This clearly shows that a) linear plots in t_h represent the apparent initial growth kinetics well and b) the slopes of the resulting plots are quite linear in potential, as seen in Figure 4.4.12. Similar plots result from the initial data points for growth under other conditions. Since the slopes of linear relationships between Q and t_h formally correspond to currents, and these slopes increase linearly with E_h, as was shown in Figure 4.4.12.; this behavior evidently corresponds to an Ohmic law. Evaluation of the resistances, R, corresponding to this behavior, give

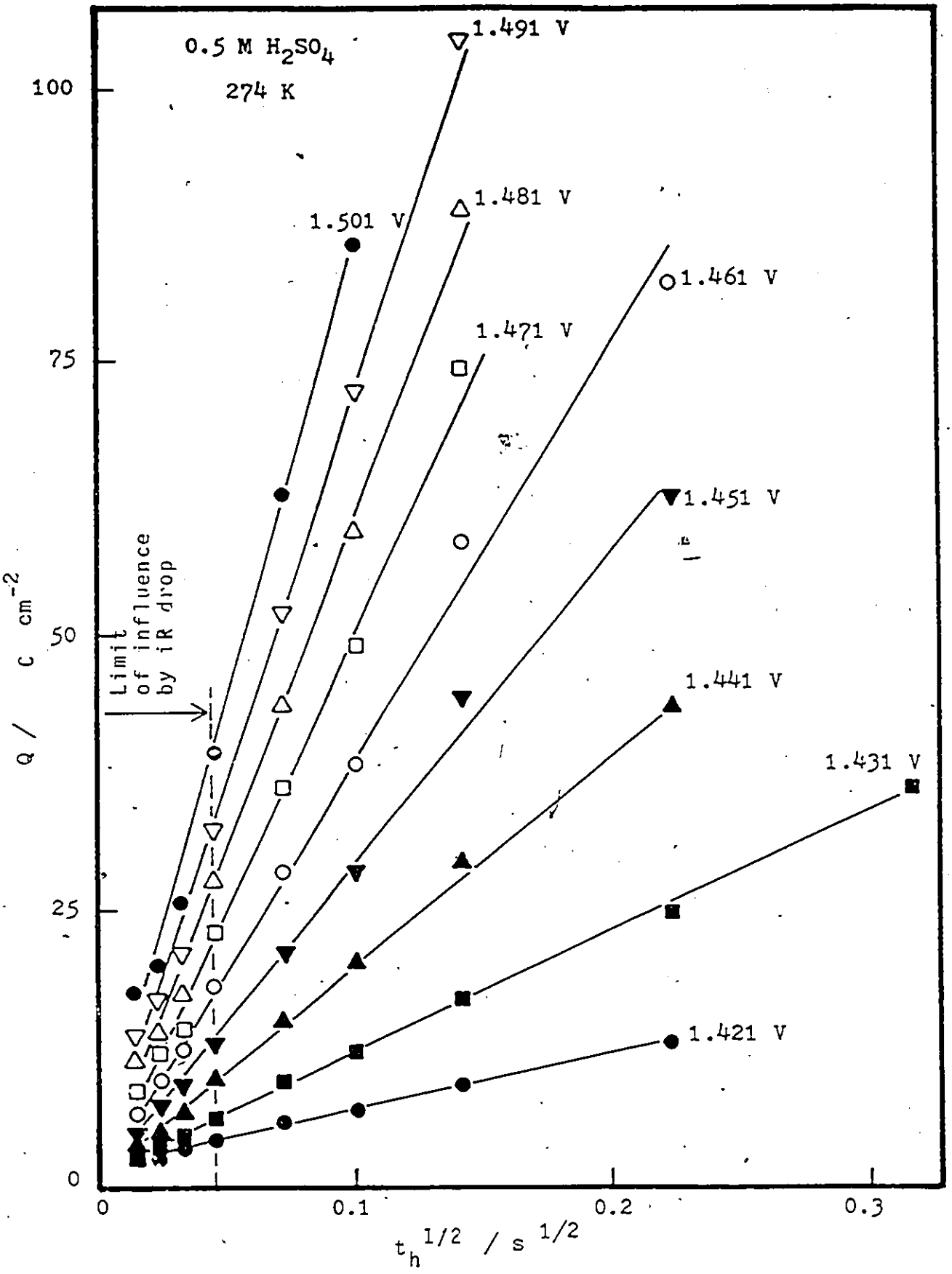

Figure 4.4.10. Variation of surface oxide charge with $t_h^{1/2}$ at Au in 0.5 M H_2SO_4 at several E_h and 274 K and t_h from 0.0002 to 0.1 s.

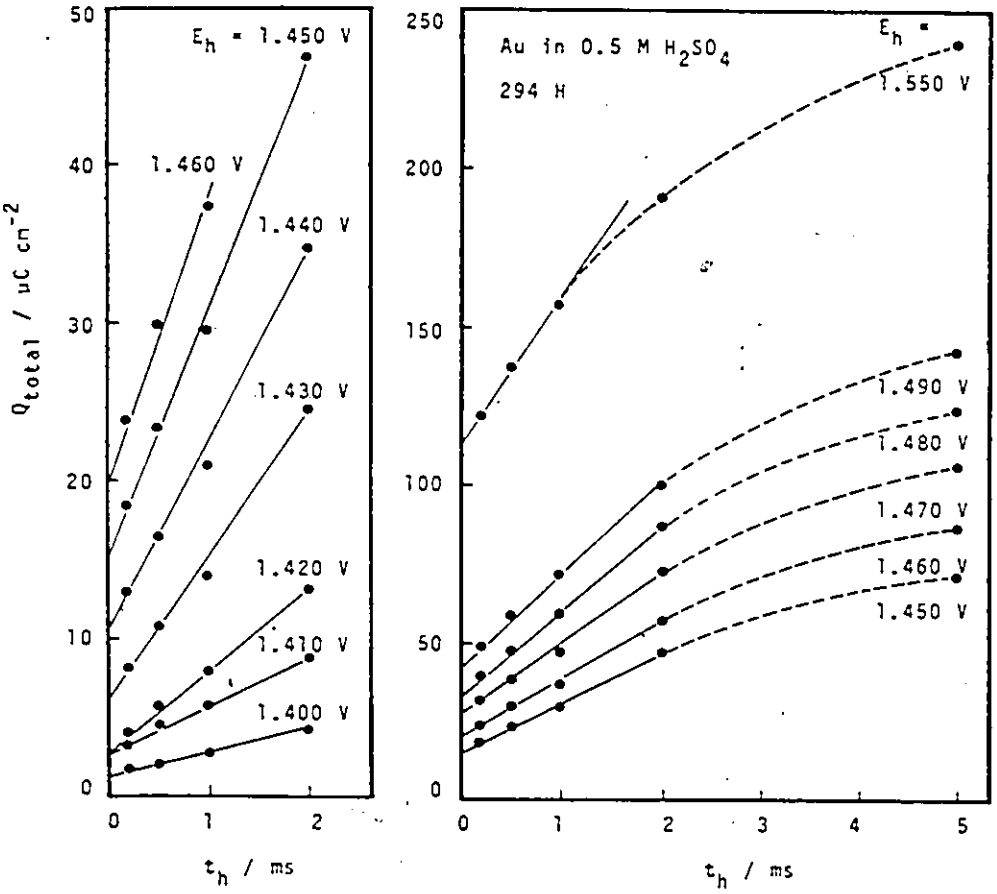

Figure 4.4.11. Variation of surface oxide charge linearly with t_h at Au in 0.5 M H_2SO_4 at several E_h and 294 K and t_h from 0.2 to 5 ms.

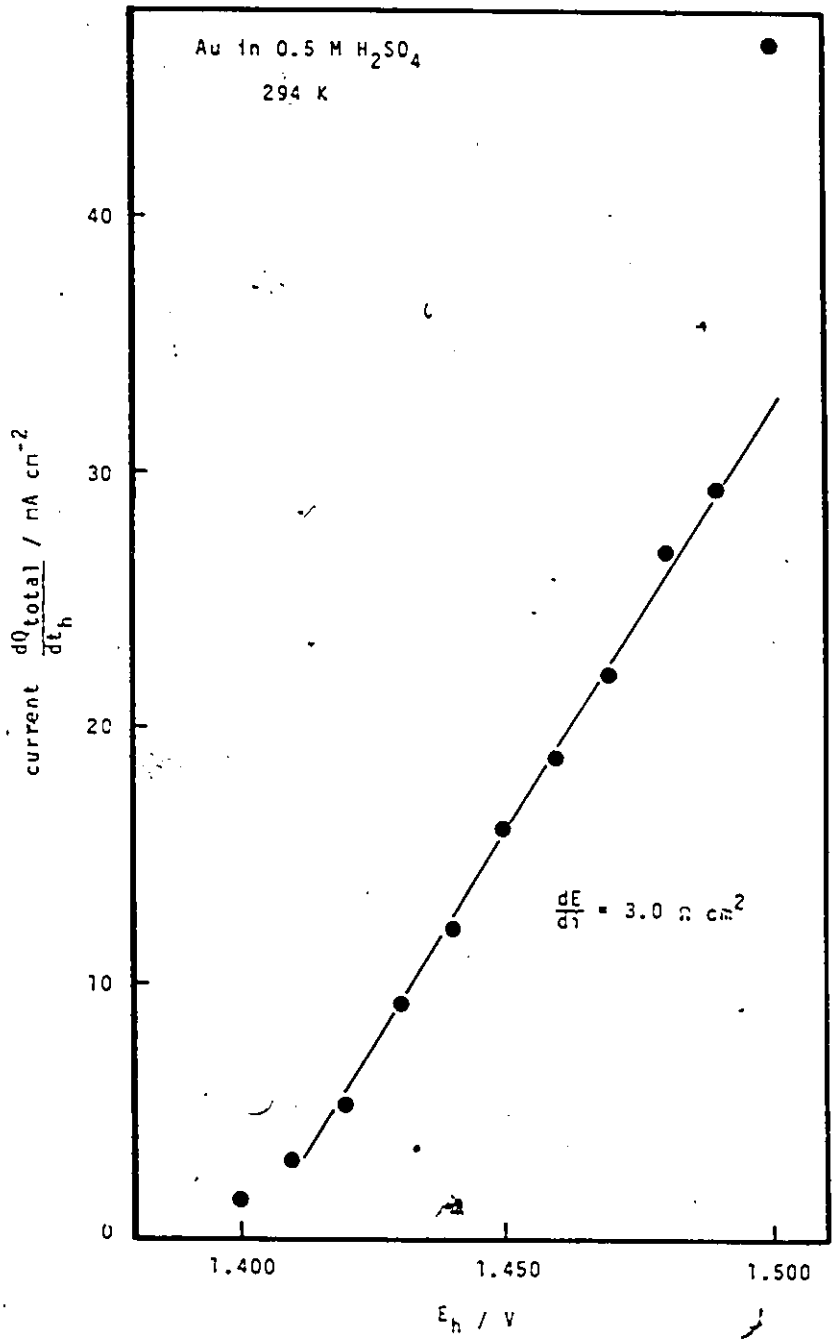

Figure 4.4.12. Slope of Q vs t_h plotted against E_h for surface oxide growth at Au in 0.5 M H_2SO_4 at 294 K.

values between 3 and 6 $\Omega\,cm^2$. This range of values for R is very close to the those obtained from solution resistance measurements of the cell in 0.5 M H_2SO_4 at room temperature, using both an interrupt technique[241] and a.c. impedance at high frequencies, giving resistances between 0.3 and 1.5 Ω, or 0.6 and 3 $\Omega\ cm^2$.

The conclusion to be reached from these plots for the initial oxide growth kinetic behavior is that the rates are controlled by electrolyte resistance, i.e. by the iR effect referred to in Section 4.3.1., before a different, chemical kinetic limitation sets in at longer times, giving the well established logarithmic behavior in t_h.

Physically, the significance of this Ohmic effect at very short t_h is that the initial low coverages by oxide at Au are generated near equilibrium conditions, so that the growth rate can be limited by the rate of passage of current in solution, i.e. through the iR effect. In hindsight, the possible significance of the iR limitation in the initial stages of oxide film growth is not difficult to appreciate, since the initial surface oxidation rates, as current densities, are on the order of 5 to 10 mA cm^{-2} over the first ms, depending upon E_h (see Figures 4.4.11.a. and b.).

The resistances corresponding to this iR limitation are shown as a function of temperature in Figure 4.4.13, from which it is seen that R decreases with T in qualitatively expected way. Because the data are based on small Q values, determined over a very short range of t_h values (0.0002 and 0.002 s), there is some inevitable spread and uncertainty in the R values. Variation of the electrolyte R values may also arise from its strong dependence upon cell geometry, since it was not possible to place the working and internal reference electrodes exactly the same distance apart for different experimental runs in the cell used during the course of this work. However, the R values are of the right order of magnitude for solution resistance effects and far too

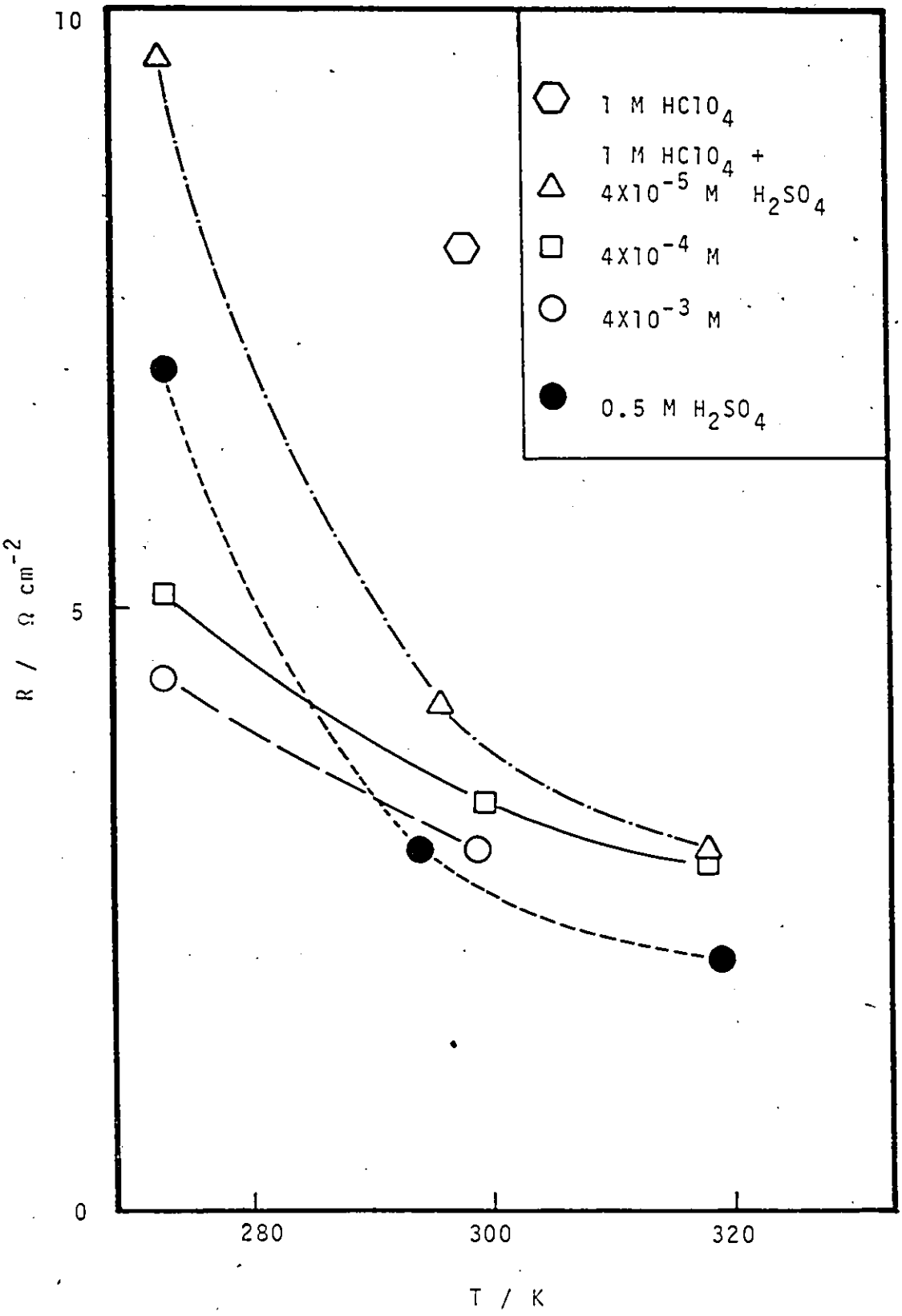

Figure 4.4.13. Resistance (from slope of dQ/dt_h vs E_h) vs temperature for different electrolyte solutions.

large to correspond to the Faradaic resistance of the OH deposition process, near equilibrium, (i.e. from linearization of the Butler-Volmer equation for small overpotentials in the initial stages of the surface oxidation process at Au).

4.4.6. Growth of OC1 Species After Formation of Species Reduced in the OC2 and OC3 Peaks

A special experiment was conducted in order to form the "initial", reversibly deposited, OC1 species after a small coverage (ca. 10 $\mu C\ cm^{-2}$) of surface oxide characterized by reduction in the OC2 and OC3 peaks had been generated at Au in 0.5 M H_2SO_4 at 294 K. This requires application of a potential of 1.33 V, well below that for the appearance of the OA1/OC1 reversible electrosorption process in a regular sweep.

The result of this experiment is shown in Figure 4.4.14. and the special potential-time program needed to achieve this result is shown in the inset of this figure.

The OC2 and OC3 type surface oxide species were grown while holding at 1.33 V for 100 s, following which the potential was swept to 1.410 V, where the OC1 type surface oxide was formed (sharp peak at the right-hand-side of the I vs E profile of Figure 4.4.14.). The resulting surface oxide species that were formed were then reduced at 50 $V\ s^{-1}$ for analysis.

The behavior shown in Figure 4.4.14. shows that it is possible to grow the states of oxide corresponding to the OC2 and OC3 peaks already at potentials less positive than those necessary to grow the OC1 or OC1' species; however, growth at such potentials is very slow. This significant result indicates that there must be some very small coverage of reversibly electrosorbed OH species at the anion covered electrode surface in 0.5 M H_2SO_4 even at these relatively low growth potentials. This condition is necessary because reversibly electrosorbed OH species of the OC1 type are indicated as the required

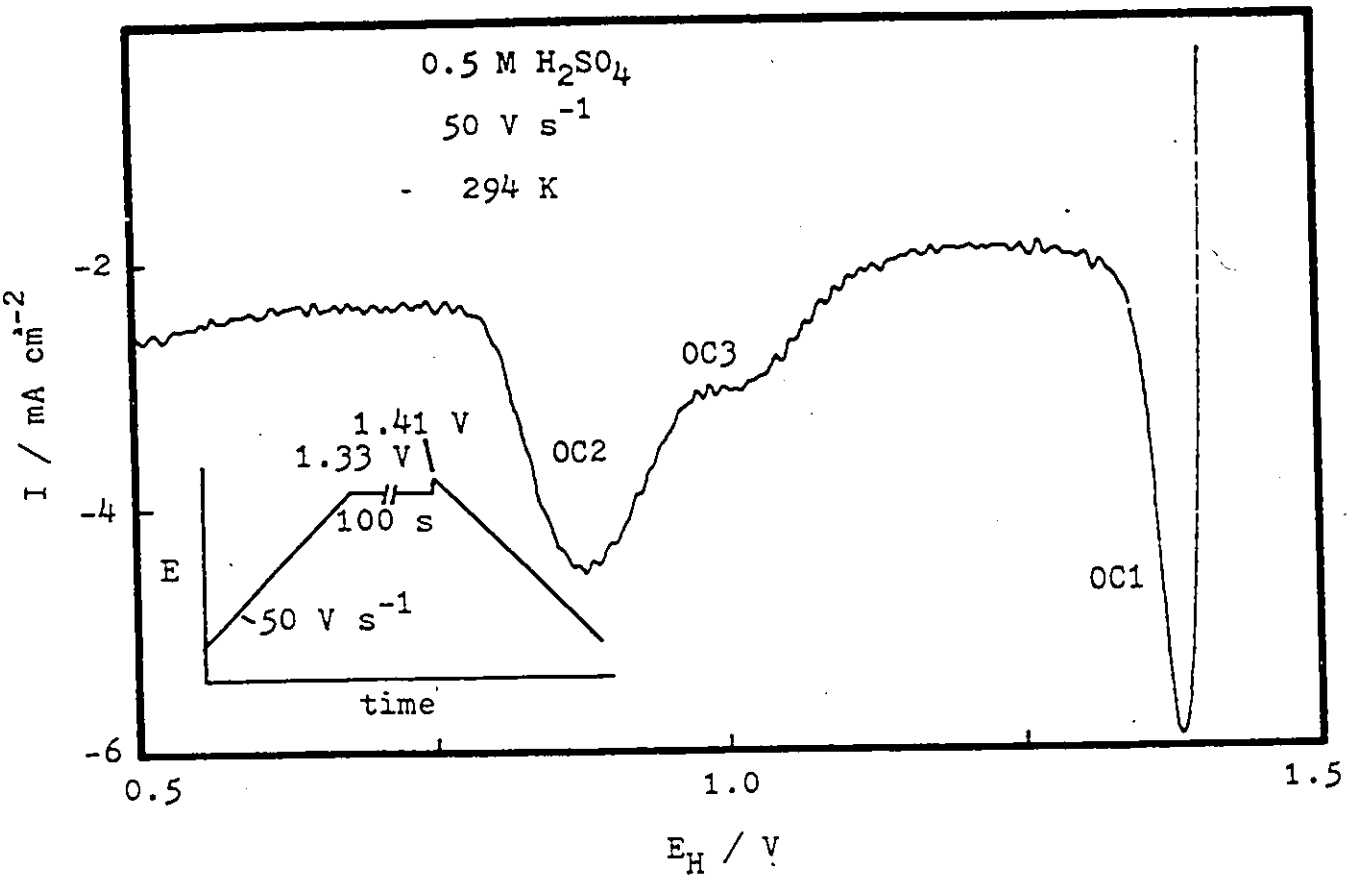

Figure 4.4.14. Potentiodynamic I vs E profile where the OC2 and OC3 peaks were grown before the reversible OC1 peak using a special potential-time program (inset).

precursors for formation of "converted" species identified by their reduction in the OC2 and OC3 peaks. The behavior observed also means that even after a small quantity of OC2 and OC3 type surface oxide species has been formed, there are still places at the surface where the OC1 species can be independently electrosorbed reversibly, i.e. provided the OC2 and OC3 coverage is sufficiently small.

4.5. Surface Oxide Growth in Mixed $HClO_4/H_2SO_4$ Electrolytes

In the preceding sections it has been shown how adsorption of anions plays a major role in surface oxide formation on Au, especially in the very earliest stages of this process. The strongly adsorbed sulfate anion evidentally has especially interesting and significant effects on surface oxide formation at gold.

In this section, results of experiments in mixed $HClO_4/H_2SO_4$ solutions are described which help to understand the role of exchange between adsorbed ClO_4^- and sulfate ions at the surface in the kinetics of the oxide film growth processes. Rapid potential-time programs, as described before, were used which, with mixed $HClO_4/H_2SO_4$ electrolytes at three compositions, lead to informative results complementary to those described in Section 4.2. Special attention was given to the study of oxide growth processes in the "anions on" situation in relation to the "anions off" situation, including investigations at more than one concentration of H_2SO_4.

The experiments described in this section arise from the observation that, under mixed electrolyte conditions in certain experiments, the I vs E profiles for conversion of OC1 species to OC2 and OC3 show a remarkable isopotential point (Figure 4.2.1.). Bearing in mind that isosbestic points of this kind arise when, for some property being measured which exhibits a peak, there is a conversion from one species to another (e.g. as in U.V. or I.R. spectroscopy), it seems likely that there is some time-dependent substitution of adsorbed ClO_4^- by the more strongly adsorbed SO_4^{2-} or HSO_4^- in the OC1 region that causes a change in the extent of electrosorption of OH and its conversion to the OC3 and the OC2 species at the anion-free areas of the Au surface.

This possibility of "ion-exchange" effects in adsorption at the Au surface led to the series of experiments and the results described in this section with mixed $HClO_4/H_2SO_4$ electrolytes. These experiments were conducted in order to

cover intermediate times of of oxide film growth from an initial "anion-free" conditions of the electrode surface ("anions off" situation) to one where an equilibrium coverage of sulfate ions was present ("anions on" situation). From the nature of such experiments, it might be expected that results on time effects from an initial "anions off" situation should eventually coincide with the behavior observed for the "anions on" condition; however, for reasons to be discussed later, this is not usually the case except for low growth potential. At intermediate times, exchange between the ions adsorbed (ClO_4^- together with HSO_4^- or SO_4^{2-}) will be taking place, coupled with time dependent conversion of OH electrosorbed amongst the anions to other states, OC2 and OC3, discussed in the preceding sections. Some of the results at longer holding times are necessarily related to those recorded in Section 4.4., as will be apparent from some of the plots which follow.

As before, the states of surface oxide developed under the two conditions ("anions off" and "anions on") are evaluated from the I vs E profiles generated in cathodic sweeps taken after various holding times, t_h. Three compositions of $HClO_4/H_2SO_4$ mixtures were investigated.

4.5.1. Results of "Anions Off" and "Anions On" Experiments on Surface Oxide Growth in 1 M $HClO_4$ with $4X10^{-4}$ M H_2SO_4

Figures 4.5.1.a. and 4.5.1.b. show the I vs E profiles for the reduction of surface oxide grown at Au electrodes in 1 M $HClO_4$ with $4X10^{-4}$ M H_2SO_4 at 1.340 V and 300 K; two potential-time programs were used as described in the inset diagrams. The potential-time program used for obtaining the results of Figure 4.5.1.a. was designed to minimize SO_4^{2-} (HSO_4^-) adsorption ("anions off" situation) and that used for the results of Figure 4.5.1.b. was arranged to allow near-equilibrium coverage to be attained of this of this anion ("anions on" situation) at the Au electrode surface before surface oxide formation was initiated.

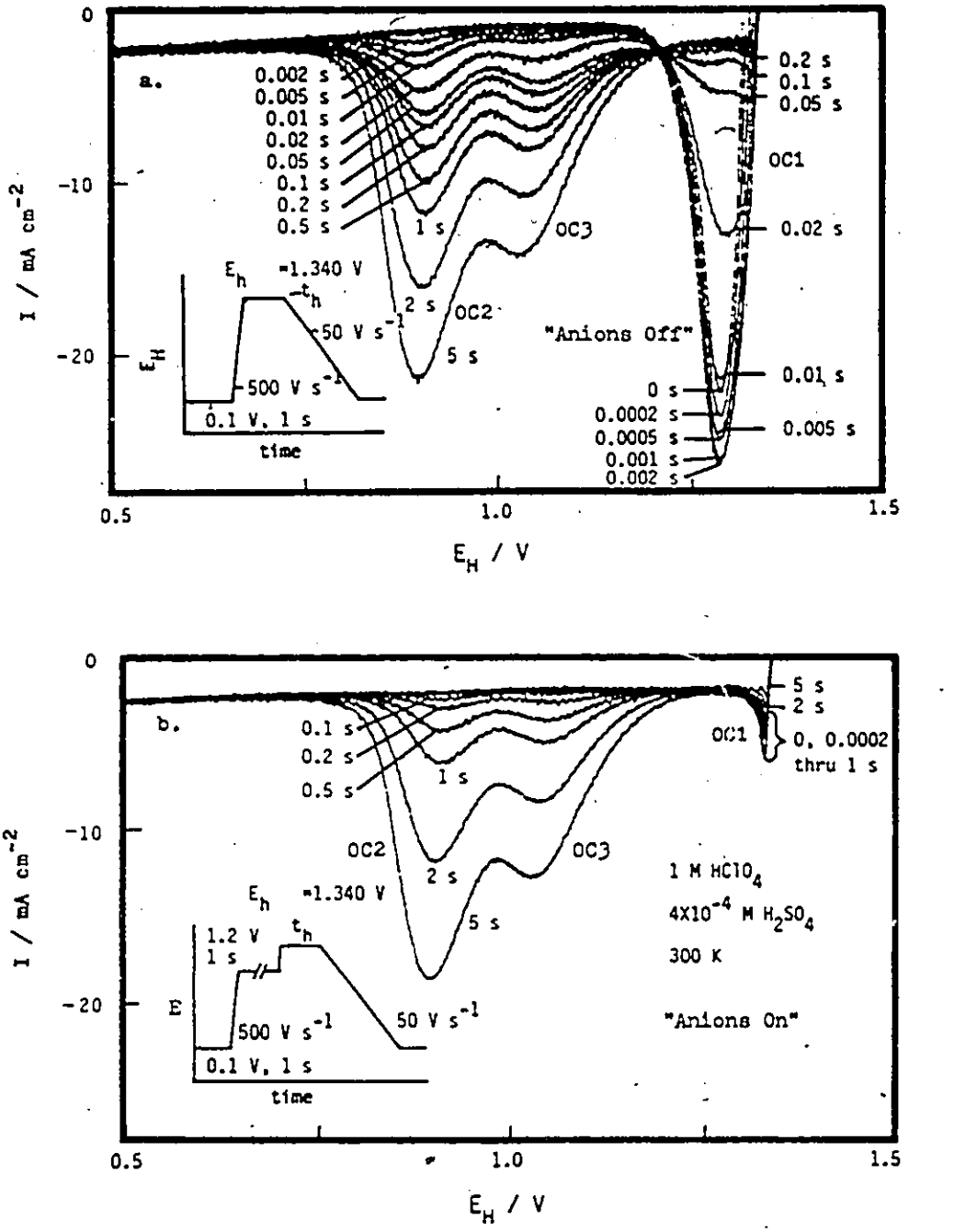

Figure 4.5.1. Series of potentiodynamic I vs E profiles for surface oxide growth at Au at E_h = 1.340 V and several t_h between 0.0002 and 5 s and at 300 K in 1 M $HClO_4$ with 4X10^{-4} M H_2SO_4. (a.) 0 s holding at 1.2 V ("anions off"); (b.) 1 s holding at 1.2 V ("anions on").

In the "anions off" potential-time program, a potential of 0.1 V was held for 1 s to allow the anions to be desorbed from the electrode surface and the potential was then very rapidly swept at 500 V s^{-1} to 1.340 V so as not to allow significant SO_4^{2-} adsorption to take place during this excursion of potential. After holding the potential for variable but controlled periods of time at the surface oxide growth potential, 1.340 V, the surface oxide formed was reduced and its states analysed by means of cathodic sweeps at 50 V s^{-1}.

In the "anions on" potential program, the potential was held for 1 s at 0.1 V, then swept at 500 V s^{-1} to 1.2 V, where the potential was held for 1 s to allow near-saturation sulfate coverage to be attained. The potential was then swept at 500 V s^{-1} to 1.340 V, where the potential was held for a variable time and states of the resulting surface oxide formed were again analysed by means of cathodic sweeps at 50 V s^{-1}.

The differences between the "anions off" and the "anions on" growth behavior are quite pronounced, as they are especially in the initial OC1 region dealt with earlier. In the "anions off" growth, the initial reversible OC1 reduction should resemble, and it does, that seen in 1 M $HClO_4$ with no added H_2SO_4 (Figure 4.3.2.). The peak corresponds to a relatively large OH coverage, the peak potential is 1.289 V; also, the I vs E profile has a very clear isopotential point at 1.145 V, which suggests the participation of a conversion process of the kind mentioned earlier. In the "anions on" case, the OC1 peak corresponds to a considerably smaller OH coverage, as expected, and the peak potential is 1.341 V; i.e. more positive than in the "anions off" case. In these ways its behavior is similar to that of the OC1 peak observed in 0.5 M H_2SO_4, even though its peak potential is about 33 mV less positive in this mixed electrolyte. This less positive peak potential is presumably due to a lower equilibrium coverage of SO_4^{2-} and correspondingly faster anion desorption kinetics at the electrode surface at the lower concentration of

H_2SO_4. In the "anions off" case, the OC1 peak current increases somewhat when the potential is held at 1.340 V for periods between 0 and 0.002 s, as explained earlier, but decreases when the potential is held for longer than 0.002 s. After a holding time of 0.05 s, a small peak positive with respect to the initial OC1 peak appears and is similar to that observed in the "anions on" case. This suggests, of course, that SO_4^{2-} anions must have been adsorbed at the surface after this period of time. This conclusion is consistent with the anion adsorption effects described in Section 4.2. for the very initial stages of Au surface oxidation.

For E_h = 1.340 V (Figure 4.5.1.) the OC2 and OC3 peaks appear after a holding time of $\geq$ 0.002 s for the "anions off" case but only after 0.1 s for the "anions on" case. From the results of Section 4.2., it is clear that this is because there is a larger coverage of the OC1 precursor species in the "anions off" case. There is also a decrease in the rate of growth of these two peaks at holding times of about 0.05 s, where the OH coverage corresponding to the OC1 peak is greatly diminished by the adsorption of SO_4^{2-} at the electrode surface. For longer holding times, it is expected that the coverage, shape and potentials of these two peaks in the "anions off" case approaches those for the "anions on" case, and this is what is observed. It should also be noted that the OC2 peak initially grows faster than the OC3 peak in both the "anions off" and the "anions on" cases, which also occurs in surface oxide growth at Au in 1 M $HClO_4$ with no added H_2SO_4.

Figures 4.5.2.a. and 4.5.2.b. show the integrated charges plotted against time on a logarithmic scale for the OC1 peaks and the total O-species, respectively, for the I vs E profiles shown in Figure 4.5.1. The charge due to the OC1 peak, after an initial increase with holding time due to the effect of iR effect (Section 4.5.1.), decreases dramatically for the "anions off" case. In the "anions on" case, the OC1 charge is much smaller and remains relatively

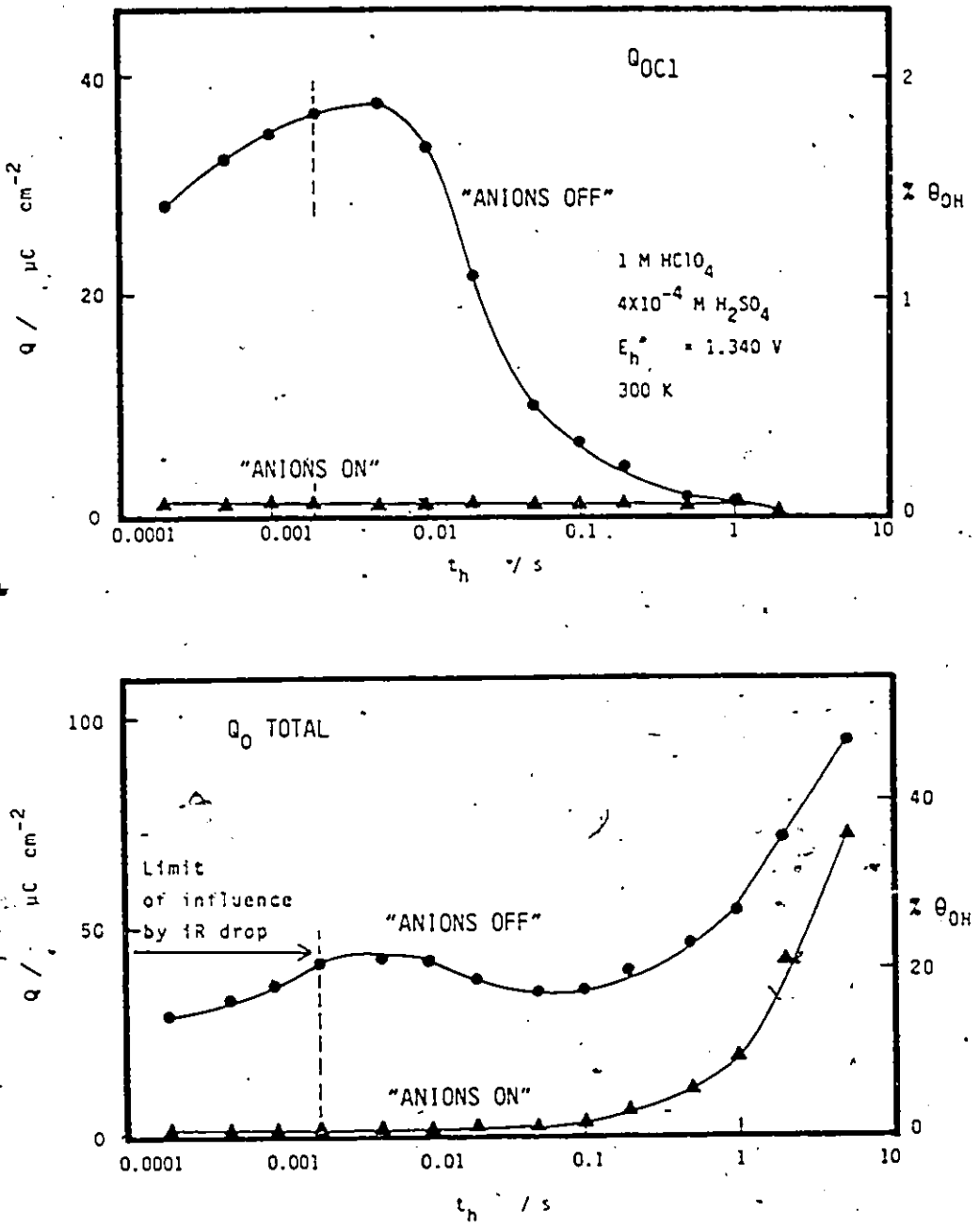

Figure 4.5.2. Variation of surface oxide charge formed at Au in 1 M $HClO_4$ with $4X10^{-4}$ M H_2SO_4 at 1.340 V and 300 K for "anions off" and "anions on" growth and t_h from 0.0002 to 5 s. (a.) OCl only; (b.) total surface oxide charge.

constant up to t_h = 1 s. The total charge, Q_{total}, in the "anions off" case actually decreases as a function of time from 0.002 to 0.2 s(Figure 4.5.2.b.), which is similar to the behavior shown in Figure 4.2.6 of Section 4.2. An explanation is that the adsorption of SO_4^{2-}, which increases with t_h, displaces the reversibly deposited OC1 species at the surface. For t_h > 0.1 s, surface oxide growth becomes significant, as manifested by the development of the OC2 and OC3 peaks, and eventually continues in the normal logarithmic way[6] in t_h.

These more stable O-species grow more slowly when SO_4^{2-} is adsorbed on the electrode surface, owing to the necessity of desorbing the SO_4^{2-} for growth to occur, but they are not displaced by the anions, as are the OC1 species. The total oxide reduction charge in the "anions on" case remains relatively small until 0.1 s, beyond which oxide growth characterised by the OC2 and OC3 peaks starts to be significant. The oxidation charges then approach those for the "anions off" case.

The stages in the <u>"anions off"</u> surface oxide growth in 1 M $HClO_4$ with $4X10^{-4}$ M H_2SO_4 may be summarized as follows:

1. A relatively SO_4^{2-}-free surface exists before surface oxide formation commences (however, less strongly adsorbed ClO_4^- ions of the supporting electrolyte still populate the surface and the double-layer);
2. Growth of the initial reversibly deposited OC1 species in between ClO_4^- anions under tonditions of little influence of adsorbed sulfate at first;
3. Adsorption of SO_4^{2-}, consequent competition with adsorbed ClO_4^- anions at the surface, causing the appearance of some OC1 species in the state found when adsorbed between sulfate anions and a dimininution the charge for all reversibly deposited OC1 species, since the equilibrium coverage of this species decreases with

increasing coverage of sulfate anions, which leads to a decrease in total surface oxide charge;

4. Desorption of SO_4^{2-} allowing formation of the less anion-sensitive OC2 and OC3 species;

5. Normal surface oxide growth.

Likewise, the stages in the "anions on" surface oxide growth can be summarized as follows:

1. A surface saturated with hydrated sulfate anions exists before surface oxide formation (OH electrodeposition) commences;

2. Formation of a reversibly deposited OC1 species of the type found in H_2SO_4, corresponding to OH deposition in between SO_4^{2-} (HSO_4^-) ions chemisorbed in arrays on the surface;

3. Gradual desorption of anions, possible appearance of some OC1' species and formation of OC2 and OC3 species;

4. Normal surface oxide growth.

Figures 4.5.3.a. and b. show charges for total O-species under "anions off" conditions plotted against time on a logarithmic scale at 300 K for several growth potentials. It should be noted that separate double-layer charging data for "anions on" and "anions off" conditions were subtracted in performing the integration of the I vs E profiles. The two sets of values differed by about 10 $\mu C\ cm^{-2}$ between the integration limits used in these calculations (over potential ranges from E_h to 0.6 V). Although the two separate sets of double-layer charging data were the best ones to use for calculating low oxide reduction charges at short growth times, this probably introduced a small error at longer times or larger surface oxide coverages where the actual double-layer charging values would be between those for "anions on" and "anions off" conditions.

At very low E_h (1.280 and 1.300 V), Q_{OC1} decreases with no apparent

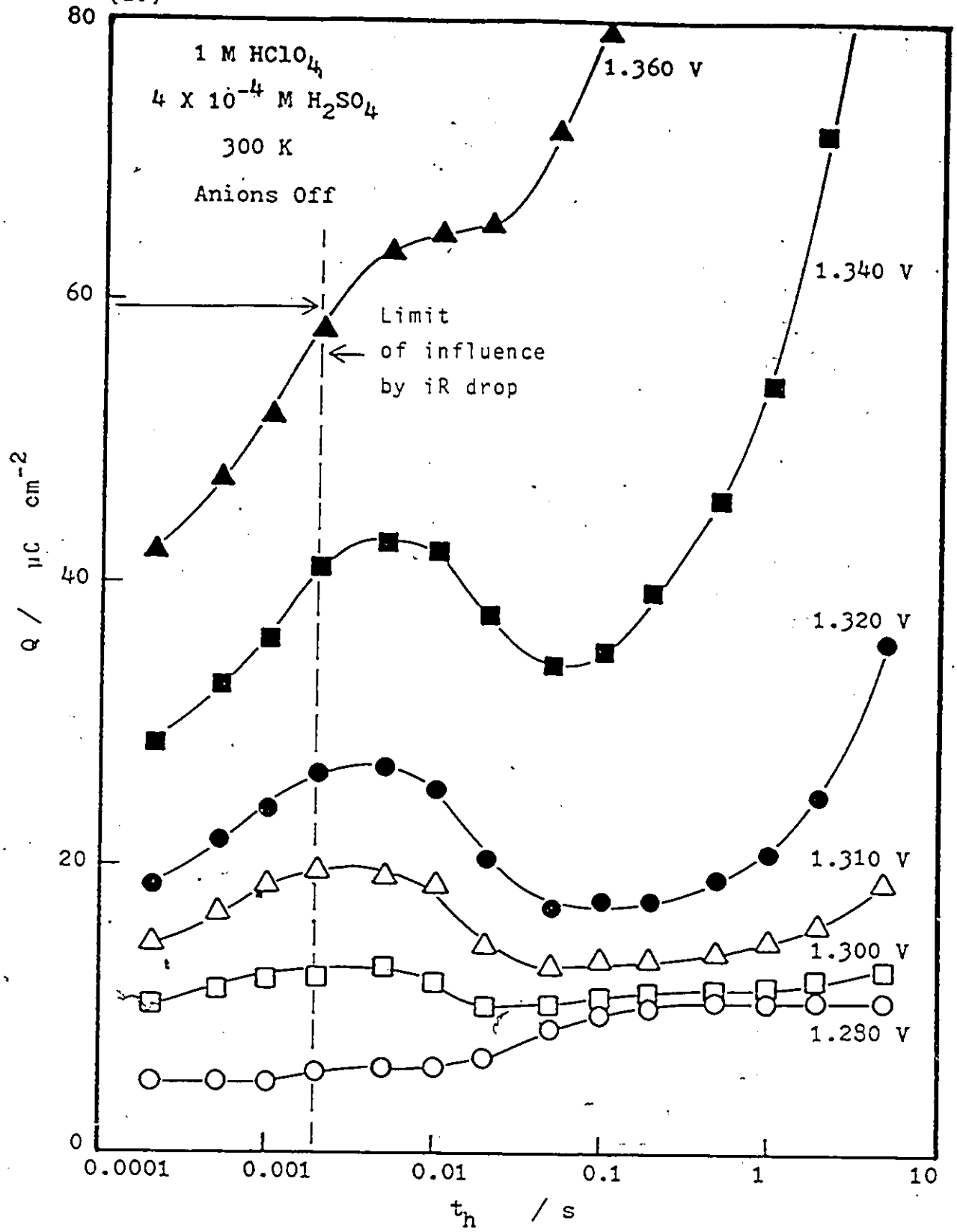

Figure 4.5.3. Variation of surface oxide charge formed at Au in 1 M $HClO_4$ with $4X10^{-4}$ M H_2SO_4 at several E_h and 300 K for "anions off" growth and t_h from 0.0002 to 5 s.

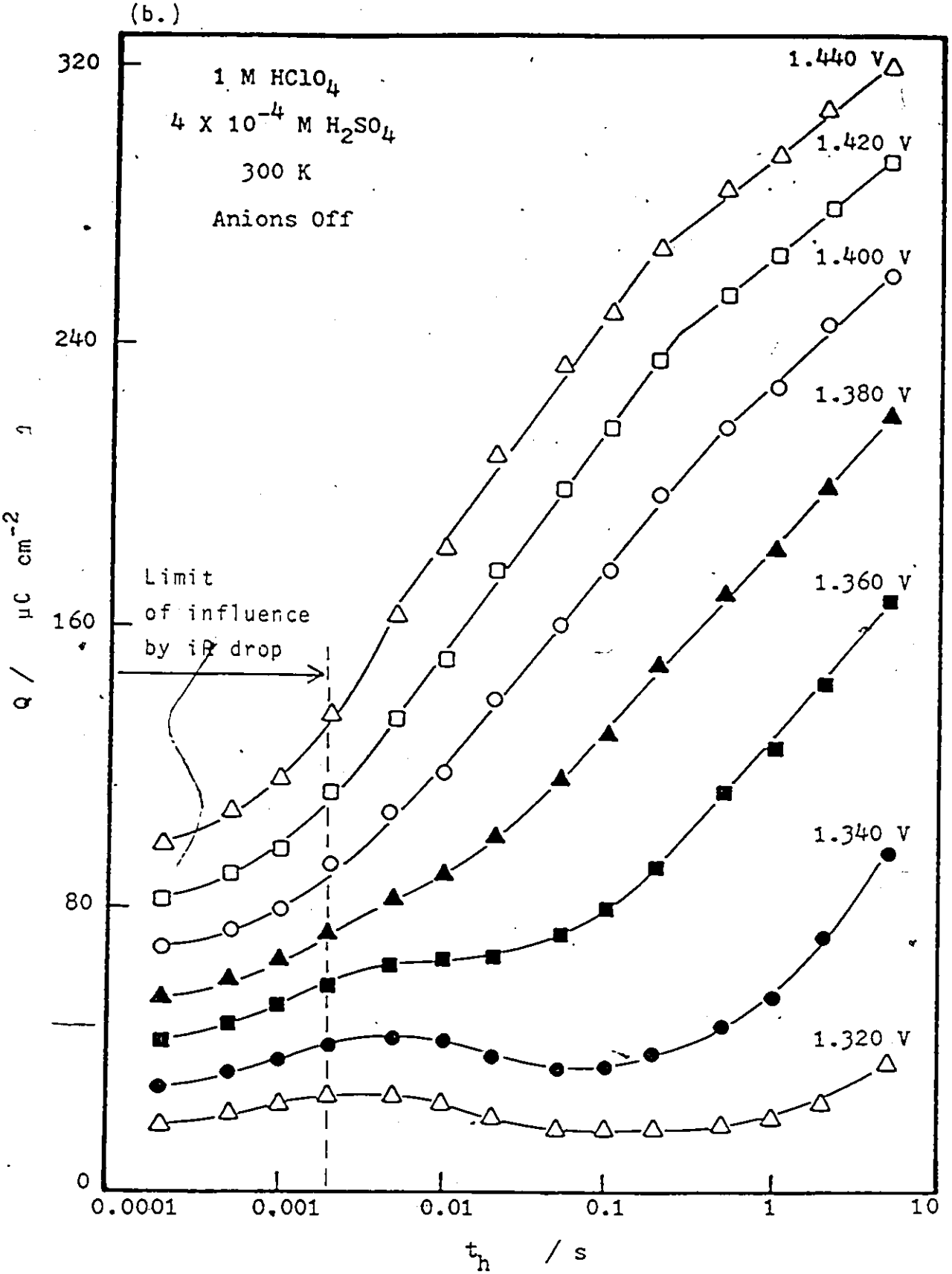
(b.)
1 M $HClO_4$
4 X 10^{-4} M H_2SO_4
300 K
Anions Off
1.440 V
1.420 V
1.400 V
1.380 V
1.360 V
1.340 V
1.320 V
Limit
of influence
by iR drop
Q / µC cm^{-2}
320
240
160
80
0
0.0001
0.001
0.01
0.1
1
10
t_h / s

growth of OC2 and OC3 charges when t_h < 5 s, as can be seen in the I vs E profiles. The increase in charge (Figure 4.5.3.a.), which is observed at these two growth potentials is due to the increase in double-layer capacitance with adsorption of SO_4^{-2} (Section 4.7.).

At growth potentials of 1.310, 1.320, 1.340 and 1.360 V, a clear decrease, or an inflection in the relation of total charge to $\log(t_h)$ is observed before normal surface oxide formation, i.e. phase-oxide development, occurs. This indicates competition between the O-species, especially those in the OC1 state and adsorbed SO_4^{2-} and ClO_4^- ions at the surface.

For E_h > 1.400 V (Figure 4.5.3.b.), initially a non-logarithmic growth region followed by logarithic growth regions with no clear decrease or plateau arises in surface oxide formation. At these higher potentials, the more stable OC2 and OC3 species grow quickly enough to prevent any significant readsorption of sulfate at the surface resulting in subsequent displacement of OH species from the surface.

In the regimes of logarithmic growth in t_h, the growth plots seem to have two characteristic slopes, $dq/d\log(t_h)$, and within each of the two regions, the lines are almost parallel. Further discussion of the logarithmic growth behavior will be given in Chapter V.

A similar plot of the charges for the "anions on" situation for total O-species against $\log(t_h)$ at 300 K for several growth potentials is shown in Figure 4.5.4. The charges for "anions on" growth are, as expected, consistently smaller than those for "anions off" growth at the same potential at relatively short holding times; however, eventually the "anions on" charges tend to approach those for the "anions off" case, as is observed at longer holding times, since, the surface oxide coverages then become comparable for the two conditions. In general, the "anions on" growth resembles, as is expected, that for 0.5 M H_2SO_4 except that the surface oxide grows somewhat

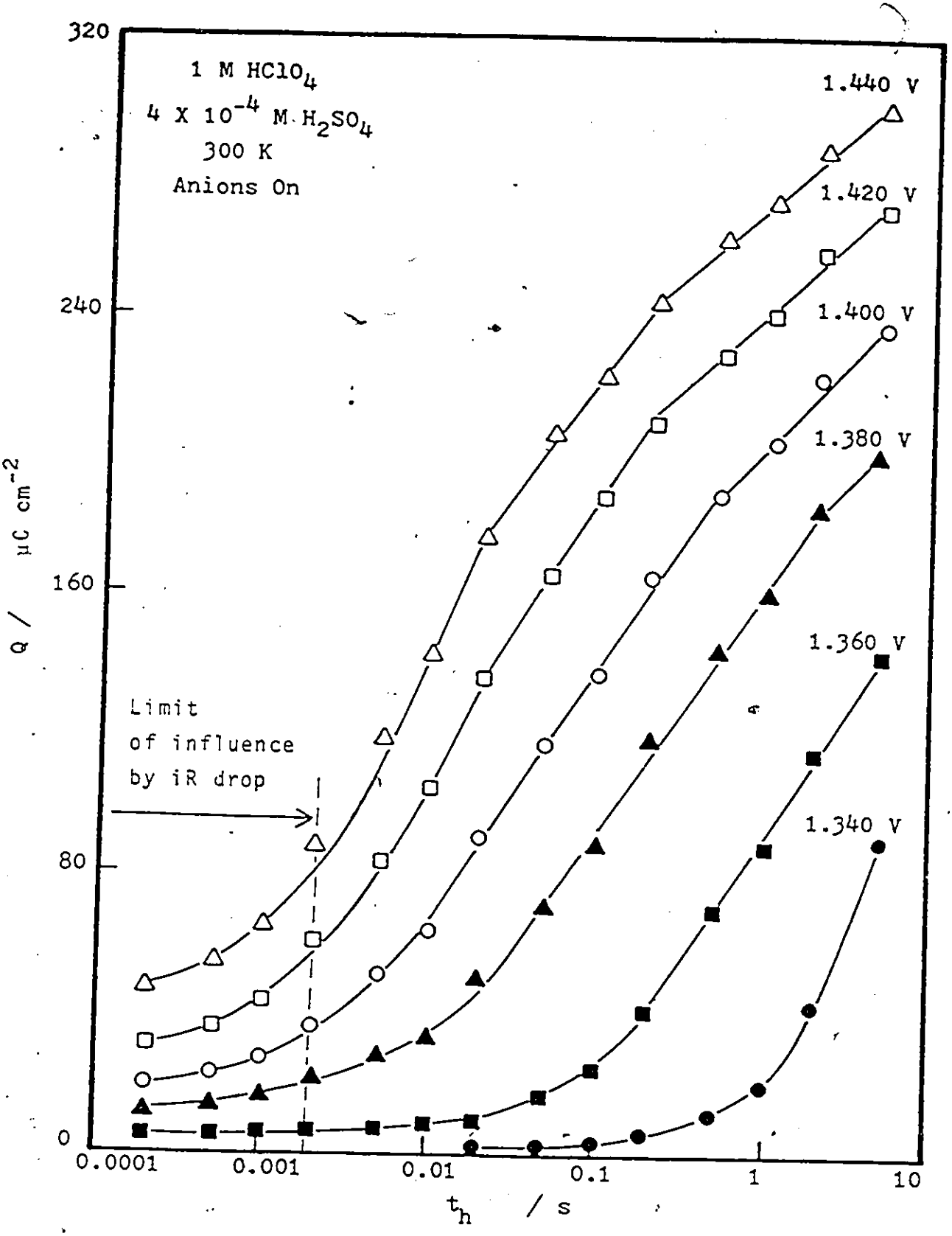

Figure 4.5.4. Variation of surface oxide charge formed at Au in 1 M $HClO_4$ with $4X10^{-4}$ M H_2SO_4 at several E_h and 300 K for "anions on" growth and t_h from 0.0002 to 5 s.

faster, since with the concentration of H_2SO_4 is lower than 0.5 M in these other cases.

4.5.2. Comparison of the OC2 and OC3 Peaks for "Anions Off" and "Anions On" Growth in 1 M $HClO_4$ with $4X10^{-4}$ M H_2SO_4

The behavior of the OC2 and OC3 peaks is different for "anions off" and "anions on" growth at relatively short holding times and low coverages, but becomes similar at longer holding times and higher coverages in the expected way. This is because at first (small t_h) the influence of adsorbed SO_4^{2-} is quite different for the OC2 and OC3 types of growth at relatively short holding times; this difference, however, diminishes with t_h as more surface oxide is developed. The peak potentials of OC2 and OC3 are sensitive to the presence of anions and show some interesting differences when examined under the two potential-time growth programs.

In Figure 4.5.5., the charges and the potentials of the OC3 peak are plotted against time on a logarithmic scale. The OC3 surface oxide charge both for "anions off" and "anions on" conditions is shown for E_h = 1.400 V in 1 M $HClO_4$ with $4X10^{-4}$ M H_2SO_4 at 300 K. Unlike the behavior of the OC1 peak, the "anions off" growth for the OC3 state is very similar to that for the "anions on" condition; however, the OC3 charge does increase somewhat more slowly with t_h for the "anions on" case and exhibits logarithmic growth at t_h > 0.1 s just as it does in 0.5 M H_2SO_4. The initial points for the logarithmic growth region actually represent some charge contributions for the OC1 peak added to those for OC3 peak (encirled points), as was also the case for growth in 0.5 M H_2SO_4. The slope of the logarithmic region is about 45 $\mu C\ cm^{-2}$ per decade for both conditions of growth in this electrolyte at 300 K.

The "anions on" peak potential for OC3 shifts to less positive potentials with increasing t_h and OC3 coverage, as was also seen in 0.5 M H_2SO_4. The "anions off" peak at low coverages and short times arises at ca. 1.045 V, which

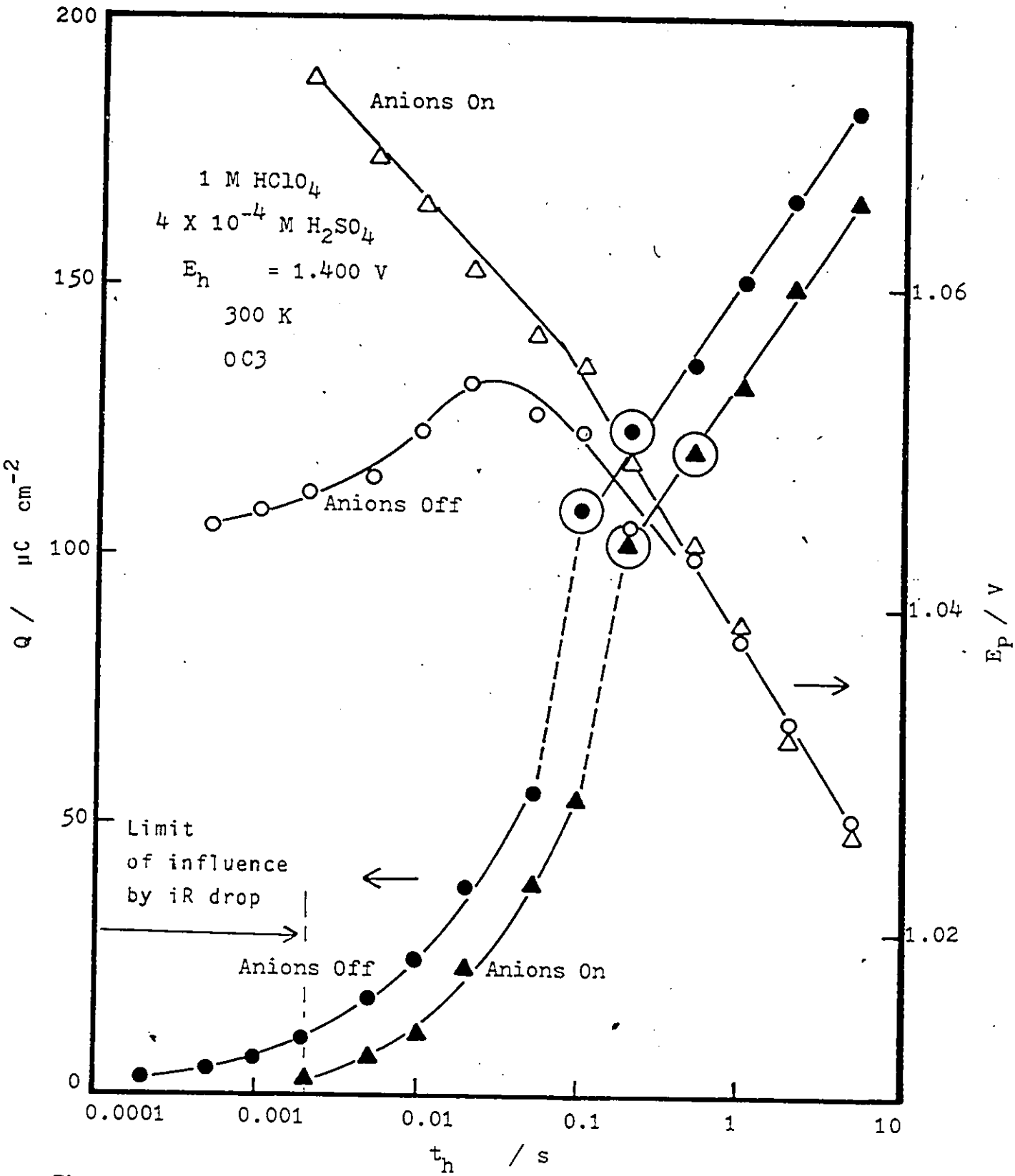

Figure 4.5.5. Comparison of "anions off" and "anions on" growth with respect to OC3 charges and peak potentials for Au in 1 M $HClO_4$ with $4X10^{-4}$ M H_2SO_4 at E_h = 1.400 V and 300 K for t_h from 0.0002 to 5 s.

is 28 mV less positive than that for the "anions on" peak at 1.073 V for low coverages. This confirms that this OC3 peak potential is quite sensitive to the presence of anions at the electrode surface. Indeed, the "anions off" peak initially shifts positively with holding time as SO_4^{2-} is allowed to become adsorbed on the electrode. Eventually, the "anions off" peak potential begins to shift to less positive potentials and finally converges to that for "anions on" as the state of the electrode surface finally becomes similar for the two kinds of growth conditions. Both types of peak potentials then shift logarithmically with t_h with a slope of about -17 mV per decade.

For the OC2 peak, under the same "anions off" and "anions on" conditions, Figure 4.5.6. shows the charges and the potentials plotted against $\log(t_h)$ for E_h = 1.400 V at 300 K. Again, the growth behavior is similar for the two conditions, except that a slightly higher saturation charge is attained under "anions off" conditions.

It is evident from both Figures 4.5.5. and 4.5.6. that the OC2 and OC3 states developed in time under "anions off" and "anions on" conditions each require about 0.5 to 1 s to attain common peak potential values with continuing time. After this time, the coverage of sulfate anions must be similar for both conditions, since these anions are readsorbing at the surface under "anions off" conditions and desorbing under "anions on" conditions because of the increasing coverage of OC3 species formed in the turn-over process.

When the OC3 and OC2 peak potentials are plotted against the peak charges for "anions off" and "anions on" growth at gold, in 1 M $HClO_4$ with $\sim 10^{-4}$ M H_2SO_4 at 300 K the relations shown in Figure 4.5.7. result for 1.400 V, 1.420 V and 1.440 V. As was also shown in Figure 4.5.5., the "anions off" and "anions on" OC3 peaks are separated by 28 mV as $\theta_{OC3} \rightarrow 0$, but the two types of peaks shift together with increasing coverage (and time) and finally converge when

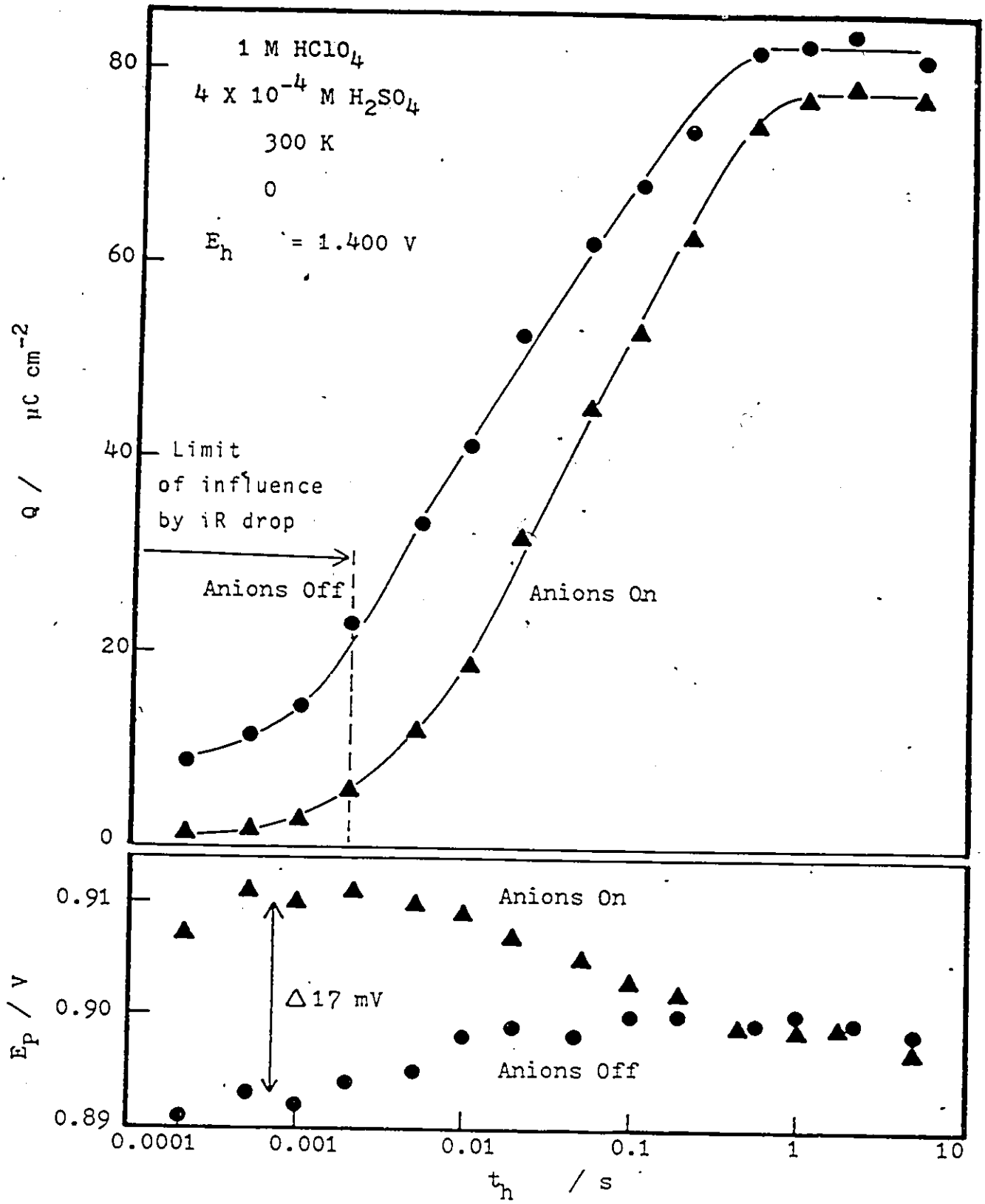

Figure 4.5.6. Comparison of "anions off" and "anions on" growth with respect to OC2 charges and peak potentials for Au in 1 M $HClO_4$ with $4X10^{-4}$ M H_2SO_4 at a growth potential of 1.400 V and 300 K for growth periods from 0.0002 to 5 s.

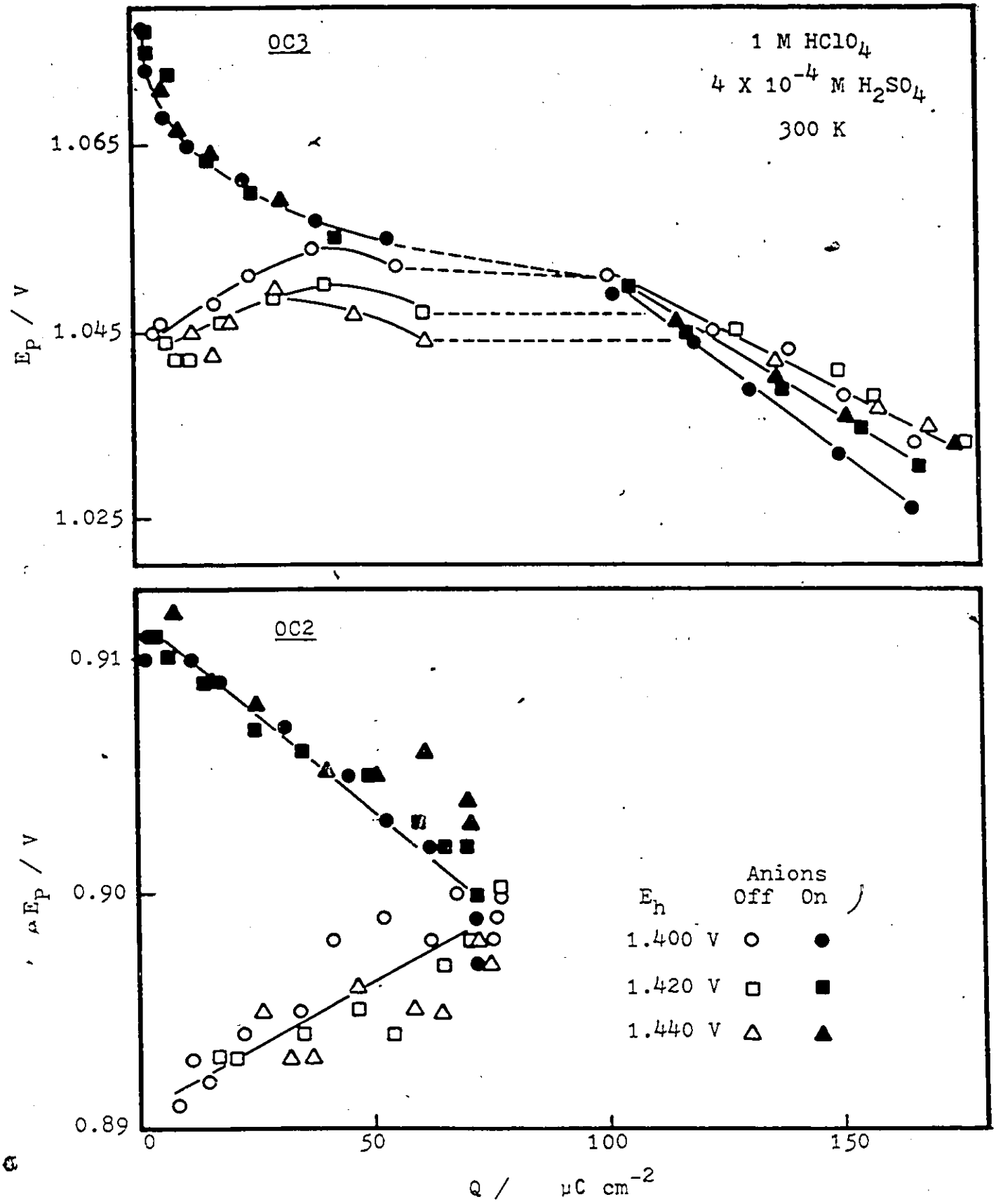

Figure 4.5.7. Comparison of "anions off" and "anions on" growth with respect to OC2 and OC3 peak potentials plotted against peak charge for Au in 1 M $HClO_4$ with $4X10^{-4}$ M H_2SO_4 at E_h = 1.400 V, 1.420 V and 1.440 V, and 300 K for t_h from 0.0002 to 5 s.

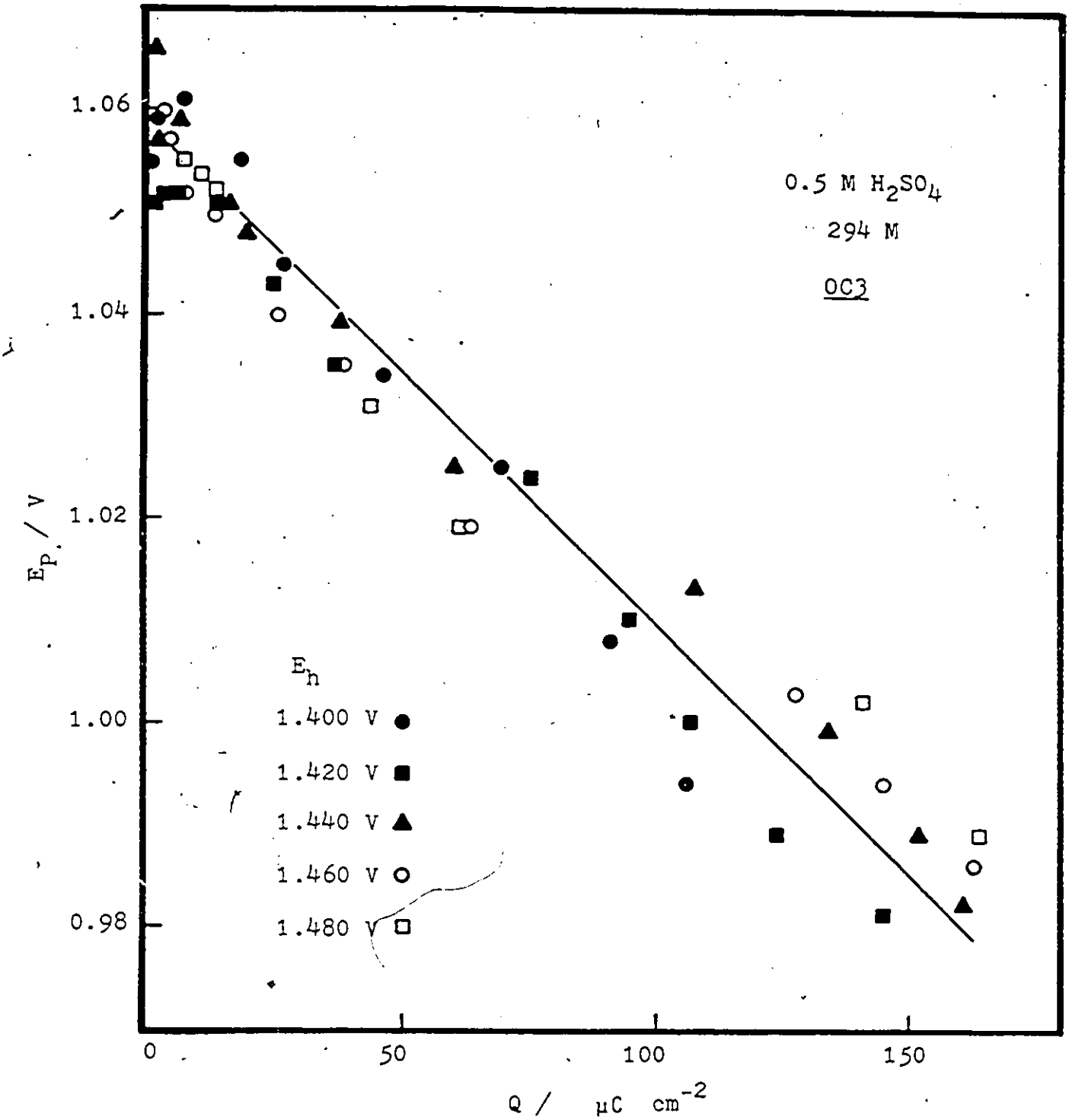

Figure 4.5.8. OC3 peak potentials plotted against peak charge for Au in 0.5 M H_2SO_4 at several E_h and 294 K for t_h from 0.0002 to 5 s.

Q_{OC3} is between 50 and 100 $\mu C\ cm^{-2}$. After convergence is reached, the peak potentials for OC3 shift linearly with increasing charge, with a slope of about -0.4 mV $\mu C^{-1} cm^2$, as is shown more clearly in Figure 4.5.8. for 0.5 M H_2SO_4 at 294 K for several surface oxide growth potentials. Under these conditions, however, this linear relationship begins at $Q_{OC3} = 0$ and the slope is about -0.5 mV $\mu C^{-1}\ cm^2$. The peak potentials for the two types of conditions converge at the saturation coverage, as was also seen in Figure 4.5.6.

4.5.3. The Effect of Temperature on Surface Oxide Formation Under "Anions Off" Conditions

Figures 4.5.9.a. and 4.5.9.b. show the I vs E profiles for the reduction of surface oxide grown using the "anions off" potential-time program in 1 M $HClO_4$ with $4X10^{-4}$ M H_2SO_4 at 1.340 V at 273 K and 318 K, respectively. The I vs E profiles for growth under similar conditions at 300 K was shown earlier in Figure 4.5.1.a. Under "anions off" conditions at all three temperatures, the OC1 peak is well defined as was noted in Section 4.2. However, this initial reversibly formed species that is reduced in this peak begins to disappear after holding times that are shorter with increasing temperature, as the rates of both SO_4^{2-} adsorption and conversion of OC1 surface oxide to changed states increase with temperature. The rate of growth of the OC2 and OC3 species increases considerably with temperature at this growth potential. The OC2 peak does not appear before 0.01 s holding at 273 K but at 318 K, it is already observed before any potential holding. The growth of the OC2 and OC3 species is, however, very slow for holding times between 0.05 and 2 s at 273 K. Some slowing of growth due to anion adsorption is seen at 300 K, but no obvious diminution arises in the growth rate for these two species at 318 K. At 273 K, the disappearance of the OC1 peak seems to be more closely related to anion adsorption at 273 K and to conversion at 318 K, but these two processes are not

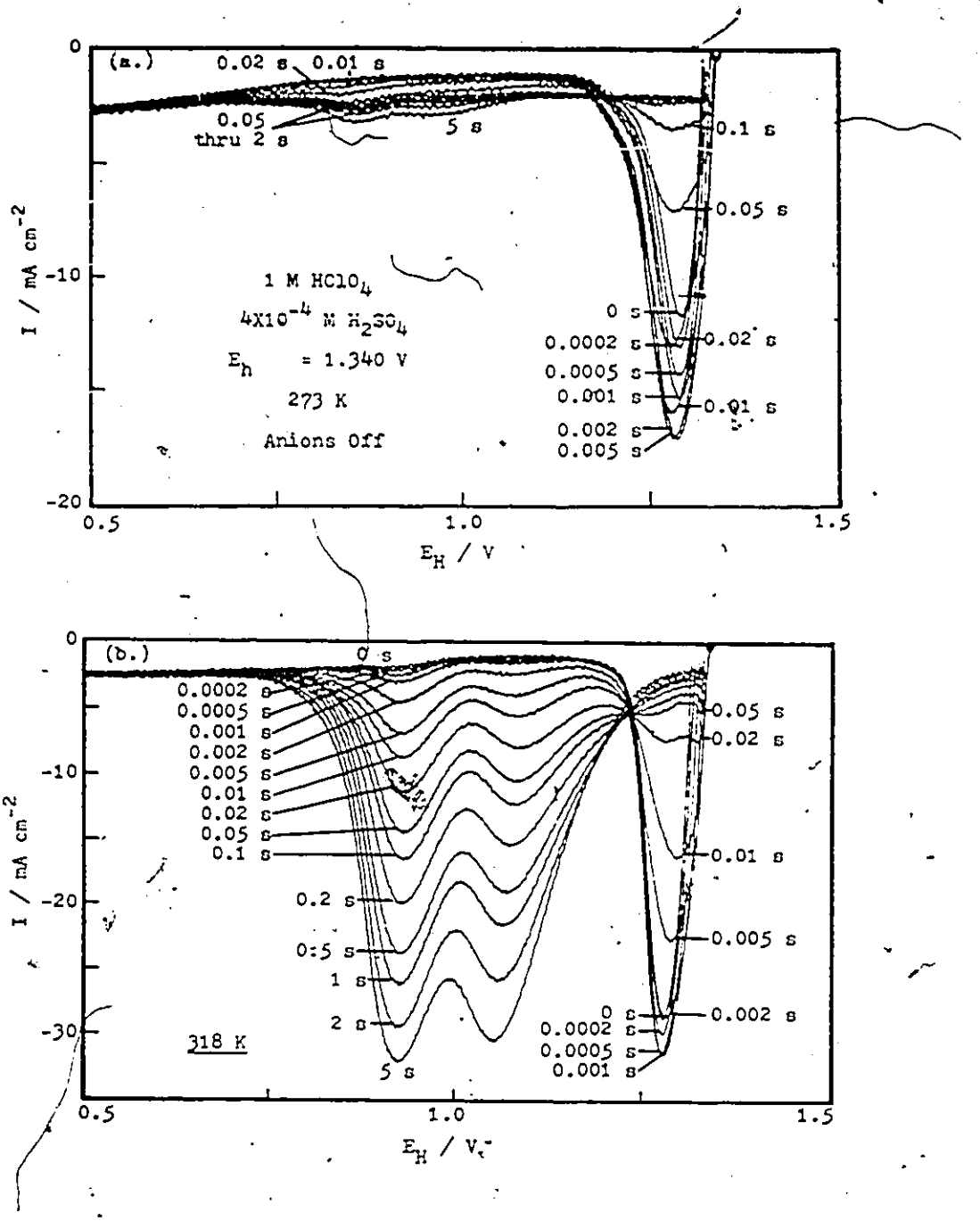

Figure 4.5.9. Series of potentiodynamic I vs E profiles for "anions off" surface oxide growth at Au at E_h = 1.340 V and several t_h between 0.0002 and 5 s in 1 M $HClO_4$ with $4X10^{-4}$ M H_2SO_4. (a.) 273 K; (b) 318 K

independent.

The growth behavior at three temperatures (273, 300 and 318 K) under "anions off" conditions is compared in Figure 4.5.10. for Au in 1 M $HClO_4$ with $4X10^{-4}$ M H_2SO_4 at E_h = 1.340 V. All three growth curves show either a decrease or an arrest in surface oxide formation rate as sulfate becomes readsorbed at the surface, but this decrease is most pronounced for growth at 273 K and only a plateau is seen at 318 K at this growth potential. Also, the 318 K curve shows a logarithmic growth region, which is not observed at the two lower temperatures at times less than 5 s at 1.340 V. Since the formation of the OC2 and OC3 species occurs more rapidly at the higher temperature, the sulfate ion is not given as long a time to become adsorbed at the surface and interfere with surface oxide formation as at the lower temperatures. These growth curves appear similar to those found at other potentials, but at the same temperature (Figure 4.5.3.a.), in this electrolyte.

Figure 4.5.11. shows the growth and disappearance the OC1 peak for "anions off" growth for the same three temperatures at 1.340 V. The maximum charge of the peak increases with temperature. The peak also begins to disappear after a shorter time at higher temperature, obviously because the sulfate ion becomes readsorbed more quickly as is seen in Figure 4.2.2. and also because the conversion process to the OC2 and OC3 species occurs more quickly at higher temperature.

A summary in which peak potentials and coverages (as OH-species) are compared for the OC1, OC2 and OC3 states for both "anions off" and "anions on" growth at the three different temperatures in 1 M $HClO_4$ with $4X10^{-4}$ M H_2SO_4 is given in Table 4.5.1. Maximum coverage of the OC1 type peaks for "anions on" type growth was not clearly found at 300 K and 318 K and so could not be given in the table. The maximum coverage of the OC1 species attained in "anions on" growth is somewhat less than that for "anions off" growth, and it decreases

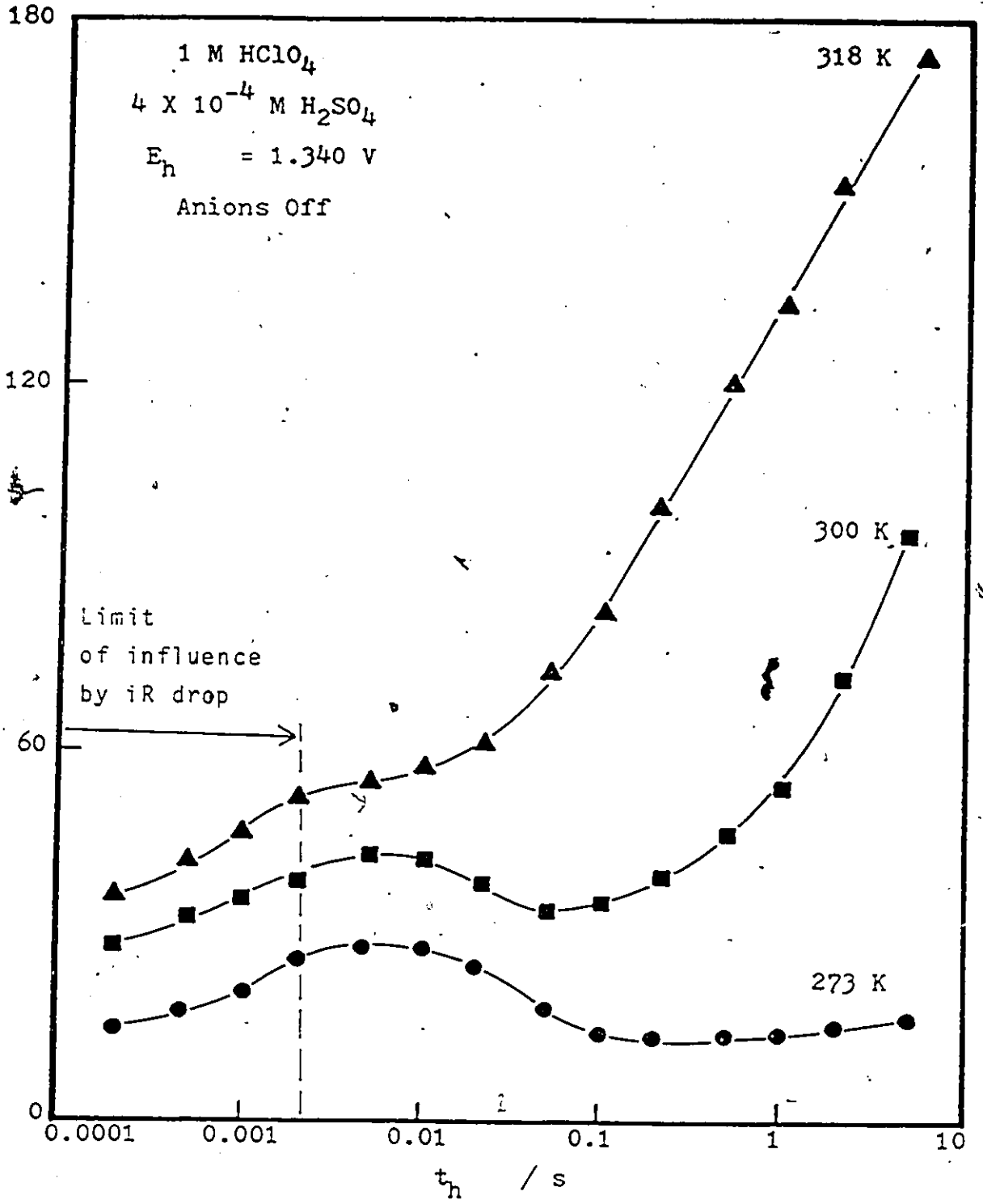

Figure 4.5.10. Variation of surface oxide charge formed at Au in 1 M $HClO_4$ with $4X10^{-4}$ M H_2SO_4 at 1.340 V and 273 K, 300 K and 318 K for "anions off" growth and t_h from 0.0002 to 5 s.

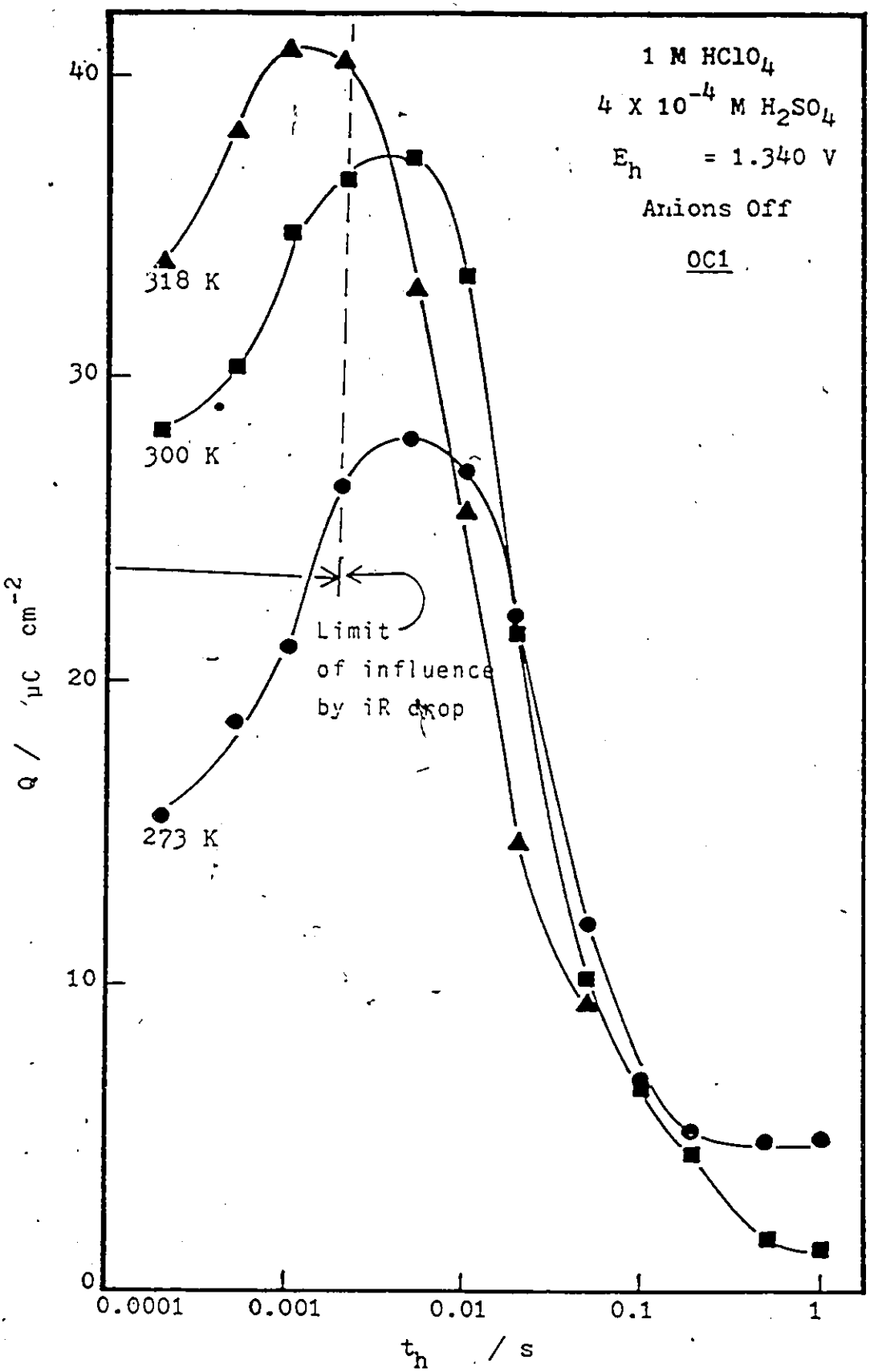

Figure 4.5.11. Variation of Q_{OC1} formed at Au in 1 M $HClO_4$ with $4X10^{-4}$ M H_2SO_4 at 1.340 V and 273 K, 300 K and 318 K for "anions off" growth and t_h from 0.0002 to 5 s.

Table 4.5.1.

Summary of Oxide Growth Behavior in 1 M $HClO_4$ with $4X10^{-4}$ M H_2SO_4 for "Anions Off" and "Anions On" Conditions

T / K	273		300		318	
Anions	off	on	off	on	off	on
OC1						
θ_{max}*	0.34	0.30	0.30	--	0.26	--
E_P / V						
OC1	1.289	1.346	1.289	1.341	1.280	1.331
OC1'	--	1.289	--	1.290	--	1.280
OC2						
θ_{max}*	0.38	0.34	0.38	0.36	0.38	0.36
E_P / V	0.834	0.857	0.892	0.910	0.928	0.943
Δ mV	23		18		15	
OC3						
E_P / V	0.983	1.018	1.045	1.073	1.075	1.095
(as θ_{OC3} -> 0)						
Δ mV	35		28		20	

* θ_{max} data are calculated here as coverages for OH-species (1 e/site).

somewhat with increasing temperature. The "anions off" OC1 peak potential does not seem to change much with temperature, but for the "anions on" it shifts to less positive potentials with temperature.

It is also interesting that the "anions on" OC1' initial peak potential is the same for that of the "anions off" OC1 peak. This seems to confirm the suggestion (Section 4.2.) that the OC1' peak appears for surface oxide growth in H_2SO_4 when the anions begin to desorb from the Au surface.

The OC2 peak saturation coverage is not much affected by temperature or the initial presence of sulfate ion at the surface before surface oxide formation commences. The OC2 and OC3 peak potentials shift positively with temperature, as was also seen for growth in 0.5 M H_2SO_4.

4.5.4. "Anions Off" and "Anions On" Surface Oxide Formation at Au in 1 M $HClO_4$ WITH $4X10^{-5}$ M H_2SO_4

Figures 4.5.12. and 4.5.13. enable comparison to be made between "anions off" and "anions on" growth for several potentials at Au in this electrolyte mixture at 296 K. The "anions off" growth curves at the lower potentials examined show dips or arrests in surface oxide formation, but these are not nearly as pronounced as those found for 1 M $HClO_4$ with $4X10^{-4}$ M H_2SO_4. This is because the sulfate anions will tend to be readsorb about ten times more slowly in the more dilute solution. For this reason also, the surface oxide grows somewhat faster in $4X10^{-5}$ M H_2SO_4 for these lower potentials than in $4X10^{-4}$ M H_2SO_4. The "anions off" growth in 1 M $HClO_4$ with $4X10^{-5}$ M H_2SO_4 seems to be intermediate between that in 1 M $HClO_4$ with $4X10^{-4}$ M H_2SO_4 and that in 1 M $HClO_4$ with no added H_2SO_4. The "anions on" growth curves are very similar to those in 1 M $HClO_4$ with $4X10^{-4}$ M H_2SO_4. This is, of course, because the surface has a near equilibrium coverage of SO_4^{2-} for "anions on" growth, and this coverage would be only slightly smaller for the lower concentration of H_2SO_4[105]. The "anions on" growth approaches the "anions off" at higher growth

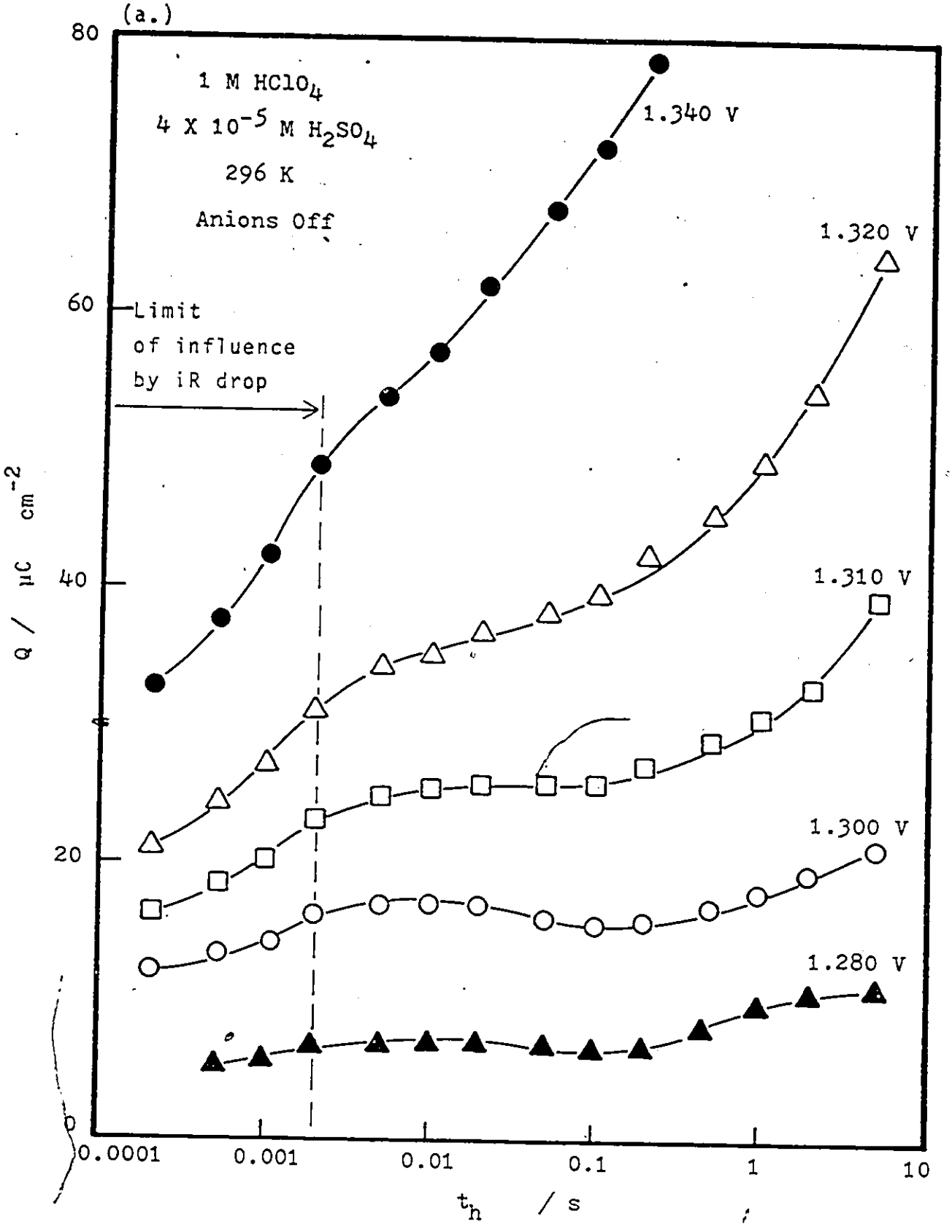

Figure 4.5.12. Variation of surface oxide charge formed at Au in 1 M $HClO_4$ with $4X10^{-5}$ M H_2SO_4 at several E_h and 296 K for "anions off" growth and t_h from 0.0002 to 5 s.

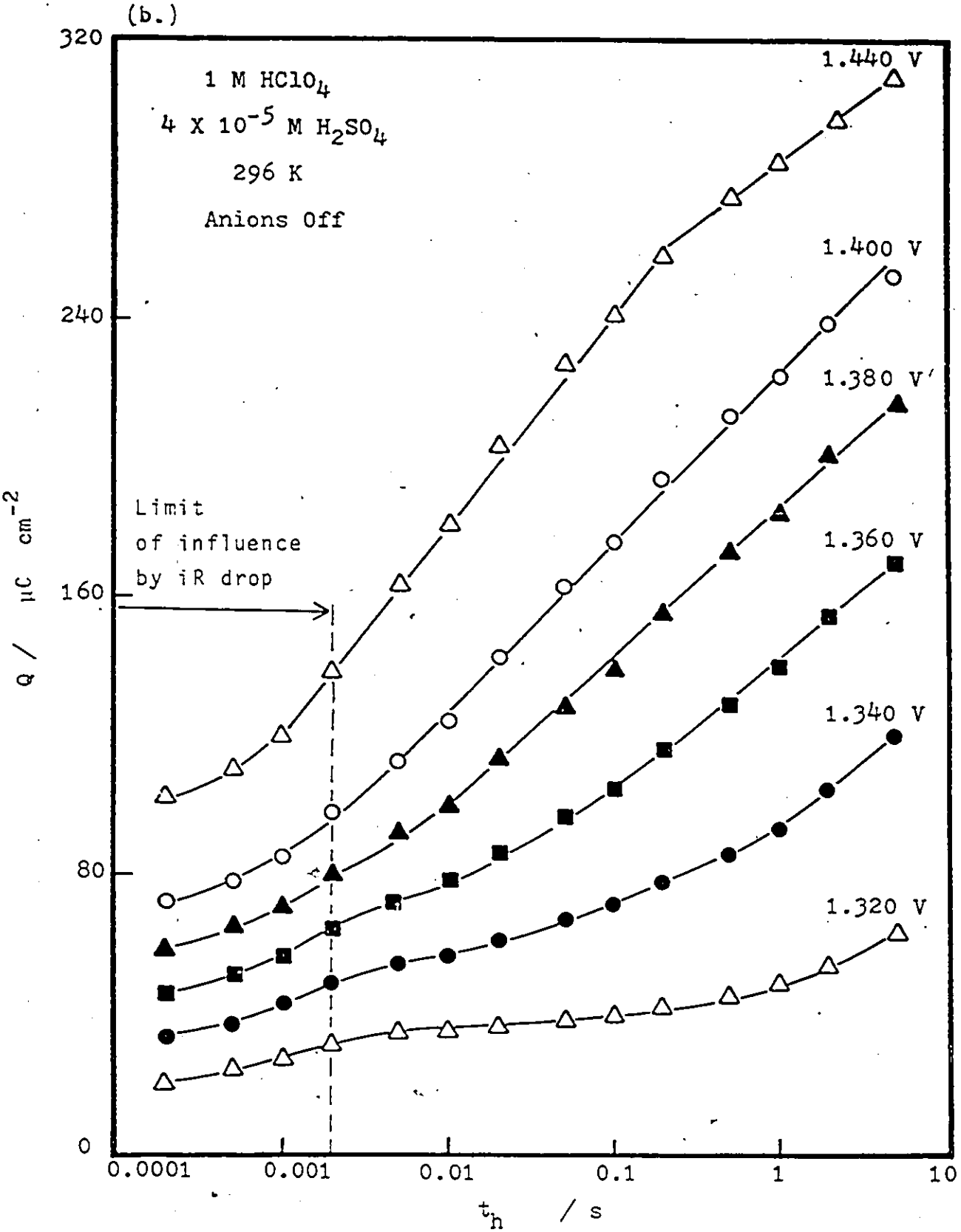
(b.)
1 M $HClO_4$
4 X 10^{-5} M H_2SO_4
296 K
Anions Off
1.440 V
1.400 V
1.380 V
1.360 V
1.340 V
1.320 V
Limit
of influence
by iR drop
Q / μC cm^{-2}
320
240
160
80
0
0.0001
0.001
0.01
0.1
1
10
t_h / s

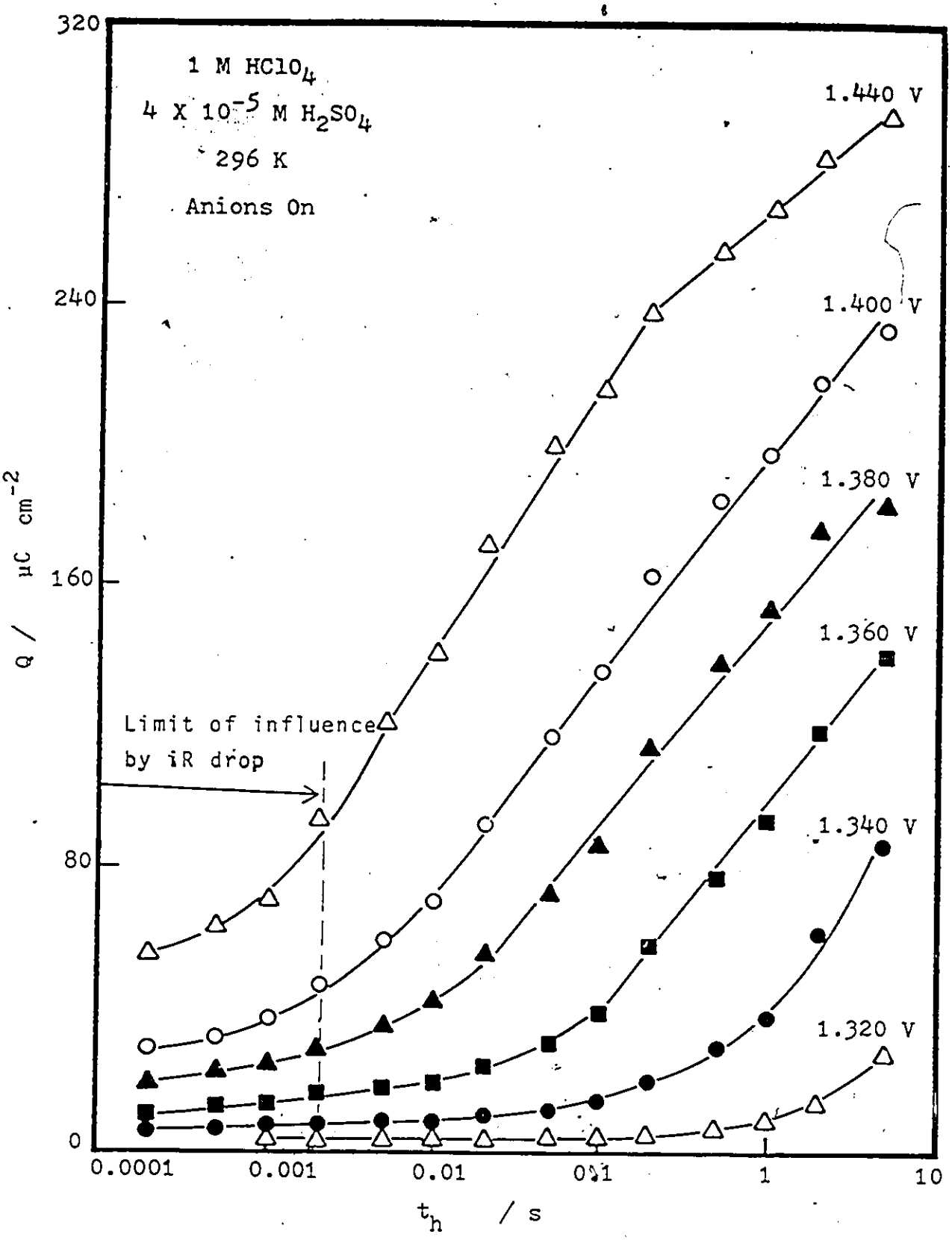

Figure 4.5.13. Variation of surface oxide charge formed at Au in 1 M $HClO_4$ with $4X10^{-5}$ M H_2SO_4 at several E_h and 296 K for "anions on" growth and t_h from 0.0002 to 5 s.

Table 4.5.2.

Summary of Oxide Growth Behavior in 1 M $HClO_4$ with $4X10^{-5}$ M H_2SO_4 for "Anions Off" and "Anions On" Conditions

T / K	273		296		318	
Anions	off	on	off	on	off	on
OC1						
θ_{max}*	0.34	0.30	0.32	0.26	0.30	0.22
E_p / V						
OC1	1.280	1.332	1.280	1.333	1.275	1.330
OC1'	--	1.280	--	1.265	--	1.280
OC2						
θ_{max}*	0.38	0.34	0.38	0.34	0.40	0.36
E_p / V	0.817	0.850	0.863	0.892	0.910	0.913
Δ mV	32		29		29	
OC3						
E_p / V	0.975	1.010	1.020	1.052	1.075	1.095
(as θ_{OC3} -> 0)						
Δ mV	35		32		20	

* θ_{max} data are calculated here as coverages for OH-species (1 e/site).

potentials and long holding times, as it did in the 1 M $HClO_4$ with $4X10^{-4}$ M H_2SO_4 electrolyte, and also as expected.

A summary in which peak potentials and coverages are compared (as OH-species) for the OC1, OC2 and OC3 states for both "anions off" and "anions on" growth at three temperatures in 1 M $HClO_4$ with $4X10^{-5}$ M H_2SO_4 is given in Table 4.5.2. In general, and as expected, the influence of SO_4^{2-} is less in this electrolyte than in 1 M $HClO_4$ with $4X10^{-4}$ M H_2SO_4 for all the surface oxide reduction peaks. In this electrolyte mixture the maximum OH coverage for the OC1 peak(s) decreases with temperature for both "anions off" and "anions on" growth, and the "anions on" coverages are consistently lower than those for "anions off" conditions.

4.5.5. Surface Oxide Formation at Au in 1 M $HClO_4$ with $4X10^{-3}$ M H_2SO_4

As in the potentiodynamic I vs E profile at 50 V s^{-1} (Figure 4.2.1.b.), surface oxide growth in 1 M $HClO_4$ with $4X10^{-3}$ M H_2SO_4 is not affected by holding at 1.2 V to allow equilibrium adsorption of sulfate to be attained at the gold surface. For 4 X 10^{-3} M, the electrode seems to be already saturated with this anion, just as in 0.5 M H_2SO_4. For this reason only the "anions off" type potential-time program was used to examine surface oxide growth in this electrolyte.

Figure 4.5.14. shows some typical I vs E reduction profiles for surface oxide growth at gold in this solution at 299 K and 1.370 V. These growth profiles very much resemble those for the "anions on" case in 1 M $HClO_4$ with $4X10^{-4}$ M H_2SO_4 except that the OC2 peak does not grow quite as quickly as the OC3 peak.

Figure 4.5.15. shows surface oxide growth curves for several potentials at gold in this electrolyte at 299 K. They resemble those for "anions on" growth in the other two mixed electrolytes studied and also those for 0.5 M H_2SO_4, with regions of non-logarithmic followed by logarithmic growth behavior.

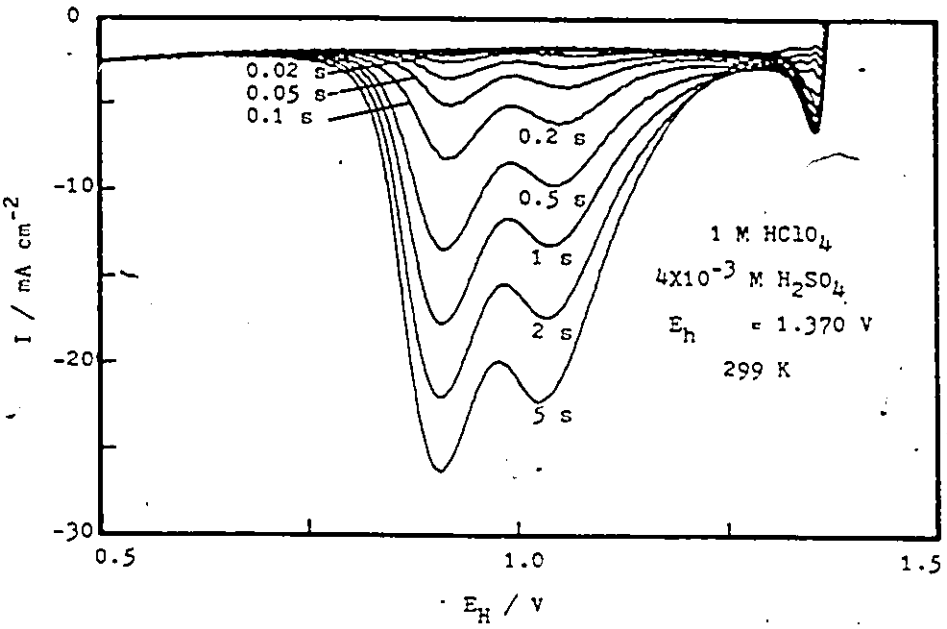

Figure 4.5.14. Series of potentiodynamic I vs E profiles for surface oxide growth at Au at E_h = 1.370 V and several t_h between 0.0002 and 5 s and at 299 K in 1 M $HClO_4$ with $4X10^{-3}$ M H_2SO_4.

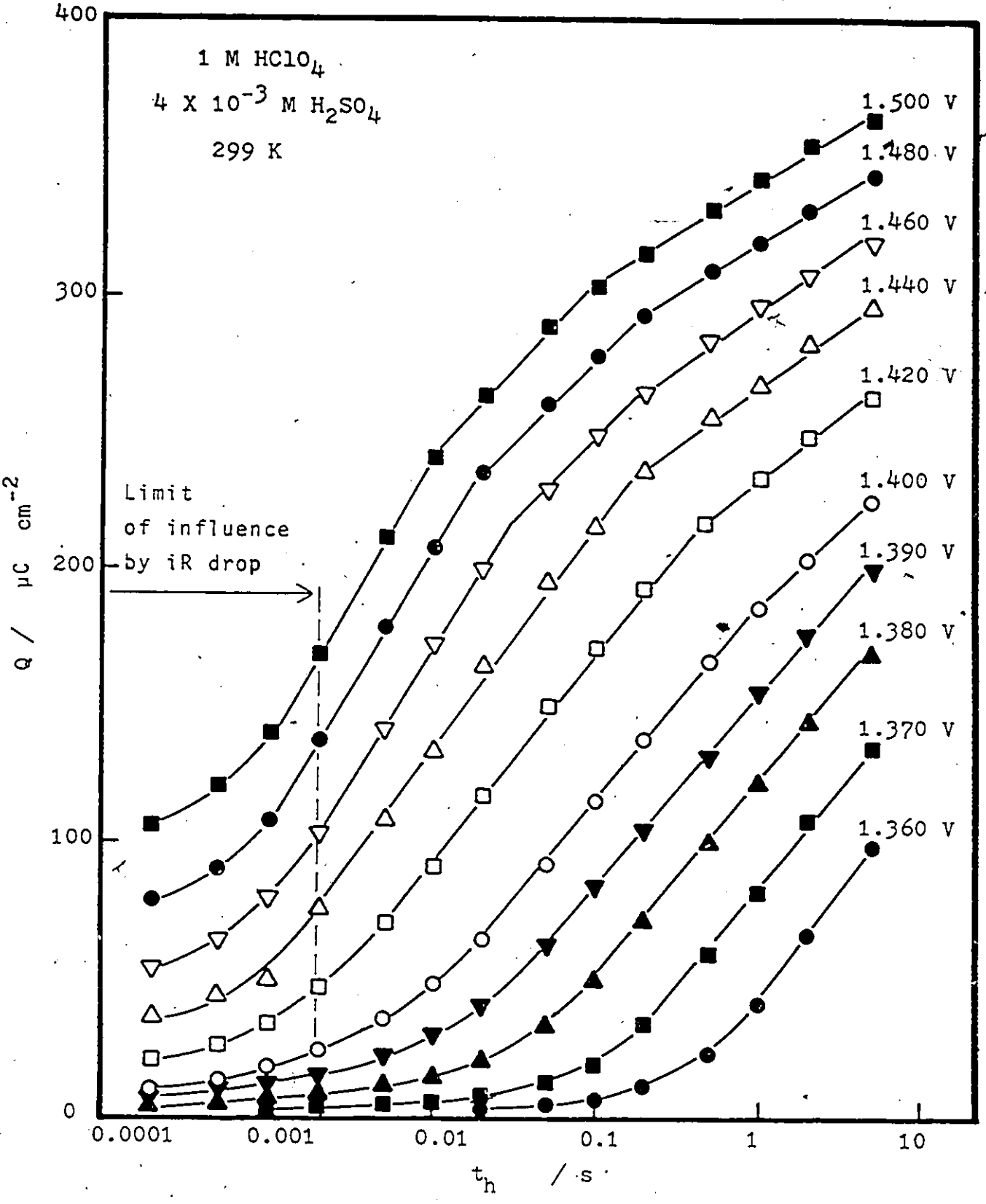

Figure 4.5.15. Variation of surface oxide charge formed at Au in 1 M $HClO_4$ with $4X10^{-3}$ M H_2SO_4 at several E_h and 299 K for t_h from 0.0002 to 5 s.

Table 4.5.3.

Summary of Oxide Growth Behavior in 1 M $HClO_4$ with $4X10^{-3}$ M H_2SO_4*

T / K	273	299	318
OC1			
θ_{max} **	0.28	0.24	0.22
E_p / V			
OC1	1.353	1.353	1.346
OC1'	1.300	1.307	1.310
OC2			
θ_{max} **	0.22	0.34	0.32
E_p / V	0.837	0.913	0.950
OC3			
E_p / V (as θ_{OC3} => 0)	1.009	1.075	1.105

* At this concentration, sulfate anions are always present on the surface, as in 0.5 M H_2SO_4.

** θ_{max} data are calculated here as coverages for OH-species (1 e/site).

A summary of peak potentials and coverages (as OH-species) for the OC1, OC2 and OC3 states arising in growth at three temperatures in 1 M $HClO_4$ with $4X10^{-3}$ M H_2SO_4 is given in Table 4.5.3. Because sulfate adsorption attains saturation in this electrolyte, these results should be compared only with those for the "anions on" conditions for the other two mixed electrolytes examined.

When these results are related to those for the other two mixed electrolytes, it is seen that all the reduction peak potentials of the surface oxide species formed become more positive with increasing H_2SO_4 concentration and coverage by sulfate ions, and the OC2 and OC3 peak potentials become more positive with increasing temperature.

Inspection of the coverage data summarized in Tables 4.5.1., 4.5.2. and 4.5.3. leads to the following general conclusions:

1. the OC1 charge tends to decrease with increasing temperature, possibly as a result of a greater rate of conversion to other states at higher temperatures;
2. The saturation OC2 charges are virtually independent of temperature over the investigated range (273 to 318 K) and independent of anion concentration, with the exception of a single result for 4×10^{-4} M H_2SO_4 at 273 K (Table 4.5.3.), For which the OC2 value is lower than the other two values. This may be due to difficulty in separating the OC2 from the OC3 peak at this temperature, since these two peaks come closer together with decreasing temperature and increasing H_2SO_4 concentration.

4.5.6. "Square-Root" Growth Behavior in Mixed Electrolytes

It was mentioned in Section 4.4.5., when some of the data for total surface oxide charge are plotted against the square-root of holding time for growth at Au, e.g. in 1 M $HClO_4$ with $4X10^{-4}$ M H_2SO_4 at 300 K (Figure 4.5.16.),

apparently linear relations arise at several growth potentials. The non-logarithmic regions of the "anions on" growth relations for mixed $HClO_4/H_2SO_4$ electrolytes seem to follow an apparent "square-root" law just as for growth in ~~0.5 M H_2SO_4~~ (Section 4.4.5.). Two examples of $t_h^{1/2}$ plots are shown in Figures 4.5.16., for 1 M $HClO_4$ with 4 X 10^{-4} M H_2SO_4, and 4.5.17., for 1 M $HClO_4$ with 4 X 10^{-3} M H_2SO_4.

As demonstrated by the exploratory linear and square-root t_h plots in Section 4.4.5., however, data points for which $t_h \leq 2$ ms (separated by the dashed line from other points at longer t_h) are determined primarily by the iR drop limitation because the initial currents are relatively large. Hence, this type of points at short t_h do not belong to a $t_h^{1/2}$ relation and, in fact, plot out linearly in time, as was shown in Figures 4.4.10.a. and b. Soon, but not immediately, after this initial iR controlled growth period, the data follows $\log(t_h)$ relations. The commencement of these logarithmic regions is marked by brackets ([ ) in Figures 4.5.16. and 4.5.17.

However, when $t_h > 0.2$ ms, and the growth rate is no longer controlled by the iR effect, and the holding potential is relatively low (1.360 to 1.390 V), Q seems to follows a $t_h^{1/2}$ relation before logarithmic growth behavior sets in. At the two lowest potentials (1.360 and 1.370 V), the increase with Q is so small that the data may be fitted equally well by a linear, square-root or logarithmic relation in t_h, so that a $t^{1/2}$ relation cannot be reliably distinguished. The growth relations that do seem to have a significant section in $t^{1/2}$ in ~~Figure 4.5.16.~~ and 4.5.17. are distinguished by the solid black points.

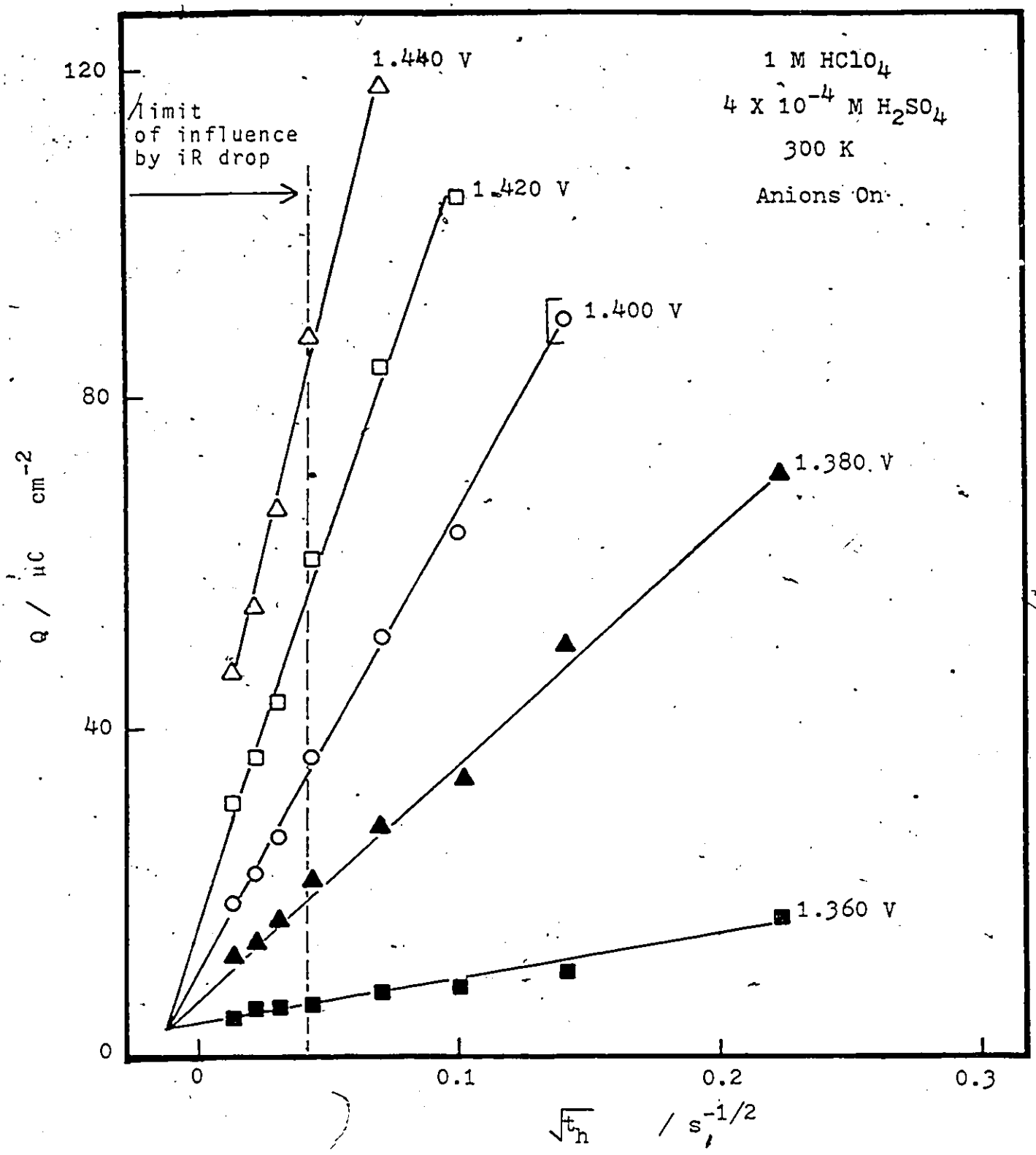

Figure 4.5.16. Variation of surface oxide charge with $t_h^{1/2}$ at Au in 1 M $HClO_4$ with $4X10^{-4}$ M H_2SO_4 at several E_h and 300 K for "anions on" growth and t_h from 0.0002 to 0.5 s.

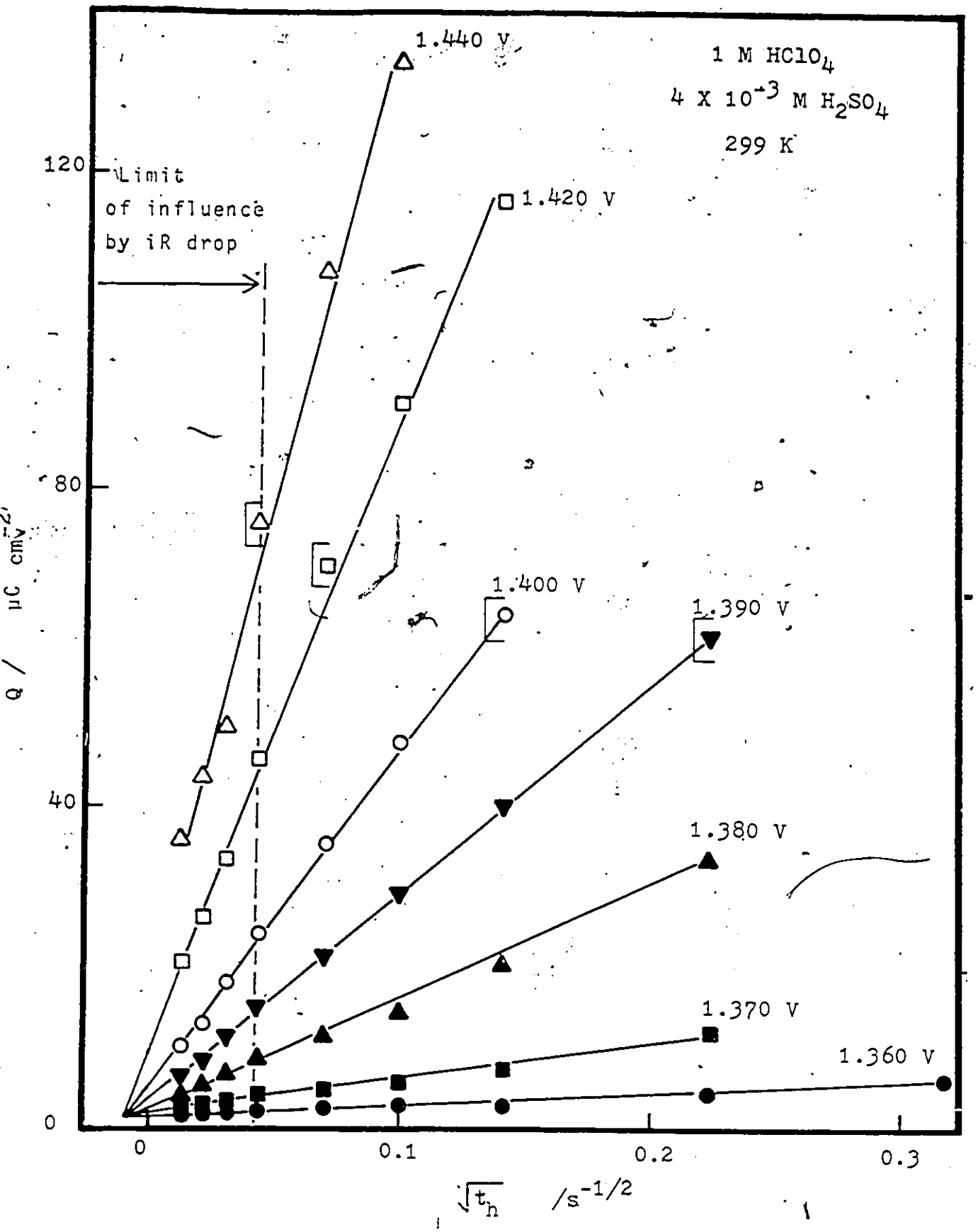

Figure 4.5.17. Variation of surface oxide charge with $t^{1/2}$ at Au in 1 M $HClO_4$ with $4X10^{-3}$ M H_2SO_4 at several growth potentials and 299 K and t_h from 0.0002 to 0.5 s.

4.6. Temperature Effects on Au Surface Oxide Formation and Reduction

Previous work in this laboratory showed that temperature has, as may be expected, important effects on the kinetics of surface oxide formation at Au[6,7]. In the present work, the effects of temperature on the first distinguishable surface oxide species and the species reduced in the main peak, OC3, was examined using cyclic-voltammetry.

First, the potentiodynamic I vs E profile for Au at 0.050 V s^{-1} in 0.5 M H_2SO_4 are shown in Figure 4.6.1. for several temperatures between 274 and 318 K. The apparent potential for the onset of surface oxide formation and the first clear anodic peak become less positive with increasing temperature. This initial sharp oxidation peak is prominent at 318 K, but its current decreases at lower temperatures, as a second, more positive peak becomes predominant. This result seems to arise from the temperature-dependence of adsorption of sulfate ions, which are more strongly adsorbed at lower temperatures.

The main reduction peak, OC3, becomes narrower and its potential shifts positively with increasing temperature. It should be noted that these I vs E profiles were measured in an isothermal cell, that is, a cell in which the H_2 reference electrode was maintained at the same temperature as the working electrode. Allowance must therefore be made for the change in potential of the H_2 reference electrode with temperature: thermo-cell measurements made in other work in this laboratory gave values of dE/dT for the H_2 electrode of 0.95 mV K^{-1} in 1 M CF_3SO_3H[241] and 0.85 mV K^{-1} in 0.1 M HCl[248]. For the present work on Au, the value 0.95 mV K^{-1} was used in making corrections to the potential scale.

In Figure 4.6.2., the current of the first clear anodic peak, OA2, shown in Figure 4.6.1. is plotted against temperature. Two linear regions are observed, the first between 273 and 300 K with a slope of 1.48 A cm^{-2} K^{-1} and

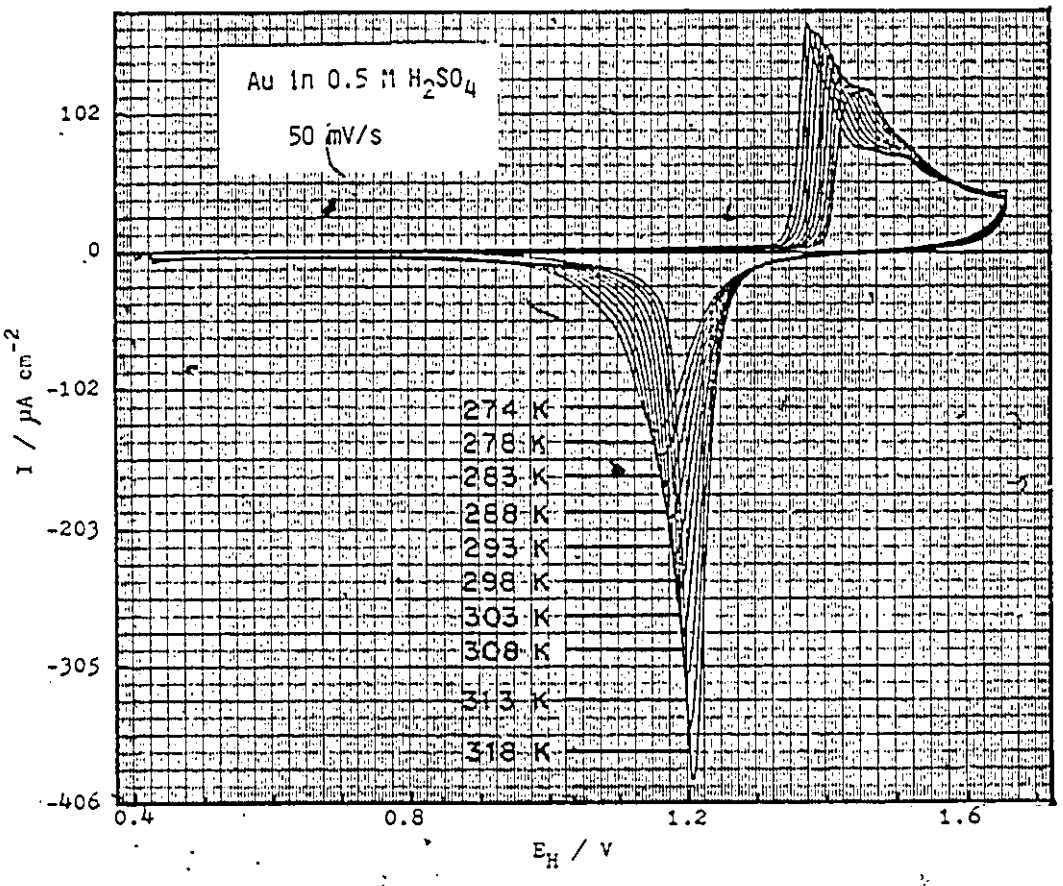

Figure 4.6.1. Potentiodynamic I vs E profiles for Au at 0.050 V s^{-1} in 0.5 M H_2SO_4 at several temperatures between 274 and 318 K.

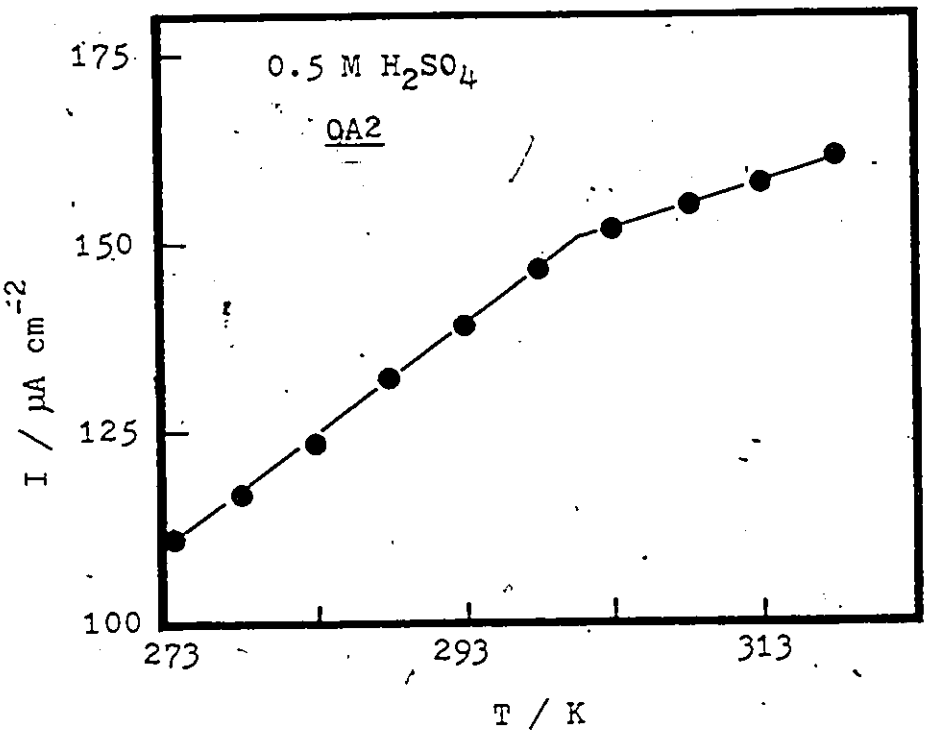

Figure 4.6.2. OA2 peak current vs temperature for Au at 0.050 V s^{-1} in 0.5 M H_2SO_4.

the second for temperatures above 300 K having a slope of 0.60 μA cm^{-2} K^{-1}. This suggests that there is a change in the kinetics of the process associated with this peak with temperature, at about 300 K. This might also due be to increasing predominance of the more anodic peak seen in Figure 4.6.1 with decreasing temperature at temperatures below 300 K.

Figure 4.6.3. shows the potential of this first large anodic peak, OA2, measured at 0.050 V s^{-1} plotted against temperature in 0.5 M H_2SO_4, and in 1 M $HClO_4$ with added H_2SO_4 present at concentrations of $4X10^{-3}$ M, $4X10^{-4}$ M and $4X10^{-5}$ M. When this peak potential is plotted against $\log[H_2SO_4]$ for four temperatures it is evident (see inset of Figure 4.6.3.) that it is linearly dependent on both temperature and $\log[H_2SO_4]$. When the slopes of these plots are corrected for the absolute temperature dependence of the H_2 reference electrode potential, the slope values are between 2.2 and 2.3 mV K^{-1}. However, the peak potential values deviate from linearity with temperatures below 283 K, where the more anodic peak became prominent, and the initial peak potential becomes difficult to measure.

The slopes of peak potential vs temperature relations for the four electrolytes examined are rather similar and are given in Table 4.6.1. The slope of peak potential vs log $[H_2SO_4]$ is about 10 mV per decade for the $HClO_4/H_2SO_4$ mixed electrolytes. The values obtained for 0.5 M H_2SO_4, however, do not fit the same linear relationship.

Table 4.6.1.

$[H_2SO_4]$ M	dE_P/dT^* mV K^{-1}
0.5	-2.27
$4X10^{-3}$	-2.19
$4X10^{-4}$	-2.28
$4X10^{-5}$	-2.30

* corrected for the temperature dependence of the H_2 electrode.

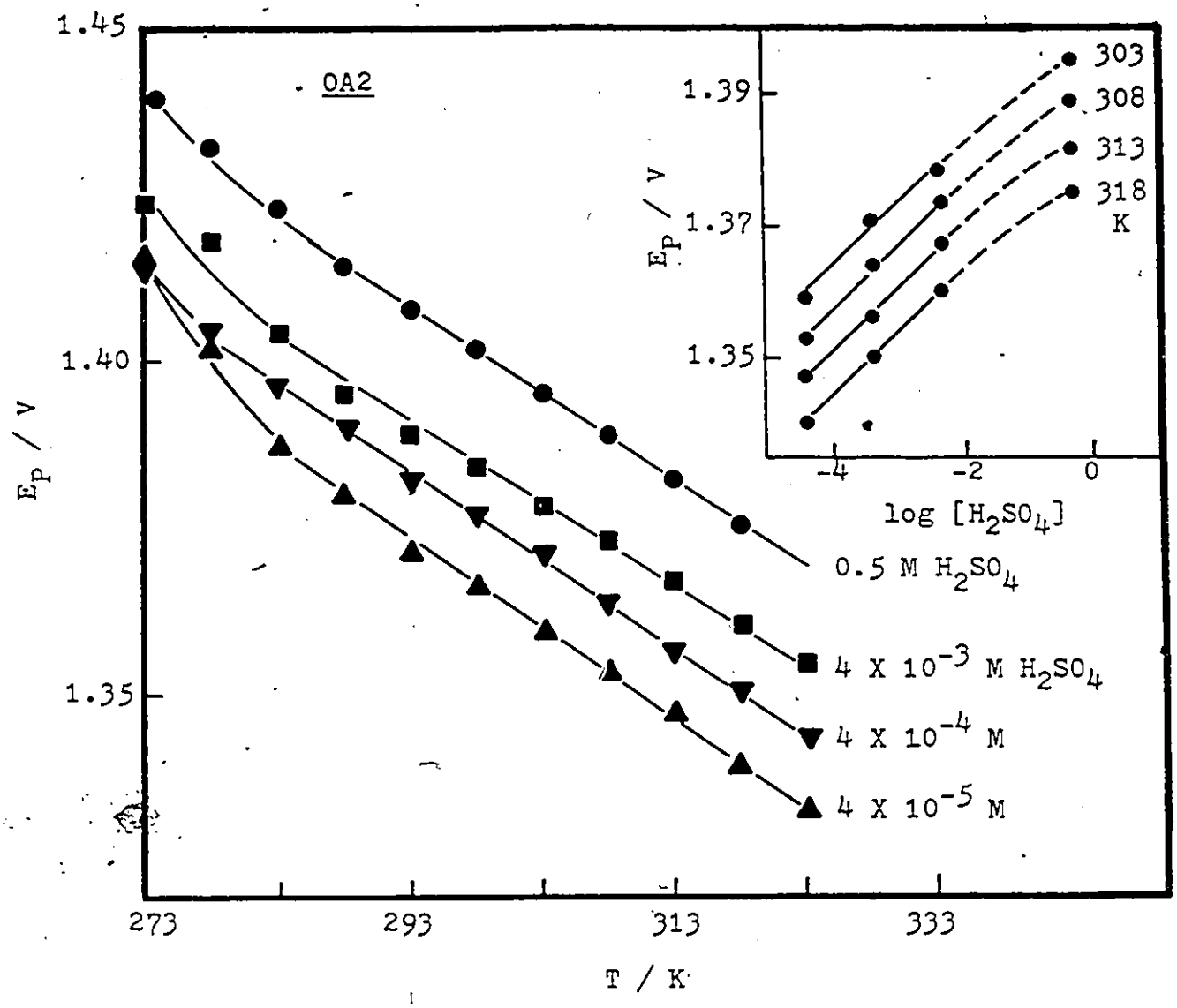

Figure 4.6.3. OA2 peak potential vs temperature and vs log [H_2SO_4] (inset) for Au at 0.050 V s^{-1} in 0.5 M H_2SO_4 and 1 M $HClO_4$ with $4X10^{-3}$, $4X10^{-4}$ and $4X10^{-5}$ M H_2SO_4.

In order to compare OC3 peak potentials and currents at different temperatures, the peaks must represent of similar charge, because these values otherwise vary with total surface oxide charge (as shown in Figure 4.1.2.) as well as with temperature. Potentiodynamic measurements of the type shown in Figure 4.1.2. were made at Au at 0.050 V s^{-1} in 0.5 M H_2SO_4 at 273, 283, 298, 319 and 343 K, taking a series of anodic end potentials, which allow different extents of surface oxidation to be attained. Figures 4.6.4., 4.6.5. and 4.6.6. show the OC3 reduction peak potentials, currents and peak half-width potentials, respectively, plotted against total surface oxide charge, using data from these potentiodynamic measurements. Surface oxide charge was measured by integrating the reduction current w.r.t. potential (and hence time) in the cathodic I vs E profiles, in the usual way.

The OC3 peak (Figure 4.6.4.) shifts to more positive potentials with increasing temperature and less positive values with increasing charge. At 273 and 283 K, the peak potential follows a linear relationship with temperature but, at higher temperatures, there are two linear regions with a break at about 200 $\mu C\ cm^{-2}$, i.e. after a single monolayer of OH has been formed. The dE_p/dQ values found are given in Table 4.6.2.

Table 4.6.2.

T / K	dE_p/dQ mV $\mu C^{-1}\ cm^{-2}$	$dI_p/d(Q^2)$ A $(\mu C\ cm^{-2})^{-2}$
273	-0.166	1410
283	-0.161	1310
298	-0.125	1360
319	-0.264 / 0.173	2160
343	-0.216 / 0.127	2900

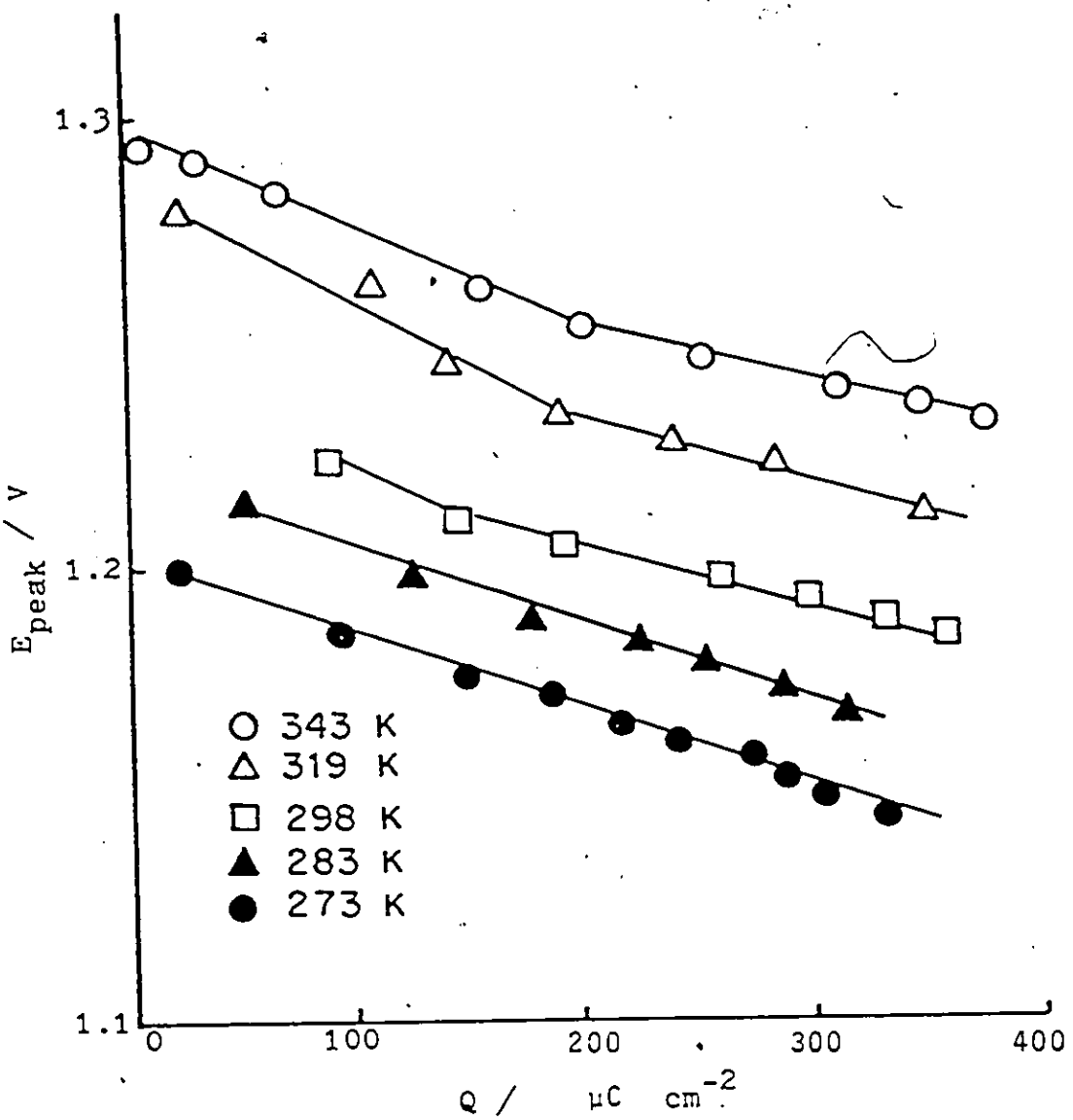

Figure.4.6.4. OC3 peak potential vs total surface oxide charge for Au at 0.050 V s^{-1} in 0.5 M H_2SO_4 at 273 K, 283 K, 298 K, 319 K and 343 K.

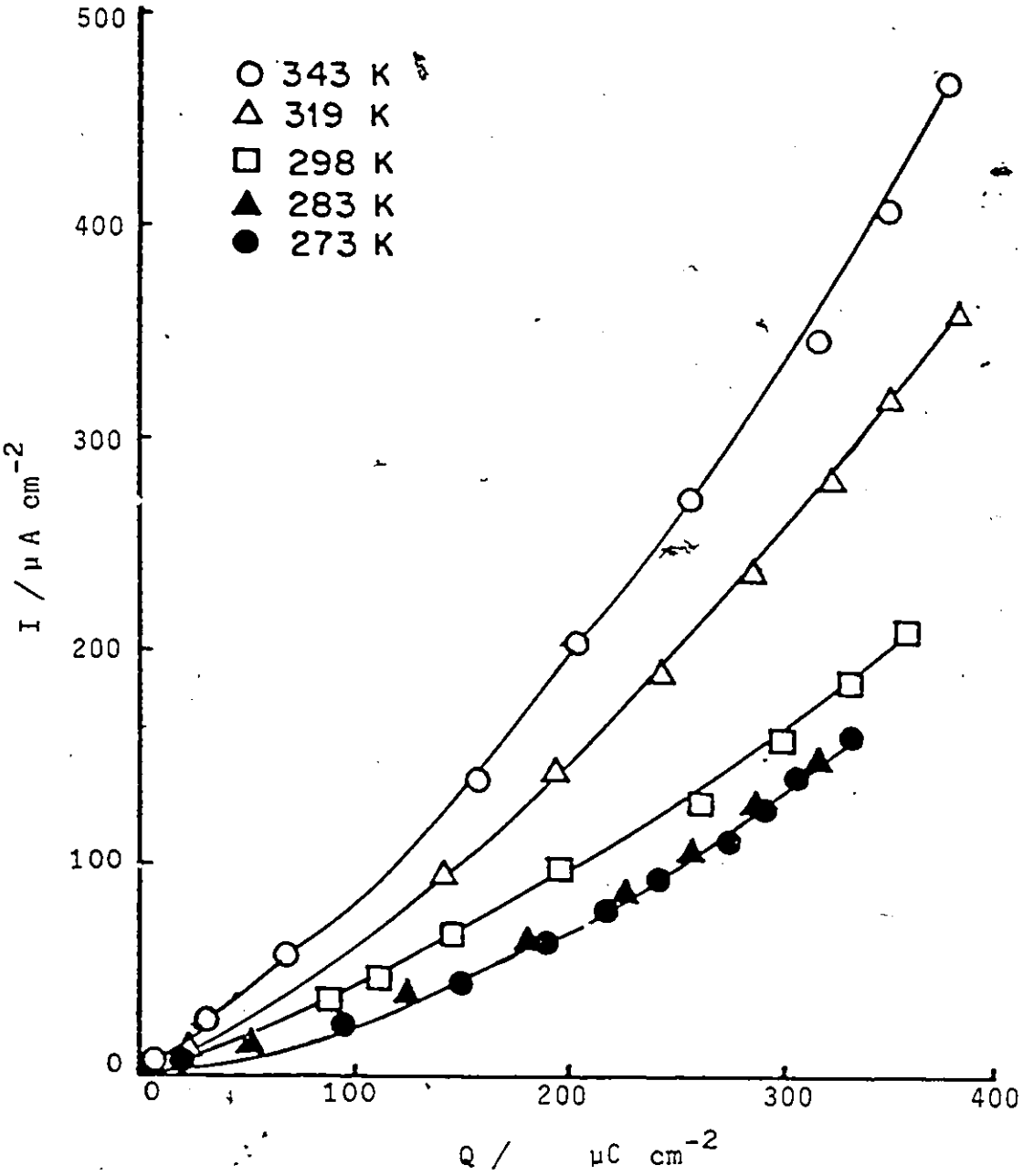

Figure 4.6.5. OC3 peak current vs total surface oxide charge for Au at 0.050 V s^{-1} in 0.5 M H_2SO_4 at 273 K, 283 K, 298 K, 319 K and 343 K.

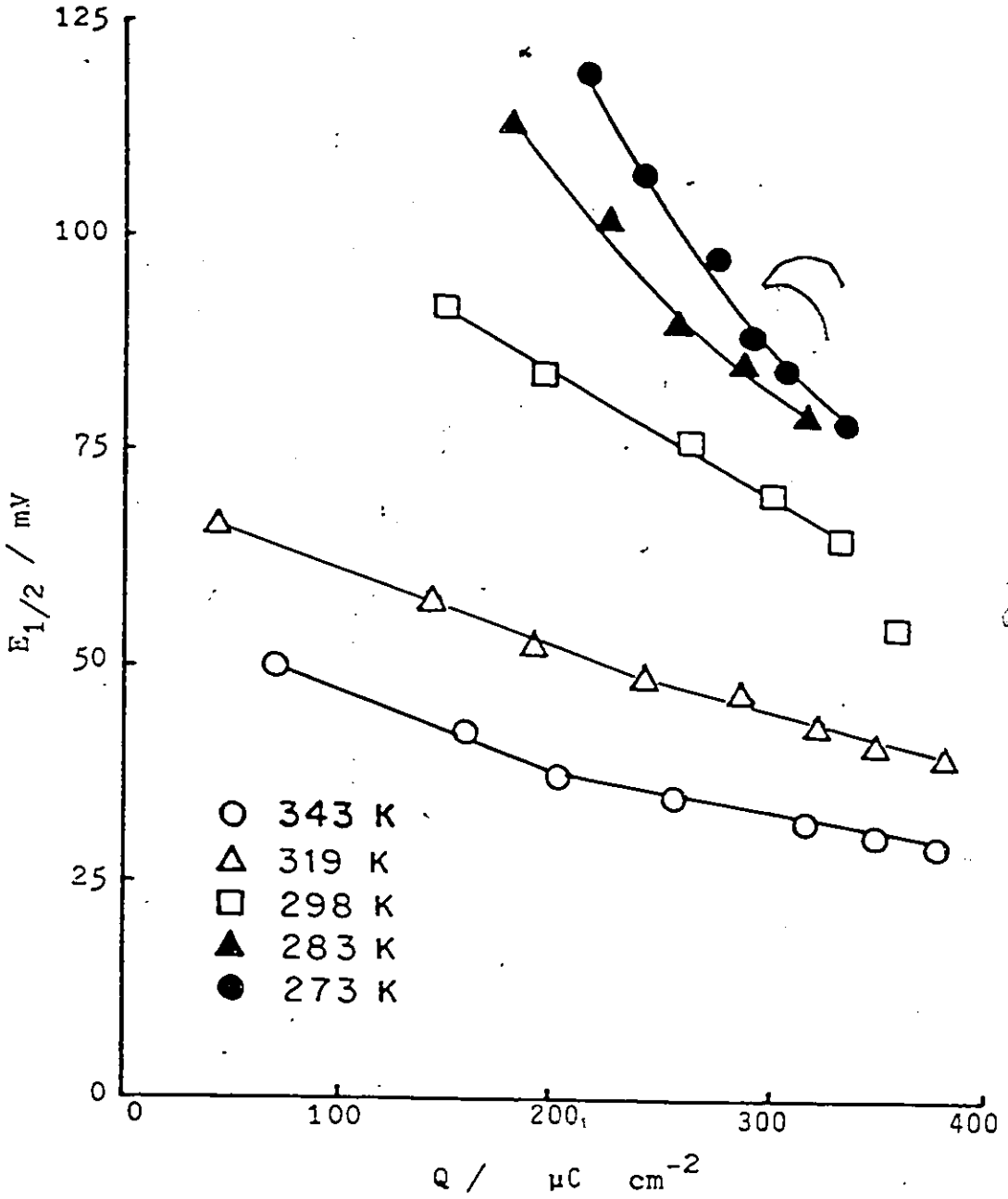

Figure 4.6.6. QCS half-width potential *vs* total surface oxide charge for Au at 0.050 V s^{-1} in 0.5 M H_2SO_4 at 273 K, 283 K, 298 K, 319 K and 343 K.

Peak currents (Figure 4.6.5.) apparently increase parabolically with charge. The $dI_p/d(Q^2)$ values obtained are also given in Table 4.6.2. The I_p values depend little on temperature in the range 273 to 283 K as the slopes, $dI_p/d(Q^2)$, are nearly the same. However, at 319 and 343 K, I_p and $dI_p/d(Q^2)$ both increase appreciably with temperature (Table 4.6.2.), indicating that the kinetics of reduction of the OC3 species at the surface differ for temperatures above and below 300 K. The half-width potential[7] of the OC3 peak (Figure 4.6.6.) decreases with increasing charge and temperature. This is expected because the peak current increases with charge squared, so the peak correspondingly becomes narrower. Formally, narrowing of peaks of this kind is known to originate from increasing 2-dimensional lateral attractive interactions between the ad-species in the surface film, ultimately leading to a single line for a well defined 3-dimensional phase, although this limit is not reached here.

4.7. Double-Layer Charging Behavior at Au in $HClO_4$ and H_2SO_4 Solutions

In the previous sections, and in earlier work[5-7], it has been shown how the early stages of oxidation of Au electrodes depend sensitively on anion adsorption in $HClO_4$ and H_2SO_4 solutions. While the present work was in progress, parallel studies were made on the oxidation of single-crystal Au surfaces by Angerstein-Kozlowska and Hamelin[194,195] in a joint project between the University of Ottawa and C.N.R.S., Meudon, France; this work demonstrated the specific role of the effects of adsorbed anions, especially at the (111) plane.

The present results and those obtained earlier require complementary studies of the adsorption of sulfate and ClO_4^- in acid solutions at Au in the double-layer charging region, i.e. before any of the processes examined in the previous section commence. In the present section, therefore, a brief account will be given of the behavior of the potential region at Au associated with double-layer charging processes, studied by means of potentiodynamic sweeps over restricted ranges of potential. These results will provide a basis for comparison of the adsorption of ClO_4^- and SO_4^{2-} (HSO_4^-) ions on the oxide-free Au surface (polycrystalline) in the potential range negative to that for initiation of the surface oxidation processes treated in the previous section, and in Chapter V which follows.

A comparison of the double-layer capacitance behavior of Au in 1 M $HClO_4$ and in 0.5 M H_2SO_4 can be made by inspecting the cyclic-voltammograms taken at 50 V s^{-1}, shown in Figure 4.7.1. for potentials negative to the onset of surface oxide formation. Since these currents are only due to capacitative charging of the metal/solution interface and electrosorption of anions of the electrolyte, the electrode's interfacial capacitance may be obtained by dividing the current by the sweep-rate. It should be mentioned that the double-layer capacitance over this potential range includes some

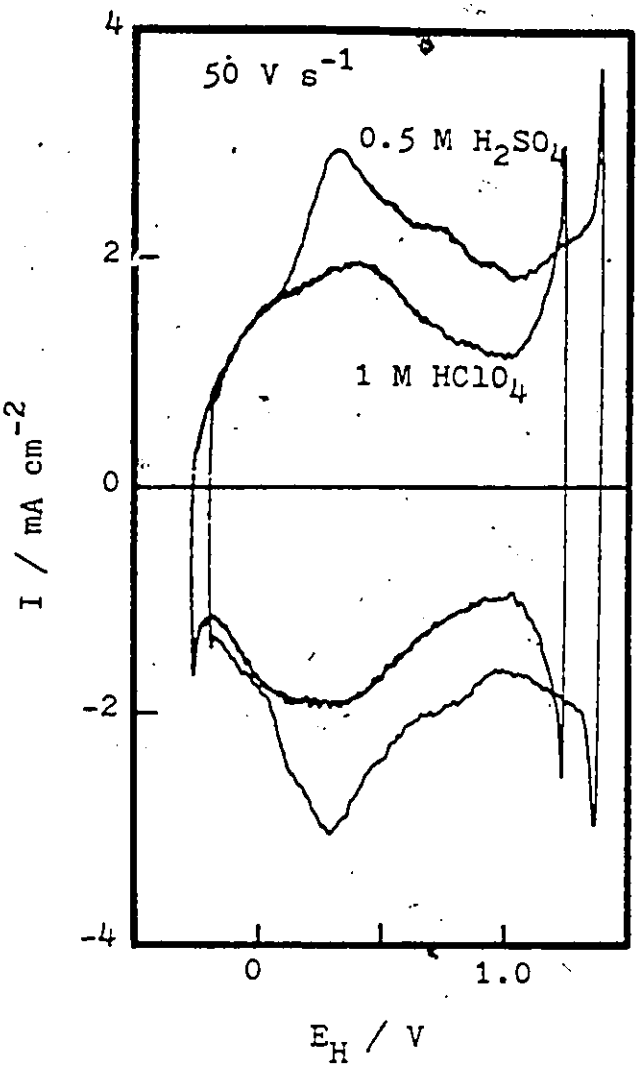

Figure 4.7.1. Potentiodynamic I vs E profiles for double layer charging of Au at 50 V s^{-1} in 0.5 M H_2SO_4 and 1 M $HClO_4$ at room temperature.

pseudocapacitance associated with chemisorption of anions that takes place with partial charge transfer[194,195] determined by the electrosorption valency factor[134].

The I vs E profiles are nearly the same for both electrolyte solutions at potentials below 0.1 V, but diverge considerably at more positive potentials, i.e. at potentials positive to the potential of zero charge (p.z.c.). The capacitance of Au in 0.5 M H_2SO_4 is approximately 20 $\mu F\ cm^{-2}$ greater than that for 1 M $HClO_4$ at potentials above 0.3 V. This potential is near the p.z.c. for Au in these solutions [143,144]. The I vs E profile in 0.5 M H_2SO_4 also shows several peaks which are not present in the profile for 1 M $HClO_4$, and probably are to be associated with charge-transfer chemisorption [194] of the sulfate ions in arrays on the surface. (Note that even on single-crystal Au surfaces, multiple peaks in the I vs E profiles also arise.)

The differences in the double-layer charging behavior of Au in these two electrolytes seems to be related to the strength of adsorption of the respective anions. At potentials below 0.1 V, which is well below the p.z.c., there should be no anions adsorbed at the negatively charged Au surface so that the double-layer charging behavior should be similar in both solutions. As the potential is made more positive and the Au surface becomes more positively charged, anions will tend to become adsorbed at the surface. Since SO_4^{2-} (HSO_4^-) is more strongly chemisorbed than ClO_4^-, giving and is associated with a greater extent of charge transfer at the surface, the corresponding capacitance should be larger. In fact, a large difference between the capacitative behavior of Au in solutions of these two anions is observed and indicates some significant charge transfer between the SO_4^{-2} (HSO_4^-) anions and the metal[195].

A similar cyclic-voltammogram is shown in Figure 4.7.2.a. for Au in 1 M $HClO_4$ with 4×10^{-4} M H_2SO_4 at 50 V s^{-1} for five potential holding times at 1.2

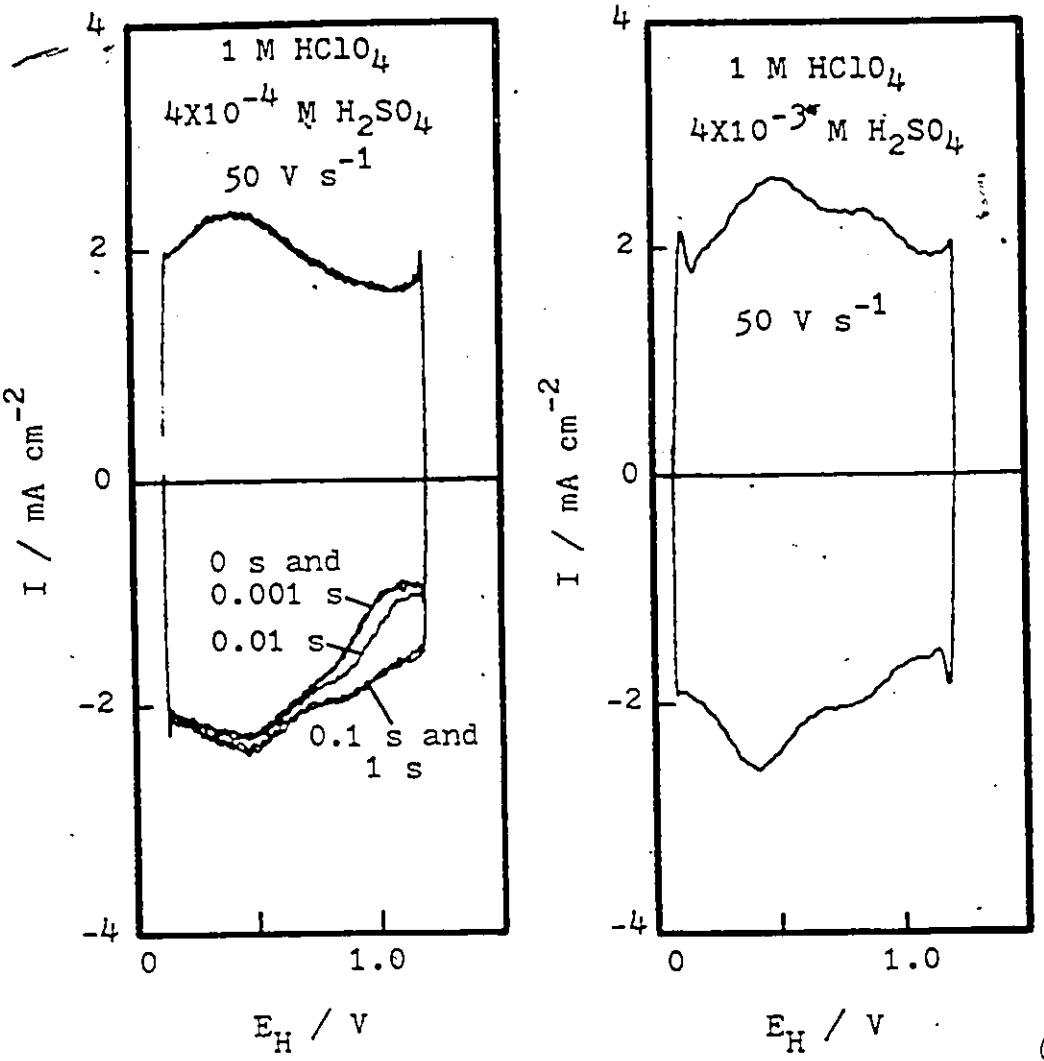

Figure 4.7.2. Potentiodynamic I vs E profiles for double layer charging of Au at 50 V s^{-1} in (a.) 1 M $HClO_4$ with $4X10^{-4}$ M H_2SO_4 at 300 K and t_n at 1.2 V between 0.001 and 1 s; (b.) 1 M $HClO_4$ with $4X10^{-3}$ M H_2SO_4 at 299 K.

V. Unlike the profiles in 1 M $HClO_4$ and 0.5 M H_2SO_4, for which the anodic and cathodic sweeps over the double-layer charging region are fairly symmetrical (as would be expected for currents due only to reversible processes associated with ion accumulation in the double-layer and chemisorption, there is a definite asymmetry around 1.2 V in the anodic and cathodic profiles of a repetitive cyclic-voltammogram taken in this solution. Also, there is an increase in the cathodic currents, especially those above 0.7 V, with increased holding times at 1.2 V. The corresponding increased charges are summarized in Table 4.7.1., along with similar results obtained in 1 M $HClO_4$ with 4 X 10^{-5} M H_2SO_4. The cathodic double-layer charging profiles do not change significantly with holding at 1.2 V in 1 M $HClO_4$, 0.5 M H_2SO_4 or 1 M $HClO_4$ with 4 X 10^{-3} M H_2SO_4 (Figure 4.7.2.b.). The effect that holding at 1.2 V has on the cathodic double-layer charging profile in 1 M $HClO_4$ with 4 X 10^{-4} M H_2SO_4 seems to be related to the increasing blocking of the onset of surface oxide formation with similar potential holding at 1.2 V in the same solution, as was previously shown in Figure 4.2.1., and presumably arises from slow sulfate ion adsorption competing with, and eventually substituting, ClO_4^- adsorption at these potentials.

If the coverage by anions at the Au surface is nearly at its equilibrium value for any particular potential during the anodic sweep, then those anions should be reversibly desorbed during the cathodic sweep. This is clearly the case for Au electrodes in 1 M $HClO_4$, 0.5 M H_2SO_4, and 1 M $HClO_4$ with 4 x 10^{-3} M H_2SO_4; thus, the anodic and cathodic sweeps for these electrolytes are fairly symmetrical (Figures 4.7.1. and 4.7.2.b.). However, the behavior observed in 1 M $HClO_4$ with 4 x 10^{-4} M H_2SO_4 electrolyte, shows that equilibrium coverage of SO_4^{2-} (HSO_4^-) is not maintained during an anodic potential sweep at 50 V s^{-1} to 1.2 V. Hence, during the initial part of the following cathodic sweep, anions will still be adsorbing at the Au surface, resulting in the asymmetry of the

anodic and cathodic I vs E profiles observed for this solution (Figure 4.7.2.a.).

Holding at 1.2 V, which is the potential for maximum anion adsorption observed by radiotracer measurements in this solution [105], allows time for the anions to be adsorbed and eventually approach their equilibrium coverage. The resulting increased coverage by anions consequently increases the corresponding double- layer capacitance observed in the cathodic I vs E profile after holding (Figure 4.7.2.a.). Since there is little difference between the effects of holding at 1.2 V for 0.1 s or 1 s, equilibrium coverage of SO_4^{2-} (HSO_4^-) must be nearly achieved after 0.1 s in this solution at this potential. In 1 M $HClO_4$ with 4 x 10^{-5} M H_2SO_4, on the other hand, equilibrium coverage of anions is not attained until 1 to 10 s holding at 1.2 V, owing to the lower sulfate concentration.

Table 4.7.1.

Double-Layer Charging Data for Au in 1 M $HClO_4$ with 4 X 10^{-4} M and 4 x 10^{-5} M H_2SO_4 at 50 V s^{-1} and 299 K

Sweep	Holding time at 1.2 V (s)	Charge passed between 0.7 and 1.19 V $\mu C\ cm^{-2}$	
		4 x 10^{-4} M H_2SO_4	4 x 10^{-5} M H_2SO_4
Anodic	--	17.7	14.1
Cathodic	0	14.6	12.0
	0.001	14.7	--
	0.01	16.4	12.4
	0.1	19.8	12.8
	1	20.2	16.2
	10	--	17.9

4.8. Electrode Roughening

A series of experiments was conducted to establish the potential at which surface roughening of Au commences in rapid oxidation/reduction cycles carried out by means of cyclic-voltammetry. Interest in this effect arises in relation to the process of OH/Au place exchange and anion desorption in the early stages or oxidation of Au surface which can lead to disorder or faceting of the atomic structure of the Au surface. Work by Bruckenstein et al.[112,141] indicates that dissolution is associated with the reduction of the place-exchanged surface oxide. Also, Arvia et al.[249] have used rapid potential cycling regimes as a way of obtaining facets of "preferred orientation" on polycrystalline electrodes, which is similar to the work presented here.

Two previously unused Au wire electrodes were roughened by rapid potential cycling, one in 0.5 M H_2SO_4 and the other in 1 M $HClO_4$. The roughening experiment in 1 M $HClO_4$ electrolyte was complicated by contamination by trace amounts of sulfate, which slowly become desorbed from the cell walls during the experiment. The actual electrochemically active surface areas of the electrodes were measured by the Burshtein method[245] at 50 mV s^{-1}. This was done before and after each roughening period. The roughening cycles were at 50 V s^{-1} from about 0.1 V to some variable anodic end potential of the sweeps, with holding at that potential for 0.01 s. The electrode was potentiostated against an internal Au reference electrode which itself was constantly monitored against an external H_2 reference electrode. Each roughening period lasted 10 minutes or longer, giving approximately 1000 or more cycles.

The anodic end potential of the anodic potential sweeps was increased with each successive cycling period to determine at which potential roughening begins in H_2SO_4. In $HClO_4$, 1.513 and 1.975 V were the only anodic end potentials used. After the electrodes were roughened, small pieces of wire were cut from their ends for examination under a scanning electron microscope

(SEM). A small piece of unused Au wire from the same manufacturer's batch as that used for the roughening experiments was also examined with the SEM as a reference.

I vs E profiles of some of the roughening cycles are given in Figure 4.8.1. for H_2SO_4 and in Figure 4.8.2. for $HClO_4$. The Burshtein electrode area and surface oxide charge measurements are summarized in Table 4.8.1. for H_2SO_4 and Table 4.8.2. for $HClO_4$. The data indicate that H_2SO_4 is much more aggressive towards Au surfaces with respect to roughening than $HClO_4$, an effect that may be due to the much stronger adsorption of SO_4^{2-} than ClO_4^- at Au surfaces. In H_2SO_4, no roughening or major changes in shape of the 50 mV s^{-1} I vs E profiles occurred during the first three roughening periods (Figure 4.8.1.a. through c.) with anodic end potentials of 1.200 V, i.e. only over the double-layer charging region, 1.392 V and 1.407 V, for which mostly reversible formation of oxide, OA1/OC1, takes place, but little or no phase oxide (OC3 species) is formed (see Figure 4.4.2.), as revealed in the reduction profiles. In the fourth roughening period (Figure 4.8.1.d.) where the OC1' reduction peak was present as well as significant charges due to the OC2 and OC3 peaks, still no increase of the electrode area could be detected by the Burshtein method, but the first two anodic oxide peaks in the 50 mV s^{-1} anodic I vs E profile did change significantly (Figure 4.8.3.). This indicates a reconstruction change of the electrode surface is taking place on an atomic level. Under these conditions, the coverage of the electrode by OH is just above a full monolayer ($\theta = 1.2$).

During the fifth roughening period (Figure 4.8.1.e.), where the OC1' peak still had not disappeared and where coverage by OH species (2 e/site) was still about one monolayer, measurable roughening took place. In H_2SO_4, electrode roughening seems to be related to the formation of the turned-over oxide. In the last and harshest roughening cycle (figure 4.8.1.f.), the coverage by O was

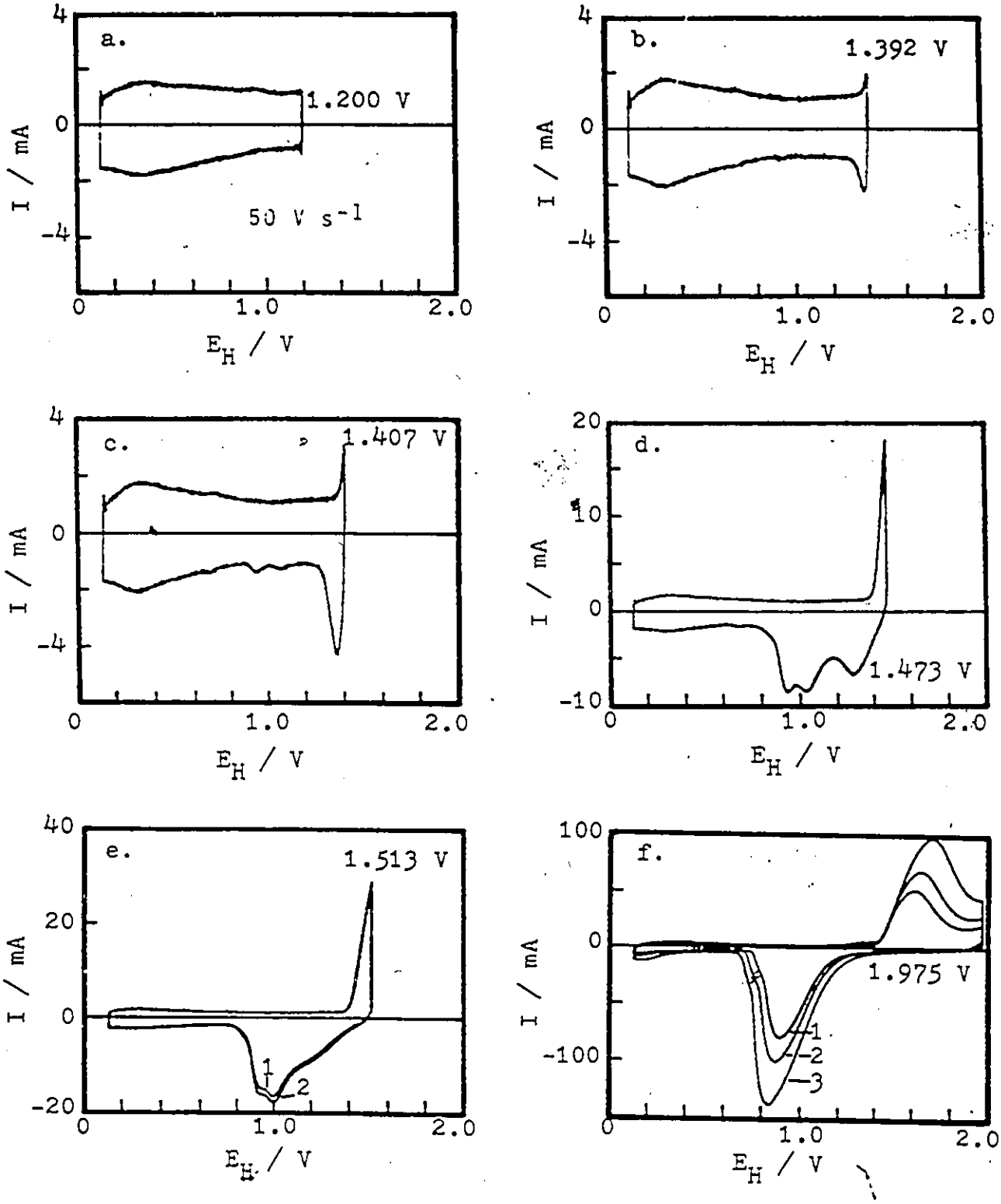

Figure 4.8.1. Potentiodynamic I vs E profiles of selected roughening cycles used on Au in 0.5 M H_2SO_4.

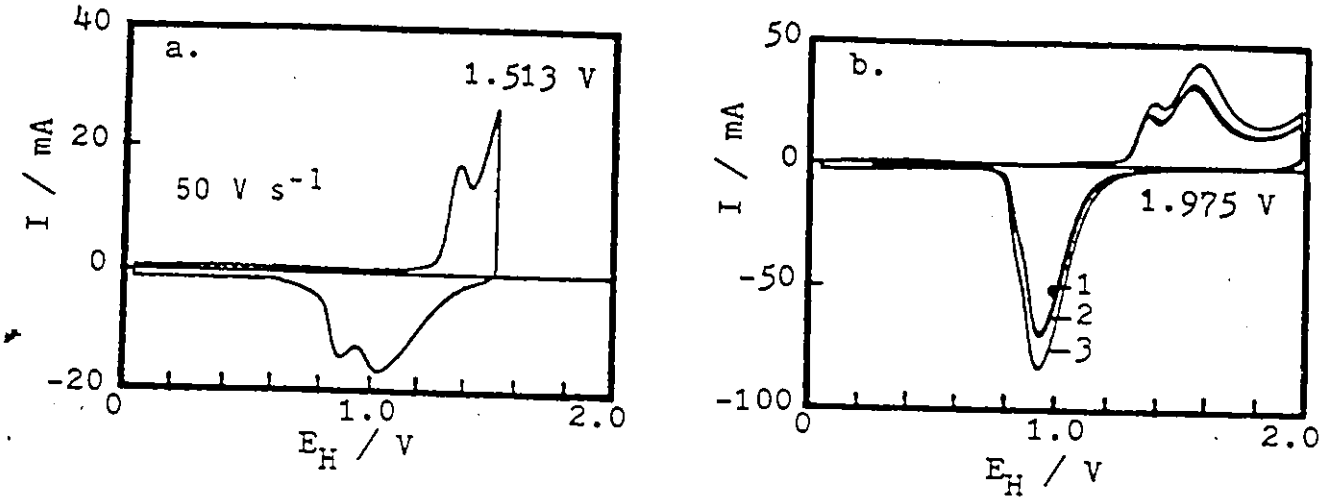

Figure 4.8.2. Potentiodynamic I vs E profiles of roughening cycles used on Au in 1 M $HClO_4$.

Table 4.8.1.

Roughening Effects at Gold in 0.5 M H_2SO_4 Under Potential Cycling

Roughening period		Electrode area by Burshtein		Oxide charge	Figure Number
Anodic end potential (V)	Time (min.) applied	cm^2	Normalized	$\mu C\ cm^{-2}$	
Before roughening	--	0.243	1.00	--	
1.200	10	0.237	0.98	--	4.8.1 a
1.392	10	0.232	0.96	2.6	b
1.407	10	0.247	1.02	26.7	c
1.475	10	0.249	1.02	245	d
1.513	10	0.262	1.08	400*	e
"	20	0.272	1.12	383*	"
"	40	0.289	1.19	367*	"
1.614	10	0.315	1.30	562	
1.857	10	0.398	1.64	844	
1.975	10	0.537	2.21	938	f
"	30	0.849	3.49	940	"

* The decrease in oxide coverage during these three roughening regimes might be due to changes of surface oxide formation kinetics at the reconstructed electrode surface.

Table 4.8.2.

Roughening Effects at Au in 1 M $HClO_4$ Under Potential Cycling

Roughening period		Electrode area by Burshtein		Oxide charge	Figure Number
Anodic end potential (V)	Time (min.) applied	cm^2	Normalized	$\mu C\ cm^{-2}$	
Before roughening	--	0.255	1.00	--	
1.513	10	0.267	1.05	455	4.8.2.a.
"	60	0.252	0.99	468	"
"	60	0.267	1.05	462	"
1.975	10	0.297	1.16	997*	b
"	90	0.379	1.49	944*	"

* The decrease in oxide coverage during these two roughening regimes might be due to changes of surface oxide formation kinetics at the reconstructed electrode surface.

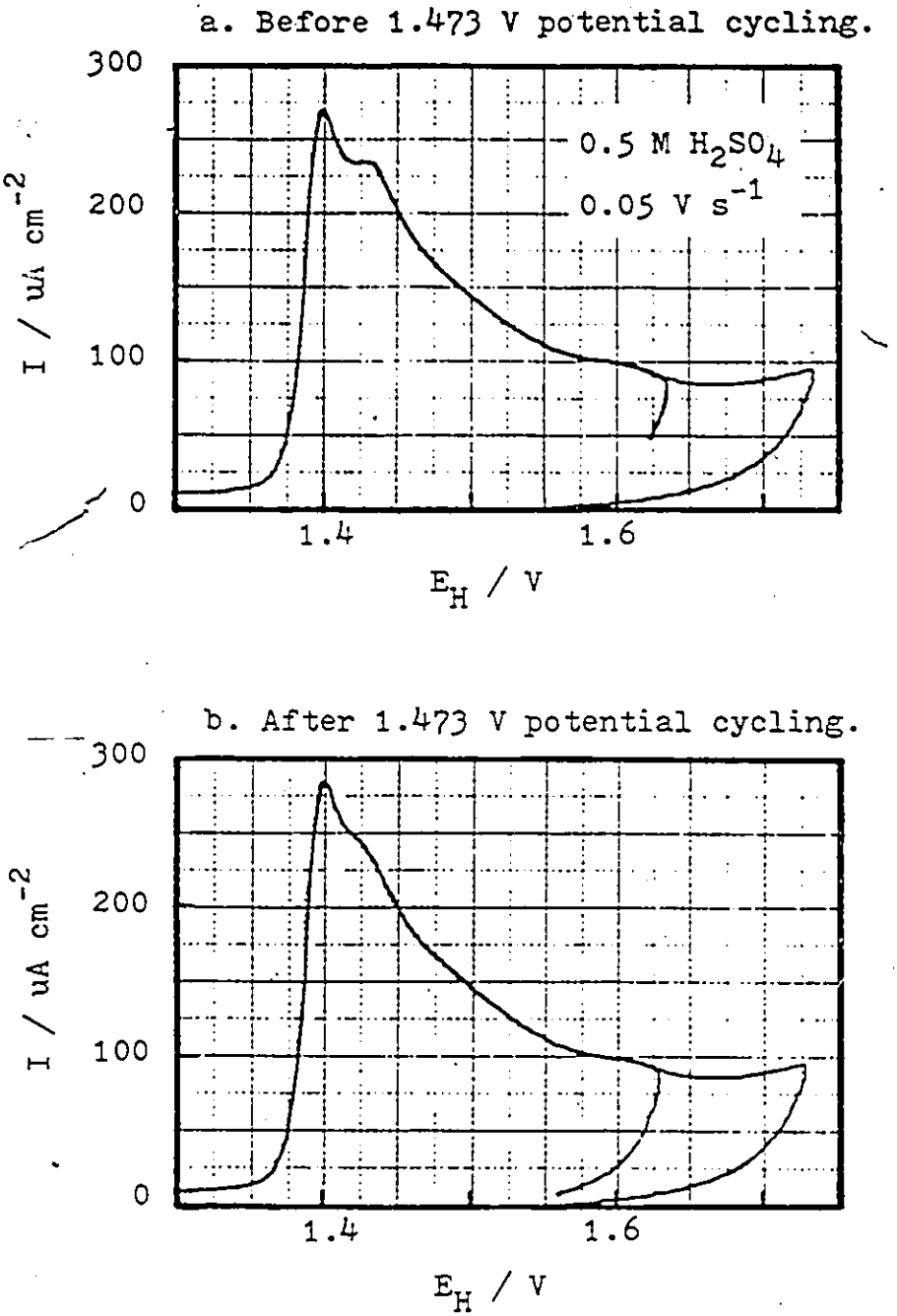

Figure 4.8.3. Potentiodynamic I vs E profiles of surface oxide formatic. Au at 0.05 V s_{-1} in 0.5 M H_2SO_4 (a.) before, and (b.) after 10 min. roughening with 1.473 V potential cycle.

above two layers,i.e. a phase-type oxide was certainly produced. Under such conditions, the electrode area was increased by a factor of 3.5 during all the roughening periods, taken cumulatively.

In $HClO_4$, after the first roughening period, with coverage by OH species just above a monolayer (Figure 4.8.2.a.), the electrode area did not increase measurably, nor did it become roughened to the extent that the electrode in H_2SO_4 had done when subjected to the same potential-sweep regime. However, measurements of the electrode area by means of the Burshtein method were complicated by slow desorption of SO_4^{2-}. During the more aggressive roughening period with θ taken to coverages greater than a monolayer of O (Figure 4.8.2.b.), definite roughening occurred, but the electrode area increased only by about one third as much as did the area of the other electrode during the same potential cycling regime in H_2SO_4. Whether this amount of roughening is due to SO_4^{2-} contamination or would also occur in very SO_4^{2-} free $HClO_4$ electrolytes remains, at the moment, unknown.

SEM pictures of a new Au wire, and of the wires roughened in $HClO_4$ and H_2SO_4, are shown in Figure 4.8.4. These indicate the same order of roughening as did the Burshtein measurements. The electrode roughened in $HClO_4$ appears etched, especially along the original scratches and flaws of the wire. The surface of the electrode roughened in H_2SO_4 has a dendritic appearance at high magnification. This indicates that, in the presence of large amounts of SO_4^{2-}, the electrode had probably become roughened by a dissolution and redeposition mechanism. This dissolution only occurs when significant coverages of non-reversible surface oxide have been formed and may be due to the formation, or the very rapid reduction of the OH/Au or O/Au place-exchanged species in the OC3 peak or of oxygen species associated with further oxide growth at the Au electrode, in the case where more than one atomic layer of place-exchanged species may have been formed. It seems that it is the

Figure 4.8.4.

SEM pictures of the state of Au wire electrodes:

(a.) New wire before any electrochemical potential cycling

(b.) and (d.) After extensive cycling at 50 V s_{-1} in 0.5 M H_2SO_4.

(c.) and (e.) After extensive cycling at 50 V.s_{-1} in 1 M $HClO_4$ ($<10^{-7}$ M H_2SO_4 contamination).


a.


b.
20Å

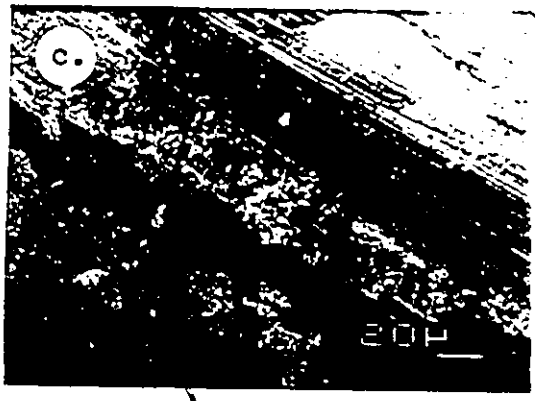
c.
20Å

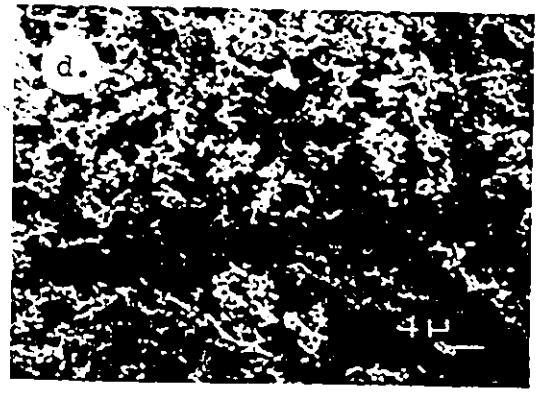
d.
4Å

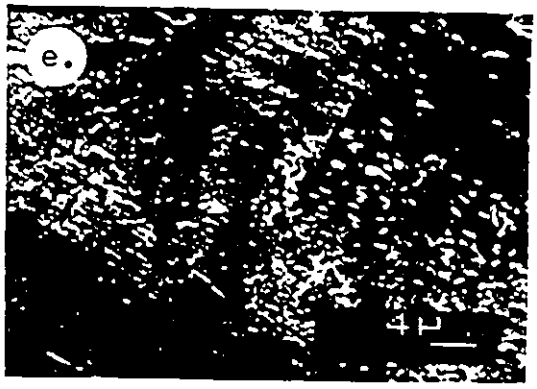
e.
4Å

reduction, especially with rapid potential sweeps, of these states of the surface oxide that causes some disorganization of the Au surface, assisted by the adsorption and desorption of anions, followed by redeposition of some dissolved Au during or after the surface oxide has been reduced.

4.9. Summary of the Results

4.9.1. The Initial Stages of Surface Oxide Formation and the Effect of Adsorbed Anions Upon this Process

Surface oxide formation and reduction at gold electrodes is found to be very sensitive to the nature of adsorbed anions at the surface, temperature, the electrochemical potential at which it is formed, as well as the microscopic structure of the electrode surface[194]. Commencement of surface oxide formation arises at less positive potentials in the presence of weakly adsorbed anions, such as ClO_4^-, than with more strongly adsorbed anions, such as SO_4^{2-} (HSO_4^-). The relative strengths of anion adsorption in terms of the effects of anions on the onset of surface oxidation at gold electrodes are found to be in the order $ClO_4^- < F^- < SO_4^{2-}$ (HSO_4^-).

In mixed $HClO_4/H_2SO_4$ electrolytes ($[H_2SO_4] = 4X10^{-4}$ M, $4X10^{-5}$ M), SO_4^{2-} anion adsorption at 1.2 V, which was studied by its displacement effect upon surface oxide formation, was found to follow adsorption kinetics which are first order in anion concentration and sites, and desorption kinetics which are first order in coverage by adsorbed anions.

In these mixed electrolytes, anions may be prevented from becoming adsorbed at the surface ("anions off" situation) or be allowed to attain almost equilibrium coverage ("anions on" situation) by using different potential-time programs. "Anions off" I vs E profiles resemble those found for 1 M $HClO_4$, and those for "anions on" resemble those found for 0.5 M H_2SO_4. It was observed that holding the potential at 1.2 V allows SO_4^{2-} anions to be adsorbed at the surface and block surface oxide formation, especially the reversible electrosorption of OH characterized by reduction in the OC1 peak. Holding at 0.1 V (a potential below the p.z.c. of Au) allows anions to be desorbed. Surface oxide grown at a potential at which OH is electrosorbed under "anions off" conditions but not under "anions on" conditions, will eventually be

displaced by readsorption of SO_4^{2-} anions, with a consequent decrease in the total charge for surface oxide formation. The anions can displace only the reversibly deposited OH species (OA1/OC1 state); they cannot displace the oxygen species that are reduced in the OC2 and OC3 peaks.

4.9.2. Comparison of Surface Oxide Growth in 1 M $HClO_4$ and 0.5 M H_2SO_4

Surface oxide growth in 1 M $HClO_4$ is characterized by the reduction of OH/O species which takes place in three cathodic peaks, OC1, OC2 and OC3. In 0.5 M H_2SO_4, however, the reduction is more complex; sometimes it may be resolved into four stages, corresponding to the OC1, OC1', OC2 and OC3 peaks. The OC1' peak is due to the reduction of OH electrosorbed at surface sites where the anions are partially desorbed. The OC1 peak for OH species deposited in $HClO_4$ arises at a less positive potential than that for the corresponding OC1 peak in H_2SO_4.

An important characteristic feature is that the coverage by the species reduced in the OC2 peak reaches a saturation limit depending on the anion and its peak potential does not shift with increasing charge. The OC3 peak is due to reduction of species involved in the beginning of phase-oxide formation, associated with the turn-over process, and its potential shifts to less positive values with increasing extent of formation of surface oxide.

Surface oxide growth in both electrolytes is characterized by an initially non-logarithmic region in time, followed by logarithmic regions. In $HClO_4$, for the least positive potentials a plateau is temporarily reached in growth after the OC1 peak has attained its maximum charge; this behavior is not observed with H_2SO_4 solutions.

The change of state (referred to as "conversion") of the intially electrosorbed OH species, reduced in the OC1 peak, to states characterized by reduction in the OC2 and especially the OC3 peak, was examined in $HClO_4$. The

charge associated with the conversion of state of the OH species, is also found to follow a logarithmic relation with time. The charge difference, $Q_{OC3} - Q_{con.}$, which represents the growth of the OC3 species beyond charges associated with the interconversion, is also found to follow a logarithmic relation in time.

The non-logarithmic region of growth in mixed $HClO_4$ and H_2SO_4 electrolytes seems to follow a "square-root" relation with time under certain conditions, intermediate in the range of t_h covered; but this is not found so simply for growth in $HClO_4$. The slope of this growth relation is also found to depend linearly on potential and temperature, but this effect may be due to the involvement of some resistive current control (iR effect at short holding times).

For surface oxide growth in 0.5 M H_2SO_4, the OC1 peak is found to shift to less positive potentials with temperature, while the the OC1', OC2 and OC3 peaks shift to more positive potentials. The OC2 peak shifts linearly with temperature, while the OC3 peak apparently shifts as the square-root of temperature, the significance of which is not clear; it may be associated with difficulty of deconvolution of the OC3 peak under certain conditions.

4.9.3. "Anions Off" and "Anions On" Surface Oxide Growth in Mixed $HClO_4/H_2SO_4$ Electrolytes

Surface oxide growth in mixed $HClO_4/H_2SO_4$ electrolytes was examined with and without SO_4^{2-} anions initially adsorbed at the electrode surface ("anions on" and "anions off" conditions, respectively). Under "anions off" conditions, the growth behavior initially resembles that found in $HClO_4$, as expected, but the electrosorbed OH species reduced in the OC1 peak are displaced by readsorption of SO_4^{2-} anions, which leads to a <u>decrease</u> in total surface oxide charge with time. The growth of OH/O species reduced in the OC2 and OC3 peak eventually becomes more important so that the total surface oxide increases

again. "Anions on" growth resembles that observed in H_2SO_4. Although the "anions off" and "anions on" growth behavior are quite different at relatively short holding times, understandably they become more similar as the time of holding, t_h, becomes longer and the electrode potential, E_h, more positive. "Anions off" growth could not be examined in 1 M $HClO_4$ with $4X10^{-3}$ M H_2SO_4 because the SO_4^{2-} anions are always at saturation coverage for that concentration of H_2SO_4.

The peak potential of the OC1' peak in "anions on" growth is the same as that for the OC1 peak in "anions off" growth. This observation supports the idea that the OC1' peak is due to the reduction of OH species electrosorbed in vacant spaces left on the surface in the initial stages of desorption of anions.

At relatively short holding times, the potentials for the OC2 and OC3 peaks are more positive for the "anions on" than for the "anions off" case, but these peaks have a common intermediate potential at longer holding times.

4.9.4. Temperature Effects

The potential of the first clear anodic peak, OA2, observed in 0.5 M H_2SO_4 at 0.050 V s^{-1} becomes less positive linearly with temperature. The current for this peak also increases linearly with temperature, with a change in slope at about 300 K.

The potential of the OC3 peak becomes less positive in a linear way with charge, Q, but becomes more positive with increasing temperature. Curiously, the current for this peak seems to increase with Q^2. There is little difference in the I_p vs Q relations between T = 273 and 283 K, but I_p and $dI_p/d(Q^2)$ increase between 298 and 343 K.

4.9.5. Double-Layer Charging Behavior and Anion Adsorption

The double-layer charging I vs E profiles for polycrystalline Au electrodes in 0.5 M H_2SO_4 and 1 M $HClO_4$ are nearly the same for E $\leq$ 0.1 V (i.e.

well negative to the p.z.c.) where no anions are adsorbed at the surface, but are quite different for more positive potentials where anion chemisorption arises. The higher capacitances observed in H_2SO_4 than in $HClO_4$ are attributed to partial charge-transfer involved in the adsorption of this anion, leading to an electrosorption pseudo-capacitance contribution. The double-layer capacitance of the polycrystalline Au interfaces in mixed $HClO_4/H_2SO_4$ electrolytes is intermediate between that for the individual $HClO_4$ and H_2SO_4 solutions, and the currents on the cathodic I vs E profile increase with holding time at 1.2 V, a situation which allows the SO_4^- (HSO_4^-) anions to become adsorbed to nearly their equilibrium extent.

4.9.6. Electrode Roughening

Roughening of Au electrodes by means of rapid potential cycling begins when the potential is sufficient on the anodic sweep for $\theta_O > 1$ to be established, i.e. when a turned-over oxide is formed, with the appearance of the OC3 and OC2 peaks on the reduction cycle, i.e. when place-exchange of the O species with Au atoms at the surface commences significantly. Gold electrodes roughen more rapidly in 0.5 M H_2SO_4 than in 1 M $HClO_4$, indicating a specific effect of the more strongly adsorbed sulfate anions on this process. The Au electrode that has been roughened in 0.5 M H_2SO_4 had a dendritic appearance under the SEM, indicating that some Au was probably dissolved and redeposited, while the electrode roughened in 1 M $HClO_4$ had an etched appearance.

CHAPTER V

CONCLUSIVE DISCUSION OF SELECTED PROBLEMS

In this concluding chapter, some selected aspects of the results will be discussed, especially some features of the observations and experimental conclusions that may have general significance. The material in this chapter is therefore complementary to that in Chapter IV.

First, a point of chemical significance must be addressed that can affect quantitative evaluations of oxide coverage in this and all other published work related to this research.

5.1 Fractional Coverage, θ, in Relation to Charge, Q

Surface concentration of species generated in the initial stages of oxidation of metals, such as Pt or Au, are best expressed in terms of fractional coverage, θ, of the metal surface by the electrosorbed species. In the electrochemical deposition of such species, the θ value can be evaluated formally from the ratio Q/Q_1, where Q is the charge required for electrosorption (or electrodesorption) of the adsorbed species and the charge, Q_1, corresponds to monolayer coverage. This implies utilization of Faraday's laws on a microscopic scale for surface species. Such evaluation of coverages has been made frequently for underpotentially deposited H at Pt.

However, for anodic electrosorption of OH or O species at noble metals, especially Au, several difficulties arise in the interpretation of Q values (which can be very accurately measured) in terms of corresponding θ[194,195]. These difficulties arise for the following reasons:

1. Electrosorption, following electrostatic physisorption, of anions with partial charge transfer occurs over a potential range just below (or in some cases overlapping with) the potential for effective onset of OH deposition amongst these anions adsorbed in arrays (formally according to equations 5.11. and 5.12. in Section 5.9.). This process provides a

lattice of adsorbed anions into which OH's are subsequently deposited (see 2. below), determining their adsorption energy, i.e. the potential range for their deposition.

2. Electrosorption of OH in the initial stages of Au surface oxidation amongst, or adjacent to, chemisorbed anions may involve an incomplete transfer of charge (equation 5.11.), i.e. there is an electrosorption valency factor, $\gamma < 1$.
3. As the surface oxidation process continues, anions previously chemisorbed with some fraction of electron transfer (see equation 5.11. of section 5.8.) become desorbed with regain of the normal charge and the OH species remaining now can be assumed to become completely discharged, with a further degree of charge transfer.
4. The extent to which anions can cover the surface are determined by the geometry of the anions and that of the surface lattice on which it is adsorbed (3 trigonal sites for a tetrahedral anions on the (111) surface), together with the extent of surface occupancy by the anion's hydration-bound water. This is represented by M_{3+X} in the formal equations 5.10. and 5.11. in Section 5.9.

When OH or O species eventually occupy sites not associated at the same time with anions (equation 5.12.), the calculation θ_{OH} or θ_O values from the relation $\theta = Q/Q_1$ becomes simple and unambiguous. This is, in fact, the basis of calculation of real areas of Au anodes by the method of evaluation of the charge, Q_O (1 monolayer), for the "Burshtein minimum".

As a result of the ambiguities introduced by the factors discussed in 1. through 4., any θ values calculated from Q data for the initially deposited species in the presence of chemisorbed anions would be unavoidably arbitrary. For this reason, extents of electrosorption of OH species in the initial stages of Au oxidation have been given in terms of charge, Q_{OH} or Q_O, except in some

cases where nominal values of θ_{OH} have been tabulated, e.g. in Tables 4.5.1., 4.5.2., 4.5.3., etc.

5.2. Is the Initial Monolayer of Surface Oxidation at Au Composed of OH or O?

One of the general questions in the study of surface oxide formation at noble metals is whether the initial monolayer is composed of OH or O species electrosorbed at the surface, i.e. with one or two electrons having been transferred per site, respectively. This obviously makes a major difference in the quantitative interpretation of the relation of charge to coverage. Although the position has been taken throughout this thesis, for the reasons indicated below, that the initial monolayer is composed of OH species, the coverages were, in some places, reported as O species calculated on the basis of 2 e/site. This is because the corresponding charges were simply divided by the Burshtein charge[245], Q_B, i.e. the anodic charge integrated under the anodic-going curve in an I vs E profile up to the minimum just before oxygen evolution, corresponding to 400 $\mu C\ cm^{-1}$, or 2 e/site. Of course Q_B may correspond to a single monolayer of O species, two layers of OH species or some combination of both species, but in the initial 200 $\mu C\ cm^{-1}$ (nominal monolayer of OH), the oxide species at the surface are probably OH's. One piece of evidence for this supposition is that the only logical explanation of the OA4 peak, especially that observed at Au(111)[195], is the passage of a second electron, as for the process in which chemisorbed OH is converted to O:

$$AuOH \rightarrow AuO + H^+ + e$$

However, only rather little supplementary, non-electrochemical evidence is available for Au in support of this 2-step process of surface oxidation.

In the analogous case at Pt, there is considerable evidence which indicates that a distinguishable monolayer of OH is attained at 1.1 V r.h.e. In particular, here are three kinds of electrochemical results which lead to this-

conclusion:

1. The initial stages of surface oxidation of Pt are selectively blocked by Cl^- up to 1.1 V [159], at which potential the charge passed is 210 $\mu C\ cm^{-2}$, corresponding to 1 OH/Pt. This blocking is selective for species formed below this potential and not those that are deposited at higher potentials,
2. The oxidation of organics at Pt[58,137] usually exhibits a minimum in oxidation currents at 1.1 V, i.e. when the surface is just filled with OH species, before it goes on to a region of further reactivity between 1.1 and 1.3 or 1.4 V, i.e. where the transition from PtOH to PtO is believed to take place with further passage of charge.
3. Using ellipsometry, Reddy et al.[23] found a qualitative change in the optical behavior of the surface oxide formed at Pt beyond 0.95 V, which they interpreted as the formation of a partial partial layer of adsorbed OH below this potential and a phase-oxide film above it.

More recently, Benzinger et al.[250] examined Pt surfaces in 1 M $HClO_4$ using an in-situ IR technique. At potentials where the reversible deposition of OH occurs, they observed a broad band between 3100 and 3500 cm^{-1}, which was interpreted as due to OH species hydrogen bonded to water, and at potentials where place exchange occurs, an OH stetch band at 3540 cm^{-1} was found. It was suggested that the reversibly formed OH at the surface cannot exhibit a free stretching mode because it is constrained by hydrogen bonding, but the turned over and thus occluded OH can. Several studies of electrochemically formed surface oxide at Pt have been made using ESCA (XPS). In an earlier examination, it was suggested that the surface oxide was composed of PtO or PtO_2[123] species, but more recent work indicates that it might be $Pt(OH)_2$[122] or $Pt(OH)_4$[125,126,188].

For gold electrodes, there are some optical measurements that indicate

that the initially formed surface oxide differs considerably from that formed at higher potentials. Gottesfeld et al.[79] found that the greatest effects of a.c. perturbation of ellipsometric and reflectometric parameters measured during oxidation of Au electrodes in 0.2 M $HClO_4$ arose over the potential range where electrochemical cyclic-voltammetry experiments showed that a reversible process is found (OA1/OC1). Chao et al.[89], using surface plasmon spectroscopy (SPS), found a shift of their SPS dispersion measurements for the initial part of surface oxide formation at gold, but with no damping; however, considerable damping was found for thicker layers of oxide. Some ESCA studies have been made of emersed Au electrodes[202,206], but no chemically conclusive indication that the initial monolayer of the surface oxide is composed of OH species has been found.

Bange et al.[166] have examined the co-adsorption of O_2 and H_2O at Ag(110) in the gas phase with thermal desorption analyzed by mass spectroscopy, and LEED. They found that water reacts with preadsorbed oxygen to form adsorbed OH species and that the OH's and additional adsorbed water form hydrogen bonded complexes. It is reasonable to assume that similar complexes of OH and H_2O may be formed at Au electrodes.

5.3. Problems Encountered in Oxide Growth Experiments at Constant Potential

Because of experimental limitations, such as iR drop or the finite time during a potential sweep, certain problems arise in the interpretation of the results for surface oxide growth at constant potential. These problems must be addressed before conclusions concerning surface oxide growth at the shortest holding times can be made. This is necessary for the discussion of certain aspects of the non-logarithmic growth region, for example the $t_h^{1/2}$ relation which is apparently followed for surface oxide growth in solutions containing sulfate anions (0.5 M H_2SO_4 and the mixed $HClO_4/H_2SO_4$ electrolytes.)

In order to study surface oxide growth at constant potential, it is desirable to reach this potential very quickly in order to minimize all electrode processes other than double-layer charging. For this reason, a potential "jump" (actually a sweep of 500 V s^{-1}) was used to reach this potential. This very fast sweep causes the electrodeposition of OH to be irreversible, as was intended, but at the holding potential, E_h, which was chosen to have values above the reversible deposition potential for OH, the overvoltage thus produced causes this reaction to proceed very quickly at first, slowing down gradually until the equilbrium coverage of OH at this potential is reached. The resulting high currents at short holding times (see Section 4.3.1.) create a potential iR drop. which decreases the real potential at the electrode with respect to applied one. Hence, this potential "jump", although necessary, influences the results at short times. The iR drop introduces an error, however the irreversibility of the electrodeposition of OH may give some incidental insight of the kinetics at high sweep-rate, s, of this initial step in the overall process.

The potential "jump", although fast, does require a finite time, which may be long enough for some processes to occur to a small, but still significant, extent. Therefore, a correction must be introduced for the time of this sweep, $t_{corr} = (E_h - E_{in}) / s$, where E_{in} is the potential for the onset of the process being examined. For surface oxide formation, E_{in} will depend somewhat on the solution composition, however it is generally about 1.2 V, and this value was used in calculating the t_{corr} values tabulated in Table 5.1. These t_{corr} values for surface oxide growth experiments are relatively small, on the order of the shortest experimental holding times used.

For anion adsorption, the value for E_{in} is just positive to the potential of zero charge, where this process begins; for the rather concentrated solutions used in these experiments, this value is about 0.1 V, or an even more

negative potential. E_{in} was taken as 0.2 V for the purpose of calculating the t_{corr} values in Table 5.1., and for an E_h of 1.400 V, gives t_{corr} = 1.2 / 500 = 0.0024 s, which is rather long in comparison to the shortest t_h values used in these experiments. In some of the experiments, a sweep-rate of 50 V s^{-1} was used, under these conditions the t_{corr} values will be 10 times larger.

Table 5.1.

Corrections, t_{corr}, for Potential Holding Experiments for s = 500 V s^{-1}

	OH electrodeposition		anion chemisorption	
E_h / V	E_{in} / V	t_{corr} / s	E_{in} / V	t_{corr} / s
1.320	1.200	2.4×10^{-4}	0.200	0.0022
1.340		2.8		0.0023
1.360		3.2		0.0023
1.380		3.6		0.0024
1.400		4.0		0.0024
1.420		4.4		0.0024
1.440		4.8		0.0025
1.460		5.2		0.0025

For anion chemisorption, full or partial charge transfer from the anion occurs at potentials more positive than that for the initial physisorption, but less positive than thoses for the onset of OH electrodeposition. This charge transfer reaction is spread over a relatively large potential range[194,195].

Under some conditions, such as low concentration of anions and short t_h, anion chemisorption with charge transfer is still taking place during potential holding, producing an anodic current which may still be significant during subsequent reduction of the deposited OH. This chemisorption current

diminishes with time as the anions reach equilbrium coverage, creating the effect of an apparent increase in the reduction charge in the OC1 peak.

In a simple reversible surface reaction, such as OH deposition or anion chemisorption with full or partial charge transfer, the charge at constant potential is independent of time. When this reaction is driven to irreversibility, the charge increases with time until equilibrium coverage is attained. It also increases when the effective electrode potential changes in time with decreasing iR drop. Other surface processes may also change the electrode surface, giving rise to changes in charge, for example charge increases when part of the blocking effect of anions at the surface is removed by their desorption, and it may also be affected by changes in the lateral interactions between species at the surface.

The peak potential for a reversible electrodeposition reaction is independent of time or charge when this charge increases due to an increase of free surface without a change of the environment of the species at the surface, i.e. without changing the lateral interactions between them. For an irreversible surface reaction, the peak potentials of the reverse reaction, for example the reduction of deposited OH, is also constant and independent of the charge passed during deposition if the lateral interactions are small enough. When strong lateral interaction occur, as was shown in previous calculations made in this laboratory[56], the peak potentials will shift with increasing charge. However, if the peak potentials shift with little change in charge, as is observed in H_2SO_4 solution, a change in the reversible potential for this reaction must arise due to changes of the environment of the reactive oxide species on the surface.

5.4. Isotherm for Adsorption of OH Reduced in the OC1 Peak

Since the initial deposition of OH between adsorbed anions at the surface (OA1/OC1 peaks) has been shown (see Section 4.3.) to be a reversible process,

it is of interest to to see if an isotherm in potential can be developed to describe it. Unfortutunately, there are many factors which complicate the measurement of the thermodynamically reversible coverage of OH at the surface at any one potential, the most important of which are:

1. Kinetic irreversiblity; because, even though the initial deposition of OH at the surface is a relatively fast process, finite times are needed to attain equilbrium coverage.
2. iR drop; because the currents encountered for surface oxide formation at very short times are quite high (several mA), the effective electrode potential will be somewhat lower than that applied. A potential difference of a few mV can be quite significant in the earliest stages of surface oxide formation. As the surface oxidation current decays, the effective electrode potential approaches that which is experimentally applied.
3. Anion desorption in time; this effect will change the coverage of ions between which the OH's are being deposited.
4. Conversion of the reversibly adsorbed OH to new, irreversibly reducible species in different states, characterized by reduction in the OC2 and OC3 peaks.

It should be noted that factors 3. and 4. may take place over relatively long periods of time when compared with factors 1. and 2., provided the growth potential is low enough, since all these factors depend upon potential. When such conditions are obtained, then the initial extent of surface oxide formation, at a given potential, should remain fairly constant over some intermediate range in time, after the effects of kinetic irreversibility and iR drop are no longer important and before anion desorption or conversion of the initially deposited OH species to irreversibly reduced states have significantly taken place. Under such conditions, a quasi-reversible

equilibrium coverage of OH can be measured a indicated by the independence in time, t_h for the formation of the OC1 state at low potentials, E_h (see e.g. Figure 4.3.3.a.).

Inspection of the surface oxide growth curves in 1 M $HClO_4$ at 298 K (Figure 4.3.4.) shows that thare are indeed ranges of time for several growth potentials where the extent of surface oxide formation is fairly constant. The charges at the very shortest times are smaller than the "equilibrium" charge, as is expected from the influence of above factors 1. and 2., ahd irreversibility sets in at longer times, but the range of time in which the charge (corresponding to all or most of the anodically generated OH species being reduced in the OC1 peak) remains essentially constant is up to 2 decades in some cases. This is clearly shown in Figure 5.1., where I vs E profiles for reduction in the OC1 peak region are given for the range of holding times 0.002 to 0.1 s at 1.290 V. The reduction profiles are nearly the same; however a small decrease in the OC1 peak is seen as a function of time due to the a small extent of conversion of OH species from one state to another (see Section 4.3.2.), as would be expected.

An isotherm for the initial reversibly deposited OH with respect to potential, under the condition described above, is presented in Figure 5.2., along with the range of holding times where the total surface oxide charge remains constant. Most of the $Q_{OC1,eq.}$ values found were measured under conditions where no appreciable conversion had yet occurred, i.e. the OC1 state had attained nearly equilibrium coverage, but for the Q values associated with the last two growth potentials (1.320 and 1.340 V), small but significant quantities of surface oxide were found to be reduced in the OC2 and OC3 peaks as a result of the conversion process.

This behavior can be seen more clearly in the series of plots of Q values for the initial stages of oxidation at six growth potentials shown in Figure

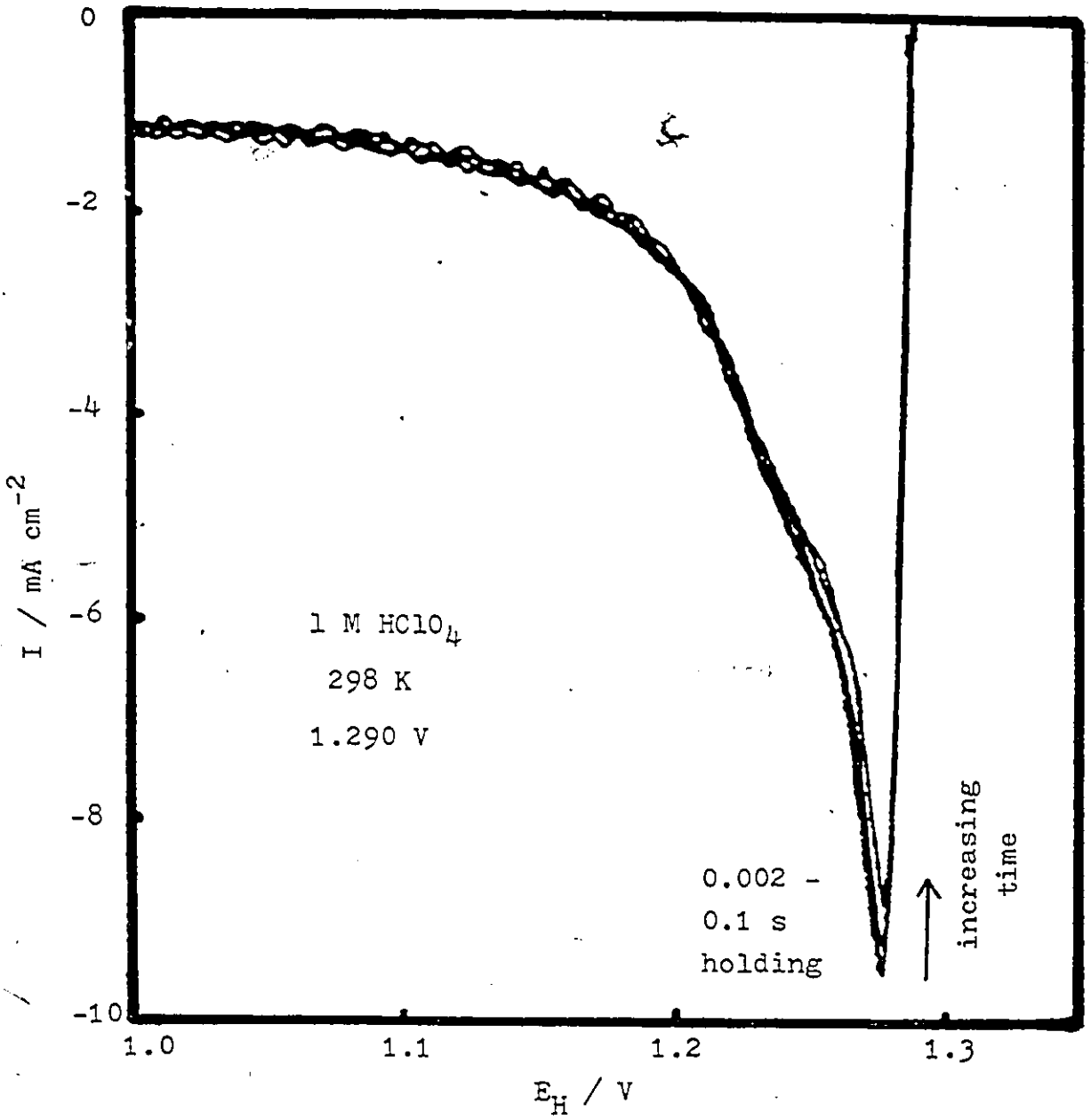

Figure 5.1. Potentiodynamic I vs E profiles for reduction in the OC1 peak for surface oxide grown at Au in 1 M $HClO_4$ at 298 K and E_h = 1.290 V for holding times where Q_{OC1} remains constant (t_h = 0.002 to 0.1 s).

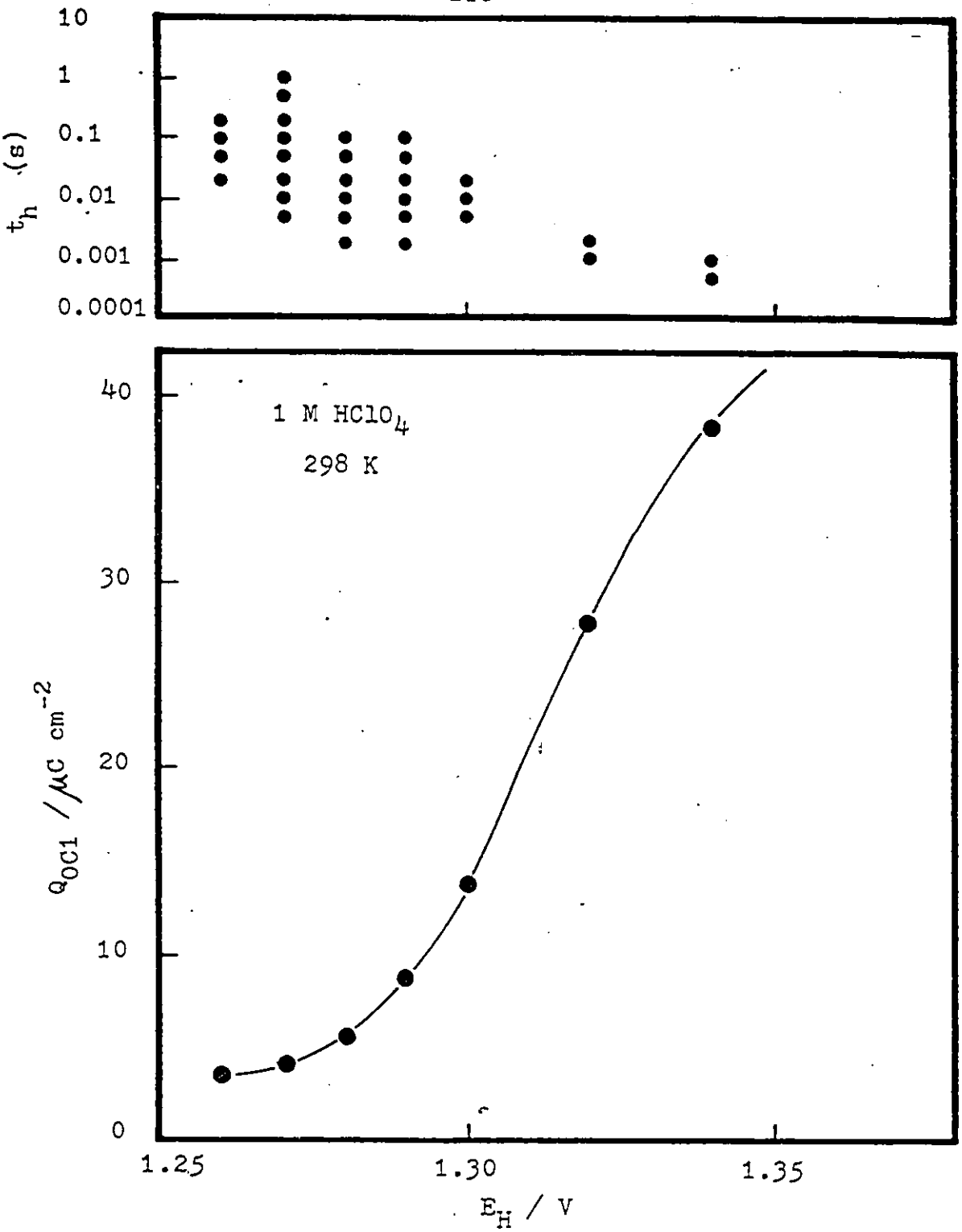

Figure 5.2. Isotherm, Q_{OC1} vs E_h, for Au in 1 M $HClO_4$ at 298 K, and range of holding times, t_h, during which Q_{OC1} does not change.

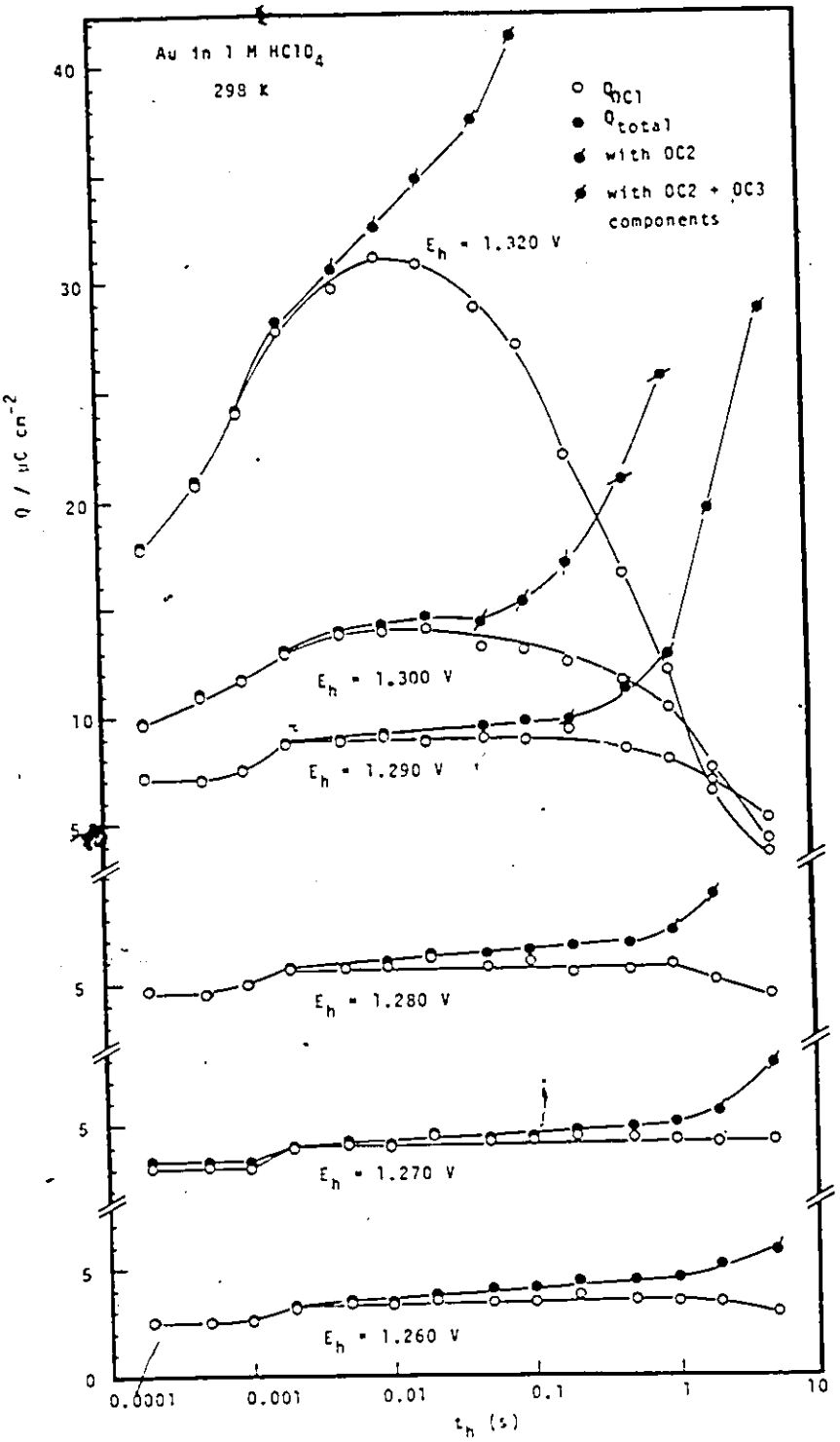

Figure 5.3. Variation of surface oxide charge associated with the OC1 peak and total O-species at Au in 1 M $HClO_4$ at 298 K and several potentials from 1.260 to 1.320 V for t_h from 0.0002 to 5 s.

5.3.; here the OC1 component (as Q_{OC1}) is distinguished from the total Q, and it is seen that the time interval over which Q_{OC1} remains almost constant progressively diminishes until, at E_h = 1.320 V, Q_{OC1} just passes through a maximum before eventually declining to a value near zero.

The equilibrium situation for OC1 species, referred to with respect to the results shown in the preceding figures, can be considered in terms of a kinectic equation. The following expression can be written for the equilibrium situation, i.e. when the rate of adsorption equals that for desorption, for adsorption of OH in the presence of preadsorbed anions:

$$k_1 \, c_{H_2O} \, (1 - \theta_A - \theta_{OH}) \exp(\beta \tfrac{zF}{RT} E) = k_{-1} \, \theta_{OH} \, c_{H^+} \exp \tfrac{-(1 - \beta)zF}{RT} E \qquad (5.1.)$$

where θ_A is the coverage by adsorbed anions. The corresponding equilibrium constant is given by

$$K_{OH} = \frac{k_1}{k_{-1}} = \frac{\theta_{OH} \, c_{H^+}}{(1 - \theta_A - \theta_{OH}) \, c_{H_2O}} \exp - \frac{zF}{RT} E \qquad (5.2.)$$

Since the surface which is not covered at saturation by OH is just the effective extent of blocking by anions, i.e. $\theta_A = 1 - \theta_{OH,sat.}$, the latter may be substituted in equation 5.2. and the expression may be further simplified to give

$$K_{OH} \frac{c_{H_2O}}{c_{H^+}} \exp - \frac{zF}{RT} E = \frac{\theta_{OH}}{(\theta_{OH,sat.} - \theta_{OH})} \qquad (5.3.)$$

Taking the logarithim of the above equation leads to

$$E = \frac{2.3 \, RT}{zF} \log \frac{\theta_{OH}}{(\theta_{OH,sat.} - \theta_{OH})} - 2.3 \frac{RT}{zF} \log \left[K_{OH} \frac{c_{H_2O}}{c_{H^+}} \right] \qquad (5.4.)$$

If it is assumed that the electrosorption of OH involves transfer of 1 e, then the plot of $\log \frac{\theta_{OH}}{(\theta_{OH,sat.} - \theta_{OH})}$ vs E_h should give a slope of 59 mV per decade. However, such a relation was not found to hold for the isotherm given

in Figure 5.2. This is possibly because it was difficult to estimate the true saturation charge for the OC1 peak, on account of the factors previously mentioned, and also because the charge values at 1.32 and 1.34 V are suspect for the same reasons.

It should be mentioned that a similar treatment of the surface oxide formation charges measured in 0.5 M H_2SO_4 and the "anions on" situation in mixed $HClO_4/H_2SO_4$ solutions is not possible because the partial desorption and relaxation of the adsorbed sulfate layer at the gold surface allows additional deposition of OH, characterized by reduction in the OC1' peak, as seen in Section 4.4. and further discussed in Section 5.11., and also because the conversion processes occurs more quickly at the higher potentials needed for OH deposition in the presence of the more strongly adsorbed sulfate anion. Surface oxide growth under "anions off" conditions is complicated by the fact that HSO_4^- is readsorbing during surface oxide formation, diminishing the charge for reduction in the OC1 peak. For these reasons, it was only possible to treat the data obtained with 1 M $HClO_4$ in the above way.

5.5. The Significance of the $t^{1/2}$ Relation for Surface Oxide Growth

It has been shown in Section 4.5.6. that the initial stages of growth of surface oxide films at Au, at constant applied potential, follow, for some conditions, a square-root law in time, $t_h^{1/2}$ (e.g. see Figures 4.5.16. and 4.5.17.). At first, it appeared that the initial oxide growth data for a number of growth conditions could be represented rather generally by a $t_h^{1/2}$ relation before the onset of the regime of logarithmic growth in t_h. However, after allowances for the initial iR effect (Section 4.3.1. and Figures 4.4.10. and 4.4.11.) and taking into account the point in the plots of the $t_h^{1/2}$ relations belonging to log t_h growth, it appears that the $t_h^{1/2}$ relation only applies under rather restricted conditions than was initially thought, as exemplified in Figures 4.5.16. and 4.5.17.

An interesting aspect of these $t_h^{1/2}$ relations for the initial stages of oxide growth is that they seem to be independent of the extent of the particular types of surface oxide species at the surface, i.e. for the states reduced in the OC1, OC2 and OC3 peaks. For some of these relations at the lower growth potentials, very little of the charge involved is due reduction of oxide in the OC2 or OC3 peaks, but for those at higher potentials, significant extents of OC2 and OC3 type surface oxide was found.

5.5.1. Common Intersection Points in the $t^{1/2}$ Relations

It has been found (see Figures 4.5.16. and 4.5.17.) that some (but not all) of the Q vs $t_h^{1/2}$ lines at different growth potentials at the same temperature and in the same electrolyte solution converge, extrapolate to a common point at negative times. Since this common intersection point for these lines is found for several growth potential under various conditions, as shown in Table 5.2., it seems likely that there is some commonality between these relations.

Table 5.2.

Common Intersection Points for the $t^{1/2}$ Relations

$[H_2SO_4]$/M	E_h/V	Intersection Point	
		t/s	Q/ $\mu C\ cm^{-2}$
0.5	1.39, 1.40, 1.41	0.0	0.8
4×10^{-3}	1.37, 1.38, 1.39, 1.40	-0.0001	1.5
4×10^{-4}	1.36, 1.38, 1.40	-0.00015	3.7
4×10^{-5}	1.36, 1.38, 1.40, 1.44	-0.0005	9.5

The fact that intersection point is at a negative time implies that surface oxide growth is effectively starting at some time earlier time than $t_h = 0$ and that there is some small, but significant oxide coverage at $t_h = 0$

on the practical time scale of holding at the growth potential. This is a reasonable, practical expectation, because of the way the experiments have been done, i.e. with a fast sweep (500 V s^{-1}) from less positive potentials to the growth potential. During this brief transient time, there is already some initial degree of surface oxide formation occuring at the higher potential end of the sweep. There may also be some small quantity of surface oxide formation in the very first part of the reduction sweep. Indeed, the I vs E profiles for reduction after 0 s holding at the growth potentials show that surface oxide can be formed under these conditions, especially that which is reduced in the OC1 peak, since these OH species are deposited quite rapidly.

5.5.2. Dependence of the $t^{1/2}$ Relations on Potential, Temperature and Sulfate Concentration

The slopes of the Q vs $t_h^{1/2}$ lines generally show a linear dependence on potential, excepting at the lowest growth potentials. The slopes of the $t_h^{1/2}$ lines also increase with temperature, as is expected, and decrease with the concentration of H_2SO_4 in the electrolyte solution, as shown in Figures 5.4.a. and b. Linear dependence on potential of the $dQ/d(t_h^{1/2})$ slope is seen in the mixed $HClO_4/H_2SO_4$ electrolytes, at both 273 K and "room temperature", and is similar to that found in 0.5 M H_2SO_4, for which relations having nearly nearly the same $(d(dQ/d(t_h^{1/2}))/dE)$ slopes are found, including that for the second (longer holding times) $t_h^{1/2}$ slope found in 4 X 10^{-5} M H_2SO_4 at 273 K. The dependence on E_h for growth in 0.5 M H_2SO_4 is more positive than those found in mixed electrolytes by about 30 mV at both temperatures. The first (shorter holding times) $t_h^{1/2}$ slopes found in 4 X 10^{-5} M H_2SO_4 at 273 K do not have the same dependence on E_h as the other lines do, but is was found that surface oxide formation under these conditions was partially influenced by diffusion from solution (see Section 4.2.) due to the low concentration of H_2SO_4 in this case.

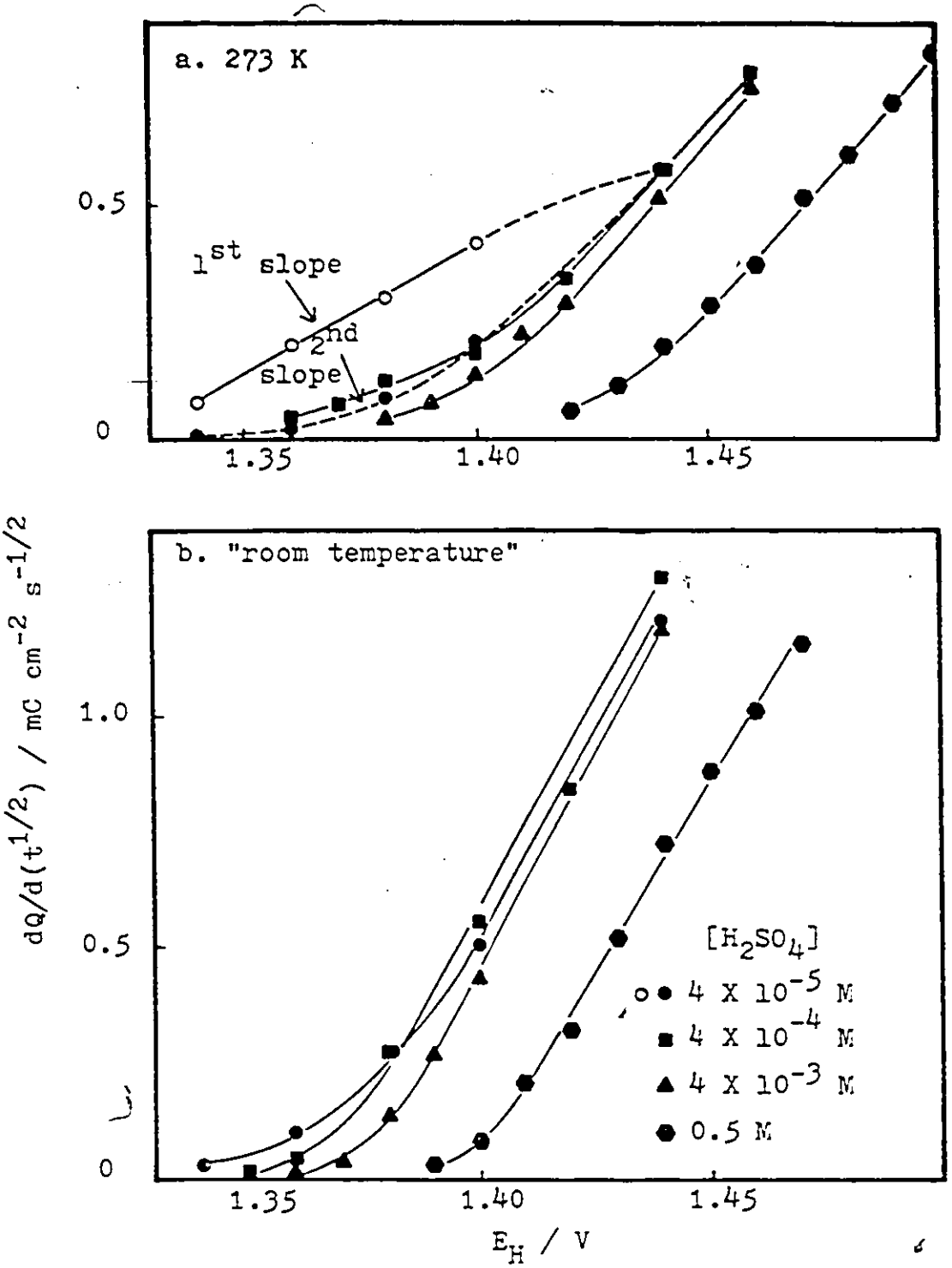

Figure 5.4. Variation of $dQ/d(t^{1/2})$ with potential, E_h, for surface oxide grown at Au in 0.5 M H_2SO_4 and in 1 M $HClO_4$ with 4 X 10^{-3}, 4 X10^{-4}, and 4 X 10^{-5} M H_2SO_4 at: a. 273 K and b. room temperature.

The kinetics for electrochemical reactions are generally expotential in potential, rather than linear, as is found for this $t_h^{1/2}$ relation of the extent of surface oxide formation. Linearization of $\exp(\frac{zFE}{RT})$ for one electron transfer holds only for a range in potential of about 5 to 10 mV, and since these slopes have been found to be linear over potential ranges up to 60 mV, these $t_h^{1/2}$ relations certainly cannot arise from an approximation of an expotential dependance of growth rate on E_h.

Electrochemical reactions which have a linear dependence on potential are usually related in some way to capacitance or resistance, i.e. that is the relation between charge and potential or field through the relation $C = \frac{Q}{E}$, or some corresponding field expression related to Ohm's law. Unfortunately, there doesn't seem to be an obvious physical basis for the dependence of the $t^{1/2}$ kinetics on capacitance.

5.5.3. Possible Mechanisms for $t^{1/2}$ Behavior

Reactions which follow $t^{1/2}$ kinetic relations suggest that some sort of diffusion control is rate-determining, either diffusion to or from bulk solution or surface diffusion. Unfortunately, there are problems in invoking diffusion to explain the square-root relations found in this work as will be discussed below. However, it is possible that these $t^{1/2}$ kinetics are not due to diffusion. A kinetic expession in which the rate of deposition of OH depends inversely on coverage will also be discussed as it can lead to a $t^{1/2}$ relation upon integration.

5.5.3.1. Diffusion from Solution

An adsorption reaction which is controlled by the so-called semi-infinite diffusion of material from solution[251,252] will give kinetics in which coverage increases as $t^{1/2}$. Since the reactant in OH deposition is water, diffusion from solution can not be considered the likely mechanism; however it might be more likely that control of the oxide growth by diffusion of desorbing anions,

which have a strong effect on the initial stages of surface oxidation, into solution maybe the one responsible for this behavior. This mechanism might be used to explain the $t^{1/2}$ relation in the solutions with the lowest concentrations of H_2SO_4, but this behavior also arises in 0.5 M H_2SO_4, where no bulk solution concentration gradients for HSO_4^- could possibly be involved. This indicates that diffusion from the solution to the surface, or of anions from the surface to the solution, is probably not the mechanism responsible for the $t^{1/2}$ relation.

Another problem with this mechanism is that diffusion control under electrochemically irreversible conditions[251] depend exponentially on potential, and it has been shown that the $t^{1/2}$ growth depends linearly on potential.

5.5.3.2 Diffusion on the Surface

Diffusion of adsorbed species (anions or OH's) on the surface itself is another possible explanation of the $t_h^{1/2}$ relation found for surface oxidation of gold at relatively short holding times. Despic and Bockris[253] have treated surface diffusion in metal crystallization, in which deposited metal adatoms diffuse on the electrode surface to growing steps. However, it is difficult to see how this process would apply the situation found in the present work. The $t_h^{1/2}$ relations seem to be independent of the relative contributions from the quantities of OC1, OC2 and OC3 species that correspond the Q values, as previously discussed. In light of this, it seems unlikely that deposited OH's diffusing along the surface to mini islands of turned-over OC3 states give rise to the $t_h^{1/2}$ relations. Also, the growth of the OC3 species seems to be more important in the logarithmic relation rather than the $t^{1/2}$ one.

Free surface diffusion of OH species would be associated with a diffusion constant of the order of 10^{-6} m^2 s^{-1}. At say $\theta_{OH} = 0.1$, the adsorbed OH species are only on the order of 1 nm apart on the average. Hence, on the basis of the Einstein equations, their root mean sqaure displacement time would

be on the order of 10^{-7} to 10^{-8} s. This is 4 to 5 orders of magnitude smaller than the smallest times involved in the $t_h^{1/2}$ relations. Hence the 2-dimensional free diffusion of OH species, as in liquid water, cannot be responsible for the experimentally observed $t_h^{1/2}$ regimes.

However, it must be recalled that the OH species are electrosorbed at Au and hence in a state of chemisorption on the various sites of the Au surface lattice. Hence a Gibbs activation energy $\Delta G^{o\ddagger}$, additional to that for the displacement amongst solvent molecules at the surface, will probably be involved. In order to account for the time scale involved in the $t_h^{1/2}$ growth region on the basis of a activated surface diffusion, the $G^{o\ddagger}$ would have to be ca 30 kJ mol^{-1}, from $\exp(-\Delta G^{o\ddagger}/RT) \triangleq 10^{-5}$. This seems to be a quite realistic figure in relation to the expected order of magnitude for the chemisorptive bond energy of a metal such as Au.

5.5.3.3 Rate Inversely Proportional to Coverage.

A rate expression which depends inversely in coverage, i.e. with a negative order in θ, could be written as:

$$\frac{d\theta}{dt} = k/\theta \qquad (5.5)$$

This integrates to an equation in which coverage depends upon $t^{1/2}$. Thus

$$\theta^2 = k\,(t + \tau)$$

or

$$\theta = k^{1/2}\,(t + \tau)^{1/2} \qquad (5.6.)$$

where τ is an integration constant. It seems logical that the rate of surface oxide formation would decrease as the coverage increases, and $1/\theta$ approximates to $(1 - \theta)$, or free space at the surface, at sufficiently low coverage values.

If the integration constant, , is sufficiently small (on the order of the smallest holding times used, 0.0002 s), then θ should vary explicitly in $t^{1/2}$ and the deviation from linearity of the $t^{1/2}$ relations should not be significant.

One of the problems with this mechanism is that the rate constant, k,

would be expected to depend exponentially on potential rather than linearly, as was experimentally found. Another problem with this mechanism is that is does not account properly for anions; in $\frac{d\theta}{dt}$, θ refers only to the coverage of OH or O species being formed only, but in k/θ, θ term should be related to coverage by everything at the surface, i.e. surface oxide species and chemisorbed anions, whose coverage is decreasing as a function of time.

It should be noted that the so-called "parabolic law" for oxide film growth was one of the results of the original treatment of Mott and Cabrera[41]. This law, corresponding to an increase of film thickness, x, with $t^{1/2}$ at constant potential, arises from integration of a rate law for dx/dt that expresses dx/dt as proportional to x^{-1}, i.e. to the field operating across the growing film, which progressively decreases as the film thickens. It is thus analogous in form to equation 5.5. Such a growth law is based on field-assisted migration of metal ions across the growing film within which the homogeneous field is assumed to exist. Thus, the Mott-Cabrera "parabolic law" can only apply to compact multilayer films and can hardly be expected physically to represent the kinetics of surface oxide growing at gold, where the $t^{1/2}$ law applies already to films corresponding to 5 to 50 % of a monolayer, before even a full nominal monolayer is established. The only basis on which a Mott-Cabrera "parabolic law" could conceivably arise under these conditions would be if the initial stages of oxide film growth at Au involved relatively thick, but small, islands of oxide material, with remaining patches of metal remaining bare except for chemisorbed anions, solvent and possibly some 2-dimensionally chemisorbed OH species. However, none of the other aspects of sub-monolayer oxide film growth at Au, characterized in this present work or in the previous related work[5,6], gives any indications that the initial stages of surface oxide film growth at Au procees by an island development and thickening mechanism. Hence the Mott-Cabrera mechanism cannot apply in this

case despite the formal identity of the $t^{1/2}$ law that arises from their mechanism and is observed in a general way here. Note also that the Mott-Cabrera "parabolic law" should give growth rate slopes, $dx/dt^{1/2}$, that are exponential rather than linear in field or potential except under the unlikely conditions that the field across the film is small enough for Tafel-type expotentials in the field or potential to be linearized.

It seems that the film extention law derived above, based on a rate equation in $d\theta/dt$ proportional to θ^{-1}, or limitingly to $1-\theta$ ($\theta^{-1} \rightarrow 1-\theta$ when $\theta \ll 1$), is formally similar to the Mott-Cabrera "parabolic law", but the physical conditions to which the two rate equations apply are entirely different, except for the rather unlikely case of small island growth referred to above.

5.6. Oxide Growth at Constant Potential: General Features

In Chapter IV, a number of examples of oxide growth plots in log t_h were presented for different electrolyte solutions, temperatures and especially for a range of controlled constant potentials, E_h, at which the oxide film was grown for times, t_h, from 0.0002 s to 5 s. Several general features of these growth curves are to be noted as illustrated schematically in Figure 5.5.

First, an initial growth region, I, is observed that involves, for short times, passage of relatively high current densities, ca. 5 to 10 mA cm^{-2}. However, analysis of this region (Section 4.3.1. and Figures 4.4.10.a. and b.) shows that these growth rates, as currents, are initially constant with t_h and increase linearly with E_h, indicating that the OH deposition process is, in fact, ohmically controlled. Hence, this region of growth curves has no fundamental significance in understanding the electrochemistry of the growth process. That it is not mechanistically connected with the growth process is indicated by the observation that the initial regions where Q is linear in t_h are independent of whether the experiments are conducted with "anions off" or

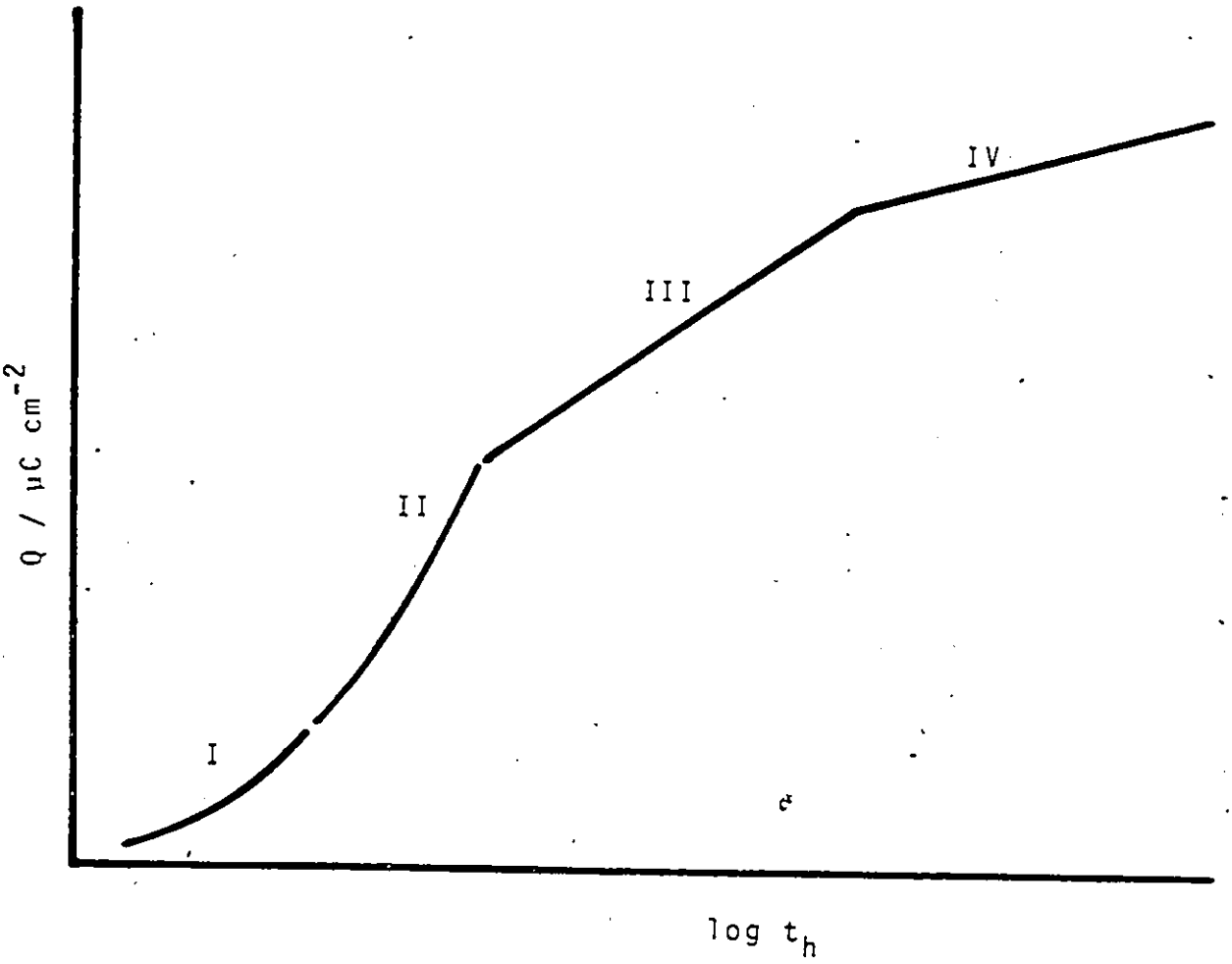

Figure 5.5. Schematic representation of the course of surface oxide growth plotted as a function of log t_h at a given potential, E_h.

Region I: growth controlled by iR effect, dependent on experimental cell arrangement and conductivity of the electrolyte solution

II: transition region to log t_h regime, which plots linearly with $t_h^{1/2}$ for some conditions.

III, IV: regimes of log t_h growth

"anions on" the electrode surface.

When these initial, iR- controlled currents have declined, under some conditions (for relatively low growth potentials), the growth continues in stage II according to the square-root relations in t_h, the slopes of which increase approximately linearly with E_h.

Probably the most important behavior is that which arises in stages III and IV, where the growth enters, and continues in, a logarithmic regime in t_h, the slopes of which (especially region IV) are almost <u>independent</u> of the growth potential, so that the growth relations in log t_h at different E_h become almost parallel (curve section IV) over an appreciable range of potentials, until the oxide layer becomes a thicker phase oxide and Mott-Cabrera type "high field" film growth determines the kinetics of further film extention.

5.7. Logarithmic Surface Oxide Growth

5.7.1. Origins of the Logarithmic Growth Law

At longer holding times and/or greater extents of surface oxidation of gold, a growth law which is directly logarithmic in time takes over from the initial linear in t_h and later $t_h^{1/2}$ relations (Figures 4.4.10a. and b. and 4.5.16. and 4.5.17.), as was seen in previous work from this laboratory by Barnett[6]. This change in the mechanism of surface oxidation arises when the turn-over process and quasi-3-dimensional phase oxide growth, characterized by reduction in the OC3 peak, becomes the major process after the initial OH deposition step. The direct logarithmic growth law was well established at Pt electrodes by previous work in this laboratory[26,200], from low submonolayer coverages, continuing into multilayer formation. However at Au, initially growth does not follow a logarithmic law, as was aready discussed in detail, and the subsequent growth exhibits two logarithmic regions in time.

The problem with kinetics which are directly logarithmic in time is that they can only arise from kinetic expressions that are zero order in OH coverage, thus those containing θ or $(1 - \theta)$ as the usual pre-expotential term in the rate equation for a surface process do not integrate to log t, but rather log θ or log $(1 - \theta)$ as a function of time.

The only type of kinetic law which integrates to give log t is one in which the driving potential is modified in time by the increasing extent of coverage by species at the surface, so that there is a change of the interfacial potential across the "layer" rather than lateral interactions between the adsorbed species[133]. When lateral interactions are predominant, so that the rate constant is exponentially dependent on θ, an expresion of the form

$$\frac{d\theta}{dt} = k \exp(-g\,\theta) \qquad (5.7.)$$

arises, where g is a 2-dimensional lateral interaction parameter or some term

of equivalent significance. This equation may be integrated to give

$$\theta_t = g^{-1} \ln(t - C/k) + \ln(kg) \qquad (5.8.)$$

where C is an integration constant. Then, for $t >> C/k$, it is seen than θ_t increases logarithmically with t_h in a relation having a slope $d\theta_t/d(\log t) = g^{-1}$. This is an interesting and significant result, since it indicates that the slopes of the Q vs log t_h plots are determined not by potential, but by the chemical interaction parameter, g. This behavior is what is experimentally observed in a general way, viz. that once the oxide film growth enters the logarithmic region (e.g. see Figures 4.4.9.a., b., c. and d., 4.5.4.and 4.5.15.), the slopes of the resulting grow are semi-quantitatively, if not exactly, constant within each of the two distinguishable log t_h parts of the growth relations, for a range of growth potentials, E_h.

The treatment according to equations 5.7. and 5.8. is, however, only a semi-quantitative approach to this problem, and no completely satisfactory explaination of a direct log t growth law has yet been made.

5.7.2. Slopes of the Logarithmic Growth Relations in Time

Evaluation of the slopes of the logarithmic regions of the oxide growth curves leads to the plots shown in Figures 5.6. and 5.7. It is seen that there are significant ranges of potential, E_h, for which the slopes, $dQ/d(\log t_h)$, are independent of E_h, although in other cases, e.g. 1 M $HClO_4$ with 4 X 10^{-4} M H_2SO_4, the slope exhibit a dependence on E_h. Generally there are two distinguishable ranges of slopes of the Q vs log t_h growth plots, the slopes for lower range of log t_h have higher values than those which are found for these relations at the higher range of times. This may be easily seen qualitatively by inspection of most of the Q vs log t_h curves themselves.

For the mixed electrolytes, the groups of values are dependent on temperature and somewhat on the added sulfate ion concentration.

At low potentials, there are some difficulties in deciding which points

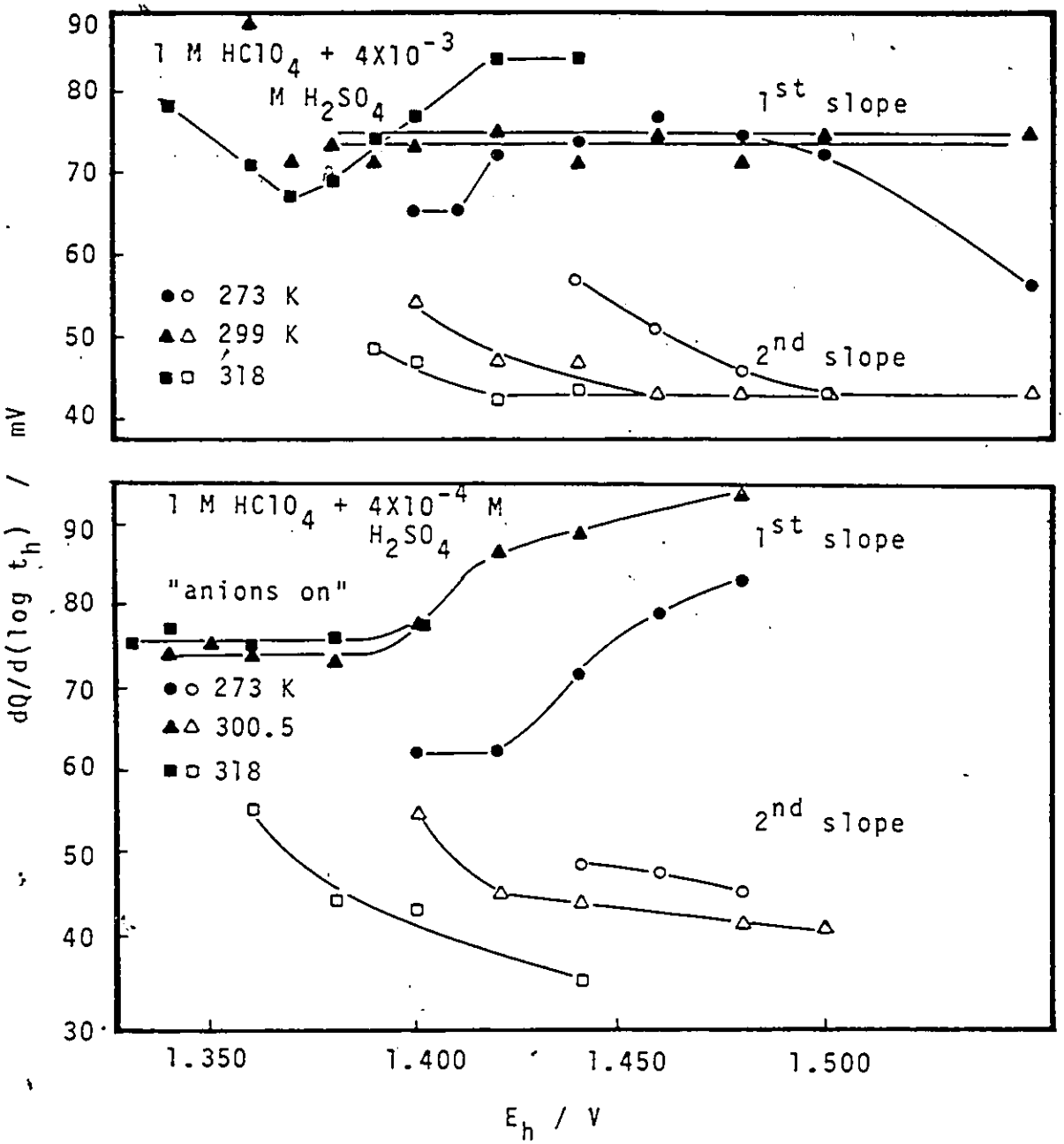

Figure 5.6. Slopes of the Q vs log t_h surface oxide growth curves, $dQ/d(\log t_h)$, for several E_h values and three temperatures in 1 M $ECl0_4$ and (a.) 4 X 10^{-3} M H_2SO_4 and (b.) 4 X 10^{-4} M H_2SO_4.

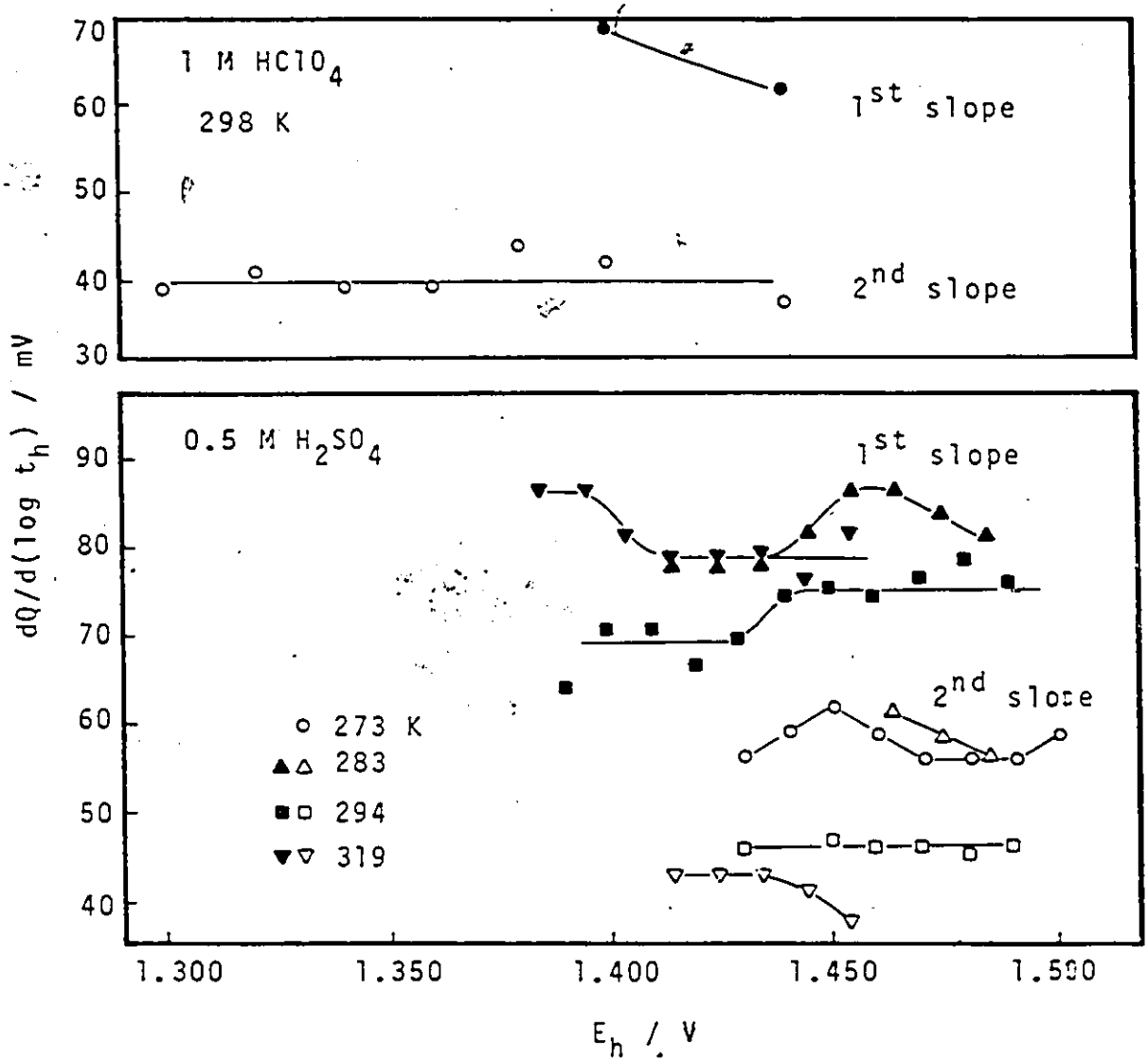

Figure 5.7. Slopes of the Q vs log t_h surface oxide growth curves, $dQ/d(\log t_h)$, for several E_h values in (a.) 1 M $HClO_4$ and (b.) 0.5 M H_2SO_4 at four temperatures.

belong to the intermediate $t_h^{1/2}$ (region II) and which belong to the beginning of the first logarithmic region. Attempts to derive resolved components of Q_{total}, i.e. Q_{OC2} and Q_{OC3}, as a function of log t_h, and plot their slopes were not very productive, as there are difficulties in reliably resolving the charge components for a range of E_h values due to overlapping of the I vs E profiles. However, regions of approximately constant $dQ_{OC2}/d(\log t_h)$ and $dQ_{OC3}/d(\log t_h)$ were found.

The numerical values of the slopes $dQ/d(\log_{h})$ for the total oxide species were ca. 75 - 90 mV per decade for the first sections of the log t_h plots and ca. 40 -55 mV per decade for the second, which enables, in most cases, the two regions to be clearly distinguished. Generally, with the limitations referred to above, the range of slopes corresponding to higher Q and log t_h values reflects the growth behavior mainly of the OC3, quasi-3-dimensional phase oxide (the turned-over species). Identification of the first, higher valued slopes region with growth of the OC2 species to their saturation coverage values is more ambiguous, and the curve resolution problem prevents more definite resolved charge plots to be made, as was previously indicated.

5.8. Conversion of OC1 to OC2 and OC3 Species in Relation to Displacement by Sulfate Ion in "Anions Off" Growth

The OC1 peak for "anions off" growth in 1 M $HClO_4$ with $4X10^{-4}$ M H_2SO_4 shows a clear and easily measured decrease with time. Unlike the decrease of the charge for OC1 in 1 M $HClO_4$, which is due mainly to conversion to OC2 and especially OC3 species, the decrease found for "anions off" growth in mixed electrolytes is complicated by displacement of surface oxide by the readsorption of SO_4^{2-} at the Au surface. Therefore, only part of the OC1 charge lost actually corresponds to conversion of the OC1 species to another state of the surface oxide species. In order to examine this phenomenon, the conversion charge, $Q_{con.}$ will be defined in the same way that it was for 1 M

$HClO_4$ (see Section 4.3.2.), that is as the maximum charge for the OC1 peak for a particular growth potential less the OC1 charge at a particular holding time after the charge under that peak has begun to decrease:

$$Q_{con.} = Q_{OC1,max.}(E) - Q_{OC1}(E,t)$$

Unfortunately, during "anions on" growth, as also fo the case of 0.5 M H_2SO_4, the decrease in the charge for OC1 is not easily measured because the OC1' state (Figure 4.4.2.) cannot be separated from the OC3 peak as the OC1' state disappears. For this reason, only the conversion and displacement of the OC1 species in the "anions off" growth regime will be discussed.

Figure 5.8. shows $Q_{con.}$ evaluated for several growth potentials for Au in 1 M $HClO_4$ with $4X10^{-4}$ M H_2SO_4 at 300 K for t_h between 0.002 and 0.5 s. These curves, unlike those for Au in 1 M $HClO_4$, have a sigmoidal shape. This is probably because of the influence of readsorbing SO_4^{2-} anions, since the extent of blocking of surface oxide formation, as a function of t_h at 1.2 V (Figure 4.2.2.), also has a sigmoidal shape when plotted vs log t_h. Conversion and displacement of species in the OC1 state seems to begin at about 0.005 s for the various potentials studied. $Q_{con.}$ increases with potential as a result of the increase of $Q_{OC1,max.}$ with potential until it reaches its maximum possible coverage.

Figure 5.9. shows $Q_{OC3} - Q_{con.}$ for some of the conversion charges recorded in Figure 5.8. Unlike the results for 1 M $HClO_4$, most of these values are less than zero, which clearly indicates that electrosorbed OH in the OC1 state must be actually displaced by anion adsorption. These values initially decrease with increasing t_h and potential, as more OC1 charge is lost on account of anion readsorption, but eventually they increase as the OC3 charge (coverage) increases (Figure 5.9.). This situation is much more complicated than that found in 1 M $HClO_4$.

Figure 5.10. shows $Q_{con.}$ and Figure 5.11. shows $Q_{OC3} - Q_{con.}$ as a function

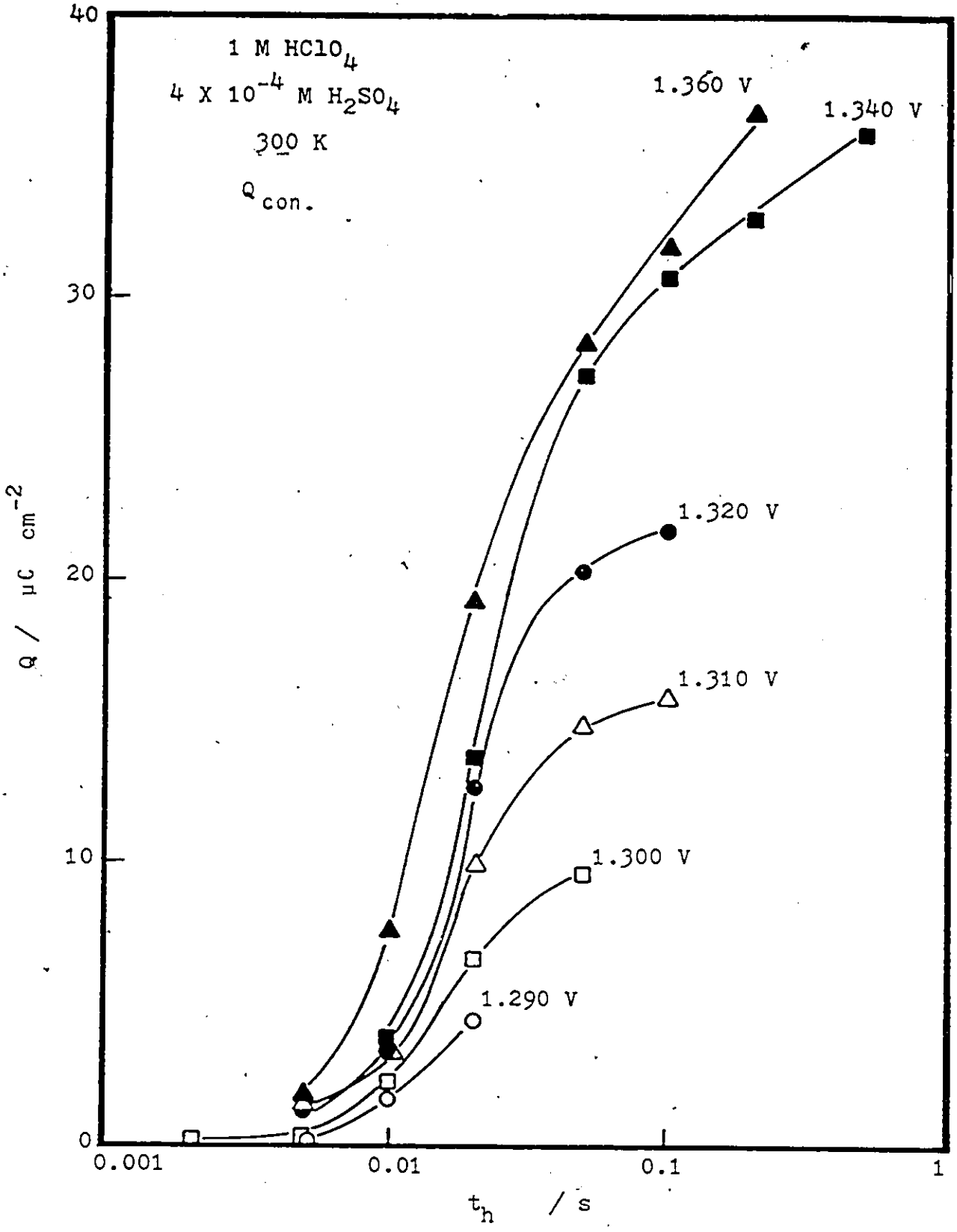

Figure 5.8. Q_{OC1} converted to OC2 and OC3 or displaced by SO_4^{2-} adsorption as a function of t_h at several E_h for "anions off" growth at Au in 1 M $HClO_4$ with $4X10^{-4}$ M H_2SO_4 at 300 K.

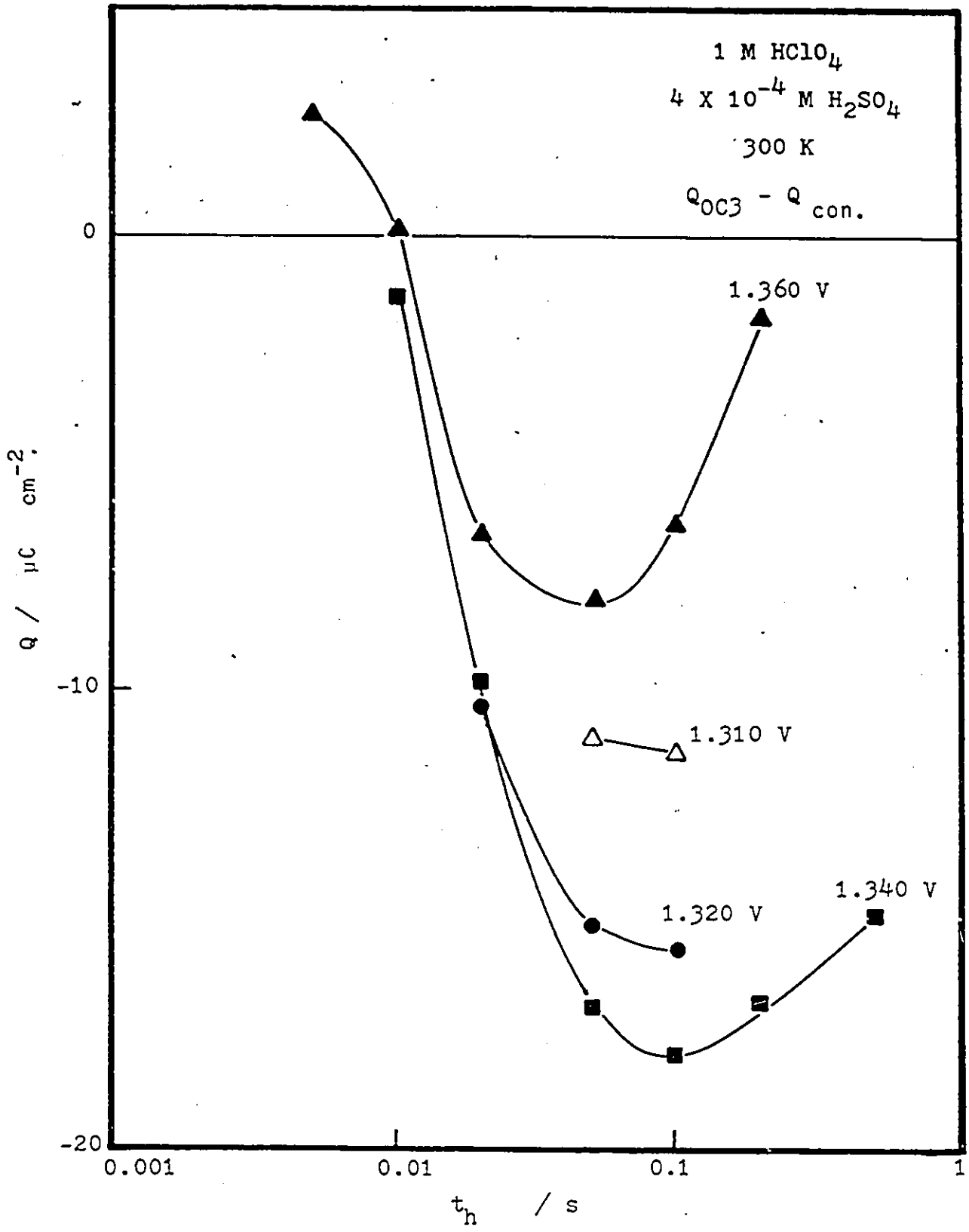

Figure 5.9. $Q_{OC3} - Q_{con.}$ vs t_h at several E_h for "anions off" growth at Au in 1 M $HClO_4$ with $4X10^{-4}$ M H_2SO_4 at 300 K.

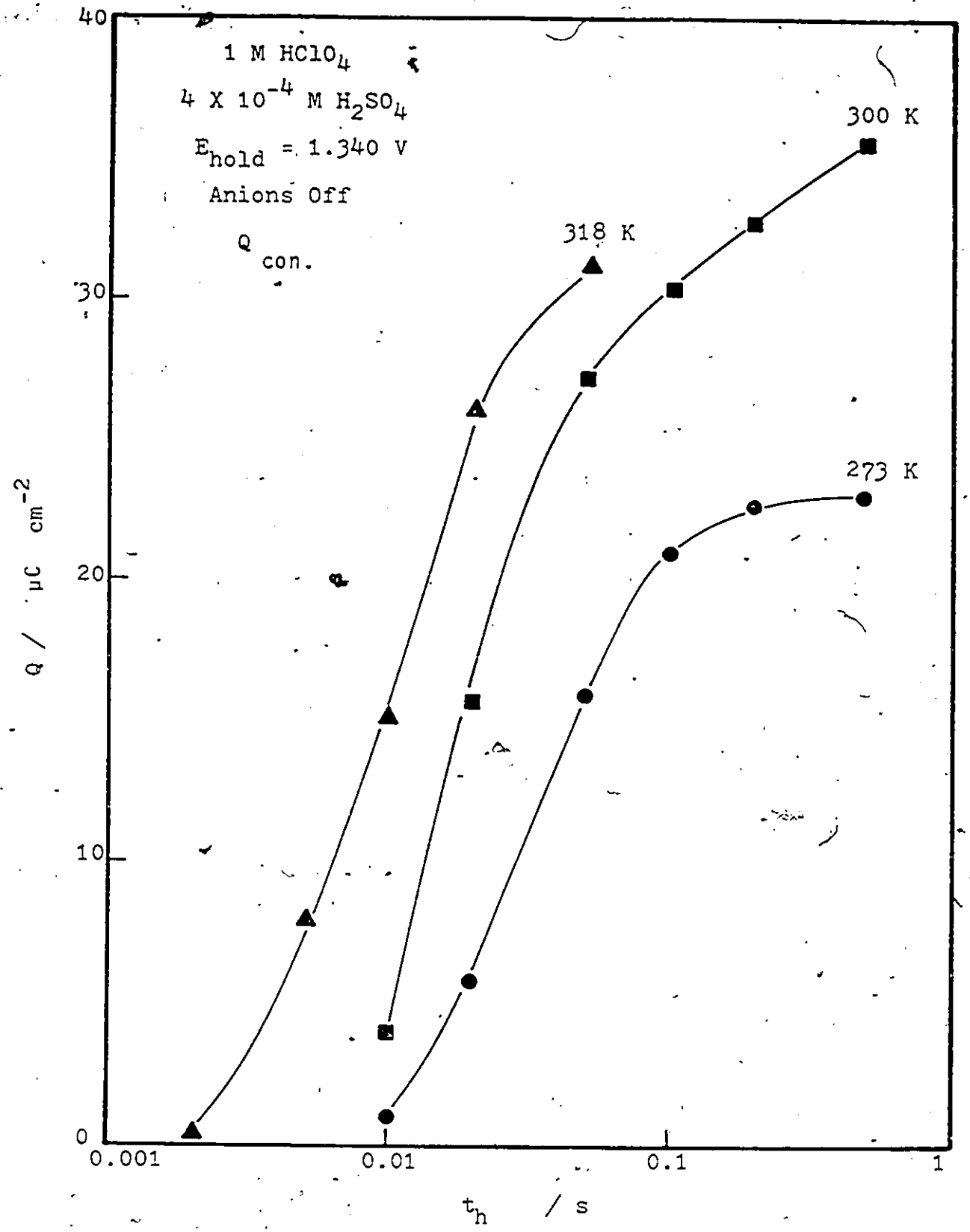

Figure 5.10. Q_{OC1} converted to OC2 and OC3 or displaced by SO_4^{2-} adsorption as a function t_h at 1.340 V for "anions off" growth at Au in 1 M $HClO_4$ with $4X10^{-4}$ M H_2SO_4 at 273 K, 300 K and 318 K.

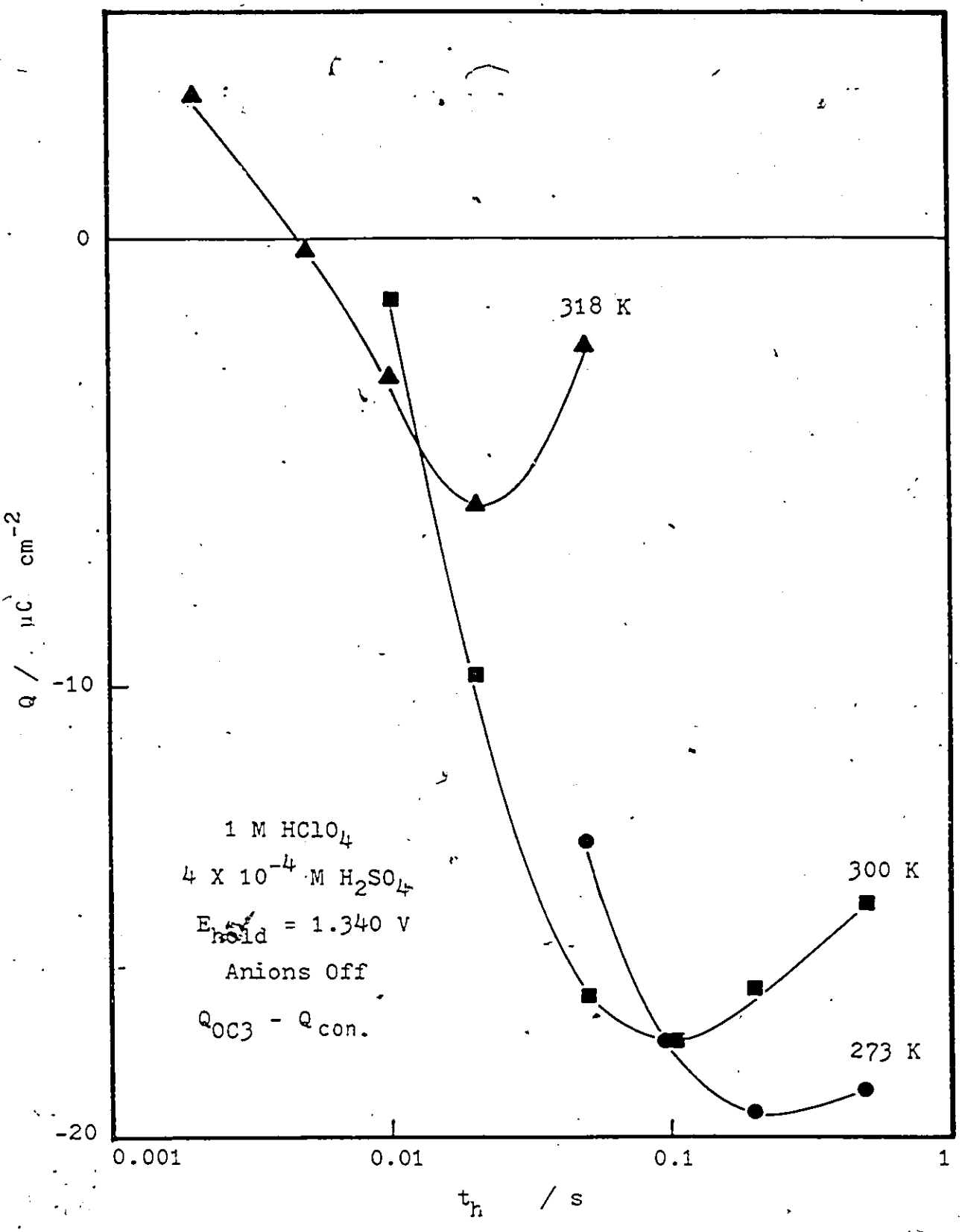

Figure 5.11. Q_{OC3} - $Q_{con.}$ *vs* t_h at 1.340 V for "anions off" growth at Au in 1 M $HClO_4$ with $4X10^{-4}$ M H_2SO_4 at 273 K, 300 K and 318 K.

of log t_h for Au in 1 M $HClO_4$ with $4X10^{-4}$ M H_2SO_4 at 1.340 V for the three temperatures of the experiments. The time after which conversion of OC1 species begins (Figure 5.10.) decreases with increasing temperature, probably because SO_4^{2-} readsorbs, of course, more quickly at higher temperatures. Again, most of the $Q_{OC3} - Q_{con.}$ differences are negative, and this trend becomes more pronounced with decreasing temperature, since growth of the OC3 species is slower for such conditions.

5.8.1. Growth and Conversion at Low Potentials

As was indicated in schematic Figure 5.5., several regimes of oxide film growth can be distinguished inthe log t_h plots. At low growth potentials, it is interesting to show how the time-dependence of the OC1 state depends on SO_4^{2-} (HSO_4^-) concentration in 1 M $HClO_4$ for four E_h values (Figures 5.12.a., b., c. and d.). The quantity of OC1 species decreases from its initial values after times that are much shorter with higher concentrations of sulfate anions. When the decrease of OC1 sets in, the total oxide species, Q_{total} in Figures 5.12.a., b., c. and d., increases. Note that in these figures, the initial, iR-influenced data points (Section 4.3.1.) are not included. These sulfate- and potential-dependent decreases of the OC1 species correspond to the conversion process previously described in this section. In sulfate-free M $HClO_4$at two lower E_h values, it is easy to identify the constancy of the OC1 charge over a large range of t_h, corresponding to attainment of equilibrium coverage by this species, referred to in Section 5.4.

5.9. General Discussion of the Mechanism of Surface Oxidation of Gold

Here a concluding representation will be given for the mechanism of the initials stages of surface oxide formation at gold, which is an extention of some initial ideas developed by Barnett[5,6] in this laboratory.

In particular, a mechanism for the initial stages of OH deposition, taking into account the effects of co-adsorbed anions, was proposed on the basis of

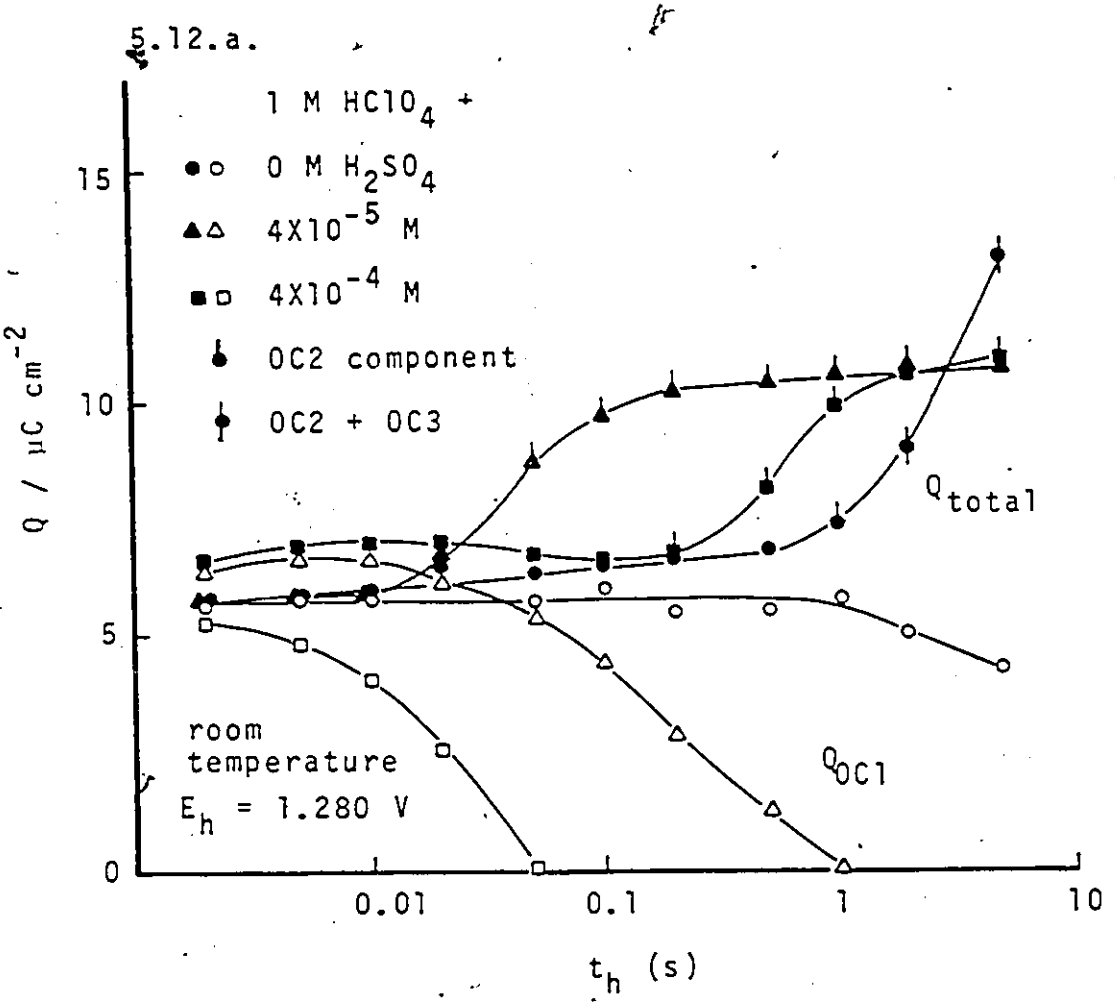

Figure 5.12. Variation of surface oxide charge associated with the OC1 peak and total O-species at Au in 1 M $HClO_4$ with $4X10^{-4}$ M, $4X10^{-5}$ M and no added H_2SO_4 at room temperature and four low E_h values: (a.) 1.280 V; (b.) 1.290 V; (c.) 1.300 V and (d.) 1.320 V.

5.12.b.

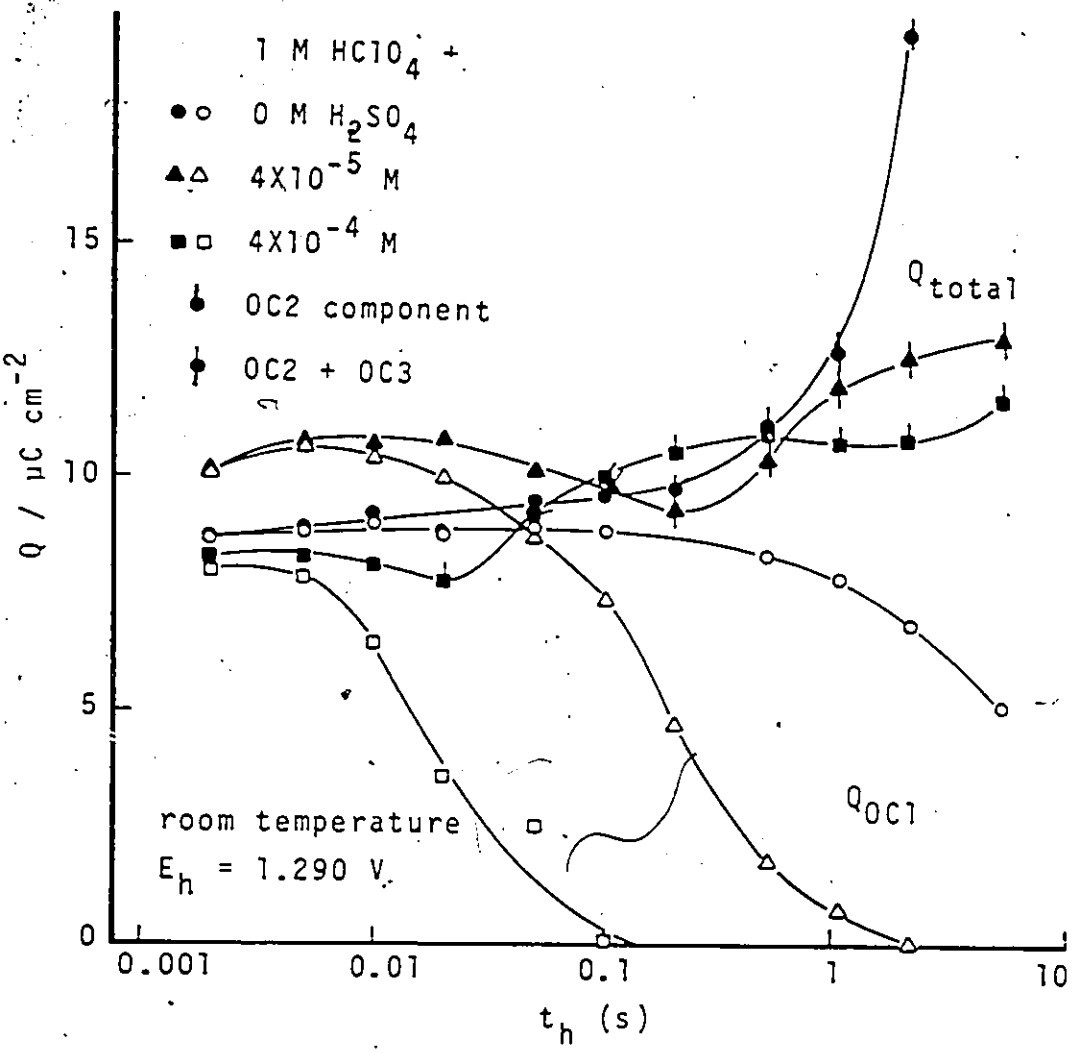
1 M HClO4 +
0 M H2SO4
4X10-5 M
4X10-4 M
OC2 component
OC2 + OC3
Qtotal
QOC1
room temperature
Eh = 1.290 V
Q / µC cm-2
th (s)
0
5
10
15
0.001
0.01
0.1
1
10

5.12.c.

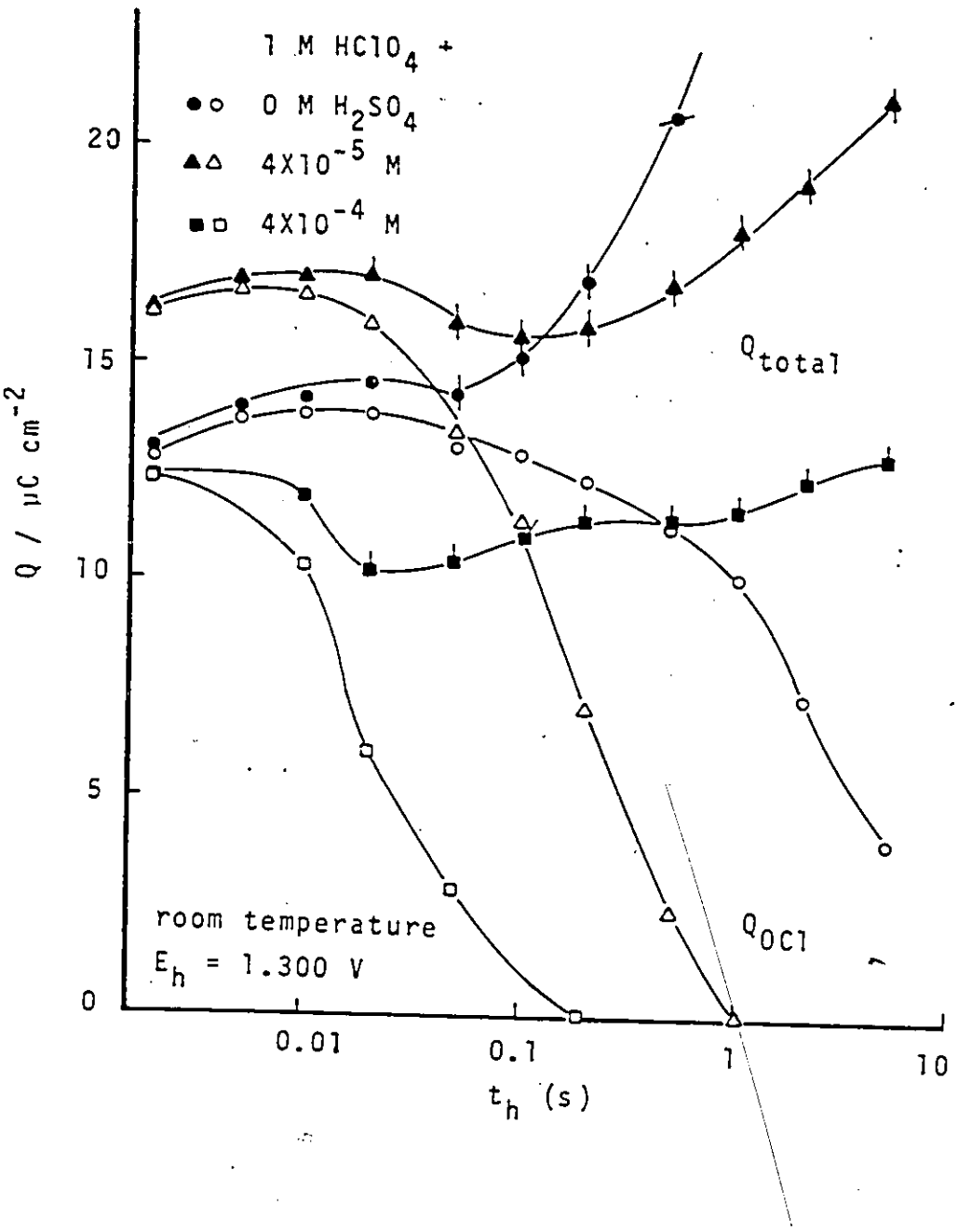
1 M HClO4 +
0 M H2SO4
4X10-5 M
4X10-4 M
Qtotal
QOCl
room temperature
Eh = 1.300 V
Q / μC cm-2
th (s)
0
5
10
15
20
0.01
0.1
1
10

5.12.d.

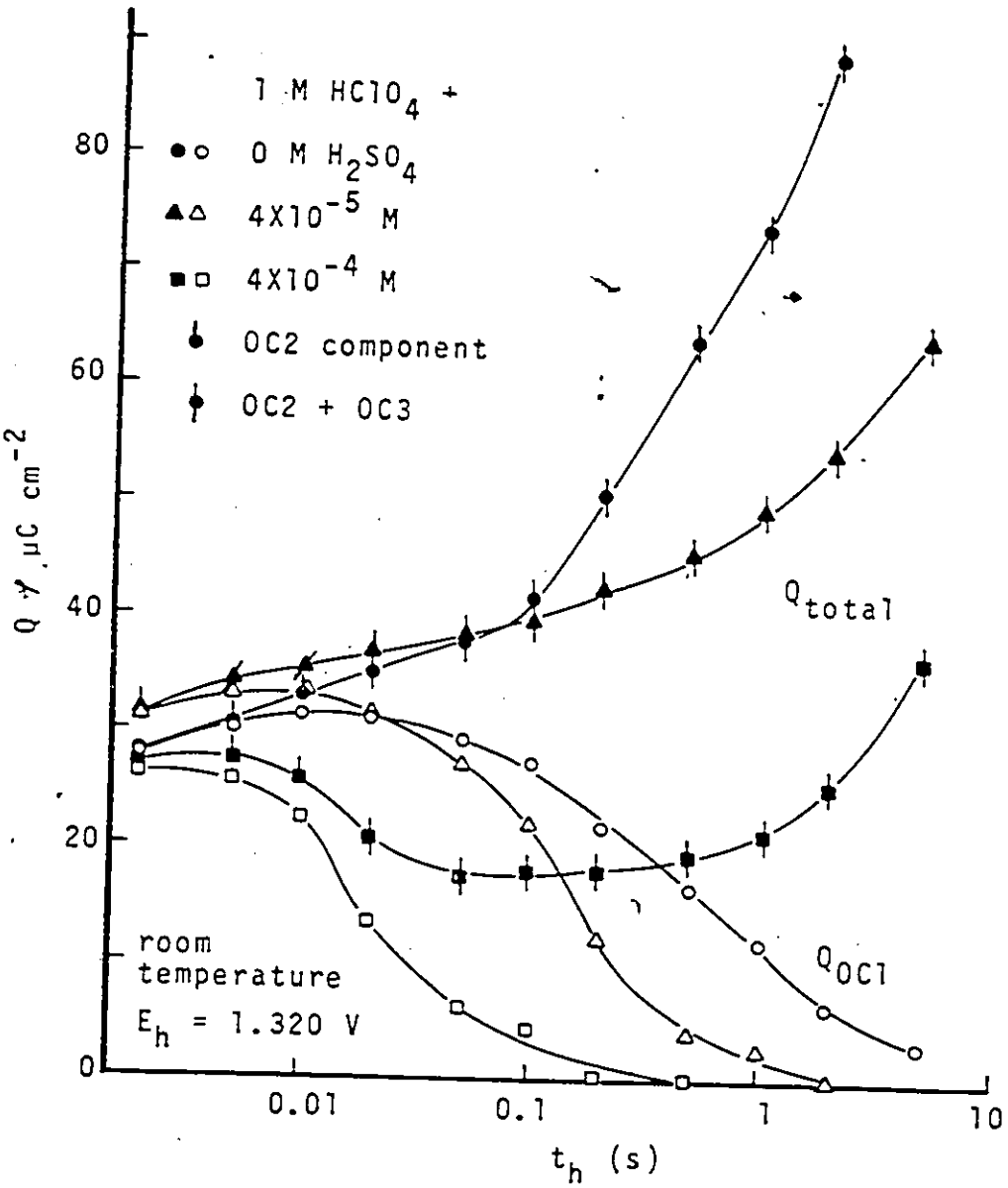
1 M HClO4 +
0 M H2SO4
4X10-5 M
4X10-4 M
OC2 component
OC2 + OC3
Q total
Q OCl
room temperature
Eh = 1.320 V
Q / µC cm-2
th (s)
0
20
40
60
80
0.01
0.1
1
10

recent studies of the oxidation of the Au(111) single-crystal surface by Kozlowska et al.[194,195] for the cases of $HClO_4$ and H_2SO_4 solutions. It can be formulated in a formal way as follows:

Prior chemisorption of the hydrated anion (A_{hyd}) with charge-transfer at potentials less positive than that for onset of OH deposition:

$$M + A_{hyd}^- \rightleftharpoons M_{3+x}\, A^-.(H_2O)_y \qquad (5.9.)$$

$$M_{3+x}\, A^-.(H_2O)_y \rightleftharpoons M_{3+x}\, A.(H_2O)_y + e \qquad (5.10.)$$

with the tetrahedral anions, ClO_4^- or SO_4^{2-} (HSO_4^-), adsorbed a trigonal (M_3) sites on the metal surface lattice (e.g. for (111)) and x other sites to accommodate the hydration water of the anions. It should be noted that perhaps somewhat more or less than 3 metal sites may be associated adsorbed anions on the less ideal polycrystalline surfaces used in the present experiments. Equation 5.10. represents the chemisorption of A^- with charge transfer that is observed experimentally[194,195] in almost reversible cyclic-voltammetry peaks prior to onset of OH deposition. It is also clearly illustrated in the thermodynamic isotherm discussed in Section 5.4.

The very initial stage of OH deposition arises from the water molecules (marked H_2O below) hydration-bound to the chemisorbed anions in a charge-transfer step represented as:

$$M_{3+x}\, A.H_2O.(H_2O)_{y-1} \rightleftharpoons M_{3+x}\, \underset{(OC1)}{[A.OH]^{\gamma-}}.(H_2O)_{y-1} + H^+ + (1-\gamma)e \qquad (5.11.)$$

giving an electrosorbed OH adjacent to an anion, A, with a net partial charge, γ^-, and the OH probably H-bonded to A (note A is an oxyanion radical) and also to the surrounding H_2O molecules. Equation 5.11. corresponds to initial discharge of OH amonst adsorbed anions (as mentioned in the Introduction), and probably in a sub-lattice arrangement of of chemisorbed anions on the surface.

The formation of the very initial state of OH, given as $[A.OH]^{\gamma-}$, is to be identified as that observed as the reversible OA1 process and its conjugate cathodic process, OC1.

The situation for OH deposition in the presence of the more strongly adsorbed sulfate ion is more complicated than that for the weaker perchlorate. This is because the adsorbed anion layer "relaxes" as a function of time, after some deposition of OH, to a new quasi-equilibrium coverage in the presence of adsorbed OH, giving rise to OH species at the surface with a slightly lower energy, characterized by shifting of the OC1 peak to less positive potentials and the appearance of the new the OC1' peak, which shifts dramatically in potential as coverage increases. This behavior was described in Section 4.3. and will be explained in greater detail in Section 5.11.

Further changes in the electrosorbed layer of OC1 type species then arise, leading to free MOH species (identified with the OC2 species) and turned-over states, OH.M (identified with the OC3 species), as follows:

$$M_{3+x}\,[A.OH]^{\gamma-}.(H_2O)_{y-1} + (1-\gamma)e \longrightarrow M_{3+x} + A_{hyd}^{-} + MOH \qquad (5.12.)$$

$$MOH \xrightarrow{\text{turn-over}} OH.M \quad (OC3) \qquad (5.13.)$$

$$M_{3+x} \xrightarrow{H_2O} MOH + H^+ + e \quad (OC2) \qquad (5.14.)$$

The transformation of OC1 species (OA1/OC1 peaks) to other states on the surface (OC3 and/or OC2) is a relatively slow process as has been demonstrated experimentally, as described in Chapter IV.

As was discussed in Section 5.4., the process shown in equation 5.12. may be slow at relatively low potentials, since it depends strongly on electrode potential. It should also be noted that, since the anions lose charge during

chemisorption, they must regain that charge during desorption; this will be discussed in Section 5.10. The adsorbed anions stablize the deposited OH species in the high energy OC1 state, preventing the replacement turn-over process from occuring until the anions have become desorbed. When anions are not present at the surface, the remaining OH's which have not been turned-over will have a lower energy state, and are characterized by reduction in the OC2 peak.

On the principal index planes of Au, there is sometimes two or more OC2 type peaks, and this behavior is thought to correspond to two or more sublattices of OH at the surface[194]. However, at polycrystalline wires, which are more disordered on an atomic scale (the I vs E profiles in 1 M $HClO_4$ actually closely resemble those observed for Au(210), which is the Miller index plane with the highest degree of microscopic roughness), it is not possible for the OC2 species to be adsorbed in such an ordered fashion on such a surface.

As the anions become desorbed, destablized patches of surface with deposited OH's, are left behind where the turn-over process can take place,

MOH MOH --> MOH OHM (5.13.)

producing more stable species that are reduced in the OC3 peak and give rise, experimentally at least, to the log t_h relation and the formation of a quasi-3-dimensional phase oxide previously discussed. This process is based on the change of energy from that of a metal-to-OH dipole in the initial state, M-OH, at the surface to the final turned-over state, OH-M, where it is more stable in the electrode field. This would give rise to the field dependence of the rate of the form $\exp((E/d)\mu/RT)$, where d is distance from the surface over which the potential E falls and μ is dipole moment.

The turn-over process is the main growth process at Au electrodes for longer times and high potentials, as measured by the charge under the OC3 peak, and continues with formation of multilayers, as shown in previous work[6] from

this laboratory. Further oxidation of Au also involves the passage of a second electron, producing O from the OH species, which corresponds to be the process giving rise to the OA4 peak; this peak is especially well resolved at the (111) plane[195].

5.10. Charge Transfer in Anion Adsorption

Recent work by Angerstein-Kozlowska et. al.[194,195] indicated that charge transfer is involved in the chemisorption of anions at gold surfaces and was found to be aproximately 1 e per adsorbed ion. This idea is further supported by the examination of the effect of relatively slow adsorption the sulfate anions (holding at 1.2 V) in mixed $HClO_4/H_2SO_4$ solutions has upon the cathodic I vs E profile for the double-layer charging region (Figure 4.7.2.a. and Table 4.7.1.). As greater coverages of adsorbed sulfate are attained at longer holding times, more cathodic charge is required to remove the chemisorbed sulfate radicals at the surface to negatively charged anions in solution; this effect is manifested in the larger currents being observed in the cathodic sweeps between 1.2 and 0.7 V.

Inspection of I vs E profiles for double-layer charging in 1 M $HClO_4$ and 0.5 M H_2SO_4 (Figure 4.7.1.) shows that considerably more charge is passed in H_2SO_4, as was discussed in Section 4.7., indicating a large coverage of ions at the surface in this solution. The double-layer capacitance for gold in the absence of any charge-transfer due to chemisorption of anions may be considered approximately 24 $\mu F\ cm^{-2}$, which corresponds to the minimum in the I vs E profile for 1 M $HClO_4$ at about 1.0 V. The currents in the double-layer charging region ($E < 1.0$ V) which correspond to capacitances greater than this minimum value may then be integrated to give the charge involved in anion adsorption. Charges of 10 $\mu C\ cm^{-2}$ and 25 $\mu C\ cm^{-2}$ were found for anion adsorption in 1 M $HClO_4$ and 0.5 M H_2SO_4, respectively, which correspond to ratios of adsorbed anions to gold surface sites (assuming 1 e/ion) of 1:20 for

ClO_4^- and 1:8 for SO_4^{2-} (HSO_4^-).

From the radiotracer results of Horanyi et al.[105], a ratio of adsorbed sulfate to gold surface sites may be calculated by assuming a Langmuir isotherm and using the surface concentrations reported for the concentrations of H_2SO_4 used in that work and extrapolating to 0.5 M H_2SO_4. A ratio of 1:27 was obtained, however, the technique used to measure the electrode surface area in the radiotracer work gives considerably higher values than the Burshtein method[245] used in the work described in this thesis, so the number of surface sites in the above ratio is probably too high, but it is uncertain by how much.

It is important to discuss the charge transfer involved in anion adsortion with respect to surface oxide formation, because, with increasing extent of OH deposition, the anions become desorbed in time, requiring ca. 1 e/ion. This cathodic charge, due to anion desorption, decreases the measured charge passed during surface oxide formation with respect to that due to the surface oxidation process (OH discharge) alone. However, the charges due to anion desorption may generally be ignored, because the blocking area of the anions and their water co-spheres is so relatively large, that many OH's (10 to 30:1) may be deposited for the desorption of any big hydrated-anion such as HSO_4^- or ClO_4^-.

5.11. The Relationship Between the Isotherms for Adsorbed Anions and OH

In the discussion of the mechanism of surface oxidation of Au, given in Section 5.9., the role of co-adsorption of OH with already chemisorbed anions was stressed. In order to discuss the earliest stages of surface oxide formation at gold, it is necessary, therefore, to have some understanding of the energetic and time-dependent relationship between the coverages of co-adsorbed anions and OH species and their associated isotherms. This is especially true for more strongly adsorbed anions, such as sulfate.

It is well known that isotherms for anion adsorption with and without the

influence of co-adsorbed OH are considerably different, as is also reciprocally the case for OH adsorption with and without the influence of anions. It has already been shown, through the present results, that anions desorb as a function of time after some initial OH is deposited, actually allowing further deposition of OH (according to equation 5.14.). This indicates that there must be a continuous readjustment of the Gibbs energies for the co-adsorbed anions and OH's with respect to each other, becoming more favorable for OH and less favorable for anions with increasing time.

For this preferential electrosorption of OH to occur, it is necessary that the elechrochemical Gibbs energies for both anion and OH adsorption both increase with potential, since both processes involve charge transfer, but one at greater rate than the other. This is qualitatively illustrated in Figure 5.13.a. for Gibbs energy vs potential and in Figure 5.13.b. for isotherms.

The line for OH deposition is shown with a steeper slope than that for anion adsorption ((1) strongly adsorbed, (2) weakly adsorbed) so that, with increasing E, OH deposition predominates over anion adsorption. The slopes differ for OH and anion adsorption due to an assumed greater degree of charge transfer for OH than for anion chemisorption (see below).

At relatively low potentials, anion adsorption is favored (equation 5.10), but above some critical potential for onset of oxidation, associated the reversible OA1/OC1 peak, OH deposition must have a more favorable energy, since it depends evidently more strongly on potential as illustrated in Figure 5.13.a. This stronger dependence on potential can only arise from a greater extent of charge transfer being associated with OH deposition relative to that for anion adsorption, owing to either or both of the following factors:

1. greater electrosorption valency, γ , for OH deposition than the anion adsorption ($\gamma_{OH} > \gamma_A$),
2. greater effective coverage of the anion and its asssociated water with

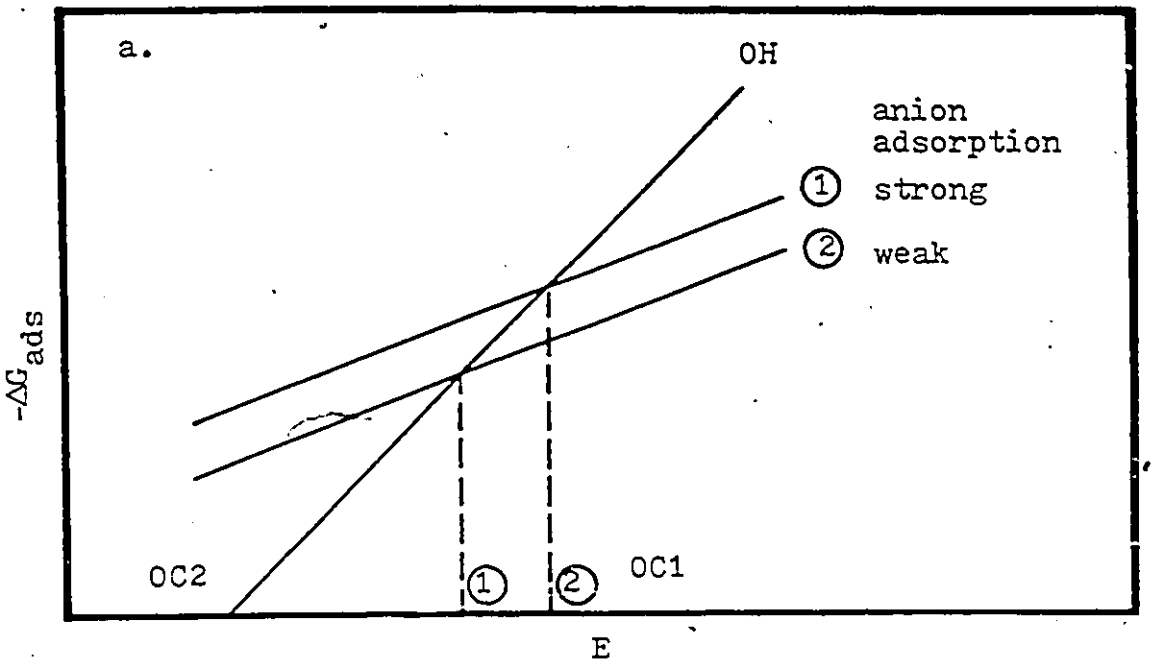

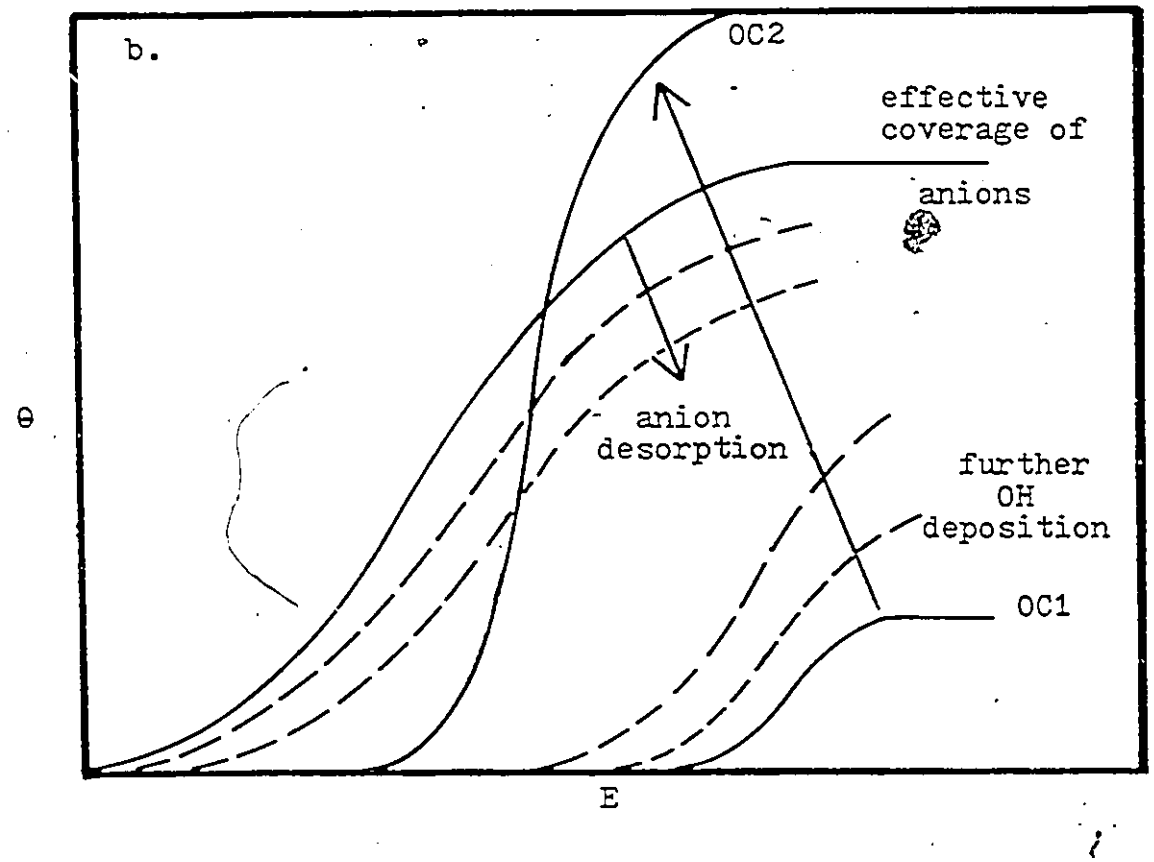

Figure 5.13. Qualitative relation between adsorbed anions and OH species reduced in the OC1 and OC2 peaks.

a. $\Delta G_{ads.}$ vs E

b. Isotherm, θ vs E

respect to deposited OH; e.g., a sulfate ion covers at least 3 sites for OH deposition at Au.

As represented in Figure 5.13.a., the onset of reversible OH deposition depends the strength (Gibbs energy) of anion adsorption, observed experimentally in the OA1/OC1 peaks which arise at less positive potentials in more weakly adsorbed anions, like perchlorate, or at more positive potentials at higher anion concentrations, i.e. greater chemical potentials.

In the presence of the OH's introduced at the surface amongst the anion lattice, the previously adsorbed anions are rendered unstable (or meta-stable) and become desorbed in time; then, as anions are removed from the surface, the Gibbs energy of the OH species at the surface is reduced, which is manifested experimentally as the reduction of these species at lower energies in the OC2 peak at less positive potentials.

In terms of adsorption isotherms, this situation is repesented in Figure 5.13.b. Here the curve labeled OC1 (a) is the isotherm for the initially deposited OH species amongst anions but, with time dependent increase of OH deposition, isotherms (b) and (c) apply with different Gibbs energies of adsorption. Simultaneously, due to a mutual interaction effect, the isotherm for anion adsorption is changed from curve (x) to curves (y) and (z) corresponding to (b) and (c) for OC1 type OH species. Thus, increase of OH deposition becomes associated with decrease of anion adsorption according to the direction of the two shorter arrows shown. As anions become desorbed with increasing OH coverage, the state of OH's becomes eventually represented by the isotherm (d) for OH, corresponding to the OC2 state.

The mechanism for sulfate desorption is probably somewhat different from that for perchlorate. The I vs E reduction profiles in 1 M $HClO_4$ show an isopotential point (Figure 4.3.4.) which is not observed in H_2SO_4 electrolyte (Figure 4.4.8.). Also, the OC1 peak does not change in potential with coverage

in $HClO_4$ nearly as much as it does in H_2SO_4, and the OC1' peak is only arises in H_2SO_4. It is suggested that the ClO_4^- desorbs more or less in those regions of the surface where the turn-over process occurs and resultant OC2 species are left, but the desorption of sulfate is a more complex process.

When OH is deposited amongst adsorbed sulfate at the surface, the free energy of the 2-dimensional joint system of the co-adsorbed anions plus OH's is changed and a non-equilbrium situation is then generated, especially at somewhat higher potentials. After some significant coverage by OH as OC1 species have been deposited (curve d, Figure 5.14.), the coverage of the joint OH + anions adsorbate system is above its equilibrium value for that potential. This unstable situation (curve b, Figure 5.14.) is then relieved by desorption of some of the anions (decending arrows from curve b to curve c) with a time dependent readjustment of the composition of the adlayer, i.e. change of coverages, to correspond to to the joint isotherm (curve c) for adsorption of A in the presence of co-adsorbed OH, representing thermodynamically, a new quasi-equilibrium state of the system at the electrode surface. As relaxation of the energy of the surface film of OH and anions takes place with anion adsorption, an increase of OH coverage is allowed, at the same electrode potential. This rather complex situation is illustrated qualitatively in the series of curves in Figure 5.14.

The new quasi-equilibrium state that tends to be reached, is characterized by reduction of the co-adsorbed OH in the OC1' peak. As the sulfate become desorbed, further OH deposition becomes allowed, causing further desorption of the ions and corresponding relaxation of the system of co-adsorbed OH and anions in time. The energy of OH at the surface is also decreasing with time, as indicated experimentally in the way the OC1' peak shifts negatively in potential with increasing OH coverage. Therefore this process involves a continuous time-dependent readjustment of the composition

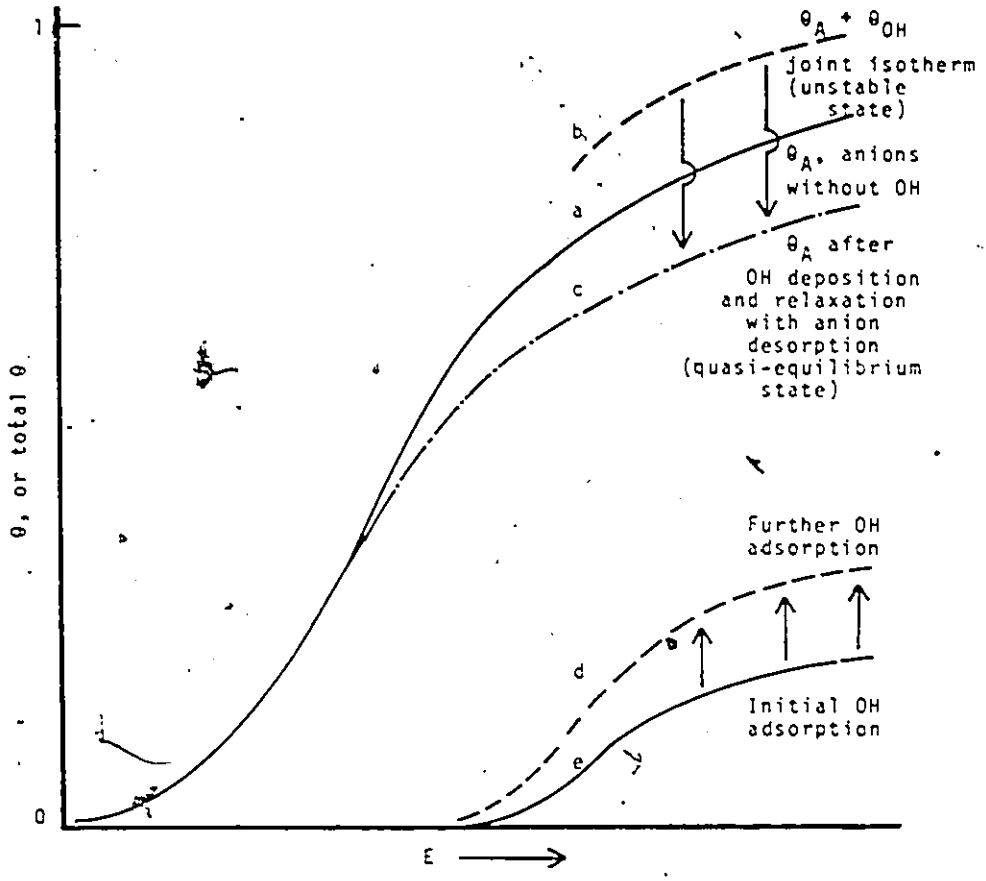

Figure 5.14. Qualitative isotherms, θ vs E, for the relation between adsorbed sulfate and deposited OH and the time-dependent relaxation in the joint isotherm.

and structure of the co-adsorbed OH and anions, in which no true equlibrium situation is achieved.

5.12. Conclusions

1. The initial stages of surface oxidation at Au probably involve OH rather than O species. O species are generated from OH species in the OA4 peak after formation of approximately a monolayer of OH.

2. An electrosorption isotherm for the OA1/OC1 type OH species in 1 M $HClO_4$ can be constructed for conditions in time and potential where the charge associated with this peak is shown experimentally to be almost constant in time.

3. At the earliest times of growth, for $t_h < 0.002$ s, the OH deposition kinetics are sufficiently rapid that the current for the OH electrosorption is iR controlled leading to linear increases of Q_{OH} with time having slopes proportional to potential (Ohmic behavior).

4. A $t_h^{1/2}$ relation for the initial stages of surface oxide growth at Au has been found under certain conditions for the relatively short time range before the well established log t relations set in. These $t_h^{1/2}$ relations were found under several conditions, i.e. different concentrations of H_2SO_4 and temperatures. However, careful examination of the relations between the apparent $t_h^{1/2}$ region and the initial iR-influenced growth and the region where growth takes place logarithmically with time, shows that the $t_h^{1/2}$ region really represents a transition region to logarithmic growth.

   The slopes of these $t_h^{1/2}$ lines, $dQ/d(t_h^{1/2})$, depend linearly on potential, rather than exponentially as would be the case for a charge transfer process displaced from equilibrium. The $t_h^{1/2}$ relation in surface oxide growth may be formally described by either surface diffusion or a rate which is inversely proportional to coverage, $\frac{d\theta}{dt} = k/\theta$, but neither of these explanations is completely satisfactory.

5. The initial stages of surface oxidation at Au involve the following processes:

   a. electrosorption of anions at potentials below the range for OH deposition;

   b. deposition of OH's amongst adsorbed anions (OA1/OC1);

   c. time-dependent desorption of the anions due to the deposition of OH's;

   d. turn-over of the MOH at the surface (OC3 peak in reduction); and

   e. OH's remaining on the surface (OC2 state in reduction).

6. Anion chemisorption involves some charge transfer, so that the negative charge must be regained as the anions desorb from the surface during continued OH deposition.

7. An important relationship exists between coverages and energies of the co-adsorbed anions and OH's, through their associated isotherms, which leads to time-dependent desorption of anions and relaxation of the adsorbed anion layer, especially for sulfate ion, where non-equilibrium conditions are obtained.

CLAIMS TO ORIGINAL RESEARCH

1. It was found that adsorbed F^- has a larger blocking effect on the initial stage of surface oxide formation at Au than ClO_4^-, but not as large that of the sulfate ion, further that the value of the OA2 peak potential in HF is between those at the same sweep-rate for $HClO_4$ and H_2SO_4 electrolytes; hence the relative strengths of adsorption of these anions is SO_4^{2-} (HSO_4^-) > F^- > ClO_4^-.
2. Special techniques were developed using a digital oscilloscope with a computer to allow the precise measurement of very low coverages (down to 0.2 % of a monolayer of OH) with surface oxide after growth periods as short as 0.0002 s.
3. The kinetics of sulfate adsorption in mixed $HClO_4/H_2SO_4$ electrolytes was examined by its blocking effect of surface oxide formation by using a special potential-time program.
4. The role of adsorbed sulfate in the surface oxide formation was studied in mixed $HClO_4/H_2SO_4$ electrolytes with a special potential-time program in which the potential was held at 1.2 V for either 0 s, to minimize sulfate adsorption at the electrode surface ("anions off" situation), or 1 s, to allow near-equilibrium coverage of sulfate ("anions on" situation). This effect was characterized by blocking of the initial peak of anodic I vs E profiles and a diminishing of the formation of species reduced in the OC1 peak in growth-type experiments.
5. The kinetics of the conversion of the initial reversibly generated state of surface oxide to states characterized by reduction in the OC2 and OC3 peaks was investigated in 1 M $HClO_4$ and mixed electrolytes.
6. Surface oxide growth was examined in mixed electrolytes under conditions where anions adsorbed at the electrode surface before surface oxide was grown was minimized ("anions off") or allowed to reach near equilibrium

coverage ("anions on"). The "anions on" growth initially resembled that in H_2SO_4 and that for "anions off" resembled that in $HClO_4$ without H_2SO_4, but during "anions off" growth, time-dependent adsorption of sulfate displaced some of the reversibly generated OH species at the surface, causing a decrease in total surface oxide charge in time.

7. The I vs E profile for the double-layer charging region in mixed $HClO_4/H_2SO_4$ electrolytes, unlike those for 1 M $HClO_4$ and 0.5 M H_2SO_4, was not found to be symmetrical, and the charge associated with the cathodic profile was found to increase with holding time at 1.2 V. This indicates that there is some partial charge transfer during the time-dependent anion adsorption in these mixed electrolytes.

8. It was determined that roughening of Au electrodes using rapid potential cycling occurs only if some turned-over oxide was formed. It was also found that Au is more effectively roughened in H_2SO_4 solution than in $HClO_4$.

9. An isotherm was developed for OH adsorption in 1 M $HClO_4$ under quasi-equilibrium conditions where the coverage of OCl species remains relatively constant with holding time.

APPENDIX I

COMPUTER PROGRAMS

This appendix contains listings of several programs and subroutines that were used in the present work. Since several of the subroutines were not written or only modified by the author, these programs are not considered to be part of the original thesis work and are only included for necessary future reference. These programs were written in either FORTRAN IV or MACRO-11 for use with a Digital PDP-11/34 mainframe computer for the following operations:

A) transfer to the computer and diskette file storage of cyclic-voltammetry data collected on a digital oscilloscope;

B) output of this data to a digital plotter; and

C) integration of this data to obtain charge and coverage information.

A. Oscilloscope Program

The program KNICFL.FOR transfers current vs. potential data from the Nicolet model 2090 III digital oscilloscope to the computer via a Nicolet model 2082 RS-232C serial interface connected between the computer and the VT-55 terminal. This is done by means of D. F. Tessier's versatile SCOPSI subroutine package developed in our laboratory. The transferred data may then be stored on diskettes.

Similar programs for handling other types of experimental data collected on the Nicolet oscilloscope, for example, from potential decay measurements, may be easily implemented by modifing the main program (KNICFL.FOR).

```
      ** KNICFL.FOR **
C
C KNICFL.FOR    VERSION 1        NICOLET DATA FILER
C
C USES DFT'S SCOPSI PACKAGE TO GET I-V DATA OFF THE NICOLET EXPLORER III
C AND STORE IT ON DISK FILES FOR THE PDP 11/34
C
C THE FILES ARE SET UP AS 32 RECORDS OF 128 WORDS.
C 1ST RECORD CONSISTS OF:
C       WORDS 1-50 - FILE ID (100 ASCII CHARACTERS)
C       WORDS 51-52 - ANODIC END POTENTIAL IN VOLTS RHE
C       WORDS 53-54 - RESISTANCE FOR MEASURING CELL CURRENT IN OHMS
C       WORDS 55-56 - SWEEP RATE IN VOLTS/SEC.
C       WORDS 57-128 - NORMALIZATION DATA FROM THE SCOPE(SEE SCOPE MANUAL AND
C                      DOCUMENTATION OF DFT'S SCOPSI)
C RECORDS 2-17 CONTAIN POTENTIAL DATA AND 18-33 CONTAIN CURRENT DATA.
C
C K.A.TELLEFSEN, U OF OTTAWA, DEC. 1982
CZ
        INTEGER IDSTR(50),ILOC,IDATA(4096),INSTD(5,8),IERR,INRES(5,8)
        REAL ANSTD(2,8),ANRES(2,8)
1       TYPE*,'INPUT ILOC'
        TYPE*,'ILOC < 0 - RETREIVE CONTENTS OF SCOPE MEMORY'
        TYPE*,'ILOC = 0 - TRANSFER CONTENTS OF DISK TRACK INDICATED ON'
        TYPE*,'           L.E.D. TO SCOPE MEMORY, THEN RETRIEVE CONTENTS'
        TYPE*,'           OF SCOPE MEMORY.'
        TYPE*,'ILOC =1-8 - TRANSFER CONTENTS OF SELECTED DISK TRACK TO'
        TYPE*,'            SCOPE MEMORY, THEN RETRIEVE CONTENTS OF SCOPE'
        TYPE*,'            MEMORY'
        ACCEPT*,ILOC
        CALL SCOPSI(ILOC,IDATA,INSTD,ANSTD,IERR,INRES,ANRES)
        TYPE*,'IERR/SCOPSI=',IERR
CPUT INTO DISK FILES
        IF(.NOT.IDECID('PUT ON DISK FILES')) GO TO 10
        TYPE*,'INPUT FILE ID - NOT MORE THAN ONE LINE'
        ACCEPT 150,IDSTR
        TYPE*,'INPUT ANODIC END POTENTIAL IN VOLTS RHE'
        ACCEPT*,E
        TYPE*,'INPUT CURRENT MEASURING RESISTOR IN OHMS'
        ACCEPT*,R
        TYPE*,'INPUT SWEEPRATE IN VOLTS/SEC.'
        ACCEPT*,S
        TYPE 100
        CALL ASSIGN(2,,-1,'NEW',,)
        DEFINE FILE 2(33,128,U,NREC)
        NREC=1
        WRITE(2'NREC)IDSTR,E,R,S,INSTD,ANSTD
D       TYPE *,'ID DATA ENTERED'
        DO 3,I=1,2
        DO 3,J=1,4096,256
        WRITE(2'NREC)(IDATA(K),K=J+I-1,J+I+253,2)
D       TYPE *,'SECTION',I,(J-1)/256,'ENTERED'
3       CONTINUE
        CALL CLOSE(2)
10      IF(IDECID('GET MORE DATA'))GO TO 1
100     FORMAT(2X,'INPUT (DEVICE) FILE NAME ->',$)
150     FORMAT(50A2)
        STOP
        END
```

```
      ** SCOPSI.FOR **
C
      SUBROUTINE SCOPSI(ILOC,IDATA,INSTD,ANSTD,IERR,INRES,ANRES)
C
C SCOPSI READS ONE COMPLETE MEMORY FROM THE NICOLET 2090
C DIGITAL OSCILLOSCOPE. IN ADDITION,  STANDARD & RESET
C NORMALIZATION DATA ARE RETURNED.
C
C INPUT PARAMETERS:
C       ILOC - AN INTEGER LOCATION CODE FOR THE TRACK/MEMORY SELECTION
C              ILOC < 0 -RETRIEVE CONTENTS OF SCOPE MEMORY
C              ILOC =0  -TRANSFER CONTENTS OF DISK TRACK INDICATED
C                       ON PANEL L.E.D. TO SCOPE MEMORY, THEN RETRIEVE
C                       CONTENTS OF SCOPE MEMORY(**SCOPE MEMORY CONTENTS
C                       ARE LOST IN THIS PROCESS**)
C              ILOC =1->8  -TRANSFER CONTENTS OF SELECTED DISK TRACK
C                       TO SCOPE MEMORY, THEN RETRIEVE CONTENTS OF
C                        SCOPE MEMORY(**SCOPE MEMORY CONTENTS
C                       ARE LOST IN THIS PROCESS**)
C
C OUTPUT PARAMETERS:
C       IDATA(4096) -THE INTEGER ARRAY IN WHICH THE
C                       UN-NORMALIZED SCOPE MEMORY CONTENTS
C                       WILL BE RETURNED
C       INSTD(5,8) - AN INTEGER ARRAY CONTAINING 5 STANDARD
C                       INTEGER NORMALIZATION VALUES FOR
C                       EACH OF THE 8 POSSIBLE MEMORY PARTS
C       ANSTD(2,8) - A REAL ARRAY CONTAINING 2 STANDARD
C                       REAL NORMALIZATION VALUES FOR
C                       EACH OF THE 8 POSSIBLE MEMORY PARTS
C       IERR - AN ERROR FLAG
C                       IERR=0 -ALL'S HUNKY DORY
C                       IERR=-1 - ILLEGAL VALUE OF ILOC WAS SUPPLIED
C       INRES(5,8) - AN INTEGER ARRAY CONTAINING 5 RESET
C                       INTEGER NORMALIZATION VALUES FOR
C                       EACH OF THE 8 POSSIBLE MEMORY PARTS
C       ANRES(2,8) - A REAL ARRAY CONTAINING 2 RESET
C                       REAL NORMALIZATION VALUES FOR
C                       EACH OF THE 8 POSSIBLE MEMORY PARTS
C
C D.F. TESSIER OTTAWA OCTOBER 1982
C
CZ
      INTEGER IDATA(4096),INSTD(5,8),INRES(5,8)
      REAL ANSTD(2,8),ANRES(2,8)
      BYTE CHAR,IWORK(270)
      IERR=0
C
C$ SUPPRESS CHARACTER ECHOING...
C
      CALL IPOKE('44,'10000.OR.IPEEK('44))    !STOP ECHO
C
CA$ SCOPE STATUS CHECK...
C
71    CALL ENVOIE('^AE3D5^B')
      DO 81 JJ=1,7
82    CHAR=ITTINR()
      IF(CHAR.LT.0)GOTO 82
      IWORK(JJ)=CHAR
81    CONTINUE
D72   WRITE(7,83)(IWORK(IJ),IJ=1,7)
D83   FORMAT(' STATUS CHECK=',5A1,2I5)
D     PAUSE 'AFTER STATUS CHECK'
C     IF(IFLAG.EQ.0)GOTO 61
      IF(IWORK(3).EQ.'@' .OR. IWORK(3).EQ.'P')GO TO 61
      WRITE(7,30)
      WRITE(7,31)             !TYPE OUT ERROR MESSAGE
      WRITE(7,30)
      PAUSE 'TYPE <RETURN> TO TRY AGAIN'
      GOTO 71
```

```
61      IF(IWORK(2).EQ.'6') GOTO 62
        WRITE(7,30)
        WRITE(7,32)             ! TYPE OUT ERROR MESSAGE
        WRITE(7,30)
        PAUSE 'TYPE <RETURN> TO TRY AGAIN'
        GOTO 71
C
CB# MEMORY OR TRACK SELECTION...
C
62      CALL TRKSEL(ILOC,IFLAG)
D       TYPE*,'IFLAG ON RETURN FROM TRKSEL=',IFLAG
D       PAUSE 'AFTER TRKSEL'
        IF(IFLAG.EQ.-1)GOTO 71  !SCOPE STATUS .NE. '@'
        IF(IFLAG.NE.-2)GOTO 63
        IERR=-1                 !INVALID ILOC SUPPLIED
        GOTO 999
C
CA      READ IN & CONVERT MEMORYFUL IN 32 128-ELEMENT CHUNKS...
C
63      DO 11 I=1,32
        IF(I.EQ.1)CALL ENVOIE('^AE3D3D200128^B')
        IF(I.GT.1)CALL ENVOIE('^AE3D200128^B')
        DO 85 II=1,262
86      CHAR=ITTINR()
        IF(CHAR.LT.0)GOTO 86
        IWORK(II)=CHAR
85      CONTINUE
        IF(.NOT.(IWORK(260).EQ.'@' .OR. IWORK(260).EQ.'P'))
        1       GO TO 71
        DO 21 II=1,256,2
        CALL FBTOB(IWORK(II),IDATA(1+(I-1)*128+II/2)) !CONVERSION HERE
21      CONTINUE
11      CONTINUE
D       PAUSE 'AFTER GETTING'
C
CC# STANDARD NORMALIZATION VALUES READ IN & DECODED...
C
        CALL ENVOIE('^AE3N1C0008^B')
        CALL CHERCH(IWORK,236,IFLAG)
        IF(IFLAG.EQ.-1)GOTO 71          !STATUS .NE. '@' OR .NE. 'P'
        CALL DECNOR(IWORK,INSTD,ANSTD)  !DECODED HERE
C
CD# RESET  NORMALIZATION VALUES READ IN & DECODED...
C
        CALL ENVOIE('^AE3N2D0008^B')
        CALL CHERCH(IWORK,236,IFLAG)
        IF(IFLAG.EQ.-1)GOTO 71          !STATUS .NE. '@' OR .NE. 'P'
        CALL DECNOR(IWORK,INRES,ANRES)  !DECODED HERE
C
CE# RESTORE CHARACTER ECHOING & MOVE CURSOR TO NEXT LINE...
C
999     CALL IPOKE('44,'167777.AND.IPEEK('44))
        WRITE(7,16)
16      FORMAT('+')
C
CF# MESSAGES...
C
30      FORMAT(1X,//,50('_'),//)
31      FORMAT(1X,'** ERROR ** ENSURE THAT:',//,
        1 ' 1) STORAGE CONTROL IS IN <HOLD LAST>',/,
        2 ' 2) NO <DISK ACTIVE> OR <DATA ERROR> LED IS ON',/,
        3 ' 3) THE RS232S INTERFACE IS TURNED ON',/,
        4 ' 4) THE <MEMORY> SETTING IS <ALL> AND',/,
        5 '    THE <TRACK SEGMENT> SETTING IS <M.F. CONTROLLED>')
32      FORMAT(1X,'** ERROR ** ENSURE THAT:',//,
        1 ' <MEMORY> SETTING IS <ALL> AND',/,
        2 ' <TRACK SEGMENT> SETTING IS <MAIN FRAME CONTROLLED>')
        RETURN
        END
```

```
      ** TRKSEL.FOR **
C
        SUBROUTINE TRKSEL(ILOC,IFLAG)
C
C       TRKSEL COPIES THE INDICATED TRACK INTO THE SCOPE MEMORY
C               (IF DESIRED)
C       ILOC - AN INTEGER LOCATION CODE FOR THE TRACK/MEMORY SELECTION
C               ILOC < 0 - CONTENTS OF MEMORY DESIRED, TAKE NO ACTION
C               ILOC =0  - CONTENTS OF TRACK INDICALED ON PANEL LED
C                       COPIED TO MEMORY
C               ILOC =1-8 - COPY SELECTED TRACK TO SCOPE MEMORY
C               ILOC > 8  -ILLEGAL LOCATION (ILOC) CHOICE, RETURN PRONTO
C RETURNED VALUES:
C               IFLAG=0 ALL OK
C               IFLAG=-1 STATUS INFO FROM SCOPE .NE. '@' OR .NE. 'P'
C               IFLAG=-2 ILLEGAL ILOC
C
C D.F. TESSIER OTTAWA OCT 1982
C
CZ
        BYTE ISTR(7),ISCRAT(5)
        INTEGER ILOC,IFLAG
        DATA ISTR /'^','A','E','3','R',0,0/
        IFLAG=0
        IF(ILOC.LT.0)RETURN     ! DATA ALREADY IN SCOPE MEMORY
        IF(ILOC.GE.0 .AND. ILOC.LE.8)GO TO 10
        IFLAG=-2        !INVALID ILOC
        RETURN
10      ISTR(6)=48+ILOC         !CONVERT TO ASCII
C
C SEND TO SCOPE...
C
        CALL ENVOIE(ISTR)
C
C GET STATUS & DELIMITER INFO FROM SCOPE...
C
        CALL CHERCH(ISCRAT,4,IFLAG)
        RETURN
        END


      ** ENVOIE.FOR  **
C
        SUBROUTINE ENVOIE(STR)
C
C ENVOIE() SENDS STRINGS TO TT: (I.E. TO THE SCOPE)
C
C       INPUT ARGUMENT:
C               STR -A BYTE STRING OF CHARACTERS TO BE SENT
C                       TO TT: (NOTE: LEN(STR) MUST BE < 26 )
C D.F. TESSIER OTTAWA OCT 1982
C
CZ
        BYTE STR(26)
        ILEN=LEN(STR)
        IF(ILEN.EQ.0)RETURN
        DO 1 I=1,ILEN
        IF(STR(I).NE.'^')GOTO 1
        STR(I)=' '
        STR(I+1)=STR(I+1)-64
        I=I+1
1       CONTINUE
        WRITE(7,3)(STR(I),I=1,ILEN)
3       FORMAT('+',25A1,$)
        RETURN
        END
```

```
      ** CHERCH.FOR **
C
      SUBROUTINE CHERCH(BYTES,NUM,IFLAG)
C
C CHERCH GETS NUM BYTE VALUES FROM TT AND STORES THRM IN
C       THE BYTE ARRAY BYTES(NUM).
C       IFLAG - AN ERROR FLAG  =0 => ALL'S WELL
C                              =-1 => STATUS .NE. '@' OR .NE. 'P'
C
C       WHEN IN USE WITH NICOLET 2090 DIGITAL OSCILLOSCOPE
C       TERMINAL ECHOING SHOULD BE SUPPRESSED BEFORE CALLING CHERCH()
C
C       THE TERMINATION OF THE INCOMING STRING IS ASSUMED
C       TO BE = ...:@<CR><LF> WHERE '@' IS A STATUS CHARACTER
C
C D.F. TESSIER OTTAWA OCT 1982
C
CZ
      BYTE BYTES(NUM)
      INTEGER IFLAG
      IFLAG=-1
      DO 2 I=1,NUM
1     CHAR=ITTINR()
      IF(CHAR.LT.0)GOTO 1
      BYTES(I)=CHAR
2     CONTINUE
      IF(BYTES(NUM-2).EQ.'@' .OR. BYTES(NUM-2).EQ.'P')IFLAG=0
      RETURN
      END


      ** DECNOR.FOR **
C
      SUBROUTINE DECNOR(IWORK,INORM,ANORM)
C
C       -DECODES NORMALIZATION ASCII DATA FROM NICOLET 2090
C        SERIES OSCILLOSCOPE RS-232S INTERFACE.
C
C INPUT PARAMETERS:
C       IWORK(270) - BYTE ARRAY CONTAINING ASCII NORMALIZATION DATA
C
C OUTPUT PARAMETERS:
C       INORM(5,8) - AN I**2 ARRAY TO RECEIVE THE I**2 NORM. DATA
C                (I.E. 5 INTEGERS FOR EACH OF 8 MEMORY SEGMENTS)
C       ANORM(2,8) - A REAL ARRAY TO RECEIVE THE REAL NORM. DATA.
C                (I.E. 2 REAL VALUES FOR EACH OF 8 MEMORY SEGMENTS)
C                SEE PG. XI-23 IN THE OPERATING MANUAL.
C
C D.F. TESSIER OTTAWA OCT 1982
C
      BYTE IWORK(270)
      INTEGER INORM(5,8)
      REAL ANORM(2,8)
C
C DECODING OF NORMALIZATION VALUES FOLLOWS...
C
      DO 45 I=1,8
      INA=(I-1)*29+1  !27 ASCII DATA + <CR><LF> PER SET
      DECODE(1,46,IWORK(INA))INORM(1,I)
      DECODE(1,46,IWORK(INA+1))INORM(2,I)
      DECODE(1,46,IWORK(INA+2))INORM(3,I)
      DECODE(5,47,IWORK(INA+3))INORM(4,I)
      DECODE(5,47,IWORK(INA+8))INORM(5,I)
      DECODE(7,48,IWORK(INA+13))ANORM(1,I)
      DECODE(7,48,IWORK(INA+20))ANORM(2,I)
46    FORMAT(I1)
47    FORMAT(I5)
48    FORMAT(E7.1)
45    CONTINUE
      RETURN
      END
```

```
        ** PBTOB.MAC **
;  CALL PBTOB(BYTS,INT)
;       BYTS IS 2 BYTES IN PRINTABLE BINARY(HI,LO):SEE
;       NICOLET 2090-SERIES OSCILLOSCOPE OPERATING MANUAL,
;       RS-232C INTERFACE SECTION.
;
;       AUTHOR: D.A. HARRINGTON, OTTAWA, OCT 1982.
;
        .PSECT CONVRT,RO,GBL,I,CON,REL
PBTOB:: ADD #2,R5       ;PASS OVER # OF ARGUMENTS
        MOV (R5)+,R2
        MOVB (R2)+,R1   ; GET HI BYTE
        MOVB (R2),R0    ; GET LO BYTE
; KILL PARITY BIT AND ANY EXTENDED SIGN BITS
        BIC #177600,R1
        BIC #177600,R0
; SUBTRACT 32
        SUB #32.,R1
        SUB #32.,R0
; EXTEND SIGN & SHIFT HI BYTE TO CORRECT PLACE
        ASH #10.,R1
        ASH #-4,R1
; ADD ON THE LO BYTE AND TRANSFER TO INT
        ADD R0,R1
        MOV R1,@(R5)
        RETURN
        .END
```

B. **Plotter Program**

The program KLEEHP.FOR and its associated subroutines plots current vs. potential data, which has been previously transferred from the Nicolet digital oscilloscope to the computer, on a Hewlett-Packard model 7470-A digital plotter. The plotter is connected between the computer and the VT-55 terminal by means of a special RS-232 "Y" connector.

The actual data is handled mostly in the relatively short subprograms NEPO (KNEPOA.FOR) and FUNC (KFUNCA.FOR), which set up the data to be plotted and supply data points to the rest of the program, respectively. In this particular program, NEPO opens and reads the desired data file. The rest of the program is used to produce attractive data output. By changing NEPO and FUNC, any data may be plotted, for example, potential vs log time as in potential decay measurements or numerical results calculated from mathematical models.

This program also uses D. A. Harrington's character string manipulation subroutine package, TERM, which has not been included in this appendix.

```
      ** KLEEHP.FOR **
C KLEEHP.FOR    PLOTS DATA FILES ON HP 7470 A GRAPHICS PLOTTER
C USES KLEE SUBROUTINE PACKAGE (HP PLOTTER VERSION), WHICH WAS INFLUENCED
C BY DFT'S PABLO
        TYPE *,'THIS PROGRAM PLOTS X-Y FILES ON THE HP 7470 A PLOTTER'
        TYPE*,'ENSURE THAT THE PLOTTER IS PROPERLY CONNECTED BETWEEN THE'
        TYPE*,'COMPUTOR AND THE TERNMINAL BY THE SPECIAL Y CONNECTOR,'
        TYPE*,'THE DIP SWITCHES ARE PROPERLY SET ( 1 THRU 8  10111010)'
        TYPE*,'AND THE PLOTTER IS SWITCHED ON.'
        TYPE*,'THEN ENTER <RETURN>'
        READ(5,15)KR
15      FORMAT(A2)
C SET UP PDP-11 / PLOTTER HANDSHAKE
        CALL HNDSHK
2       TYPE*,'INPUT ICODE(1-MENU ,2-AUTO)'
        ACCEPT*,ICODE
        IF (ICODE.NE.1.AND.ICODE.NE.2) GO TO 2
        IF(I1.EQ.2) GO TO 6
4       CALL NEPO(NELEM)
6       CALL KLEE(NELEM,ICODE,IERR)
        TYPE*,'IERR=',IERR
        TYPE *,' 1 =      SAME FILE -      SAME PARAMETERS'
        TYPE *,' 2 =      SAME FILE - DIFFERENT PARAMETERS'
        TYPE *,' 3 = DIFFERENT FILE -      SAME PARAMETERS'
        TYPE *,' 4 = DIFFERENT FILE - DIFFERENT PARAMETERS'
        TYPE *,' 5 = FINISHED GRAPHING'
        TYPE *,' WHAT DO YOU WANT?'
        ACCEPT *,I1
        ICODE = 3
        GO TO (6,2),I1
        CALL CLOSE(2)
        GO TO (4,2) I1-2
        STOP 'PROGRAM OVER'
        END
```

```
C*************************************************************************
C HP PLOTTER SUPPORT SUBROUTINES
C THESE SUBROUTINES WERE DEVELOPED FOR INTERFACING THE HP PLOTTER WITH THE
C PDP-11/34 COMPUTOR.
      SUBROUTINE HNDSHK
C THIS SUBROUTINE SETS UP THE XON/XOFF HANDSHAKE PROTOCOL FOR INTERFACING THE
C HP 7470 A PLOTTER WITH THE PDP 11/34 COMPUTOR.  IT HAS NO PARAMETERS.
C THE PLOTTER MUST BE CONNECTED BETWEEN THE COMPUTOR AND THE CRT TERMINAL BY
C THE SPECIAL RS-232 Y CONNECTOR ( P. 10-11  PLOTTER MANUAL ) . THE "DIP"
C SWITCHES ON THE PLOTTER MUST BE SET AS FOLLOWS:
C
C      SWITCH #        ON OR OFF        DETAILS
C
C       1               ON OR OFF        S2 -PARITY SWITCH
C       2               OFF              S1 -NO PARITY
C       3               ON               Y  -EAVESDROP MODE
C       4               ON               US -SET PAPER SIZE
C       5               ON               B4 -NEXT 4 SWITCHES USED TO SET BAUD
C       6               OFF              B3 - RATE TO 9600 AND ONE STOP BIT
C       7               ON               B2 -
C       8               OFF              B1 -
C
C IN THE EAVESDROP MODE, THE PLOTTER IS IN AN "OFF" STATE, THAT IS IT IGNORES
C INFORMATION TO PASS BETWEEN THE COMPUTOR AND THE TERMINAL BUT DOESN'T RESPOND
C TO ANYTHING UNTIL IT RECEIVES A PLOTTER "ON" SIGNAL FROM THE COMPUTOR. AFTER
C IT RECIEVES THIS SIGNAL FROM THE COMPUTOR, IT INTECEPTS ALL INFORMATION FROM
C THE COMPUTOR, NOT ALLOWING IT TO PASS TO THE TERMINAL, AND RESPONDS TO
C APPROPRIATE HP PLOTTER COMMANDS. UPON RECEIVING A PLOTTER "OFF" COMMAND, THE
C PLOTTER RETURNS TO ITS "OFF" STATE.
C
C REF. HP 7470 A GRAPHICS PLOTTER INTERFACING AND PROGRAMMING MANUAL
C
C COPYRIGHT 1984, K.TELLEFSEN, U. OF OTTAWA
CZ
      BYTE ESC,A1,A2
C DEFINE <ESC> AS ASCII 27
      ESC=27
C TURN PLOTTER "ON",SET UP HANDSHAKE AND CHECK FOR INTERFACE ERROR
2     WRITE(7,5)ESC,ESC,ESC,ESC,ESC
5     FORMAT('+',A1,'.Y',A1,'.RIN;',A1,'.I81;;17:'
      1,A1,'.N;19:',A1,'.E',$)
C*************************************************************************
C EXPLAINATION OF PLOTTER COMMAND STRING
C
C  ESC .Y IS THE PLOTTER "ON" SIGNAL
C
C  ESC .R RESETS ALL HANDSHAKE PARAMETERS TO THEIR DEFAULT VALUES
C
C IN      RESETS THE PLOTTER'S GRAPHIC CONDITIONS TO INITIAL POWER ON STATE
C
C  ESC .I SETS UP HANDSHAKE MODE
C      PARAMETERS:
C              81              XOFF SIGNAL IS SENT WHEN BUFFER HAS
C                              81 FREE BYTES LEFT
C
C              "NOTHING"       XON/XOFF HANDSHAKE MODE (DEFAULT)
C
C              17              THE ASCII CHARACTER FOR THE DECIMAL VALUE 17
C                              IS THE XON SIGNAL
C
C <ESC>.N SETS ADDITIONAL HANDSHAKE PARAMETERS
C      PARAMETERS:
C              "NOTHING"       NO INTERCHARACTER DELAY IN HANDSHAKE
C
C              23              THE ASCII CHARACTER FOR THE DECIMAL VALUE 19
C                              IS THE XOFF SIGNAL
C
C <ESC>.E TELLS THE PLOTTER TO SEND RS-232 INTERFACE ERROR CODE
C
C ; AND : ARE TERMINATION CHARACTERS
C
C*************************************************************************
```

```
C
C READ INTERFACE ERROR CODE
        READ(5,10) A1,A2
10      FORMAT(2A1)
C TURN PLOTTER OFF
        WRITE(7,80)ESC
80      FORMAT('+',A1,'.Z')
C <ESC>.Z TURNS PLOTTER OFF
C CHECK INTERFACE ERROR
        IF(A1.EQ.'0') RETURN
C IF NO INTERFACE ERROR (IE ERROR CODE = 0'), RETURN TO MAIN PROGRAM
C DISPLAY INTERFACE ERROR CODE
        WRITE(7,90)A1,A2
90      FORMAT(' PLOTTER RS-232 INTERFACE ERROR = ',2A1)
        TYPE*,'CHECK HP 7470 A GRAPHICS PLOTTER INTERFACING AND
        1 PROGRAMING MANUAL'
        TYPE*,'PAGE 10-27 FOR ERROR CODE MEANING'
        TYPE*,'ENSURE THAT THE DIP SWITCHES ON THE PLOTTER ARE
        1 PROPERLY SET'
        TYPE*,'SWITCH #   : 1 : 2 : 3 : 4 : 5 : 6 : 7 : 8 :'
        TYPE*,'SETTING    : 1 : 0 : 1 : 1 : 1 : 0 : 1 : 0 :'
        TYPE*,'INPUT 1 TO TRY PLOTTER SET UP AGAIN, 2 TO EXIT
        1 PROGRAM'
        ACCEPT*,ANS
        IF(ANS.EQ.1) GO TO 2
        STOP
        END
```

```
      ** HPSEND.FOR **
C HP PLOTTER SUPPORT SUBROUTINES
C
        SUBROUTINE PSEND(STR)
C
C PSEND SENDS STRINGS TO TT: (I.E. TO THE PLOTTER)
C
C       INPUT ARGUMENT:
C               STR -A BYTE STRING OF CHARACTERS TO BE SENT
C                       TO TT: (NOTE: LEN(STR) MUST BE < 40 )
C
C THIS SUBROUTINE FACILLITATES SENDING COMMAND STRINGS TO THE HP PLOTTER
C AS IT IS IMPOSSIBLE TO USE THE <ESC> CHARACTER NEEDED FOR CERTAIN PLOTTER
C COMMANDS WHEN IN THE RS-11 EDITOR, THE CHARACTER ~ IS ENTERED IN ITS STEAD
C AND IS TRANSLATED BY THE SUBROUTINE TO BE ASCII 27 <ESC>.
C
C D.F. TESSIER OTTAWA OCT 1982 (FOR USE WITH NICOLET SCOPE)
C MODIFIED OCT 1984 FOR USE WITH HP 7470 A PLOTTER, K TELLEFSEN
C
CZ
        BYTE STR(40)
C FIND LENGTH OF STRING
        ILEN=LEN(STR)
        IF(ILEN.EQ.0)RETURN
C CHECK STRING FOR ~ CHARACTER
        DO 1 I=1,ILEN
C ~ IS TRANSLATED TO BE <ESC>  ASCII 27
        IF(STR(I).EQ.'~') STR(I)=27
1       CONTINUE
C SEND THE STRING TO THE PLOTTER
        WRITE(7,3)(STR(I),I=1,ILEN)
3       FORMAT('+',39A1,$)
        RETURN
        END
```

```
      ** KNEPOA.FOR **\
C KNEPO.FOR     FILE OPENER FOR DISPLAYING NICOLET FILES ON X-YRECORDER
C
C SEPT 30,1983  WARNING!!!  THIS A STREAMLINED VERSION OF NEPO WHICH ONLY
C ASKS FOR FILE NAMES.  NO SAFETY CHECKS!!!
C
C KNEPO OPENS NICOLET EXPLORER III FILES CREATED BY KNICFL FOR DISPLAY
C ON AN X-Y RECORDER BY KLEE (SEE KLEE.FOR FOR DETAILS)
C
C THE FILES WERE SET UP AS 32 RECORDS OF 128 WORDS.
C 1ST RECORD CONSISTS OF:
C       WORDS 1-50 - FILE ID (100 ASCII CHARACTERS)
C       WORDS 51-52 - ANODIC END POTENTIAL IN VOLTS RHE
C       WORDS 53-54 - RESISTANCE FOR MEASURING CELL CURRENT IN OHMS
C       WORDS 55-56 - SWEEP RATE IN VOLTS/SEC.
C       WORDS 57-128 - NORMALIZATION DATA FROM THE SCOPE(SEE SCOPE MANUAL AND
C                      DOCUMENTATION OF DFT'S SCOPSI)
C RECORDS 2-17 CONTAIN POTENTIAL DATA AND 18-33 CONTAIN CURRENT DATA.
C
C N.A.TELLEFSEN, U OF OTTAWA, DEC. 1982
CZ
      SUBROUTINE NEPO(NELEM)
C SOME PARAMETERS USED:
C       IDSTR   - FILE ID STRING
C       E       - ANODIC END POTENTIAL
C       R       - RESISTANCE
C       S       - SWEEP RATE
C       INSTD   - INTEGRAL NORMALIZATION DATA
C       ANSTD   - REAL NOMALIZATION DATA
C       IPOT    - RAW POTENTIAL DATA
C       ICUR    - RAW CURRENT DATA
CZZ
      INTEGER IDSTR(50),IPOT(2048),ICUR(2048),INSTD(5,8)
      REAL ANSTD(2,8)
      COMMON/SCOPE/E,R,S,XSC,YSC,TPT,DIF,IPOT,ICUR
      NELEM=2048
1     TYPE *,'WARNING!  NO CHECKS, MAKE SURE THIS IS THE RIGHT FILE!'
      TYPE 100
      CALL ASSIGN(2,,-1,'OLD',,)
      DEFINE FILE 2(33,128,U,NREC)
      NREC=1
      READ(2'NREC)IDSTR,E,R,S,INSTD,ANSTD
      DO 3,J=1,2043,128
      NREC=(J-1)/128+2
      READ(2'NREC)(IPOT(K),K=J,J+127)
      NREC=(J-1)/128+18
      READ(2'NREC)(ICUR(K),K=J,J+127)
3     CONTINUE
      XSC=ANSTD(1,1)
      YSC=ANSTD(1,2)
      TPT=ANSTD(2,1)
      TYPE *,'IS THIS THE DATA YOU WANT?'
      TYPE 150,(IDSTR(I),I=1,38)
      TYPE *,'ANODIC END POTENTIAL =',E,'V'
      TYPE *,'R =',R,'OHMS','SWEEPRATE =',S,'V/S'
      TYPE *,'X SCALE= ',XSC,' Y SCALE = ',YSC
      TYPE *,'TIME PER POINT = ',TPT
      CALL CLOSE(2)
100   FORMAT(2X,'INPUT (DEVICE) FILE NAME ->',$)
150   FORMAT(2X,38A2)
170   FORMAT(' ',I4,7X,F6.3,2X,E11.4)
47    RETURN
      END
      INTEGER FUNCTION MAX(IARRAY,NP)
      INTEGER IARRAY(NP)
      MAX=IARRAY(1)
      DO 10,I=2,NP
      IF(IARRAY(I).GT.MAX)MAX=IARRAY(I)
10    CONTINUE
      RETURN
      END
```

```
      ** KFUNCA.FOR **
        REAL FUNCTION FUNC(I,NXORY,NELEM)
        INTEGER IPOT(2048),ICUR(2048)
        COMMON/SCOPE/E,R,S,XSC,YSC,TPT,DIF,IPOT,ICUR
        IF(NXORY.EQ.2)GO TO 20
        FUNC=IPOT(I)*XSC+DIF
        RETURN
20      FUNC=ICUR(I)*YSC/R
        RETURN
        END


      ** KLEE2.FOR **
C SUBROUTINE KLEE(NELEM,ICODE,IERR)
C
C KLEE IS A VERY SLIGHT MODIFICATION OF DFT'S PABLO.
C PABLO GRAPHS POINTS ON AN X-Y RECORDER.
C
C ARGUMENTS:
C       NELEM - THE NUMBER OF ELEMENTS IN THESE VECTORS
C               WHICH ARE TO BE PLOTTED, COUNTING FROM THE
C               FIRST ELEMENT;
C       ICODE - A CONDITION FLAG
C               ICODE=1 - VIEW THE MENU OF GRAPH OPTIONS
C               ICODE=2 - FULLY AUTOMATIC PLOT PARAMETER SELECTION
C               ICODE=3 - USE THE SAME PARAMETERS AS THE LAST TIME
C       IERR - AN ERROR FLAG
C               IERR=0 NO ERRORS
C               IERR=1 INVALID ICODE
C               IERR=2 NELEM IS LESS THAN 1
CZ
        SUBROUTINE KLEE(NELEM,ICODE,IERR)
        INTEGER IPICK(16),IAX(4),ITIK(4)
        COMMON/TIMZZZ/TLOWR,TRAISE,TSETL,TCONTI
        ICOD=ICODE
C ERROR CHECKS:
        IF(.NOT.( (ICOD.LT.1).OR.(ICOD.GT.3)))GO TO 10
        IERR=1          !ICODE .NE. 1 OR 2 OR 3
        GO TO 99        !RETURN
10      IF(NELEM.GE.1)GO TO 20
        IERR=2          !NELEM < 1
        GO TO 99        !RETURN
20      IF(ICOD.EQ.3) GO TO 94
C SET UP TIMES
        TLOWR=0.01
        TRAISE=0.05
        TSETL=0.8
        TYPE*,'INPUT THE CONTINUING TIME (0.01 USUALLY
        1 GOOD)'
        ACCEPT*,TCONTI
        DO 21 I=1,16
        IPICK(I)=1
21      CONTINUE
        IF(ICOD.NE.1)GO TO 50
25      IF(ICOD.EQ.1)CALL GMENU(IPICK)
50      IMODE=IABS(IPICK(2)-2)
C X-SCALE:
        CALL SCALED(IPICK(3),NELEM,'X',XHI,XLO,XTKINC,IERR)
C Y-SCALE:
        CALL SCALED(IPICK(4),NELEM,'Y',YHI,YLO,YTKINC,IERR)
C WHICH AXES?:
        CALL QAXIS(IPICK(5),IAX,IERR)
C WHICH TICKS?:
        CALL QTIKS(IPICK(6),ITIK,IERR)
C ABSOLUTE LENGTH OF AXES...
        CALL ABSIZE(IPICK(9),XWD,YHT,IERR)
C PLOT GRAPH:
94      CALL PLOTXY(NELEM,XHI,XTKINC,XLO,YHI,YTKINC,
        1       YLO,IAX,ITIK,IMODE,IPICK(7),IPICK(8),XWD,YHT)
99      RETURN
        END
```

```
      ** GMENU.FOR **                    (written by D. F. Tessier)
C SUBROUTINE GMENU(IPICK)
C
C GMENU GENERATES A CHOICE TABLE FOR GRAPHING PURPOSES.
C
C ARGUMENTS:
C       IPICK - A 16-ELEMENT INTEGER ARRAY
C               IPICK(1)=0 - HYBRID MANUAL/AUTO SELECTION
C               IPICK(1)=1 - FULLY AUTO
C               IPICK(1)=2 - FULLY MANUAL
C               IPICK(ITEM)=0 - ITEM NOT DESIRED;      FOR MENU ITEMS
C               IPICK(ITEM)=1 - AUTO                   ITEMS 2-8
C               IPICK(ITEM)=2 - MANUAL
C
C REMARKS:1)SEE TEXT OF MENU FOR DETAILS
CZ
        SUBROUTINE GMENU(IPICK)
        BYTE ITT        ! CHOICE POINTERS
        INTEGER IPICK(16)
        CALL SETUP(,,ITT,,)
        NITEMS=9        ! # MENU ITENS
CO SET ALL IPICK(I) INITIALLY TO ZERO.
76      DO 77 I=1,16
77      IPICK(I)=1      ! SET ALL TO AUTO
C3 BELOW: THE MENU IS PRINTED...
67      IF(ITT)CALL INIT
        CALL UPDATE(IPICK,9)
        IF(ITT)CALL PLOTSS(9,0,0)
        WRITE(7,701)
701     FORMAT('+','          PLOTTING OPTIONS MENU   ')
        WRITE(7,702)
702     FORMAT(' ','-------------------------------------')
        WRITE(7,10)
10      FORMAT(1X,'  #   MENU ITEM   :     OPTION      #')
        WRITE(7,803)
803     FORMAT(' ','-------------------------------------')
        WRITE(7,11)
        WRITE(7,110)
        WRITE(7,12)
        WRITE(7,120)
        WRITE(7,13)
        WRITE(7,130)
        WRITE(7,14)
        WRITE(7,140)
        WRITE(7,15)
        WRITE(7,150)
        WRITE(7,16)
        WRITE(7,160)
        WRITE(7,17)
        WRITE(7,170)
        WRITE(7,18)
        WRITE(7,180)
        WRITE(7,19)
        WRITE(7,190)
11      FORMAT(' ','  1 ALL ITEMS     - FULLY AUTO       1')
110     FORMAT(' ','                   - FULLY MANUAL     2')
12      FORMAT(' ','  2 PLOT MODE      - DISCRETE POINT   1')
120     FORMAT(' ','                   - CONTINUOUS       2')
13      FORMAT(' ','  3 X-AXIS SCALE   - AUTO SCALING     1')
130     FORMAT(' ','                   - MANUAL SCALING   2')
14      FORMAT(' ','  4 Y-AXIS SCALE   - AUTO SCALING     1')
140     FORMAT(' ','                   - MANUAL SCALING   2')
15      FORMAT(' ','  5 CHOOSE AXES    - AUTO             1')
150     FORMAT(' ','                   - MANUAL           2')
16      FORMAT(' ','  6 CHOOSE TICS    - AUTO             1')
160     FORMAT(' ','                   - MANUAL           2')
17      FORMAT(' ','  7 ZERO LINE      - AUTO             1')
170     FORMAT(' ','                   - MANUAL           2')
18      FORMAT(' ','  8 WINDOW         - AUTO             1')
180     FORMAT(' ','                   - MANUAL           2')
19      FORMAT(' ','  9 GRAPH SIZE     - AUTO             1')
190     FORMAT(' ','                   - MANUAL           2')
        WRITE(7,708)
708     FORMAT(' ','-------------------------------------')
```

```
C4 BELOW: CHOOSING PROCEDURE IS PRINTED...
        IXPOS=41
        IYPOS=2
        IF(ITT)CALL PLOTSS(9,IXPOS,IYPOS)  !MOVE TO IXPOS,IYPOS
        TYPE*,'SELECTION PROCEDURE:'
        IF(ITT)CALL PLOTSS(9,IXPOS,IYPOS+2)  ! MOVE TO .,.
        TYPE*,'1) KEY IN THE DESIRED ITEM # AND'
        IF(ITT)CALL PLOTSS(9,IXPOS,IYPOS+3)  ! MOVE TO .,.
        TYPE*,'   OPTION # ,THEN PRESS <RETURN>.'
        IF(ITT)CALL PLOTSS(9,IXPOS,IYPOS+5)  ! MOVE TO .,.
        TYPE*,'2)TO ELIMINATE A MENU ITEM,KEY IN'
        IF(ITT)CALL PLOTSS(9,IXPOS,IYPOS+6)
        TYPE*,'  A VALID ITEM # AND CHOICE # = 0'
        IF(ITT)CALL PLOTSS(9,IXPOS,IYPOS+8)  ! MOVE TO .,.
        TYPE*,'3)ITEM# <0 :REPLOT CURRENT TABLE.'
        IF(ITT)CALL PLOTSS(9,IXPOS,IYPOS+10)  ! MOVE TO .,.
        TYPE*,'4)OPTION# < 0 : MENU SESSION OVER.'
        IF(ITT)CALL PLOTSS(9,IXPOS,IYPOS+12)  ! MOVE TO .,.
        TYPE*,'5)ITEM# = OPTION# = 0 :RESTART THE '
        IF(ITT)CALL PLOTSS(9,IXPOS,IYPOS+13)  ! MOVE TO .,.
        TYPE*,'       . MENU SESSION.'
C5 BELOW: PROMPTER -> IS TYPED...
69      IF(ITT)CALL PLOTSS(9,IXPOS,IYPOS+16)  ! MOVE TO .,.
        TYPE*,'-> '
        IF(ITT)CALL PLOTSS(9,IXPOS+3,IYPOS+16)  ! MOVE TO .,.
C6 INPUT MENU SELECTION...
        ACCEPT*,ITEM,IOPT
        IF(ITT)CALL PLOTSS(9,IXPOS,IYPOS+17)  ! MOVE TO .,.
        IF(ITT)CALL PLOTSS(11,,)  ! DELETE TO LINE END
        IF(ITT)CALL PLOTSS(9,IXPOS,23)  ! MOVE TO .,.
        IF(ITT)CALL PLOTSS(11,,)  ! DELETE TO LINE END
C7 ANALYZE ITEM & IOPT HERE...
        IF(ITEM.LT.0)GO TO 67 !REPLOT MENU TABLE
        IF(ITEM.EQ.0 .AND. IOPT.EQ.0)GO TO 76   !RESTART SESSION
        IF(IOPT.LT.0)GO TO 66 !MENU SELECT SESSION OVER
        IF(((ITEM.GE.1).AND.(ITEM.LE.NITEMS)).AND.((IOPT.EQ.1).OR.
       1 (IOPT.EQ.2).OR.(IOPT.EQ.0)))GO TO 72
C8 ERROR MESSAGE...
68      IF(ITT)CALL PLOTSS(9,IXPOS,23)
        TYPE*,'INVALID INPUT: TRY AGAIN'
        GO TO 69
C9 UPDATE PICK(16):
72      IF(ITEM.EQ.1 .AND. IOPT.EQ.1)GO TO 610
        IF(ITEM.EQ.1 .AND. IOPT.EQ.2)GO TO 6201
        IF(ITEM.EQ.1 .AND. IOPT.EQ.0)GO TO 620
        IF(ITEM.NE.1 .AND. IOPT.NE.1)GO TO 630
C HERE IF ITEM.NE.1 & IOPT.EQ.1
        IPICK(ITEM)=IOPT
        GO TO 901
620     DO 621 I=1,16
621     IPICK(I)=0
        GO TO 901
6201    DO 6202 I=1,16
6202    IPICK(I)=2
        GO TO 901
630     IPICK(ITEM)=IOPT
        IPICK(1)=0
        GO TO 901
610     DO 611 I=1,16
611     IPICK(I)=1
901     CALL UPDATE(IPICK,NITEMS)
        GO TO 69
66      IF(ITT)CALL PLOTSS(9,IXPOS,23)  ! MOVE TO .,.
        TYPE*,'MENU SESSION OVER'
        RETURN
        END

        SUBROUTINE UPDATE(IPICK,NITEMS)
C10 UPDATE DISPLAY (VT-55)
        BYTE IDUM1,IDUM2,IBLNK,IPLUS,ITT        ! CHOICE POINTERS
        INTEGER IPICK(16)
        CALL SETUP(,,ITT,,)
901     IF(.NOT.ITT)GO TO 69
        IPLUS='+'
        IBLNK=' '
```

** GUDIES.FOR ** (written by D. F. Tessier)

```
C
C SUBROUTINE GUDIES(YMAX1,YMIN1,BUTMAX,BUTMIN,TIKINT,IERR)
C
C GUDIES REDUCES ESTHETICALLY PLEASING LIMITS FOR GRAPHING
C       REAL-VALUED NUMBERS.
C
C     ( PARAMETERS:
C
C               YMAX - THE USER-SUPPLIED VALUE OF THE LARGEST ELEMENT IN
C                       THE DATA TO BE PLOTTED.
C
C               YMIN - THE USER-SUPPLIED VALUE OF THE SMALLEST ELEMENT IN
C                       THE DATA TO BE PLOTTED.
C
C               BUTMAX - IS THE RESULTING UPPER LIMIT FOR THE PLOT.
C                        (NOTE: BUTMAX IS A BEAUTIFUL NUMBER)
C
C               BUTMIN - IS THE RESULTING LOWER LIMIT FOR THE PLOT.
C                        (NOTE: BUTMIN IS A BEAUTIFUL NUMBER)
C
C               TIKINT - IS THE SUGGESTED 'TICK INTERVAL' FOR THE PLOT.
C                        (NOTE: TIKINT IS A BEAUTIFUL NUMBER)
C
C               IERR - IS AN ERROR FLAG:
C                       IERR=0 NO ERRORS ENCOUNTERED;
C                       IERR=1 YMAX LESS THAN OR EQUAL YMIN. NO ACTION
C                              TAKEN AND CONTROL RETURNED TO CALLING ROUTINE.
C
C       REMARKS:
C               1) GUDIES INCLUDES THE ESPECIALLY BEAUTIFUL
C                  NUMBER 0 IF 0 LIES WITHIN 0.25*(BUTMAX-BUTMIN)
C                  OF EITHER BUTMAX OR BUTMIN.
C               2) IF YMAX1=YMIN1 (OR NELEM=1), THE AUTO FEATURE
C                  USES YMAX=2*YMAX1 &YMIN=0.5*YMIN1 AND THEREFROM
C                  DETERMINES THE BEAUTIFUL NUMBERS BUTMAX & BUTMIN.
C                  IF YMAX1=YMIN1=0 , YMAX IS TAKEN AS 1 & YMIN AS 0
CZ
      SUBROUTINE GUDIES(YMAX1,YMIN1,BUTMAX,BUTMIN,TIKINT,IERR)
      IERR=1
      IF(YMAX1.LT.YMIN1)GO TO 5
      IERR=0
      YMAX=YMAX1
      YMIN=YMIN1
      IF(YMAX.NE.YMIN)GO TO 200
      IF(YMAX.EQ.0)GO TO 69
      YMAX=2*YMAX
      YMIN=0.5*YMIN
      GO TO 200
69    YMAX=1.
      YMIN=0.
200   DELTA=(YMAX-YMIN)*0.25
C IS YMAX1 JUST BELOW  ZERO? IF SO USE YMAX=0 FOR CALCULATION...
      IF((YMAX1.LT.0.).AND.(-YMAX1.LE.DELTA))YMAX=0.
C IS YMIN1 JUST ABOVE  ZERO? IF SO USE YMIN=0 FOR CALCULATION...
      IF((YMIN1.GT.0.).AND.(YMIN1.LE.DELTA))YMIN=0.
C CHOOSE A BEAUTIFUL TICK INTERVAL...
      I=2
7     I=I+1
      FIF=(YMAX-YMIN)/FLOAT(I)
      FACTOR=10.**INTIER(ALOG10(FIF))
      INTTIK=INTIER(FIF/FACTOR)+1
      IF(.NOT.((INTTIK.EQ.1).OR.(INTTIK.EQ.2).OR.(INTTIK.EQ.5)))
     $     GO TO 7
      TIKINT=FACTOR*FLOAT(INTTIK)
      BUTMAX=TIKINT*FLOAT(1+INTIER(YMAX/TIKINT))
      IF(YMAX.EQ.0.)BUTMAX=0.
      BUTMIN=TIKINT*FLOAT(INTIER(YMIN/TIKINT))
5     RETURN
      END
```

```
CB      INTEGER FUNCTION INTIER(I) DOES THE FOLLOWING:
C
C       FOR VAL<0. INTIER(VAL)=INT(VAL)-1
C       FOR VAL=0. INTIER(VAL)=INT(VAL) (=0)
C       FOR VAL>0. INTIER(VAL)=INT(VAL)+1
CY
        INTEGER FUNCTION INTIER(VAL)
        INTIER=INT(VAL)
        IF(VAL.LT.0.)INTIER=INT(VAL)-1
        RETURN
        END


     ** KSCANW.FOR **
CA
C SUBROUTINE SCALER(ICODE,NELEM,ICODE,ICHAR,BUTMAX,BUTMIN,TIKINT,IERR)
C
C SCALER SETS UP SCALE PARAMETERS FOR GRAPHING.
C
C ARGUMENTS:
C       ICODE - A FLAG;
C               ICODE=1 AUTO, NO QUERY. AN IMPRESSIVELY INTELLIGENT CHOICE
C                       OF PARAMETERS IS MADE FOR THE USER.
C               ICODE=2 MANUAL SCALING, QUERY. ADVICE IS OFFERED TO
C                       THE BRAVE-HEARTED , LEST SHE (OR HE) OTHERWISE
C                       MAKE AN ILL-ADVISED CHOICE.
C       NELEM - THE NUMBER OF ELEMENTS, STARTING FROM THE FIRST,
C               TO BE CONSIDERED IN ARRAY VEC.
C       ICHAR - A BYTE VARIABLE, ='X' OR 'Y' TO ACT AS A TAG WHEN USING
C               SCALER(...) TO SCALE A DATA VECTOR.
C       BUTMAX - THE UPPER LIMIT FOR THE GRAPH.
C       BUTMIN - THE LOWER LIMIT FOR THE GRAPH.
C       TIKINT - THE AXIS TICK INTERVAL.
C               (NOTE: BUTMAX,BUTMIN & TIKINT AS RETURNED FROM THE AUTO
C                MODE ARE ALL BEAUTIFUL NUMBERS.)
C       IERR - AN ERROR FLAG
C               IERR=0 - NO ERRORS
C               IERR=1 - INVALID ICODE
C               IERR=2 - ATTEMPT TO FIND MAX. & MIN. VALUES IN VEC
C                       RESULTED IN A MAX. VALUE < MIN. VALUE
C
C REMARKS:1)IN SUBSEQUENT ROUTINES, TIKINT WILL USUALLY BE APPLIED
C            BEGINNING WITH BUTMIN.
C
C (C) D. F. TESSIER AUG. 1982
C       U. OF OTTAWA
C       OTTAWA, CANADA
C
C SCALER REACHES DIZZYING HEIGHTS IN THE QUEST FOR BEAUTIFUL NUMBERS
C FOR GRAPH SCALING BY USING SUBROUTINE GUDIES WHICH IS BASED ON A
C CLEVER AND YET EMMINENTLY USEFUL SUGGESTION COMMUNICATED PRIVATELY
C TO THE AUTHOR BY D.A. HARRINGTON, PH.D.
C
C SCALED IS A MODIFIED SCALER WHICH USES A FUNCTION TO GET POINTS RATHER THAN
C HAVING ARRAYS- THIS IS AN IDEA OF DAH AND DFT.        kat.
CZ
        SUBROUTINE SCALED(ICODE,NELEM,ICHAR,BUTMAX,BUTMIN,
     $       TIKINT,IERR)
        BYTE ICHAR,ITT
        REAL VEC(NELEM)
        CALL SETUP(,,ITT,,)
        IF( (ICODE.EQ.1).OR.(ICODE.EQ.2) )GO TO 10
        IERR=1  !ICODE INVALID
        GO TO 40        !RETURN
10      IERR=0
        NXY=1
        IF(ICHAR.EQ.'Y') NXY=2
        VECMAX=RMAX(NXY,NELEM)
        VECMIN=RMIN(NXY,NELEM)
```

```
17      IF(.NOT.ITT).AND.(ICODE.EQ.2))CALL INIT
11      CALL GUBIES(VECMAX,VECMIN,BUTMAX,BUTMIN,TIKINT,IFAULT)
        IF( IFAULT.NE.1 )GO TO 20
        IERR=2              !VECMAX < VECMIN
        GO TO 40            !RETURN
20      IF(ICODE.EQ.1)GO TO 40
C MANUAL...
        TYPE*,'-------------------------------------------------------'
30      TYPE*,' '
        TYPE*,'    *** MANUAL SCALER ***'
        TYPE*,' '
        WRITE(7,31)ICHAR
31      FORMAT(1X,'THE MAXIMUM AND MINIMUM ',A1,'-DATA VALUES ARE:')
        TYPE*,'MAX=',VECMAX,' MIN=',VECMIN
        TYPE*,' '
        TYPE*,'THE GRAPHICS AUTO-SCALING FEATURE'
        TYPE*,'RECOMMENDS THE FOLLOWING LIMITS:'
        WRITE(7,32)BUTMAX,BUTMIN
32      FORMAT(1X,'UPPER LIMIT=',1PE8.1,' LOWER LIMIT=',1PE8.1)
        WRITE(7,33) ICHAR,TIKINT
33      FORMAT(1X,'RECOMMENDED ',A1,'-AXIS TICK MARK INTERVAL=',1PE8.1)
        TYPE*,' '
        IF(IDECID('ARE THESE VALUES SATISFACTORY')) GO TO 49
        TYPE*,' '
        TYPE*,'** YOU ASKED FOR IT **'
        TYPE*,'INPUT THE UPPER LIMIT,LOWER LIMIT, TICK INTERVAL'
        ACCEPT*,BUTMAX,BUTMIN,TIKINT
        IF( (BUTMAX.GT.BUTMIN).AND.(TIKINT.GT.0).AND.
        $       TIKINT.LE.(BUTMAX-BUTMIN))GO TO 49
        TYPE*,'*ERROR* - TRY AGAIN'
        GO TO 11
49      TYPE*,'-------------------------------------------------------'
        TYPE*,' '
40      RETURN
        END
C
C FUNCTION RMAX(NXY,NELEM) =THE FIRST OCCURRING MAX. VALUE IN ARRAY()
C
        FUNCTION RMAX(NXY,NELEM)
5       RMAX=FUNC(1,NXY,NELEM)
        DO 6 I=2,NELEM
        VAL=FUNC(I,NXY,NELEM)
        IF(VAL.GT.RMAX)RMAX=VAL
6       CONTINUE
20      RETURN
        END
C
C RMIN(NXY,NELEM)= THE FIRST OCCURRING MIN. VALUE IN ARRAY()
C
        FUNCTION RMIN(NXY,NELEM)
5       RMIN=FUNC(1,NXY,NELEM)
        DO 2 I=2,NELEM
        VAL=FUNC(I,NXY,NELEM)
        IF(VAL.LT.RMIN)RMIN=VAL
2       CONTINUE
        GO TO 20
20      RETURN
        END
```

```
      ** KHPLOT.FOR **
C       ************************************************
C       ************ HP 7470 A PLOTTER VERSION ************
C       ************************************************
C
        SUBROUTINE PLOTXY(NELEM,XHI,XTKINC,XLO,YHI,YTKINC,
       #        YLO,IAX,ITIK,IMODE,IZERO,IWIND,XWD,YHT)
C
C THIS VERSION OF SUBROUTINE PLOTXY (KHPLOT) HAS BEEN WRITTEN TO ALLOW
C PLOTTING ON THE HP 7470 A PLOTTER USING THE KLEE GRAPHICS SUBROUTINES
C WITH MINIMAL CHANGES TO THE OTHER SUBROUTINES.
C
C PARAMETERS:
C       NELEM   - THE TOTAL NUMBER OF POINTS IN THE FILE PLOTTED
C       XHI     - THE HIGH X AXIS LIMIT
C       XTKINC  - THE X AXIS TICK INCREMENT
C       XLO     - THE LOW X AXIS LIMIT
C       YHI     - THE HIGH Y AXIS LIMIT
C       YTKINC  - THE Y AXIS TICK INCREMENT
C       YLO     - THE LOW Y AXIS LIMIT
C       IAX     - AN ARRAY CONTAINING 4 AXIS DRAWER FLAGS, 0 = OFF & 1 = ON
C                       IAX(1)  - Y AXIS
C                       IAX(2)  - X AXIS
C                       IAX(3)  - Y BLOCK AXIS
C                       IAX(4)  - X BLOCK AXIS
C       ITIK    - AN ARRAY CONTAINING 4 AXIS TICK DRAWER FLAGS
C                       ITIK(1) - Y AXIS TIK
C                       ITIK(2) - X AXIS TIK
C                       ITIK(3) - Y BLOCK AXIS TIK
C                       ITIK(4) - X BLOCK AXIS TIK
C       IMODE   - PLOT TYPE CONDITION FLAG
C                       IMODE = 0       CONTINUOUS PLOTTING
C                       IMODE = 1       POINT BY POINT PLOTTING
C       IZERO   - ZERO LINE DRAWER CONDITION FLAG, 0 = OFF & 1 = ON
C       IWIND   - DATA WINDOW CONDITION FLAG, 0 = OFF & 1 = ON
C                 THE DATA WINDOW ALLOWS ONLY THOSE POINTS WITHIN THE AXIS
C                 LIMITS TO BE PLOTTED.
C       XWD     - PLOT WIDTH, MUST BE BETWEEN 0 AND 35
C                       ACTUAL PLOT WIDTH = 9 IN. * ( XWD / 35. )
C       YHT     - PLOT HEIGHT, MUST BE BETWEEN 0 AND 25
C                       ACTUAL PLOT HEIGHT = 6 IN. * ( YHT / 25. )
C
C REF. HP 7470 A GRAPHICS PLOTTER INTERFACING AND PROGRAMMING MANUAL
C
C ************************************************************
CZ
        INTEGER ITIK(4),IAX(4)
C DEFINE POINT 1 AND POINT 2 TO BE SENT TO PLOTTER
C POINT 1 GIVES THE LOWER LEFT HAND CORNER OF THE PLOTTING AREA
C IN HP PLOTTER UNITS. (SEE REF.)
        PX1=1000. !     POINT 1 IS (1000.,1000.)
        PY1=1000.
C POINT 2 GIVES THE UPPER RIGHT HAND CORNER OF THE PLOTTING AREA
        PX2=(XWD/35.)*9000.+1000.
        PY2=(YHT/25.)*6000.+1000.
C DEFINE CONVENIENT USER SCALE UNITS BETWEEN POINTS 1 AND 2
        USCX0=0.0       ! MIN. X SCALE IS 0
        USCX1=10000.0   ! MAX. X SCALE IS 10000
        USCY0=0.0       ! MIN. Y SCALE IS 0
        USCY1=10000.0   ! MAX. Y SCALE IS 10000
C TURN PLOTTER 'ON' AND SEND IT THE VALUES OF POINTS 1 AND 2
        CALL PSEND('~.YIP')
        WRITE(7,1000)PX1,PY1,PX2,PY2
C EXPLAINATION OF PLOTTER COMMAND STRING
C       <ESC>.Y         TURN PLOTTER 'ON' ( ~ = <ESC> )
C       IP              INPUT COORDINATES OF P1 AND P2
C
C DEBUGGER, SET UP MONITOR MODE SO WE SEE WHATS WRONG
C       CALL PSEND(';~.@;12:')
        CALL PSEND(';SC')       ! SET UP USER SCALE
        WRITE(7,1000)USCX0,USCX1,USCY0,USCY1
```

```
        CALL PSEND(';IW')       ! INPUT HARD CLIP PLOTTER WINDOW
        WRITE(7,1000)PX1-1,PY1-1,PX2+1,PY2+1
        CALL PSEND(';SP1;~.Z')
C EXPLAINATION OF PLOTTER COMMAND STRING
C       SP1             PICK UP PEN 1
C       <ESC>.Z         TURN PLOTTER 'OFF'
C
C GET THE FIRST AND LAST POINTS IN THE DATA WINDOW
        CALL WINDOW(IWIND,XHI,XLO,YHI,YLO,NP1,NP2,NELEM)
C
C MAPPING FUNCTIONS DEFINED HERE:**********************************
        XMAP(XDUMMY)=(XDUMMY-XLO)/(XHI-XLO)*(USCX1-USCX0)
        YMAP(YDUMMY)=(YDUMMY-YLO)/(YHI-YLO)*(USCY1-USCY0)
C DISPLAY THE FOLLOWING INFORMATION ON THE MONITOR
        TYPE*,'-------------------------------------------------'
        TYPE*,' '
        TYPE*,'    **** GRAPH PARAMETERS (PABLO) ****'
        TYPE*,' '
        TYPE*,'NO. ELEMENTS=',NELEM
        WRITE(7,701)XLO,XHI,XTKINC
701     FORMAT(1X,'X-RANGE FROM ',1PE8.1,'TO ',1PE8.1,' (TIC INCREMENT=',
        +       1PE8.1,')')
        WRITE(7,702)YLO,YHI,YTKINC
702     FORMAT(1X,'Y-RANGE FROM ',1PE8.1,'TO ',1PE8.1,' (TIC INCREMENT=',
        +       1PE8.1,')')
        TYPE*,'X-WIDTH & Y-HEIGHT =',XWD,YHT
        TYPE*,'-------------------------------------------------'
        TYPE*,' '
C
C SET UP PLOTTER FOR X-Y PAIRS
        XM=XMAP(FUNC(NP1,1,NELEM))      ! DEFINE 1ST POINT TO BE PLOTTED
        YM=YMAP(FUNC(NP1,2,NELEM))
C SEND PLOTTER PEN TO 1ST POINT
        CALL PSEND('~.YPA')     ! TURN PLOTTER 'ON' AND PLOT ABSOLUTE
        WRITE(7,1000)XM,YM
        CALL PSEND('PD;')       ! PEN DOWN
        IF(IMODE.EQ.0)GO TO 50  !CONTINUOUS...
        IF(IMODE.EQ.1)GO TO 20  !POINT BY POINT...
        IERR=2
        GO TO 300
C CONTINUOUS:
50      DO 55 I=NP1+1,NP2
C DEFINE POINT TO BE PLOTTED
        XM=XMAP(FUNC(I,1,NELEM))
        YM=YMAP(FUNC(I,2,NELEM))
C IF THE POINT ISN'T WITHIN THE PLOTTING LIMITS, DON'T PLOT IT
        IF(XM.GT.USCX1.OR.XM.LT.USCX0)GO TO 55
        IF(YM.GT.USCY1.OR.YM.LT.USCY0)GO TO 55
C SEND THE POINT TO THE PLOTTER
        WRITE(7,1000)XM,YM
55      CONTINUE
        GO TO 100
C POINT BY POINT:
20      DO 25 I=NP1+1,NP2
C DEFINE POINT TO BE PLOTTED
        XM=XMAP(FUNC(I,1,NELEM))
        YM=YMAP(FUNC(I,2,NELEM))
C IF THE POINT ISN'T WITHIN THE PLOTTING LIMITS, DON'T PLOT IT
        IF(XM.GT.USCX1.OR.XM.LT.USCX0)GO TO 25
        IF(YM.GT.USCY1.OR.YM.LT.USCY0)GO TO 25
C SEND THE POINT TO THE PLOTTER
        CALL PSEND('PU;')       ! PEN UP
        WRITE(7,1000)XM,YM
        CALL PSEND('PD;')       ! PEN DOWN
25      CONTINUE
C DATA PLOTTING COMPLEATED, LIFT PEN TO GET READY FOR AXIS DRAWER
100     CALL PSEND('PU;')
```

```
C*************************************************************
C AXIS DRAWER:*************************************************
C*************************************************************
C Y AXIS:
      IF(IAX(1).NE.1)GO TO 110 ! IS Y AXIS ASKED FOR?
C YES, THEN SEND PEN TO UPPER LEFT HAND CORNER
      WRITE(7,1000)USCX0,USCY1
      CALL PSEND('PD,')        ! PEN DOWN
C DRAW Y AXIS
      WRITE(7,1000)USCX0,USCY0
      CALL PSEND('PU,')        ! PEN UP
C*************************************************************
C X AXIS:
110   IF(IAX(2).NE.1)GO TO 130 ! IS X AXIS ASKED FOR?
C YES, THEN SEND PEN TO LOWER LEFT HAND CORNER.
      WRITE(7,1000)USCX0,USCY0
      CALL PSEND('PD,')        ! PEN DOWN
C DRAW X AXIS
      WRITE(7,1000)USCX1,USCY0
      CALL PSEND('PU,')        ! PEN UP
C*************************************************************
C Y BLOCK AXIS:
130   IF(IAX(4).NE.1) GO TO 150       !IS Y BLOCK AXIS ASKED FOR?
C YES, THEN SEND PEN TO LOWER RIGHT HAND CORNER.
      WRITE(7,1000)USCX1,USCY0
      CALL PSEND('PD,')        !PEN DOWN
C DRAW Y AXIS BLOCK
      WRITE(7,1000)USCX1,USCY1
      CALL PSEND('PU,')        ! PEN UP
C*************************************************************
C X BLOCK AXIS:
150   IF(IAX(4).NE.1)GO TO 180        !IS X BLOCK AXIS ASKED FOR?
C YES, THEN SEND PEN TO UPPER RIGHT HAND CORNER.
      WRITE(7,1000)USCX1,USCY1
      CALL PSEND('PD,')        ! PEN DOWN
C DRAW X BLOCK AXIS
      WRITE(7,1000)USCX0,USCY1
      CALL PSEND('PU,')        ! PEN UP
C*************************************************************
C ZERO LINE DRAWER
180   IF(IZERO.EQ.0.OR.YHI.LE.0.OR.YLO.GE.0) GO TO 200
C IS ZERO LINE ASKED FOR AND Y = 0 WITHIN THE Y AXIS LIMITS?
C YES, THEN DEFINE Y COORDINATE FOR ZERO
      YZERO=YMAP(0)
C SEND PEN TO THE LOWER X AXIS LIMIT AND Y = 0
      WRITE(7,1000)USCX0,YZERO
      CALL PSEND('PD,')        ! PEN DOWN
C DRAW ZERO LINE
      WRITE(7,1000)USCX1,YZERO
      CALL PSEND('PU,')! PEN UP
C*************************************************************
C HATCH MARKER:************************************************
C DEFINE TICK PARAMETERS
200   TLEN=100         ! TICK LENGTH IS 1/10 INCH
      NYTK=(YHI-YLO)/YTKINC+0.5       ! # OF Y AXIS TICK DIVISIONS
      YTLEN=(USCY1-USCY0)/NYTK        ! DEFINE Y TICK INCREMENT
      NXTK=(XHI-XLO)/XTKINC+0.5       ! # OF X AXIS TICK DIVISIONS
      XTLEN=(USCX1-USCX0)/NXTK        ! DEFINE X TICK INCREMENT
C Y AXIS TICKS: ***********************************************
C ARE Y AXIS TICKS ASKED FOR?
      IF(ITIK(1).NE.1) GO TO 220
C YES, THEN DRAW TICKS.
      XTT=USCX0+TLEN
      DO 210 I=1,NYTK-1
C DEFINE TICK POSITION
      YT=USCY0+YTLEN*I
C SEND PEN TO TICK POSITION
      WRITE(7,1000)USCX0,YT
      CALL PSEND('PD,')        ! PEN DOWN
C DRAW TICK
      WRITE(7,1000)XTT,YT
      CALL PSEND('PU,')        ! PEN UP
210   CONTINUE
```

```
C X AXIS TICKS: ***************************************************
C ARE X AXIS TICKS ASKED FOR?
220     IF(ITIK(2).NE.1) GO TO 240
C YES, THEN DRAW TICKS.
        YTT=USCY0+TLEN
        DO 230 I=1,NXTK-1
C DEFINE TICK POSITION
        XT=USCX0+XTLEN*I
C SEND PEN TO TICK POSITION
        WRITE(7,1000)XT,USCY0
        CALL PSEND('PD,')       ! PEN DOWN
C DRAW TICK
        WRITE(7,1000)XT,YTT
        CALL PSEND('PU,')       ! PEN UP
230     CONTINUE
C Y BLOCK AXIS TICKS: *********************************************
C ARE Y BLOCK AXIS TICKS ASKED FOR?
240     IF(ITIK(3).NE.1) GO TO 260
C YES, THEN DRAW TICKS.
        XTT=USCX1-TLEN
        DO 250 I=1,NYTK-1
C DEFINE TICK POSITION
        YT=USCY0+YTLEN*I
C SEND PEN TO TICK POSITION
        WRITE(7,1000)USCX1,YT
        CALL PSEND('PD,')       ! PEN DOWN
C DRAW TICK
        WRITE(7,1000)XTT,YT
        CALL PSEND('PU,')       ! PEN UP
250     CONTINUE
C X BLOCK AXIS TICKS: *********************************************
C ARE X BLOCK AXIS TICKS ASKED FOR?
260     IF(ITIK(4).NE.1) GO TO 300
C YES, THEN DRAW TICKS.
        YTT=USCY1-TLEN
        DO 270 I=1,NXTK-1
C DEFINE TICK POSITION
        XT=USCX0+XTLEN*I
C SEND PEN TO TICK POSITION
        WRITE(7,1000)XT,USCY1
        CALL PSEND('PD,')       ! PEN DOWN
C DRAW TICK
        WRITE(7,1000)XT,YTT
        CALL PSEND('PU,')       ! PEN UP
270     CONTINUE
C TERMINATE PLOT ABSOLUTE COMMAND (;) AND TURN PLOTTER 'OFF'
300     CALL PSEND(';~.Z')
        RETURN
C FORMAT FOR SENDING PAIRS OF REAL NUMBERS TO THE PLOTTER
1000    FORMAT('+',F11.4,',',F11.4,',',$)
        END
```

```
      ** KWIND.FOR **
C DRIVER
C       CALL NEPO(NELEM)
C       TYPE *,' INPUT UPPER & LOWER X & Y LIMITS RESPECTIVELY'
C       ACCEPT*,XH,XL,YH,YL
C       CALL WINDOW(1,XH,XL,YH,YL,NELEM,N1,N2)
C       TYPE *,'STARTING PT. #',N1,'ENDING PT. #',N2
C       STOP
C       END
C KWIND.FOR     WINDOW LIMIT PICKER
C SUBROUTINE WINDOW ALLOWS AUTOMATIC LIMIT PICKING FOR POINT PLOTTING
C IT ALLOWS ONLY THE POINTS(+ OR - 5 %) WHICH ARE FOUND IN THE PLOTTING
C RANGE TO BE PLOTTED.
        SUBROUTINE WINDOW(IW,XHI,XLO,YHI,YLO,N1,N2,NELEM)
        N1=1
        N2=NELEM
        NB=1    ! SET UP INITIAL SEARCH NUMBER
        IF (IW.EQ.0) RETURN
5       DO 10,I=NB,NELEM
D       TYPE *,'1ST',I
        X=FUNC(I,1,NELEM)
        Y=FUNC(I,2,NELEM)
        IF(X.GT.XHI.OR.X.LT.XLO.OR.Y.GT.YHI.OR.Y.LT.YLO) GO TO 10
        N1=I
        GO TO 12
10      CONTINUE
        TYPE *,'**ERROR**       NO WINDOW FOUND'
        TYPE *,'PLOTTING LIMITS SET TO POINT',1,'AND',NELEM
        N1=1
        N2=NELEM
        GO TO 40
12      XHIN=XHI+.05*(XHI-XLO)
        XLON=XLO-.05*(XHI-XLO)
        YHIN=YHI+.05*(YHI-YLO)
        YLON=YLO-.05*(YHI-YLO)
C 5 % NOISE ALLOWANCE
        XX=X    !SET MARKER X VALUE EQUAL TO THAT AT BEGINING OF WINDOW
        NERX=0  !10% OF X FULL SCALE ERROR FLAG IS SET ON
        YY=Y    !SET MARKER Y VALUE EQUAL TO THAT AT BEGINING OF WINDOW
        NERY=0  !10% OF Y FULL SCALE ERROR FLAG IS SET ON
C FIND 2ND LIMIT OF WINDOW
        DO 20,K=N1+1,NELEM
D       TYPE *,'2ND',K
        X=FUNC(K,1,NELEM)
        Y=FUNC(K,2,NELEM)
C IF X VALUE < 10% FULL SCALE DIFFERENT THAN INITIAL X, NERX IS OFF
        IF(ABS(XX-X)*10.GT.XHI-XLO) NERX=1
C IF Y VALUE < 10% FULL SCALE DIFFERENT THAN INITIAL Y, NERY IS OFF
        IF(ABS(YY-Y)*10.GT.YHI-YLO) NERY=1
C IS POINT WITHIN LIMITS + OR - 5% ?
        IF(X.LT.XHIN.AND.X.GT.XLON.AND.Y.LT.YHIN.AND.Y.GT.YLON) GO TO 20
C NO. SO SET END LIMIT.
        N2=K-1
        GO TO 30
20      CONTINUE
        N2=NELEM-1
30      NB=N2+1 ! SET SEARCH NUMBER EQUAL TO END LIMIT + 1
C CONDITIONS FOR AN ACCEPTABLE WINDOW
        IF(NERX.EQ.0.OR.NERY.EQ.0)GO TO 5
C ERROR FLAG FOR 10% F.S. MUST BE OFF
C IF THESE CONDITIONS AREN'T MET, THE SEARCH BEGINS AGAIN
40      RETURN
        END
```

```
      ** QTIKS.FOR **    (written by D. F. Tessier)
CA
C SUBROUTINE QTIKS(ICODE,ITIK,IERR)
C
C QTIKS DETERMINES WHICH TICKS ARE TO BE DRAWN.
C
C ARGUMENTS:
C       ICODE - A FLAG;
C               ICODE=0 NO AXIS TICKS AT ALL
C               ICODE=1 AUTO, NO QUERY. X- & Y-AXIS TICKS ONLY;
C               ICODE=2 MANUAL CHOICE, QUERY.
C       ITIK(4) -INTEGER ARRAY CONTAINING DECISIONS.
C               ITIK(I)=0 - NO TICKS
C               ITIK(I)=1 - TICKS REQUIRED
C               ITIK(1) - Y-AXIS TICKS
C               ITIK(2) - X-AXIS TICKS
C               ITIK(3) - Y-BLOCK TICKS
C               ITIK(4) - X-BLOCK TICKS
C
C       IERR - AN ERROR FLAG.
C               IERR=0 - NO ERRORS
C               IERR=1 - INVALID ICODE
C
CZ
        SUBROUTINE QTIKS(ICODE,ITIK,IERR)
        BYTE ITT
        INTEGER ITIK(4)
C AUTO X- & Y-TICKS ONLY...
        CALL SETUP(,,ITT,,)
        DO 3 I=1,2
        ITIK(I)=1
3       ITIK(I+2)=0
        GO TO (707,70,20),ICODE+1
        IERR=1
        GO TO 70
C  NO TICKS...
707     DO 708 I=1,4
708     ITIK(I)=0
        GO TO 70
C MANUAL...
20      IF(ITT)CALL INIT
        TYPE*,' '
        TYPE*,'-------------------------------------------------------'
        TYPE*,' '
        TYPE*,'*** CHOOSE AXIS TICKS ***'
        TYPE*,' '
        ITIK(1)=0
        ITIK(2)=0
        IF(IDECID('WANT Y-AXIS TICK '))ITIK(1)=1
        IF(IDECID('WANT X-AXIS TICK '))ITIK(2)=1
        IF(IDECID('WANT Y-BLOCK TICK'))ITIK(3)=1
        IF(IDECID('WANT X-BLOCK TICK'))ITIK(4)=1
        IF(.NOT.IDECID('ARE THESE DECISIONS ACCEPTABLE?'))GO TO 20
C       TYPE*,' '
        TYPE*,'-------------------------------------------------------'
        TYPE*,' '
70      RETURN
        END
```

** QAXIS.FOR ** (written by D. F. Tessier)

```
C^
C SUBROUTINE QAXIS(ICODE,IAX,IERR)
C
C QAXIS DETERMINES WHICH AXES ARE TO BE DRAWN.
C
C ARGUMENTS:
C       ICODE - A FLAG;
C               ICODE=0 NO AXES DESIRED
C               ICODE=1 AUTO, NO QUERY. BOX SELECTED;
C               ICODE=2 MANUAL CHOICE, QUERY.
C       IAX(4) -INTEGER ARRAY CONTAINING DECISIONS.
C               IAX(I)=0 - NO AXIS
C               IAX(I)=1 - AXIS REQUIRED
C               IAX(1) - Y-AXIS
C               IAX(2) - X-AXIS
C               IAX(3) - Y-BLOCK
C               IAX(4) - X-BLOCK
C       IERR - AN ERROR FLAG
C               IERR=0 - NO ERRORS
C               IERR=1 - INVALID ICODE
CZ
        SUBROUTINE QAXIS(ICODE,IAX,IERR)
        INTEGER IAX(4)
        IERR=0
C AUTO X- & Y-AXES + X- & Y-BLOCKS...
        DO 3 I=1,4
3       IAX(I)=1
        GO TO (747,70,20),ICODE+1
        IERR=1
        GO TO 70        !RETURN
C
C MANUAL...
20      TYPE*,' '
        TYPE*,'** CHOOSE AXES ***'
        IF(.NOT.IDECID('IS Y-AXIS WANTED?'))IAX(1)=0
        IF(.NOT.IDECID('IS X-AXIS WANTED?'))IAX(2)=0
        IF(.NOT.IDECID('IS Y-AXIS BLOCK WANTED?'))IAX(3)=0
        IF(.NOT.IDECID('IS X-AXIS BLOCK WANTED?'))IAX(4)=0
        GO TO 70
747     DO 748 I=1,4
        IAX(I)=0
748     CONTINUE
70      RETURN
        END
```

```
** KINIT.FOR **\
 SUBROUTINE INIT
 CALL PLOTS5(2,512,)
 CALL PLOTS5(9,0,0)
 CALL PLOTS5(10,,)
 RETURN
 END
```

(written by D. F. Tessier)

```
      ** ABSIZE.FOR **
C SUBROUTINE ABSIZE(ICODE,XWD,YHT,IERR)
C
C ABSIZE DETERMINES THE ABSOLUTE GRAPH SIZE FOR RECORDER OUTPUT(CM)
C
C ARGUMENTS:
C       ICODE - A FLAG
C               ICODE=0 - SAME AS ICODE=1
C               ICODE=1 - SET X-WIDTH=35 CM & Y-HEIGHT =25 CM.
C               ICODE=2 - MANUAL SPECIFICATION OF X-WIDTH & Y-HEIGHT
C       XWD,YHT - THE RESULTING X-WIDTH & Y-HEIGHT
C       IERR - AN ERROR FLAG
C               IERR=0 -NO ERRORS
C               IERR=1 - INVALID ICODE
C
CZ
        SUBROUTINE ABSIZE(ICODE,XWD,YHT,IERR)
        IERR=0
        XLMAX=35.
        YLMAX=25.
        GO TO (45,45,42),ICODE+1
        IERR=1
        GO TO 70          !RETURN
45      XWD=XLMAX
        YHT=YLMAX
        GO TO 70
C
C MANUAL...
42      TYPE*,'*** GRAPH SIZE ***'
        WRITE(7,41)XLMAX,YLMAX
41      FORMAT(1X,'MAXIMUM SIZE: X-WIDTH=',F8.1,
        $       'CM , Y-HEIGHT=',F8.1,'CM.')
        TYPE*,'INPUT X-WIDTH & Y-HEIGHT (CM)'
        ACCEPT*,XWD,YHT
        IF( (XWD.LE.XLMAX).AND.(XWD.GT.0.).AND.(YHT.LE.YLMAX).AND.
        1       (YHT.GT.0.) )GO TO 70
        TYPE*,'UNACCEPTABLE VALUES! TRY AGAIN.'
        GO TO 42
C69     TYPE*,'X-WIDTH & Y-HEIGHT=',XWD,'&',YHT,' (CM) .'
C       IF(.NOT.IDECID('IS THIS SATISFACTORY?') )GO TO 42
70      RETURN
        END
```

(written by D. F. Tessier)

```
      ** IDECID.FOR **
C LOGICAL FUNCTION DECIDE(ISTR)
C 1)TYPES OUT THE MESSAGE STRING ISTR (MAX. 25 CHARACTERS);
C 2) RETURNS .TRUE IF USER ANSWERS YES (Y) TO THE MESSAGE;
C 3)RETURNS .FALSE FOR ANY OTHER INPUT.

        LOGICAL FUNCTION IDECID(ISTR)
        BYTE ISTR(50),PROMT(12)
        DATA PROMT/' ','[','Y',' ','O','R',' ','N',']',' ','?',' '/
12      WRITE(7,100)(ISTR(I),I=1,LEN(ISTR)),PROMT
100     FORMAT('$',80A1)
        READ(5,55)IYN
55      FORMAT(A1)
        IF( IYN.EQ.'N' .OR. IYN.EQ.'Y' )GO TO 109
        GO TO 12
109     IF(IYN.EQ.'Y')GO TO 2
        IDECID=.FALSE.
        GO TO 6
2       IDECID=.TRUE.
6       RETURN
        END
```

C. Integration Program

The program KOC12.FOR calculates charges by integrating cathodic sweep currents with respect to time between two potential limits that are set as input from the keyboard for cyclic-voltammetry data transferred from the Nicolet digital oscilloscope. These charges were used in this work to determine coverages of O-species produced during oxide growth experiments. Appropriate double-layer charges are automatically subtracted during the charge calculation.

```
      ** KOC12.FOR **
C KOC1.FOR      VERSION 2       INTEGRATES NICOLET DATA
C
C       THIS PROGRAM INTGRATES DATA GOTTEN OFF THE NICOLET EXPLORER III USING
C KNICFL (NICOLET DATA FILER).  THE INTEGRATION LIMITS MUST BE SUPPLIED BY THE
C USER.  THE DOUBLE  LAYER CHARGING IS CALCULATED BY INTEGRATING
C A GIVEN FILE CONTAINING DL I-V DATA UP TO SOME MAXIMUM POTENTIAL (USER GIVEN)
C AND BY A GIVEN 'AVERAGE' DL CURRENT ABOVE THIS POTENTIAL. THIS PROGRAM IS
C SPECIFICALLY TAILORED FOR OXIDE GROWTH EXPERIMENTS REQUIRING INTEGRATION OF
C CATHODIC REDUCTION CURVES (ESPECIALLY THE AU 'OC1' EXPERIMENTS) BY MODIFYING
C THE MORE GENERAL KOC1 PROGRAM. IT CAN ONLY BE USED FOR INTEGRATING CATHODIC
C SWEEPS.
CZ
      INTEGER IDSTR(50),INSTD(5,8),IPOT(2048),ICUR(2048),IDSTRD(50),
      1 INSTDD(5,8),IPOTDL(2048),ICURDL(2048)
      REAL ANSTD(2,8),ANSTDD(2,8)
      TYPE *,'SET UP DL CHARGING DATA'
      CALL NICRD(IDSTRD,EDL,RDL,SDL,INSTDD,ANSTDD,IPOTDL,ICURDL)
      TYPE *,'INPUT MAXIMUM POTENTIAL IN VOLTS RHE FOR DL FILE
      1 INTEGRATION.'
      ACCEPT *, EMAX
      TYPE *,'INPUT THE AVERAGE DL CURRENT IN AMPS.'
      ACCEPT *,DLI
      TYPE *,'SET UP OXIDE GROWTH DATA'
1     CALL NICRD(IDSTR,E,R,S,INSTD,ANSTD,IPOT,ICUR)
20    TYPE *,'INPUT POTENTIALS FOR 1ST AND 2ND INTEGRATION LIMITS'
      ACCEPT *,ELIM1,ELIM2
      IF(ELIM1.GT.E.OR.(ELIM1.LT.ELIM2)) GO TO 20
      IEL1=(ELIM1-E+MAX(IPOT,2048)*ANSTD(1,1))/ANSTD(1,1)
      IEL2=(ELIM2-E+MAX(IPOT,2048)*ANSTD(1,1))/ANSTD(1,1)
      QDL=0
      IF(ELIM2.GT.EMAX) GO TO 15
      ELIMD1=ELIM1
      IF(ELIM1.GT.EMAX) ELIMD1=EMAX
      IELDL1=(ELIMD1-EDL+MAX(IPOTDL,2048)*ANSTDD(1,1))/ANSTDD(1,1)
      IELDL2=(ELIM2-EDL+MAX(IPOTDL,2048)*ANSTDD(1,1))/ANSTDD(1,1)
      NNN=0
      DO 40, I=1,2047
      IF(NNN.EQ.1) GO TO 33
      IF(I.GT.2046) GO TO 31
      IF(.NOT.(IELDL1.LE.IPOTDL(I).AND.IELDL1.GE.IPOTDL(I+1).AND.
      1 IPOTDL(I+1).GT.IPOTDL(I+2))) GO TO 40
      LIMDL1=I
      NNN=1
      GO TO 40
33    IF(.NOT.(IELDL2.LE.IPOTDL(I).AND.IELDL2.GE.IPOTDL(I+1))) GO TO 40
      LIMDL2=I
      GO TO 43
40    CONTINUE
```

```
43      DO 90,I=LIMDL1+1,LIMDL2
        QDL=QDL+((ICURDL(I-1)+ICURDL(I))*ANSTDD(1,2)/(2*RDL))*ANSTDD(2,2)
90      CONTINUE
        EMX=EMAX
        GO TO 16
15      IF(ELIM2.GT.EMAX) EMX=ELIM2
16      IF(ELIM1.LT.EMAX) GO TO 17
        QDL=QDL+(DLI*(ELIM1-EMX)/SDL)
17      NN=0
        DO 30, I=1,2047
        IF(NN.EQ.1) GO TO 23
        IF(I.GT.2046) GO TO 31
22      IF(.NOT.(IEL1.LE.IPOT(I).AND.IEL1.GE.IPOT(I+1).AND.IPOT(I+1).GT.
        1       IPOT(I+2))) GO TO 30
        LIM1=I
        NN=1
        GO TO 30
23      IF(.NOT.((IEL2.LE.IPOT(I).AND.IEL2.GE.IPOT(I+1)).OR.(IEL2.GE.
        1       IPOT(I).AND.IEL2.LE.IPOT(I+1)))) GO TO 30
        LIM2=I
        GO TO 32
30      CONTINUE
31      TYPE *,'YOUR LIMITS COULD NOT BE FOUND- TRY AGAIN'
        GO TO 20
32      TYPE *,ELIM1,'= PT # ',LIM1,' AND ',ELIM2,'= PT # ',LIM2
C INTEGRATION
50      Q=0
        ELIM1=((IPOT(LIM1)+IPOT(LIM1+1))/2-MAX(IPOT,2048))*ANSTD(1,1)+E
        ELIM2=((IPOT(LIM2)+IPOT(LIM2+1))/2-MAX(IPOT,2048))*ANSTD(1,1)+E
        DO 60,I=LIM1+1,LIM2
        Q=Q+((ICUR(I-1)+ICUR(I))*ANSTD(1,2)/(2*R))*ANSTD(2,2)
60      CONTINUE
        Q=Q-QDL
        TYPE 150,(IDSTR(I),I=1,38)
        TYPE*,'ANODIC END POTENTIAL =',E,'V'
        TYPE*,'R =',R,'OHMS','SWEEPRATE =',S,'V/S'
        TYPE *,'TIME PER PT = ',ANSTD(2,2)
        TYPE *,'INTEGRATION LIMITS ',ELIM1,' TO ',ELIM2
        TYPE *,'DOUBLE LAYER CHARGE',QDL,' COUL. '
        TYPE *,'OXIDE CHARGE = ',Q,' COUL.'
        IF(IDECID('ANOTHER INTEGRATION-SAME FILE')) GO TO 20
        IF(IDECID('ANOTHER FILE'))GO TO 1
100     FORMAT(' WHAT DO YOU WANT?',$)
150     FORMAT(2X,38A2)
        STOP
        END
```

```
      ** KNICR2.SUB **
C
C KNICRD.FOR    VERSION 1       NICOLET DATA READER
C
C READS FILES CREATED BY KNICFL OF I-V DATA OFF THE NICOLET EXPLORER III
C
C THE FILES ARE SET UP AS 32 RECORDS OF 128 WORDS.
C 1ST RECORD CONSISTS OF:
C       WORDS 1-50 - FILE ID (100 ASCII CHARACTERS)
C       WORDS 51-52 - ANODIC END POTENTIAL IN VOLTS RHE
C       WORDS 53-54 - RESISTANCE FOR MEASURING CELL CURRENT IN OHMS
C       WORDS 55-56 - SWEEP RATE IN VOLTS/SEC.
C       WORDS 57-128 - NORMALIZATION DATA FROM THE SCOPE(SEE SCOPE MANUAL AND
C                       DOCUMENTATION OF DFT'S SCOPSI)
C RECORDS 2-17 CONTAIN POTENTIAL DATA AND 18-33 CONTAIN CURRENT DATA.
C
C K.A.TELLEFSEN, U OF OTTAWA, DEC. 1982
CZ
```

```
      SUBROUTINE NICRD(IDSTR,E,R,S,INSTD,ANSTD,IPOT,ICUR)
C ARGUMENTS:
C       IDSTR   - FILE ID STRING
C       E       - ANODIC END POTENTIAL
C       R       - RESISTANCE
C       S       - SWEEP RATE
C       INSTD   - INTEGRAL NORMALIZATION DATA
C       ANSTD   - REAL NOMALIZATION DATA
C       IPOT    - RAW POTENTIAL DATA
C       ICUR    - RAW CURRENT DATA
CZZ
      INTEGER IDSTR(50),IPOT(2048),ICUR(2048),INSTD(5,8)
      REAL ANSTD(2,8)
1     TYPE 100
      CALL ASSIGN(2,,-1,'OLD',,)
      DEFINE FILE 2(33,128,U,NREC)
      NREC=1
      READ(2'NREC)IDSTR,E,R,S,INSTD,ANSTD
      DO 3,J=1,2048,128
      NREC=(J-1)/128+2
      READ(2'NREC)(IPOT(K),K=J,J+127)
      NREC=(J-1)/128+18
      READ(2'NREC)(ICUR(K),K=J,J+127)
3     CONTINUE
      TYPE *,'IS THIS THE DATA YOU WANT?'
      TYPE 150,(IDSTR(I),I=1,38)
      TYPE*,'ANODIC END POTENTIAL =',E,'V'
      TYPE*,'R =',R,'OHMS','SWEEPRATE =',S,'V/S'
      TYPE*,'NORMALIZATION DATA'
      DO 5,I=1,8
5     TYPE*,(INSTD(J,I),J=1,5),ANSTD(1,I),ANSTD(2,I)
      IF(IDECID('TELL ME')) GO TO 4
      CALL CLOSE(2)
      TYPE *,'GET ANOTHER FILE THEN'
      GO TO 1
4     TYPE*,'INPUT 1 FOR NO DATA OUTPUT'
      TYPE*,'      2 FOR RAW DATA OUTPUT'
      TYPE*,'      3 FOR CALCULATED DATA OUTPUT - E (V RHE),I (AMPS)
      1,C (I/S)'
      ACCEPT*,NQ
      GO TO (47,20,20),NQ
20    INC=1
      IF(IDECID('ABREVIATED DATA (128 PTS)')) INC=16
      TYPE*,' '
      GO TO (47,30,40) NQ
30    TYPE*,'   #  RAW POTENTIAL/RAW CURRENT'
      DO 8,I=1,2048,INC
8     TYPE 160,I,IPOT(I),ICUR(I)
      GO TO 47
40    TYPE*,'   #: POTENTIAL/V:   CURRENT/A:PSEUDOCAP./COUL/V'
      DIF=E-MAX(IPOT,2049)*ANSTD(1,1)
      DO 45,I=1,2048,INC
      POT=IPOT(I)*ANSTD(1,1)+DIF
      CUR=ICUR(I)*ANSTD(1,2)/R
      CAP=CUR/S
45    TYPE 170,I,POT,CUR,CAP
47    CALL CLOSE(2)
100   FORMAT(2X,'INPUT (DEVICE) FILE NAME ->',$)
150   FORMAT(2X,38A2)
160   FORMAT(' ',I4,10X,I5,6X,I5)
170   FORMAT(' ',I4,7X,F6.3,2X,E11.4,2X,E11.4)
      RETURN
      END
      INTEGER FUNCTION MAX(IARRAY,NP)
      INTEGER IARRAY(NP)
      MAX=IARRAY(1)
      DO 10,I=2,NP
      IF(IARRAY(I).GT.MAX)MAX=IARRAY(I)
10    CONTINUE
      RETURN
      END
```

REFERENCES

1. J. Fontenrose, Python, a Study of the Delphic Myth and Its Origins, University of California Press, Los Angelos, (1959); M. Eliade, Patterns in Comparative Religion, Meridian Books, Cleveland, Ohio, (1965)
2. A.W. Adamson, Physical Chemistry of Surfaces, Interscience Publisher, New York, (1968)
3. M.J. Dignam in Comprehesive Treatise of Electrochemistry, Vol. 4, J.O'M. Bockris, B.E. Conway, E. Yeager and R.E. White, editors, Plenum, New York (1981)
4. G. Belanger and A.K. Vijh in Oxides and Oxide Films, Vol. 5, p. 1 - 104, A.K. Vijh, editor, Marcel Dekker, New York (1977)
5. H. Angerstein-Kozlowska, B.E. Conway, B. Barnett and J. Mozota, J. Electroanal. Chem. 100 (1979) 417
6. B.M. Barnett, Ph. D. Thesis, U. of Ottawa (1980)
7. W.B.A. Sharp, Ph. D. Thesis, U. of Ottawa (1976)
8. M.D. Goldshtein, Ts.I. Zalkind, V.I. Veselovskii, Elektrokhim. 8 (1972) 606
9. M.D. Goldshtein, Ts.I. Zalkind, V.I. Veselovskii, Elektrokhim. 9 (1973) 699
10. J.O'M. Bockris and A.K.N. Reddy, Modern Electrochemistry, Vol. 2, Plenum Press, New York (1970)
11. U.R. Evans, The Corrosion and Oxidation of Metals, St. Martins, New York (1960)
12. D.B. Gibbs, B. Rao, R.A. Griffins and M.J. Dignam, J. Electrochem. Soc. 122 (1975) 1167
13. J.A. Mc Millan, Chem. Rev. 62 (1962) 65
14. D.C.W. Kanangara, Ph.D. Thesis, U. of Ottawa (1985)
15. U.F. Frank, Techn. Hochschule Aachem. Get. Werkstoffe Korrosion 14 (1963) 367
16. R. Simpraga and B.E. Conway, J. Electroanal. Chem., in press

17. T.P. Hoar in Modern Aspects of Electrochemistry, Vol. 2, J.O'M. Bockris, editor, Academic Press, New York (1959)

18. I. Young, Anodic Oxide Films, Academic Press, New York, (1961)

19. D.A. Vermilyea in Advances in Electrochemistry and Electrochemical Engineering, Vol. 3, P. Delahay and C.W. Tobias, editors, Interscience, New York (1963)

20. U.R. Evans, Electrochim. Acta 16 (1971) 1825

21. A.K. Vijh, Electrochemistry of Metals and Semiconductors, Marcel Dekker, New York (1973)

22. S.W. Feldberg, C.G. Enke, and C.E. Bricker, J. Electrochem. Soc. 110 (1963) 863

23. A.K.N. Reddy, M.A. Genshaw and J.O'M. Bockris, J. Chem. Phys. 48 (1969) 671

24. D. Gilroy and B.E. Conway, Can. J. Chem. 46 (1968) 875

25. K.J. Vetter and J.W. Schultze, J. Electroanal. Chem. 34 (1972) 131; 141

26. D.Gilroy, J. Electroanal. Chem. 71 (1976) 257

27. D. Dickertmann, J.W. Schultze and K.J. Vetter, J. Electroanal. Chem. 55 (1974) 429

28. M.M. Lohrengel and J.W. Schultze, Electrochim. Acta 21 (1976) 957

29. J.W. Schultze and M.M. Lohrengel, Ber. Busenges. 80 (1976) 552

30. W.E. Reid and J. Kruger, Nature 203 (1964) 402

31. A.C. Macrides, J. Electrochem. Soc. 113 (1966) 1158

32. J.W. Schultze and K.J. Vetter, Ber. Bunsenges. 75 (1971) 470

33. W. Visscher and M.A.V. Devanathan, J. Electroanal. Chem. 8 (1964) 127

34. J.L. Ord and F.C. Ho, J. Electrochem. Soc. 118 (1971) 46

35. A. Damjanovic, A.T. Ward, B. Ulrich and M. O'Jea, J. Electrochem. Soc. 122 (1975) 471

36. A. Damjanovic and L.-S.R. Yeh, J. Electrochem. Soc. 126 (1979) 555

37. L.B. Harris and A. Damjanovic, J. Electrochem. Soc. 122(1975) 593

38. A. Damjanovic, L.-S.R. Yeh and J.F. Wolf, J. Electrochem. Soc. 127 (1980) 1945, 1951

39. M.A.H. Lanyon and B.M.W. Trapnell, Proc. Roy. Soc. A227 (1955) 387

40. G. Tammann and W. Koster, Z. Anorg. Chem. 123 (1922) 196

41. N. Cabrera and N.F. Mott, Rep. Prog. Phys. 12 (1948) 163; N.F. Mott, Trans. Faraday Soc. 36 (1940) 472

42. E. Yeager and J. Kuta in Physical Chemistry: an Advanced Treatise, V. 91, ch. 4, H. Eyring, Henderson and Jost, editors, Academic Press, New York (1970)

43. B.E. Conway and H. Angerstein-Kozlowska, Acc. Chem. Res. 14 (1981) 49

44. B.E. Conway and H. Angerstein-Kozlowska, National Bureau of Standards Special Publication 455 (1976) 107

45. B.E. Conway, H. Angerstein-Kozlowska and F.C. Ho, J. Vac. Sci. Technol. 14 (1977) 351

46. A. Sevcik, Coll. Czech. Chem. Comm. 13 (1948) 349

47. F.G. Will and C.A. Knorr, Z. Electrochem. 64 (1960) 258

48. F.P. Bowden and E.K. Rideal, Proc. Roy. Soc. A120 (1928) 59; Ibid. 80; A126 (1929) 107

49. A. Slygin and A.N. Frumkin, Acta Physiochim URSS 3 (1935) 791

50. J.A.V. Butler and J. Pearson, Trans. Fara. Soc. 34 (1938) 1163

51. J.A.V. Butler and G. Drever, Trans. Fara Soc. 32 (1936) 426

52. A. Hickling, Trans. Fara. Soc. 38 (1942) 27

53. H.A. Kozlowska, B.E. Conway and W.B.A. Sharp, J. Electroanal. Chem. 43 (1973) 9

54. H. Angerstein-Kozlowska, J. Klinger and B.E. Conway, J. Electroanal. Chem. 75 (1977) 45, 61

55. H. Angerstein-Kozlowska, B.E. Conway and J. Klinger, J. Electroanal. Chem. 87 (1978) 301, 321

56. J. Klinger, Ph.D. Thesis, U. Of Ottawa, (1976)

57. B.E. Conway, E. Gileadi and M. Dziechiuch, Electrochim. Acta 8 (1963) 143

58. B.E. Conway and E. Gileadi, Can. J. Chem. 42 (1964) 90

59. H. Angerstein-Kozlowska and B.E. Conway, J. Electroanal. Chem. (1976)

60. M. Sotto, J. Electroanal. Chem. 69 (1976) 229; 70 (1976) 291; 72 (1976) 287

61. N.R. de Tacconi, J.O. Zerbino, M.E. Folquer and A.J. Arvia, J. Electroanal. Chem 85 (1977) 213

62. C.M. Ferro, A.J. Calandra and A.J. Arvia, J. Electroanal. Chem. 50 (1974) 403; 55 (1974)291; 59 (1975) 239

63. R. Cordova O., M.E. Martins and A.J. Arvia, J. Electrochem. Soc. 126 (1979) 1172; Electrochim. Acta 24 (1979) 469, 25 (1980) 453

64. M.E. Martins, R. Cordova and A.J. Arvia, Electrochim. Acta 26 (1981) 1547

65. M.I. Florit, M.E. Martins and A.J. Arvia, J. Electroanal. Chem. 151 (1983) 209

66. L.D. Burke and M. McRann, J. Electroanal. Chem. 125 (1981) 387

67. L.D. Burke, M.M. McCarthy and M.B.C. Roche, J. Electroanal. Chem. 167 (1984) 291

68. L.D. Burke, M.I. Casey, V.J. Cunnane, O.J. Murphy and T.A.M. Twomey, J. Electroanal. Chem. 189 (1985) 353

69. L.D. Burke, M.E. Lyons and D.P. Whelan, J. Electroanal. Chem. 139 (1982) 131

70. E. Yeager, Surf. Sci. 101 (1980) 1

71. J.D.E. McIntire in Advances in Electrochemistry and Electrochemical Engineering, Vol 9., R.H. Mueller, editor, Wiley, New York, 1973

72. G. Blondeau and E. Yeager, Prog. Solid State Chem., 11 (1976) 153

73. D.M. Kolb in Advances in Electrochemistry and Electrochemical Engineering, Vol 11., H. Gerisher and C.W. Tobias, editors, Wiley, New York, 1973

74. B.D. Cahan and R.F. Spanier, Surf. Sci. 16 (1969) 166

75. B.D. Cahan, Surf. Sci. 56 (1976) 354

76. R. Greef, J. Chem. Phys. 51 (1969) 3148

77. B.E. Conway, Symp. Fara. Soc. 4 (1970) 95

78. B.E. Conway and S. Gottesfeld, J. Chem. Soc. Faraday Trans. I 69 (1973) 1090

79. S. Gottesfeld, M. Babai and B. Reichman, Surf. Sci. 56 (1976) 373

80. W.E. Reid and J. Kruger, Nature 203 (1964) 402

81. R.S. Sirohi and M.A. Genshaw, J. Electrochem. Soc. 116 (1969) 910

82. T. Takamura, K. Takamura, W. Nippe and E. Yeager, J. Electrochem. Soc. 117 (1970) 626

83. C. Nguyen Van Huong, C. Hinnen, J. Lecoeur and R. Parsons, J. Electroanal. Chem. 92 (1978) 239; C. Hinnen, C. Nguyen Van Huong, A. Rousseau and J.P. Dalbera, J. Electroanal. Chem. 106 (1980) 175; C. Nguyen Van Huong, C. Hinnen and J. Lecoeur, Ibid. 185

84. W. Boeck and D.M. Kolb, Surf. Sci. 118 (1982) 613

85. S.H. Lui, C. Hinnen, C. Nguyen Van Huong, N.R. De Tacconi and K.M. Ho, J. Electroanal. Chem. 176 (1984) 325

86. A. Otto, Surf. Sci. 101 (1980) 99

87. F. Abeles, T. Lopez-Rios and A. Tadjeddine, Solid State Commun. 16 (1975) 843

88. F. Chao, M. Costa and A. Tadjeddine, J. Physique C5 (1977) 97

89. F. Chao, M. Costa, A. Tadjeddine, F. Abeles, T. Lopez-Rios and M.L. Theye, J. Electroanal. Chem. 83 (1977) 65

90. A. Tedjeddine, J. Electroanal. Chem. 169 (1984) 129

91. W. Schultze, Electrochim. Acta 17 (1977) 451

92. B. Pettinger, U. Wenning and H. Wetzel, Surf. Sci. 101 (1980) 742; U. Wenning, B. Pettinger and H. Wetzel, Chem. Phys. Lett. 70 (1980) 49

93. I. Pockrand, Chem. Phys. Lett. 85 (1982) 37

94. C.C. Busby and J.A. Creighton, J. Electroanal. Chem. 140 (1982) 379

95. P.R. Griffiths, Chemical Infrared Fourier Transform Spectroscopy, Wiley-Interscience, N.Y. (1975)

96. P.R. Griffiths in Analytical Applications of FT-IR to Molecular and Biological Systems, NATO Advanced Study Institute, Florence (1980), J.R. Durig, D. Reidel, editors, Dordrecht, Holland

97. A. Bewick and K. Kunimatsu, Surf. Sci. 101 (1980) 131

98. J.W. Foley, C. Korzeniewski, J. Daschbach, and S. Pons, in Electroanalytical Chemistry, Vol. 14, A.J. Bard, editor, Marcel Dekker, New York (1987)

99. H.Masuda, A. Fujishima and K. Honda, Bull. Chem. Soc. Jap. 53 (1980) 1542

100. A. Fujishima, H. Masuda and K. Honda, Chemistry Letters (Chem. Soc. Jap.) (1979) 1063

101. A. Fujishima, H. Masuda, K. Honda and A.J. Bard, Anal. Chem. (1980) 52 682

102. T. Watanabe and H. Gerisher, J. Electroanal. Chem. 117 (1981), 185; 122 (1981) 73

103. G. Horanyi, Electrochim. Acta 25 (1980) 43

104. G. Horanyi, J. Solt and F. Nagy, J. Electroanal. Chem. 31 (1971) 95; G. Horanyi and E.M. Rizmayer, J. Electroanal. Chem. 36 (1972) 496; G. Horanyi, E.M. Rizmayer and G. Inzelt, J. Electroanal. Chem. 93 (1978) 93; G. Horanyi and E.M. Rizmayer, Electrochim. Acta 30 (1985) 923

105. G. Horanyi, E.M. Rizmayer and P. Joo, J. Electroanal. Chem. 152 (1983) 211

106. G. Horanyi and E.M. Rizmayer, J. Electroanal. Chem. 165 (1984) 288

107. H. Shimizu, Electrochim Acta. 13 (1968) 27, 45, 55

108. W.N. Hansen, Surf. Sci. 16 (1969) 205

109. D.L. Rath, Ph.D. Thesis, Utah State University (1979)

110. R.I. Tucceri and D. Posadas, J. Electroanal. Chem. 191 (1985) 387

111. W.N. Hansen, Surf. Sci. 101 (1980) 109

112. S. Bruckenstein and M. Shay, J. Electroanal. Chem. 188 (1985) 131

113. W.N. Hansen, C.L. Wang and T.W. Humpreys, J. Electroanal. Chem. 90 (1978) 137; 90 (1978) 87

114. D.M. Kolb and W.N. Hansen, Surf. Sci. 79 (1979) 205

115. W.N. Hansen and D.M. Kolb, J. Electroanal. Chem. 100 (1979) 493

116. A.T. Hubbard, R.M. Ishikawa and J. Katekaru, J. Electroanal. Chem. 86 (1978) 271

117. P.N. Ross, Surf. Sci. 102 (1981) 463

118. M. Sumino and S. Shibata, Denki Kagaku 44 (1976) 425

119. M. Peukert and H.P. Bonzel, Surf. Sci. 145 (1984) 239

120. K.S. Kim, N. Winograd and R.E. Davis, J.A.C.S. 93 (1971) 6296

121. J.S. Hammond and N. Winograd, J. Electroanal. Chem., 78 (1977) 55

122. G.C. Allen, P.M. Tucker, A. Capon and R. Parsons, J. Electroanal. Chem. 50 (1974) 335

123. T. Dickinson, A. Povey, P.M.A. Sherwood, J. Chem. Soc., Fara. Trans. I 71 (1975) 298

124. L. Kover, C.S. Ujhelyi, D. Berenyi, D. Varga, I. Kadar, A. Kover and J. Miller, J. Electron Spectrosc. Relat. Phenom. 14 (1978) 201

125. M. Peuckert, F.P. Coenen and H.P. Bonzel, Electrochim. Acta 29 (1984) 1305

126. E. Rach and J. Heitbaum, Electrochim Acta 31 (1986) 477

127. W.N. Hansen, D.M. Kolb, D.L. Rath and R. Wille, J. Electroanal. Chem. 110 (1980) 369

128. D. Scherson, S. Krause and D.M. Kolb, J. Electroanal. Chem. 176 (1984) 363

129. H. Neff and E.R. Kotz, J. Electoanal. Chem. 151 (1983) 305

130. E.R. Kotz, H. Neff and K. Muller, J. Electroanal. Chem. 215 (1986) 331

131. D.L. Rath and D.M. Kolb, Surf. Sci. 109 (1981) 641

132. G.J. Hansen and W.N. Hansen, J. Electroanal. Chem. 150 (1983) 193

133. B.V. Tilak, H. Angerstein-Kozlowska and B.E. Conway, J. Electroanal. Chem. 148 (1973) 1

134. J.W. Schultze and K.J. Vetter, J. Electroanal. Chem. 43 (1973) 63

135. D.H. Everett and W.I. Whitton, Trans. Fara. Soc. 48 (1952) 749

136. C.M. Quinn and M.W. Roberts, Trans. Fara. Soc. 60 (1964) 899; M.W. Roberts and B.R. Wells, Disc. Fara. Soc. 41 (1966) 162; Surf. Sci. 15 (1969) 325

137. E.J. Rudd and B.E. Conway in Comprehensive Treatise of Electrochemistry, Vol. 7, B.E. Conway, J.O'M. Bockris, E. Yeager, S.U.M. Khan and R.E. White, editors, Plenum, New York (1983)

138. P. Stonehart, H.A. Kozlowska and B.E. Conway, Proc. Roy. Soc. A 310 (1969) 541

139. N. Sato and M. Cohen, J. Electrochem. Soc. 111 (1964) 512, 519, 624

140. S. Schuldiner and T.B. Warner, J. Electrochem. Soc. 112 (1965) 212; T.B. Warner and S. Schuldiner, ibid. 853; S. Schuldiner, T.B. Warner and B.J. Piersma, J. Electrochem. Soc. 114 (1967) 343

141. S.H. Cadle and S. Bruckenstein, Anal. Chem. 46 (1974) 16

142. D.C. Grahame, Chem. Rev. 41 (1947) 441

143. G.M. Schmid and M.E. Curley-Fiorino in Encyclopedia of Electrochemistry of the Elements, Vol. 4, A.J. Bard, editor, Marcel Dekker, New York (1975)

144. A. Hamelin, T. Vitanov, E. Sevastyanov and A. Popov, J. Electroanal. Chem. 145 (1983) 225

145. B.E. Conway, H. Angerstein-Kozlowska and W.B.A. Sharp, Z. Phys. Chem. Neue Folge 98 (1975) 61

146. A. Clark, The Chemisorptive Bond, Academic Press, New York (1974)

147. S. Levine, G.M. Bell and D. Calvert, Can J. Chem. 40 (1964) 518

148. Khr.Iv. Noninski and E.M. Lazarova, Electrokhimiya 9 (1973)

149. G. Valette, J. Electroanal. Chem. 122 (1981) 285

150. A. Hamelin, J. Electroanal. Chem. 138 (1982) 395

151. A. Hamelin and A. Le Lan, C.R. Acad. Sci. (Paris) C295 (1982) 161

152. A. Hamelin, Z. Borkowska and J. Stafiej, J. Electroanal. Chem. 189 (1985) 85

153. G. Valette, A. Hamelin and R. Parsons, Z. Phys. Chem. Neue Folge 113 (1978) 71

154. A. Hamelin, J. Electroanal. Chem. 142 (1982) 299

156. J. Lipkowski, C. Nguyen Van Huong, C. Hinnen, R. Parsons and J. Chevalet, J. Electroanal. Chem. 143 (1983) 396

157. V.S. Bagotsky, Y.B. Vassilyev, J. Weber and J.N. Pirtskhalova, J. Electroanal. Chem. 27 (1970) 31

158. M.V. Breiter, Electrochim. Acta 8 (1963) 925

159. B.E. Conway and D.M. Novak, J. Chem. Soc., Fara. Trans. I 75 (1979) 2454; D.M. Novak and B.E. Conway, ibid. 77 (1981) 2341

160. A.N. Frumkin, Z. Phys. Chem. 35 (1926) 792; 164 (1933) 121

161. R. Parsons, J.Electroanal. 21 (1969) 35

162. W.R. Fawcett and S. Levine, J. Electroanal. Chem. 84 (1977) 303

163. S. Sathyanaryana, J. Electroanal. Chem. 50 (1974) 195

164. R. Guidelli, J. Electroanal. Chem. 53 (1974) 205; 74 (1976) 347

165. F.T. Wagner and T.E. Moylan, Surf. Sci. 182 (1987) 125

166. K. Bange, T.E. Madey, J.K. Sass and E.M. Stuve, Surf. Sci. 183 (1987) 334; K. Bange, K.J. Sass and R. Parsons, to be published

167. B.E. Conway, Elektrokhimiya 13 (1977) 822; J. Electroanal. Chem. 65 (1975) 491

168. D.M. Kolb and J. Schneider, Electrochim. Acta 31 (1986) 929

169. J. Lecoeur, J. Andro and R. Parsons, Surf. Sci. 114 (1982) 320

170. A.S. Homa, E. Yeager and B.D. Cahan, J. Electroanal. Chem. 150 (1983) 181

171. D.M. Kolb, G. Lehmpfuhl and M.S. Zei, J. Electroanal. Chem. 179 (1984) 289; D.M. Kolb and J. Schneider, Surf. Sci. 162 (1985) 764

172. J. Lecouer, J. Andro and R Parsons, Surf. Sci. 114 (1982) 320

173. M. Bacchetta, A. Francesconi, S. Trassati, L. Duubova and A. Hamelin, J. Electroanal. Chem. 218 (1987) 355

174. J.E.B. Randles and K.S. Whiteley, Trans. Fara. Soc. 52 (1956) 1509

175. A. Hamelin, L. Stoicoviciu and F. Silva, Electrochem. Soc. Meeting, Toronto, 1985

176. A. Hamelin, J. Electroanal. Chem. 210 (1986) 303

177. U.A. Esin and B.E. Markov, Acta Psysicochem. U.S.S.R. 10 (1939) 353

178. J. Clavilier and C. Nguyen Van Huong, J. Electroanl. Chem 80 (1977) 101

179. A.G. Zelinski, R.Yu. Beck, A.I. Makurin and S.D. Abdulov, Elektrokhimia 14 (1978) 1740

180. F.G. Will, J. Electrochem. Chem. 112 (1965) 451

181. K. Yamamoto, D.M. Kolb, R. Kotz and G. Lehmpfuhl, J. Electroanal. Chem. 96 (1979) 133

182. R.R. Adzic, W.E. O'Grady and S. Srinivasan, Surf. Sci. 94 (1980) L191

183. E. Yeager, W.E. O'Grady, M.Y.C. Woo and P. Hagen, J. Electrochem. Soc.

184. A.T. Hubbard, J. Electroanal. Chem. 86 (1978) 271

185. P.N. Ross, J. Electroanal. Chem. 76 (1977) 139

186. J. Clavilier, R. Faure, G. Guinet and R. Durand, J. Electroanal. Chem. 107 (1980) 205

187. C.L. Scortichini and C.N. Reilly, J. Electroanal. Chem. 139 (1982) 247

188. F.T. Wagner and P.N. Ross, J. Electroanal. Chem. 150 (1983) 141

189. A.S. Homa, E. Yeager and B.D. Cahan, J. Electroanal. Chem. 150 (1983) 181

190. J.P. Bellier, J. Lecoeur and A. Rousseau, J. Electroanal. Chem. 200 55

191. A. Hamelin and M. Sotto, C.R. Acad. Sci. Paris C271 (1970) 609

192. M. Sotto, C.R. Acad. Sci. Paris C274 (1972) 1776

193. M. Sotto, C.R. Acad. Sci. Paris C276 (1973) 141

194. H. Angerstein-Kozlowska, B.E. Conway, A. Hamelin and L. Stoicovciu, Electrochim. Acta 31 (1986) 1051

195. H. Angerstein-Kozlowska, B.E. Conway, A. Hamelin and L. Stoicovciu, to be published

196. M.A. Van Hove, R.J. Koestner, P.C. Stair, J.P. Biberian, L.L. Kesmodel, I. Bartos and G.A. Somorjai, Surf. Sci. 103 (1981) 189, 218

197. D.G. Fedak, J.V. Florio and W.D. Robertson in The Structure and Chemistry of Solid Surfaces, G.A. Somorjai, editor, Wiley, New York (1969)

198. G. Ertl, Surf. Sci. 152/153 (1985) 328

199. S. Motoo and N. Furuya, J. Electroanal. Chem. 167 (1984) 309

200. S. Hadzi-Jordanov, H. Angerstein-Kozlowska and B.E. Conway, J. Electrochem. Soc. 125 (1978) 1471

201. A. Damjanovic, L.-S.R. Yeh and J.F. Wolf, J. Electrochem. Soc. 129 (1982) 55

202. K.S. Kim, C.D. Sell and N. Winograd in Proc. Electrocatalysis, Electrochem. Soc., M.W. Breiter, editor, (1974) 242

203. D.A.J. Rand and R. Woods, J. Electroanal. Chem. 31 (1971) 29

204. H.A. Laitinen and M.S. Chao, J. Electrocnem. Soc. 108 (1961) 726

205. S.B. Brummer and Makrides, J. Electrochem. Soc. 111 (1964) 1122

206. M. Peuckert, F.P. Coenen and H.P. Bonzel, Surf. Sci. 141 (1984) 515

207. F. Jirsa and O. Buryanek, Z. Elektrochem. 29 (1923) 126; F. Jirsa and H. Jelinek, Z. Elektrochem. 30 (1924) 286

208. Davis and G. Somorjai, Surf. Sci. 91 (1980) 73

209. R.W. McCabe and D. Schmidt, Surf. Sci. 60 (1976) 85, Surf. Sci. 65 (1977) 189

210. S. Evans, J. Peilaszek and J.M. Thomas, Surf. Sci. 56 (1976) 644

211. H. Niehus and G. Comsa, Surf. Sci. 93 (1980) L147

212. T. Matsushima, D.B. Almy and J.M. White, Surf. Sci. 67 (1977) 89

213. C.R. Helms, H.P. Bonzel and S. Kelemen, J. Chem. Phys. 65 (1976) 1773

214. R. Ducros and R.P. Merrill, Surf. Sci. 55 (1976) 227

215. C.E. Smith, J.P. Biberian and G. Somorjai, J. Catal. 57 (1979) 426

216. D.M. Collins, J.B. Lee and W.E. Spicer, Surf. Sci. 55 (1976) 389

217. W.H. Weinberg, D.R. Monroe, V. Lampton and R.P. Merrill, J Vacuum Sci. Technol.14 (1977) 444

218. D.G. Castner and G.A. Somorjai, Chemical Reviews 79 (1979) 233

219. M.R. McClellan, F.R. McFeely and J.L. Gland, Surf. Sci. 123 (1983) 188

220. J.L. Gland and V.N. Korchak, Surf.Sci 75 (1978) 73

221. J.L. Gland, Surf. Sci. 93 (1980) 487

222. B.J. Wood, J. Phys. Chem. 75 (1971) 2186

223. A.F. Benton and J.C. Elgin, J.A.C.S. 49 (1927) 2426

224. P.A. Thiessen and H. Schutza, Z. Anorg. Chem. 243 (1932) 32

225. M.E. Schrader, J. Colloid Interfac. Sci. 59 (1987) 456

226. N.B. Bazhutin, G.K. Boreskov and V.I. Savchenko, Reaction Kinetics Catalysis Letters 104 (1979) 337

227. M.A. Chesters and G.A. Somorjai, Surf. Sci. 52 (1975) 21

228. D.D. Eley and P.B. Moore, Surf. Sci. 76 (1978) 1599

229. D.D. Eley and C.F. Knights, Proc. Roy. Soc. A294 (1966) 1

230. P. Legare, L. Hilaire, M. Sotto and G. Maire, Surf. Sci. 91 (1980) 175

231. M.E. Schrader, Surf. Sci. 78 (1978) L227

232. N.D.S. Canning, D.Outka and R.J. Madix, Surf. Sci. 141 (1984) 240

233. J.J. Pireaux, M. Chtaib, J.P. Delrue, P.A. Thiry, M. Liehr and R. Caudano, Surf. Sci. 141 (1984) 211

235. U. Stimming and W. Schmickler, J. Electroanal. Chem., 150 (1983) 125; U. Frese, T. Iwasita, W. Schmickler and U. Stimming, J. Chem. Phys. 89 (1985) 409; U. Frese and U. Stimming, J. Electroanal. Chem. 198 (1986) 409; T. Dinan and U. Stimming, J. Electrochem. Soc. 133 (1987) 2662

235. M.W. Roberts and C.S. McKee, The Chemistry of the Metal-Gas Interface, Oxford University Press, Oxford (1978)

236. B.E. Conway, H. Angerstein-Kozlowska, W.B.A. Sharp and E.E. Criddle, Anal. Chem. 45 (1973) 1331

237. J.I. Konikoff (to G.E. Schenectedy, N.Y., U.S.A.), U.S. Patent 3,127,243 (C1.23-24) Mar. 31, 1964; Canadian Patent 675,829 (C1.201-29) Dec. 10, 1963

238. B.E. Conway, Proc. Roy. Soc. (London) A256 (1960) 128

239. J. Mozota, B. Barnett, D.F. Tessier, H. Angerstein-Kozlowska and B.E. Conway, Anal. Chim. Acta 183 (1981) 191

240. J.M. Mozota, Ph.D. Thesis, U. of Ottawa (1981)

241. D.F. Tessier, Ph.D. Thesis, U. of Ottawa (1985)

242. B.E. Conway, H. Angerstein-Kozlowska, F.C. Ho, J. Klinger, B. Mc Dougall and S. Gottesfeld, Fara. Disc. Chem. Soc. 56 (1973) 29

243. T. Beiger, D.A.J. Rand and R. Wood, J. Electroanal. Chem. 29 (1971) 269

244. B.E. Conway and L. Bai, Electrochim. Acta 31 (1986) 1013

245. A.A. Michri, A.G. Pshchenichnikov, R.Kh. Burshtein, Electrokhimia 8 (1972) 364

246. A. Hamelin, J. Electroanal. Chem 195 (1985) 175

247. B. Barnett, unpublished results

248. D.W. Wilkinson, Ph.D. Thesis, U. of Ottawa (198?)

249. A.J. Arvia, J.C. Canullo, E. Custidiano, C.L. Perdreil and W.E. Triaca, Electrochim. Acta 31 (1986) 1359; C.L. Perdreil, A.J. Arvia and M. Ipohorski, J. Electroanal. Chem. 215 (1986) 317; M.C. Galindo, C.L. Perdreil, M.E. Martins and A.J. Arvia, to be published

250. J.B. Benzinger, F.A. Pascal, S.L. Bernasek, M.P. Soriaga and A.T. Hubbard, J. Electroanal. Chem. 198 (1986) 65

251. B.B. Damaskin, The Principles of Current Methods for the Study of Electrochemical Reactions, McGraw-Hill New York (1967)

252. A.K. Reddy in Electrosorption, E. Gileadi, editor, Plenum, New York (1967)

253. A. Despic and J.O'M. Bockris, J. Chem. Phys. 32 (1960) 389

254. R.Z. Schrebler-Gazman, J.R. Vilche and A.J. Arvia, J. Electrochem. Soc. 125 (1978) 1578

255. A.J. Bard, Encycl. Electrochem., Vol. 2, (1974) p. 242

256. F.G. Will and C.A. Knorr, Z. Elektrochem., 64 (1960) 270

257. G. Gruneberg, Electrochim. Acta, 10 (1965) 339

258. M.W. Breiter, Electrochim. Acta, 10 (1965) 543

259. T. Takamura, K. Takamura, W. Nippe and E. Yeager, J. Electrochem. Soc., 117 (1970) 629

260. M. Bonnemay, C. Bernard, G. Magner and M. Savy, C.R. Acad. Sci., Paris, 270 (1970) 1628